EFFECT OF METFORMIN ON BREAST CANCER METABOLISM



Thesis submitted by:
Simon Richard Lord
Christ Church

For the degree of:
Doctor of Philosophy
Department of Oncology
Trinity Term 2014
University of Oxford

Supervisor:
Professor Adrian L. Harris

ABSTRACT

There is a great and growing interest in the anti-cancer effects of the diabetes drug metformin as evidenced by the 50 clinical trials worldwide investigating the role of metformin in cancer treatment that are actively recruiting patients. Metformin's potential anti-cancer effects were first brought to light following a series of epidemiological studies showing that treatment with metformin, as opposed to other diabetes drugs, correlated with a reduction in the incidence of cancer in these patients. A subsequent retrospective clinical study of diabetic patients has suggested potential synergy with chemotherapy and several published in vitro and in vivo studies have clearly demonstrated evidence of an anti-cancer effect. However there is still not a consensus as to the mode of action by which metformin achieves this. Many in vitro studies of both cancer and non-cancer cells have shown that metformin can inhibit complex 1 of the mitochondrial respiratory transport chain and subsequently activate the energy sensing kinase, AMPK. The downstream catabolic effects subsequent to AMPK activation would be expected to be antiproliferative in nature in the cancer setting. However, it is also postulated that metformin derives its anticancer effect instead from downregulation of the 'host's' insulin axis, an indirect effect. Hence, there were 3 aims to this thesis project: to gain greater insight into its anticancer mechanism of action, to study pathways that might be targeted to synergise with metformin and to set up a 'window of opportunity' clinical study to develop potential biomarkers of its anticancer and metabolic effect and further investigate its mechanism of action in vivo. This thesis describes the novel finding that in vitro and in vivo metformin treatment results in the marked accumulation of fatty acid

triglyceride in cancer cells and that this phenomenon is secondary to the inhibition of fatty acid oxidation. It is also shown that etomoxir, another inhibitor of fatty acid oxidation, has an additive effect with metformin both in terms of inhibition of fatty acid oxidation, triglyceride fatty acid accumulation and the antiproliferative effect. In vitro work also showed the importance of glutamine in maintaining cancer cell growth for metformin treated cells and evidence of marked synergy with several compounds that inhibit the steps of the glutaminolysis and reductive carboxylation pathways, and also glutamine uptake. Lastly, this thesis describes a clinical study in which 2 weeks of metformin treatment was given to women with early breast cancer prior to any other treatment being initiated. Pharmacodynamic assays were carried out pre- and post-metformin, the study tests including breast core biopsies assayed for changes in gene expression using next generation sequencing, immunohistochemistry and metabolomics. Dynamic ^{18}[F]-FDG PET-CT scans were also carried out along with measurement of 'host' serum metabolic markers. Preliminary gene sequencing data from the clinical study demonstrates striking changes in the expression of genes encoding for the units of the mitochondrial electron transport chain (including complex 1) and the regulatory enzymes of glycolysis, glutaminolysis and fatty acid oxidation consistent with a direct metabolic effect on breast cancer cells by metformin. However, insulin secretion was also lowered by metformin in this cohort of non-diabetic breast cancer patients, suggesting that downregulation of the host's insulin axis may also play a role.

LIST OF PUBLICATIONS RELATED TO THESIS

Lord S, Collins JM, Fielding B, Pinnick K, Clark A, Wigfield S, Harjes U, Jha P, Hoefler G, Harris AL, Karpe F. Inhibition of fatty acid oxidation contributes to metformin's anticancer effect. Submitted to Cancer Discovery.

Lord S, Patel N, Liu D, Fenwick J, Gleeson F, Buffa FM, Harris AL. Neoadjuvant window studies of metformin and biomarker development for drugs targeting cancer metabolism. Accepted for publication by JNCI monographs.

Favaro E, **Lord S**, Harris AL, Buffa FM. Gene expression and hypoxia in breast cancer. Genome Medicine. 2011 Dec:3(83): doi:10.1186/gm271.

Lord S, Favaro E, Harris AL. Cancer metabolism as a target for therapy. MIMS Oncology. 2011 Mar:5(1):14-17.

Lord S, Harris AL, Angiogenesis - still a worthwhile target for breast cancer therapy? Breast Cancer Research. 2010 Dec;12(Suppl 4):S19.

ACKNOWLEDGEMENTS

Back in the Autumn of 2009 and the midst of the credit crunch I had been planning to follow a PhD in Leeds and the Mayo clinic examining NK cell biology and its relevance to the immune response to cancer. Although, after a struggle, I managed to secure a year of funding I am glad that I did not take this up! My time in the Harris lab has been the most fulfilling and interesting of my career and has enabled me to meet, and interact with, a great number of talented people, many of whom have become close friends.

Firstly I have to thank my supervisor Adrian Harris. From start to finish his enthusiasm and optimism were so important to getting this project off the ground. His ability to give advice when needed but allow me to have enough independence to learn form my mistakes was invaluable in my development as an investigator. I look forward to him acting as my mentor for years to come.

My collaborators Jennifer Collins, Fredrik Karpe, Dan Liu and John Fenwick were always available for advice and the story presented in this thesis could not have been generated without their help in carrying out the assays and analyzing the data. Neel Patel spent many of his weekends drawing round tumour VOIs or playing golf with me and he has become a good friend. Take it from me he is better at drawing round VOIs.

I have made many friends in my time in the Harris lab. My initiation involved several boozy dinners at Christ Church hosted by Chris Blick and Andrew Lomas that I often

had to leave prematurely… In particular my thanks go to Simon Wigfield and Ulrike Harjes who were both sources of advice and help, Dean Singleton for his rosy outlook on life and Helen Sheldon, Alan Mcintyre, Elena Favaro, Karim Bensaad and Ana Ramachandran for always being helpful no matter how daft a question was asked of them.

Most of all I have to thank my parents. The attributes I learnt from my journalist father in always finishing to a deadline mean I am not still writing this thesis now whilst my mother taught me many life skills that came in handy in dealing with the diverse range of characters I worked with in Oxford! Lastly, my time in the Harris' lab coincided with my marriage to my wonderful wife, Emily. Her support and calmness (in general) when yet again I was 45 minutes late for dinner (even when I was supposed to be cooking it) were invaluable in enabling me to finish this thesis.

LIST OF ABBREVIATIONS

ACC	Acetyl-CoA carboxylase
ACLY	ATP Citrate Lyase
AIC	Akaike Information Criteria
AICAR	5-Aminoimidazole-4-carboxamide ribonucleotide
AIF	Arterial input function
ADP	Adenosine diphosphate
AGPAT	Acylglycerophosphate acyltransferase
AKT	Protein Kinase B
AMP	Adenosine monophosphate
AMPK	AMP-activated protein kinase
ATGL	Adipose triglyceride lipase
ATP	Adenosine triphosphate
BMI	Body mass index
BODIPY	Boron-dipyrromethene
BPTES	Bis-2-(5-phenylacetamido-1,3,4-thiadiazol-2-yl)ethyl sulfide
BRCA1	Breast Cancer Susceptibility Gene 1
BSA	Bovine serum albumin
CAMMK	Calcium-calmodulin-dependent protein kinase
CBP	CREB binding protein
CDK	Cyclin dependent kinases
CI	Confidence interval
CKI	Cyclin-CDK inhbitors

CoA	Coenzyme A
CPT1	Carnitine palmitoyltransferase-1
CR	Complete radiological response
CREB	cAMP response element-binding protein
CRTC2	CREB-regulated transcription co-activator-2
DAPI	4',6-diamidino-2-phenylindole
DEPC	Diethylpyrocarbonate
DG	Diglyceride
DGAT	Diacyglycerol acyltransferase
2-DG	2-deoxyglucose
DMEM	Dulbecco’s modified Eagle's minimal essential medium
DNL	De novo lipogenesis
DON	6-Diazo-5-oxo-L-norleucine
DTT	Dithiothreitol
eGFR	Estimated glomerular filtration rate
EGFR	Epidermal growth factor receptor
ECAR	Extracellular acidification rate
ECOG	Eastern Cooperative Oncology Group
EDTA	Ethylenediaminetetraacetic acid
EIF4B	Eukaryotic translation initiation factor 4B
EIF4E	Eukaryotic translation Initiation factor 4E
4E-BP1	Eukaryotic translation initiation factor 4E-binding protein 1
ELOVL	Elongation of very long chain fatty acids protein
ER	Oestrogen receptor
ETC	Electron transport chain

ETF	Electron transfer flavoprotein
ETF:QO	Electron transfer flavoprotein dehydrogenase
FA	Fatty acid
FABP	Fatty acid binding protein
FA CoA	Fatty acid Coenzyme A
FACS	Fluorescence-activated cell sorting
FAME	Fatty acid methyl esters
FAS	Fatty acid synthase
FBS	Foetal bovine serum
FCCP	Mesoxalonitrile 4-trifluoromethoxyphenylhydrazone
^{18}[F]-FDG	2-deoxy-2-(^{18}F)fluoro-D-glucose
FEC	Fluorouracil-epirubicin-cyclophosphamide
GβL	G protein beta subunit-like
GC	Gas chromatography
GCP	Good clinical practice
GLUT	Glucose transporter
GPAT	Glycerol-3-phosphate
GPNA	L-γ-glutamyl-p-nitroanilide
GTP	Guanosine triphosphate
HDL	High-density lipoprotein
HER2	Human epidermal growth factor receptor 2
HIF	Hypoxia inducible factor
HMG-CoA	3-hydroxy-3-methylglutaryl-co-enzyme A
$^{2}H_2O$	Deuterated water
HOMA	Homeostasis model assessment

HRP	Horseradish peroxidase
HSL	Hormone sensitive lipase
H_2SO_4	Sulphuric acid
IDH	Isocitrate dehydrogenase
IGF	Insulin-like growth factor
IGF-BP3	Insulin-like growth factor-binding protein-3
IR	Insulin receptor
K_1	Dynamic PET-CT rate constant 1
k_2	Dynamic PET-CT rate constant 2
k_3	Dynamic PET-CT rate constant 3
k_4	Dynamic PET-CT rate constant 4
KBq	Kilobecquerel
KEGG	Kyoto Encylcopedia of Genes and Genomes
KOH	Potassium hydroxide
LDL	Low-density lipoprotein
LKB1	Liver kinase B1
LPA	Lysophosphatidic acid
MAG	Monoacylglycerol
MAGL	Monoacylglycerol lipase
MAPK	Mitogen-activated protein kinase
MCT	Monocarboxylate transporter
MEF	Mouse embryonic fibroblast
MPP	1-methyl-4 phenylpyridimium iodide
mTOR	Mammalian target of rapamycin
mRNA	Messenger ribonucleic acid

MRI	Magnetic resonance imaging
MS	Mass spectrometry
MTS	3-(4,5-dimethylthiazol-2-yl)-5-(3-carboxymethoxyphenyl)-2- (4-sulfophenyl)-2H-tetrazolium
NAD/NADH	Nicotinamide adenine dinucleotide
NADPH	Nicotinamide adenine dinucleotide phosphate
NH4	Ammonium
NMR	Nuclear Magnetic Resonance
NNK	4-(methylnitrosamino)-1-(3-pyridyl)-1-butanone
NOD	nucleotide-binding oligomerisation
NRF2	Nuclear factor (erythroid-derived 2)-like 2
OCR	Oxygen consumption rate
OCT1	Organic cation transporter-1
PA	Phosphatidic acid
pACC	phosphorylated Acetyl-CoA carboxylase
PAP	Phosphatidic acid phosphohydrolase
PK	Pyruvate kinase
PKC	Protein kinase C
pS6	phosphorylated S6 kinase
pAMPK	phosphorylated AMP-activated protein kinase
p4E-BP1	phosphorylated Eukaryotic translation initiation factor 4E-binding protein 1
PBS	Phosphate buffered saline
pCR	Complete pathological response
PDE3B	Phosphodiesterase 3B

PDK	Pyruvate dehydrogenase kinase
PDH	Pyruvate dehydrogenase
PET-CT	Positron emission tomography–computed tomography
PI3K	Phosphoinositide 3-kinase
PKC	Protein Kinase C
PL	Phospholipid
PML	Promyelocytic leukemia gene
PNPLA2	Patatin-like phospholipase domain containing 2
PPAR	Peroxisome proliferator-activated receptor
PR	Partial radiological response
PRKAA	Protein Kinase, AMP-Activated, Alpha, Catalytic Subunit
PRKAB	Protein Kinase, AMP-Activated, Beta, Non-Catalytic Subunit
PRKAG	Protein Kinase, AMP-Activated, Gamma, Non-Catalytic Subunit
PTEN	Phosphatase and tensin homologue deleted on chromosome 10
RCF	Relative centrifugal force
RIN	RNA integrity number
RNASeq	Next generation RNA sequencing
ROS	Reactive Oxygen Species
RPMI	Roswell Park Memorial Institute medium
RRN3	RNA polymerase I-specific transcription initiation factor
RT-PCR	Reverse transcription polymerase chain reaction
S6	ribosomal protein S6
S6K	ribosomal protein S6 kinase
Scr	Scrambled
SCD	Stearoyl-CoA desaturase

SD	Stable disease
SEM	Standard error of the mean
SLC1A5	Solute carrier family1 member 5
SLC22A1	Solute carrier family 22 member 1
SLC38A1	Solute carrier family 38 member 1
SLC38A2	Solute carrier family 38 member 2
SLC38A5	Solute carrier family 38 member 5
SI	Metric unit
SHP	Small heterodimer partner
SRB	Sulforhodamine B
SREBP-1	Sterol regulatory element-binding protein-1
STAT3	Signal transducer and activator of transcription 3
SUL	SUV lean
SUV	Standardised uptake value
SUV_{Max}	Maximum standardised uptake value
TCA	Tricarboxylic acid
TG	Triglyceride
TMA	Tissue microarray
TNFR1	Tumour necrosis factor receptor 1
TSC	Tuberous sclerosis complex
TUNEL	Terminal deoxynucleotidyl transferase
VEGF	Vascular endothelial factor
VEGFR2	Vascular endothelial growth factor receptor 2
VOI	Volume of interest
WHO	World Health Organsiation

TABLE OF CONTENTS

TITLE PAGE 1

ABSTRACT 2

LIST OF PUBLICATIONS RELATED TO THESIS 4

ACKNOWLEDGEMENTS 5

LIST OF ABBREVIATIONS 7

TABLE OF CONTENTS 14

LIST OF FIGURES 24

LIST OF TABLES 28

CHAPTER 1: INTRODUCTION

1.1: Overview of metformin and its role in treatment of diabetes mellitus 30

1.1.1: Historical context 30

1.1.2: Chemical structure and formulations of metformin 31

1.1.3: Pharmacokinetics, metabolism and distribution of metformin 31

1.1.4: Tolerability 33

1.1.5: Metformin's effects on glucose and lipid metabolism in diabetes 34

1.2: Basis for growing interest in the potential for metformin as an anticancer drug 36

1.2.1: Epidemiological and retrospective clinical studies 36

1.2.2: In vitro and in vivo studies of metformin's anticancer effect 39

1.2.3: Metformin and cancer prevention 41

1.2.4: Obesity, diabetes and breast cancer 42

1.3: Proposed mechanisms of action of metformin in cancer 44

1.3.1: Direct versus indirect theory of effect 44

1.3.1.1: Direct effect 45

1.3.1.2: Indirect effect 46

1.3.2: AMPK activation 47

1.3.3: Inhibition of Mitochondrial complex 1 50

1.3.4: Limitations of preclinical models 53

1.4: Cancer metabolism 55

1.4.1: Overview 55

1.4.2: The Warburg effect: glucose metabolism in cancer cells 55

1.4.3: Glutamine metabolism in cancer 59

1.4.4: Cancer lipid metabolism 60

1.4.4.1: Overview 60

1.4.4.2: Summary of structure and function of lipids 62

1.4.4.3: Fatty acid synthesis in cancer cells 63

1.4.4.4: Fatty acid uptake into cancer cells 66

1.4.4.5: Fatty acid desaturation in cancer cells 67

1.4.5.5: Fatty acid oxidation in cancer cells 67

1.4.5.6: Storage and lipolysis of lipid in cancer cells 68

1.5: Biomarker trials of metformin 72

1.5.1: Overview 72

1.5.2: Published window of opportunity studies and metformin 73

1.5.3: Role of functional imaging, gene sequencing and metabolomics in cancer drug development 76

1.5.3.1: Functional imaging 76

1.5.3.2: RNA sequencing 76

1.5.3.3: Metabolomics 77

1.5.4: Potential biomarkers of metformin's clinical effect in breast cancer 78

1.5.5: Mechanism's of resistance to metformin's indirect effect 78

1.5.6: Mechanism's of resistance to metformin's direct effect 80

1.6: Summary and aims 83

1.6.1: Summary 83

1.6.2: Aims 83

CHAPTER 2: MATERIALS AND METHODS

2.1: Materials 84

2.1.1: Cell lines 84

2.1.2: Chemicals 84

2.1.3: Antibodies 84

2.2: Cell culture and in vitro techniques 85

2.2.1: Cell culture 85

2.2.2: Hypoxic exposure 85

2.2.3: RNA interference 85

2.3: Cell growth assays 86

2.3.1 Cell counting 86

2.3.2 Cell number assays 86

2.3.3: Spheroid formation and volume quantification 86

2.3.4: Proliferation assays 87

2.3.4.1 Sulforhodamine B (SRB) assay 87

2.3.4.2 Cyquant™ assay 87

2.4: Assays of cellular metabolism 87

2.4.1: Glucose and lactate measurement 87

2.4.2: Oxygen consumption and extracellular acidification experiments 88

2.4.3: ATP estimation 88

2.4.4: Estimation of oleate oxidation 89

2.4.5: Measurements of Total lipolysis, HSL and ATGL activity 89

2.5: RT-PCR 91

2.5.1: RNA extraction 91

2.5.2: cDNA synthesis 91

2.5.3: Quantitative PCR (qPCR) 92

2.5.4: Quantification of gene expression 92

2.6: Protein extraction and analysis 93

2.6.1: Protein extraction 93

2.6.2: Protein electrophoresis and antibody detection 93

2.7: In vivo experiments 94

2.8: Flow cytometry 94

2.8.1: BODIPY uptake analysis 94

2.9: Electron microscopy techniques 95

2.10: Gas chromatography mass spectrometry techniques 95

2.10.1: Preparation of samples 95

2.10.2: Gas chromatography 98

2.10.3: Use of stable isotopes and mass spectrometry 98

2.11: LD540 Staining 99

2.11.1: LD540 staining of cells in vitro 99

2.11.2: LD540 staining of xenograft sections 100

2.12: Immunohistochemistry techniques for clinical study 100

2.12.1: Cell pellet generation for validation and controls 100

2.12.2: Summary of Immunohistochemistry antibody optimization 101

2.12.3: Validation of pAMPK antibody 102

2.12.4: pS6 staining validation 102

2.12.5: pEIF4-BP1 staining validation 103

2.12.6: Ki67 staining 104

2.12.7: Collection of biopsies for immunohistochemistry and handling 104

2.13: Analysis of ^{18}[F]-FDG PET-CT scans 108

2.13.1: PET-CT protocol 108

2.13.2: Analysis of static PET-CT 110

2.13.3 Analysis of dynamic PET-CT 110

2.14: Gene sequencing of breast biopsy samples 112

2.14.1: Collection of biopsies and handling 112

2.14.2: RNA preparation from biopsy samples 112

2.14.4: Quantification and quality control of samples 113

2.14.5: Next generation sequencing of samples 113

2.15: Clinical serum metabolic markers 114

2.15.1: Serum sample for glucose, insulin, IGF-1, IGF-2, IGF-BP-3, C-peptide, lactate and leptin 114

2.15.2: EDTA sample for HDL, total cholesterol and triglycerides 114

2.15.3: Processing of serum and EDTA samples 115

2.16: Statistical methodology 115

2.16.1: Data from in vitro and in vivo models 115

2.16.2: Bioinformatic analysis of gene sequencing data 115

2.16.3: Immunohistochemistry data 117

CHAPTER 3: METFORMIN ALTERS SUBSTRATE UTILISATION IN BREAST CANCER CELLS

3.1: Introduction 118

3.11: Current understanding of metformin's direct (insulin independent) effects on cancer cells 118

3.1.2: Glucose, glutamine and the cancer phenotype 118

3.1.3: Aims 121

3.2: Results 122

3.2.1: Effect of metformin on the proliferation of a panel of breast cancer cell lines 122

3.2.2: Metformin and activation of AMPK in MCF7 cells 125

3.2.3: Metformin inhibits mitochondrial respiration and depletes cellular ATP 128

3.2.4: Metformin alters mitochondrial morphology in MCF7 cells but not MDA-MB-231 cells 131

3.2.5: Metformin treatment leads to an increase in the glycolytic rate in breast cancer cell lines 134

3.2.6: Depletion of glucose enhances the anti-proliferative effect of metformin in sensitive breast cancer cell lines 137

3.2.7: Effect of metformin on the individual contributions of glucose, glutamine and lactate as substrates for de novo lipogenesis in MCF7 cells 140

3.2.8: Withdrawal of glutamine enhances the anti-proliferative effect of metformin in sensitive breast cancer cell lines 143

3.2.9: A screen of inhibitors of key modulators of glutamine metabolism in combination with metformin reveals promising synergy 144

3.3: Discussion 153

3.3.1: Sensitivity to metformin between cancer cell lines is not determined by mitochondrial resistance or their capacity to upregulate glycolysis 153

3.3.2: Metformin activates AMPK at lower doses under hypoxic conditions 153

3.3.3: Synergy between inhibitors of glutamine metabolism and metformin offers a promising cancer treatment strategy 154

3.3.4: Future work 155

CHAPTER 4: EFFECT OF METFORMIN ON BREAST CANCER LIPID METABOLISM

4.1: Introduction 157

4.1.1: Metformin and its effects on lipid metabolism 157

4.1.2: Are metformin's effects on lipid metabolism a potential link to its anticancer effect? 158

4.1.3: Aims 159

4.2: Results 160

4.2.1: Metformin treatment of breast cancer cell lines leads to an accumulation of triglyceride and lipid droplet formation in vitro and in vivo 160

4.2.2: Effect of metformin on fatty acid desaturation and elongation 165

4.2.3: Metformin reduces the proportion of triglyceride fatty acid derived from de novo lipogenesis 171

4.2.4: Metformin increases fatty acid uptake in MCF7 and MDA-MB-468 cells 172

4.2.5: Metformin reduces the proportion of exogenous fatty acid directed toward cellular phospholipid 175

4.2.6: Metformin reduces fatty acid oxidation in MCF7 and MDA-MB-468 cells 177

4.2.7: Etomoxir and metformin have an additive effect in suppressing the growth of breast cancer cell lines in vitro 178

4.2.8: Metformin treatment does not affect lipolysis in breast cancer cell lines 181

4.2.9: Activation of AMPK does not mediate metformin's effects on triglyceride accumulation 183

4.2.10: Rotenone mimics metformin's effects on triglyceride accumulation 186

4.2.11: Addition of palmitic acid and oleic acid does not alter metformin's effect on breast cancer cell line proliferation 187

4.3: Discussion 188

4.3.1: Metformin's inhibition of fatty acid oxidation is in contrast to previous studies and is a novel explanation for its anticancer effect 188

4.3.2: Metformin's effect on trigyceride accumulation needs further assessment in vivo – future work 191

CHAPTER 5: CLINICAL STUDY

5.1: Introduction 193

5.1.1: Metformin and its place in the breast cancer clinic 193

5.1.2: Focus of published biomarker studies to date 193

5.1.3: Aims 194

5.2: Study design 195

5.3: Patient and clinical characteristics 199

5.4: ^{18}[F]-FDG PET-CT analysis 202

5.4.1: Analysis of static ^{18}[F]-FDG PET-CT 202

5.4.1.2: Bowel uptake of ^{18}[F]-FDG 205

5.4.2: Analysis of dynamic ^{18}[F]-FDG PET-CT 206

5.5: Next generation RNA sequencing 213

5.5.1: Overview 213

5.5.2: Electron Transport Chain 217

5.5.3: TCA cycle 221

5.5.4: Glycolysis and glucose uptake 224

5.5.5: Glutamine metabolism 226

5.5.6: Lipid metabolism 228

5.5.7: Insulin, AMPK, PI3K and MTOR signaling 230

5.6: Immunohistochemical analysis 233

5.6.1: Ki67 233

5.6.2: pAMPK 233

5.6.3: pS6 234

5.6.4: pE4-BP1 234

5.7: Serum metabolic markers 239

5.8: Discussion 243

5.8.1: mRNA sequencing analysis is consistent with 'direct' effect of metformin on cancer cells 243

5.8.2: Change in K_2 of ^{18}[F]-FDG on dynamic PET-CT is a possible biomarker of metformin's metabolic effect 244

5.8.3: Future work 244

CHAPTER 6: FINAL DISCUSSION

6.1: Overview 246

6.2: Inhibition of Fatty acid oxidation contributes to metformin's anticancer effect 247

6.3: Targeting of glutamine metabolism in conjunction with metformin treatment should be pursued as a treatment strategy 248

6.4: Gene expression data from clinical **samples correlates well with in vitro work** 249

6.5: Future directions 250

REFERENCES 252

LIST OF FIGURES

Figure 1.1: Chemical structure of metformin 31

Figure 1.2: Direct and indirect hypotheses of metformin's mechanism of anticancer effect 44

Figure 1.3: Activation of AMPK 47

Figure 1.4: Key pathways regulated by AMPK 49

Fig 1.5: Complex 1 structure and function 52

Fig 1.6: Predominant fates of glucose and glutamine in cancer cells 58

Fig 1.7: Altered lipid metabolism in cancer 61

Fig 1.8: Triglyceride storage and breakdown 71

Figure 2.1: Example of a chromatogram 97

Figure 2.2: pAMPK antibody validation on cell pellets and TMAs 105

Figure 2.3: pS6 antibody validation on cell pellets and TMAs 106

Figure 2.4: p4E-BP1 antibody validation on cell pellets and TMAs 107

Figure 2.5: Example of a dynamic PET-CT ^{18}[F]-FDG time activity curve 112

Figure 3.1: Overview of glucose and glutamine substrate utilization 120

Figure 3.2: SRB dose response curves for metformin for the MCF7, MDA-MB-468 and MDA-MB-231 cell lines 123

Figure 3.3: Western blots of effect of metformin on AMPK signaling in MCF7 cells 127

Figure 3.4: Effect of metformin on oxygen consumption in MCF7 and MDA-MB-231 cells 130

Figure 3.5: Effect of metformin on mitochondrial morphology in MCF7 and MDA-MB-231 cells 133

Figure 3.6: Effect of metformin on glycolysis parameters 136

Figure 3.7: Effect glucose depletion on cell growth in metformin treated cells 139

Figure 3.8: Importance of glutamine in maintaining cell proliferation in metformin treated cells 141

Figure 3.9: Compounds targeting the glutaminolysis and reductive carboxylation pathways 145

Figure 3.10: Cyquant dose response curves to compounds targeting glutamine metabolism in MCF7 cells 150

Figure 3.11: Effect of metformin on cell number in combination with 8 different compounds that target glutamine metabolism 151

Figure 4.1: Effect of metformin on intracellular TG fatty acid accumulation in a panel of breast cancer cell lines 161

Figure 4.2: Effect of metformin on lipid droplet accumulation in vitro and in vivo 163

Figure 4.3: Effect of metformin on fatty acid profile in 6 breast cancer cell lines 167

Figure 4.4: Effect of metformin on fatty acid desaturation and elongation 170

Figure 4.5: Effect of metformin on accumulation of DNL derived fatty acid 172

Figure 4.6: Effect of metformin on fatty acid uptake 174

Figure 4.7: Effect of metformin on accumulation of DNL derived fatty acid 176

Figure 4.8: Effect of combination of metformin and etomoxir on cell number and ATP levels 180

Figure 4.9: Effect of metformin on lipolysis 182

Figure 4.10: Effect of modulation of AMPK on TG fatty acid accumulation 185

Figure 4.11: Effect of rotenone on TG fatty acid accumulation 186

Figure 4.12: Effect of addition of oleic acid and palmitic acid on cell growth in presence of metformin 187

Figure 4.13: Summary of metformin's effects on lipid metabolism 190

Figure 5.1: Schema for 'window of opportunity' metformin clinical study 197

Figure 5.2: Example of coronal PET scan images pre- and post-metformin 203

Figure 5.3: Baseline and post-metformin SUV_{max} 204

Figure 5.4: Bowel uptake of ^{18}[F]-FDG 205

Figure 5.5: Change ^{18}[F]-FDG flux 209

Figure 5.6: Change in K_1, K_2, K_3 and K_4 210

Figure 5.7: Correlation of dynamic PET-CT variables with BMI 211

Figure 5.8: Correlation of dynamic PET-CT variables with ER status 212

Figure 5.9: Genecodis KEGG pathway map of genes encoding mitochondrial components of the electron transport chain 218

Figure 5.10: Significantly upregulated and downregulated genes encoding regulators of the TCA cycle 223

Figure 5.11: Significantly upregulated and downregulated genes encoding regulators of the glycolysis pathway 225

Figure 5.12: Significantly upregulated and downregulated genes encoding regulators of the glutaminolysis and reductive carboxylation pathways 227

Figure 5.13: Significantly upregulated and downregulated genes encoding regulators of the lipid metabolism 229

Figure 5.14: Significantly upregulated and downregulated genes encoding regulators of the PI3K, AMPK and mTOR pathways 232

Figure 5.15: Baseline and post-metformin immunohistochemical Ki67 expression 235

Figure 5.16: Baseline and post-metformin immunohistochemical pAMPK expression 236

Figure 5.17: Baseline and post-metformin immunohistochemical pS6 expression 237

Figure 5.18: Baseline and post-metformin immunohistochemical p4E-BP1 expression 238

Figure 5.19: Baseline and post-metformin serum levels glucose, lactate, insulin, c-peptide, IGF-1, IHF-2, IGF2:IGF1 ratio, IGF-BP3 and HOMA index 241

Figure 5.20: Baseline and post-metformin serum levels of total cholesterol, HDL-cholesterol, triglyceride and leptin 242

LIST OF TABLES

Table 1.1: Metformin (Glucophage preparation) pharmacokinetic profile in healthy non-diabetic adults 32

Table 1.2. Epidemiological studies to date examining the link between metformin and cancer incidence 37

Table 1.3: Neoadjuvant studies of potential metformin biomarkers of effect in breast cancer patients 75

Table 1.4: Metformin's effects on cancer cell proliferation and colony formation 78

Table 1.5: Potential mechanisms of resistance to metformin's anticancer effect relevant to direct and indirect anticancer effects of metformin 79

Table 2.1: Summary of ^{18}[F]-FDG PET-CT protocol for both static and dynamic scans 109

Table 5.1: Inclusion exclusion criteria for clinical study 196

Table 5.2: Summary of clinical study assays 198

Table 5.3: Patient and clinical characteristics 201

Table 5.4: Top 50 upregulated KEGG pathways on Genecodis analysis 215

Table 5.5: Top 50 downregulated KEGG pathways on Genecodis analysis 216

Table 5.6: Differential expression of significantly differentially expressed genes encoding units of the electron transport chain 219

Table 5.7: Differential expression of significantly differentially expressed genes encoding regulators of the TCA cycle 222

Table 5.8: Differential expression of significantly differentially expressed genes encoding regulators of the glycolysis pathway 224

Table 5.9: Differential expression of significantly differentially expressed genes encoding regulators of the glutaminolysis and reductive carboxylation pathway 226

Table 5.10: Differential expression of significantly up and down regulated genes encoding regulators of lipid metabolism. 228

Table 5.11: Differential expression of significantly up and down regulated genes encoding regulators of the PI3K, AMPK and mTOR pathways 231

CHAPTER 1: INTRODUCTION

1.1: OVERVIEW OF METFORMIN AND ITS ROLE IN TREATMENT OF DIABETES MELLITUS

1.1.1: HISTORICAL CONTEXT

It is only relatively recently that there has been interest in the anticancer effects of metformin. The biguanide drugs, metformin and phenformin, were in fact first developed in the 1950's to treat hyperglycaemia in type 2 diabetes mellitus. Both are derivatives of guanidine which was the active ingredient in goat's rue or french lilac used to treat diabetes by herbalists in the middle ages [1]. Metformin or 1,1-Dimethylbiguanide hydrochloride is now believed to be the most widely prescribed diabetes drug worldwide. In many countries phenformin was initially the biguanide drug of choice but it was withdrawn from use in the 1970's in most of the Western World due to concerns over a high rate of lactic acidosis and associated deaths.

Metformin has been shown to have beneficial effects other than just the control of blood glucose levels in diabetes. The seminal UKPDS study demonstrated that type 2 diabetic patients taking metformin had a lower all cause mortality compared to two other oral antihyperglycaemic drugs, chlorpropamide and glibenclamide, and also insulin [2]. Metformin has also been shown to reduce microvascular and macrovascular complications [3] and improve the serum lipid profile in diabetic patients (see *section 1.1.6* for more on effects of metformin on lipid metabolism in diabetes) [2, 4-6]. The use of metformin has now extended to the treatment of

polycystic ovarian syndrome [7], non-alcoholic steatohepatitis [8] and premature puberty [9], all conditions associated with insulin resistance.

1.1.2: CHEMICAL STRUCTURE AND FORMULATIONS OF METFORMIN

The molecular formula for metformin is $C_4H_{11}N_5$. It is freely soluble in water and the pH of a 1% aqueous solution is 6.68. Its structure is shown in **Figure 1.1** [10]. In the UK metformin is either available in its standard formulation (trade name Glucophage) or as an extended release formulation, Glucophage XR. Formulations are also available that combine metformin with newer oral hypoglycaemic drugs including pioglitazone, saxagliptin, sitagliptin and vildagliptin [11].

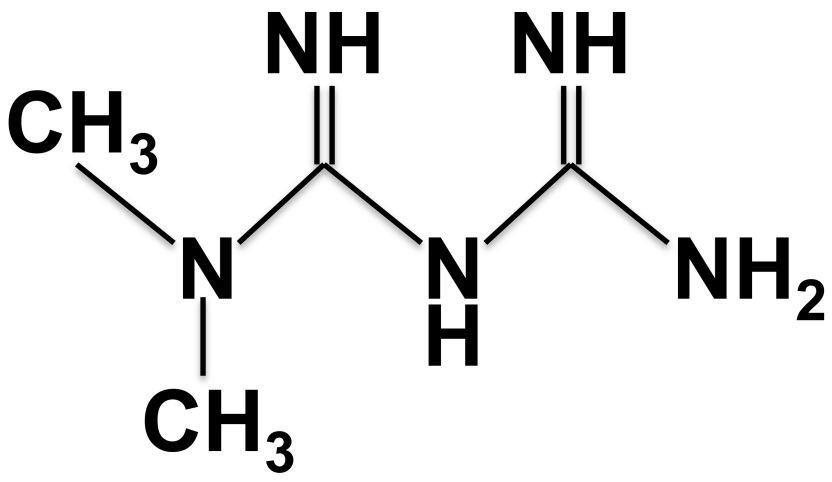


Fig 1.1: Chemical structure of metformin

1.1.3: PHARMACOKINETICS, METABOLISM AND DISTRIBUTION OF METFORMIN

The oral bioavailability of metformin ranges between 50 and 60% [12, 13] and given that there is an inverse relationship between the oral dose and relative absorption this

occurs most probably via an active and saturable process [14]. Therapeutic oral doses range from 0.5-2 g [11]. It does not bind to plasma proteins [12] and in healthy

Metformin dose	Cmax (μg/ml)	Tmax (hrs)	Renal clearance (ml/min)
500mg single dose	1.03 (+/-0.33)	2.75 (+/-0.81)	600 (+/- 132)
850mg single dose	1.60 (+/-0.38)	2.64 (+/-0.82)	552 (+/-139)
850mg three times daily for 19 doses*	2.01 (+/-0.42)	1.79 (+/-0.94)	642 (+/-173)

Table 1.1: Metformin (Glucophage preparation) pharmacokinetic profile in healthy non-diabetic adults from Bristol Myers Squibb [15]. Cmax, peak plasma concentration; Tmax, time to peak plasma concentration; * = kinetic study following dose 19.

individuals peak plasma concentration is 1 to 3 μg/ml at 1 to 3 hours after an oral dose of 500 to 1000 mg (**Table 1.1** – see comparison to levels in preclinical models in *section 1.3.4*). The plasma elimination half-life is estimated to be approximately 6 hours and 90% of metformin is eliminated within 24 hours [15]. Metformin undergoes renal excretion and there is a close correlation between creatinine clearance and elimination of metformin [12, 16]. Metformin does not undergo hepatic metabolism and there are no known metabolites of metformin [17]. This is in contrast to phenformin, at least in mammalian models, which is hydroxylated to p-hydroxyphenformin in the liver [18]. Metformin is not known to inhibit the metabolism of other drugs [19].

One study using ^{14}C-radiolabelled metformin in mice demonstrated that after administration metformin becomes most highly concentrated in the liver, kidneys, small intestinal wall and salivary glands. The high concentration in the small intestine compared to colon in the mouse is suggestive of this being the main site of uptake [20]. However, in humans, the metformin stimulated ^{18}[F]-FDG uptake response in the colon is just as great as that seen in the small intestine [21] which may mean that a different absorption pattern applies in humans.

1.1.4: TOLERABILITY

The most serious clinical risk associated with metformin is the development of lactic acidosis for which the mortality is reported to approach 50%. Typically this occurs in patients with impaired renal function and hence poor drug clearance. It is characterised by serum lactic acid concentrations of >5 mmol/L, electrolyte disturbance and a metabolic acidosis [22]. However, metformin, which has a shorter half-life than phenformin, has a far better safety profile. 1 in 40,000 to 80,000 patients on metformin develop lactic acidosis as opposed to 1 in 4000 on phenformin, and this has never been reported in the setting of a clinical trial where patients would be appropriately selected [23]. The commonest side effects are gastrointestinal and include diarrhea, abdominal bloating, nausea, a metallic taste and anorexia. Side effects typically improve after the first few days of taking the drug and can often be avoided by increasing the drug dose slowly in a stepwise fashion. Vitamin B12 deficiency has also been reported to be associated with metformin although the mechanism is unclear [24].

1.1.5: METFORMINS EFFECTS ON GLUCOSE AND LIPID METABOLISM IN DIABETES

The exact mechanism by which metformin lowers serum glucose in diabetes is still debated but there is a growing consensus that inhibition of hepatic gluconeogenesis plays a central role [25, 26]. The preferential effect in the liver can be explained by 2 observations. Firstly, accumulation of metformin in the liver has been shown in mice [20]. Secondly, organic cation transporter 1 (OCT1), a transporter protein that has been demonstrated to mediate cellular uptake of metformin, is highly expressed in the liver [27]. Deletion of the SLC22A1 gene (which encodes for OCT1) in the hepatocytes of mice and SLC22A1 polymorphisms in humans have been shown to significantly reduce the effectiveness of metformin in lowering serum blood glucose levels [27].

The molecular basis for how metformin inhibits hepatic gluconeogenesis is increasingly understood. There is now substantial data to show that the inhibition of hepatic gluconeogenesis is secondary to metformin's inhibition of complex 1 of the mitochondrial respiratory chain and subsequent AMPK activation (see *sections 1.3.2 and 1.3.3* for greater detail on complex 1 and the AMPK axis.) The first study to suggest metformin's blood glucose lowering effects might be mediated by AMPK did so by demonstrating that mice with LKB1 null hepatocytes (an upstream kinase with an important role in the activation of AMPK) had a minimal anti-hyperglycaemic response to metformin [28]. Several mechanisms for metformin's AMPK mediated inhibition of gluconeogenesis have been put forward but studies to date point toward a leading role for the transcriptional coactivator, cAMP response element-binding protein (CREB). He et al showed that metformin treatment leads to the

phosphorylation of CBP (CREB binding protein) at serine 436 through AMPK induced protein kinase C (PKC) activation. This leads to the dissociation of the CREB-CBP-CRTC2 transcription complex and subsequent reduced gluconeogenic gene expression [29]. Transcription factors also seem to play a role in metformin's modulation of CREB activity. AMPK activation in hepatocytes results in greater expression of the orphan nuclear receptor, small heterodimer partner (SHP) [30]. SHP then acts as a transcriptional repressor by competing with CREB-regulated transcription co-activator-2 (CRTC2) binding in the CREB-CBP complex [31].

Metformin has also been shown to have beneficial effects on lipid metabolism in diabetics. Several clinical studies have demonstrated an associated reduction in serum trigylcerides and total and LDL cholesterol and possibly increased HDL cholesterol [2, 4-6]. Current evidence suggests that AMPK activation is also key to metformin's effects on lipid metabolism, at least in the liver. In hepatoma HepG2 cells metformin leads to increased ACC phosphorylation, in an AMPK dependent manner, and a subsequent reduction in triglyceride cellular content secondary to increased fatty acid oxidation and reduced de novo lipogenesis (DNL) [32]. In primary rat hepatocytes metformin decreases the activity of the transcription factor, sterol-regulatory-binding-protein-1c (SREBP-1c), again in an AMPK dependent manner, and subsequently lipogenic gene expression [33]. Lastly, in hepatocytes, metformin has been shown to inhibit expression of SCD1, the gene that encodes for the key enzyme involved in desaturation of fatty acids [34].

1.2: BASIS FOR GROWING INTEREST IN THE POTENTIAL FOR METFOMRIN AS AN ANTICANCER DRUG

1.2.1: EPIDEMIOLOGICAL AND RETROSPECTIVE CLINICAL STUDIES

Growing evidence suggests that there is the potential for metformin to reduce cancer risk and perhaps be used as a cancer therapy. The interest in the potential of metformin as an anticancer agent was initially sparked by a series of epidemiological studies, solely in diabetic patients, that suggested it had a protective effect against cancer [35-37]. A meta-analysis of these studies put the reduction in relative risk in the order of 31% (SRR, 0. 69; 95% CI , 0. 61- 0. 79) [38]. In the largest study to date the reduced risk for breast, bowel and lung cancer was of a similar magnitude to that of all cancers. However a review of all epidemiological studies did suggest a trend towards a greater decrease in relative risk for pancreatic and colon cancer [37, 38]. More specifically, with regard to breast cancer, a recent study of 68,019 postmenopausal women participating in the Women's Health Initiative Trials in the USA, including 3273 diabetics at study entry, showed that the incidence of invasive breast cancer was lower in diabetics taking metformin compared to all women in the study (HR, 0. 75; 95% CI, 0. 57 - 0. 99). In contrast, for women taking other diabetes medications the incidence of invasive breast cancer was slightly higher compared to all women in the study (HR, 1.16; 95% CI, 0. 93 – 1.45). In this study metformin use was associated with a lower incidence of breast cancers positive for the oestrogen and progesterone receptors (HR, 0.64; 95% CI, 0. 45 – 0.92) [39].

Study type	Outcome	Sample size	Comparison	Site	Results (HR/OR/RR and 95% CI)	Reference
Case control	Incidence	11,876	Any vs no metformin	Multiple	OR 0.86 (0.73-1.02)	Evans et al (2005)
Retrospective cohort	Mortality	10,309	Metformin Insulin Sulphonylureas	Multiple	HR 1.0 HR1.9 (1.5-2.4) HR 1.3 (1.1-1.6)	Bowker et al (2006)
Case control	Incidence	390	Any vs no metformin	Multiple	OR 0.28 (0.13-0.57)	Monami et al (2009)
Retrospective cohort	Incidence	8,170	Any vs no metformin	Bowel Lung Breast Overall	HR 0.60 (0.38-0.94) HR 0.70 (0.43-1.15) HR 0.60 (0.32-1.10) HR 0.63 (0.49-0.81)	Libby et al (2009)
Retrospective cohort	Incidence	62,809			HR relative to metformin users	Currie et al (2009)
			Sulphonylureas	Breast Colorectal Pancreas	HR 0.98 (0.69-1.41) HR 1.80 (1.29-2.53) HR 4.95 (2.74-8.96)	
			Metformin & Sulphonylureas	Prostate Breast Colorectal Pancreas Prostate	HR 1.07 (0.76-1.49) HR 0.90 (0.67-1.21) HR1.43 (1.05-1.94) HR 0.38 (0.13-1.12) HR 1.18 (0.89-1.57)	
			Insulin	Breast Colorectal Pancreas Prostate	HR 1.07 (0.79-1.44) HR 1.69 (1.23-2.33) HR 4.63 (2.64-8.10) HR 1.10 (0.79-1.52)	
Prospective cohort	Mortality	1,353	Any vs no metformin	Multiple	HR 1.47 (1.22-1.76)	Landman et al (2010)
Case control	Incidence	973	Insulin Insulin secretalogues Thiazolidinediones Metformin	Pancreas	OR 5.04 (2.38-10.7) OR 1.74 (0.80-3.77) OR 1.65 (0.71-3.87) OR 0.41 (0.19-0.87)	Li et al (2009)
Case control	Incidence	1,001	Any vs no metformin	Prostate	OR 0.56 (0.32-1.00)	Wright & Stanford et al (2009)
Case control	Incidence	1,573	Insulin or SU Metformin	Liver	OR 2.99 (1.34-6.65) OR 0.33 (0.1-0.7)	Donadon et al (2009)
Case control	Incidence	1,524	Biguanides Thiazolidinediones Sulphonylureas Insulin	Liver	OR 0.3 (0.2-0.6) OR 0.3 (0.1-0.7) OR 7.1 (2.9-16.9) OR 1.9 (0.8-4.6)	Hassan et al (2010)
Case control	Incidence	305	Any vs no metformin	Breast	OR 0.44 (0.24-0.82)	Bodmer et al (2010)
Prospective cohort	Incidence	480,984	Any vs no metformin	Colorectal Liver Pancreas Overall	HR 0.36 (0.13-0.98) HR 0.06 (0.02-0.16) HR 0.15 (0.03-0.79) HR (0.12 (0.08-0.19)	Lee et al (2011)
Retrospective cohort	Mortality	595	Any vs no metformin	Colorectal	HR 1.45 (1.08-1.93)	Lee et al (2012)
Retrospective cohort	Mortality	3,685	Metformin Insulin	Multiple	HR 0.56 (0.34-0.94) HR 1.56 (1.22-1.99)	Bo et al (2012)
Case control	Incidence	10,781	Metformin Sulphonylureas Insulin	Ovarian	OR 0.61 (0.30-1.25) OR 1.26 (0.65-2.44) OR 2.29 (1.13-4.65)	Bodmer et al (2011)
Nested case control	Incidence	8,098	Any vs no metformin	Prostate	RR 1.23 (0.99-1.52)	Azoulay et al (2011)
Case control	Incidence	4,323	Any vs no metformin	Breast	OR 0.81 (0.63-0.96)	Bosco et al (2011)
Case control	Incidence	1,340	Metformin Sulphonylureas	Multiple	OR 0.46 (0.25-0.85) OR 0.75 (0.39-1.45)	Monami et al (2011)

Table 1.2. Epidemiological studies to date examining the link between metformin and cancer incidence. HR, Hazard Ratio; RR, Relative Risk; OR, Odds Ratio. Used from Dowling et al [40].

Besides these epidemiological studies examining for differences in cancer incidence several retrospective clinical studies have been carried out investigating for potential links between metformin treatment and outcome in cancer patients. The first such study to be published looked at whether patients with breast cancer receiving neoadjuvant chemotherapy, who were taking metformin in the context of type 2 diabetes, had a greater rate of pathological complete response (pCR), an excellent marker of longterm outcome. For those diabetic patients taking metformin the pCR rate was 24% (95% CI, 13-34) compared to 8% (95% CI, 2.3-14) for those not ($p = 0.007$). The improved pCR rate was confirmed on multivariate analysis after adjustment for known independent risk factors and compared favorably with the 16% pCR rate seen in non-diabetic patients treated in the same centre and over the same time period [41]. However, another retrospective study of women that had undergone adjuvant chemotherapy for breast cancer did not demonstrate any survival benefit for metformin, although diabetic metformin treated patients in general were slightly less likely to subsequently develop distant metastases [42].

Other cancer sites have been studied too. Garrett et al showed that in a cohort of 424 type 2 diabetic patients taking metformin that were undergoing treatment for colorectal cancer the median overall survival in the metformin cohort was 76.9 months (95% CI, 61.4–102.4) compared to 56.9 months (95% CI, 44.8–68.8) for those patients not taking metformin ($p = 0.048$) [43]. A case control study of diabetic patients and lung cancer risk reported that, although metformin seemed to reduce the risk of developing lung cancer, diabetic lung cancer patients on metformin alone had a higher risk of metastatic disease at diagnosis and shorter survival (HR, 1.47; 95% CI, 1.12 – 1.92, $p = 0.005$) when compared to their insulin or thiazolidinedione

treated counterparts [44]. One retrospective study examined the effects of metformin in diabetic patients with advanced non small cell lung cancer undergoing palliative chemotherapy concluding that, when compared with other oral hypoglycaemic drugs or insulin, those patients on metformin fared better (overall survival 8.4 months vs 4.7 months vs 6.4 months, respectively; $p = 0.007$). However, there were no significant differences in the chemotherapy response rate [45]. Data from prospective studies of metformin's effects in cancer is also starting to emerge and this is discussed in detail in *section 1.5.2.*

1.2.2: IN VITRO AND IN VIVO STUDIES OF METFORMIN'S ANTICANCER EFFECT

Early preclinical studies showed that metformin can inhibit the growth of breast cancer cell lines and colony formation and that this does not seem to be dependent on oestrogen receptor or HER2 status [46, 47]. In vitro, Metformin has been shown to induce dose dependent cell cycle arrest at the G1 checkpoint and in some breast cancer cell lines has also been shown to induce apoptosis [46, 48, 49]. In vivo several xenograft studies have shown that metformin can inhibit the tumour growth and engraftment of breast cancer cell lines [50, 51] and other tumour types, including renal, colon, pancreatic and hepatocellular cancer [52-55].

More recent studies have suggested that there is a differential response to metformin between different breast cancer subtypes. Liu et al suggested that triple negative breast cancer cell lines had unique responses to metformin with partial S phase arrest and increased apoptosis. However, these observations were made using a very high concentration of metformin (30mM) (please see section 1.3.4 for discussion for

difference in metformin concentration in preclinical models and that seen in clinical samples) [49]. Another in vitro study provided evidence that cell growth inhibition and apoptosis induced by metformin in triple negative breast cancer cell lines was mediated by inhibition of the transcription factor, signal transducer and activator of transcription 3 (STAT3). However, again high concentrations were necessary to demonstrate this effect [56]. Vazquez-Martin et al suggested that metformin may have specific anti HER2 effects, showing that metformin suppresses HER2 overexpression and that this effect was probably secondary to mTOR inhibition [57]. A panel of HER2 positive breast cancer cell lines with induced HER2 resistance has been shown to be especially sensitive to metformin, in fact more so than a panel of trastuzumab sensitive cell lines [58]. Similar anticancer effects have been seen in other cancer cell types including prostate, glioma, ovarian and endometrial cancer cell lines [48, 52, 59-62].

There is growing evidence of synergy between metformin and established cancer therapies. In mouse xenograft models the combination of doxorubicin and metformin seems to be especially effective over either treatment alone. There is also intriguing evidence that metformin selectively kills breast cancer stem cells in 4 'genetically different' breast cancer cell lines. This was in contrast to the anthracycline chemotherapy drug, doxorubicin, which in vitro kills breast cancer cells but not 'resistant' cancer stem cells (as defined by the putative stem cell marker $CD44^{high}/CD24^{low}$) [63]. A further study showed that no $CD44^{high}/CD24^{low}$ cells could be isolated from xenografts treated with metformin [63]. Other in vivo work has shown that metformin has synergy, not just with anthracyclines, but a variety of chemotherapy agents [51]. Similarly, metformin has also been shown, in prostate

cancer cell lines, to have synergy with the antiandrogen bicalutamide, in vitro and in vivo [64]. In breast adipose stromal cells, aromatase, an enzyme responsible for a key step in the biosynthesis of oestrogens, has been shown to be down regulated at low concentrations of metformin in an AMPK dependent manner [65] and there is some evidence of synergy with the anti-oestrogen, tamoxifen, in the oestrogen receptor positive breast cancer cell line, MCF7 [66]. The potential of metformin to act as a radiosensitiser has also been investigated. Substantial synergy with radiotherapy has been shown in vitro and in vivo and achieved at clinically achievable doses [67, 68].

1.2.3: METFORMIN AND CANCER PREVENTION

On the back of the epidemiological data in diabetics demonstrating a preventative role for metformin against cancer, the effect of metformin in several models of tumorigenesis has been investigated. A mouse model of lung carcinogenesis using the agent 4-(methylnitrosamino)-1-(3-pyridyl)-1-butanone (NNK) showed that oral metformin reduced tumour burden but that intraperitoneal administration (with associated higher plasma levels of metformin) was even more effective [69]. Anisimov et al showed that metformin treatment of transgenic HER2/neu mice had a significant reduction in the incidence, time to development and size of mammary adenocarcinomas [70]. For mice heterozygous for the tumour suppressor, phosphatase and tensin homologue deleted on chromosome 10 (PTEN), metformin delayed tumour onset [71]. A study of a cohort of mice treated with metformin from young or ‘middle age’ demonstrated both increased lifespan and reduced tumour incidence (by 22 and 25%, respectively) [72]. A small clinical study from Japan reported that metformin had a chemopreventative effect on the formation of aberrant crypt foci (considered a marker of colorectal cancer risk) and reduced colonic epithelial proliferation [73].

1.2.4: OBESITY, DIABETES AND BREAST CANCER

Weight gain and obesity has been estimated in the US population to have caused approximately 20% of cancers over the past 25 years [74]. This may in fact be an underestimate given that the overall population has had significant weight gain over this time period with the prevalence of obesity in the US having increased from 15% to 30% between 1980 and 2000 [75]. A meta-analysis of European obesity studies suggested that in the European population obesity accounted for 9% of breast cancers, 11% of colon cancers, 39% of endometrial cancers, 37% of oesophageal cancers and 25% of kidney cancers [76]. Obesity has also been implicated in increased risk of cancer related mortality of 52% for men and 62% for women [74]. There may be a link between obesity and breast cancer subtype. Two studies have suggested that obese premenopausal women are more likely to develop triple negative breast cancer [77, 78]. Over the past 30 years there has also been an increase in the incidence of Type 2 diabetes presumed to be secondary to this population weight gain [79]. Type 2 diabetes has similarly been linked to increased cancer risk [80]. A meta-analysis of several studies suggested that the greatest risk was for cancers of the liver, pancreas and endometrium (2-fold) but that to a lesser extent the incidence of breast cancer also increases in diabetes (1.2 fold) [81, 82].

Increased insulin-like growth factor-1 (IGF-1) and insulin signaling, oestradiol production, circulating inflammatory cytokines, hypoxia and the effects of adipocyte stem cells have all been suggested as causes for the increased incidence and poorer prognosis of cancer in obese individuals [83, 84]. For postmenopausal women the predominant source of aromatase-mediated oestrogen is adipose tissue. Circulating

oestradiol levels in obese postmenopausal women are increased and this is directly proportional both to weight and breast cancer risk. Indeed, if breast cancer risk is adjusted for levels of circulating oestradiol this relationship is lost [85-87]. Metformin has been shown to downregulate aromatase expression in an AMPK dependent manner and it has been proposed that this may contribute to its anticancer effect in breast cancer [65].

However, it is the effects of obesity on the insulin axis that most strongly link diabetes and obesity cancer risk. Circulating levels of insulin and free IGF-1 have been shown to be higher in obese individuals [88]. Binding of insulin to the insulin receptor results in multiple pro-tumorigenic downstream effects in particular activation of the PI3K/AKT/mTOR and mitogen-activated protein kinase (MAPK) pathways [89]. Tumour cells have been shown to commonly express the IGF-1 receptor and its stimulation has also been linked to tumorigenesis [90]. Similarly, the insulin receptor is often more highly expressed in breast cancer cells [91, 92]. Higher fasting insulin levels have been correlated with increased BMI and in turn poor prognosis in breast cancer patients [93]. Similarly increased expression of the IGF-1 gene signature has been shown to be a poor prognostic marker in breast cancer [94]. Analysis of gene expression in 103 breast cancer tumour samples from obese patients identified a signature that correlated with known IGF-1 signaling pathways [95]. In the liver, metformin's activation of AMPK acts to inhibit gluconeogenesis, hence decreasing circulating glucose and insulin levels and also inhibiting the IGF-1 axis. In vivo models have shown that caloric restriction can reduce tumour growth and so the reduction in circulating glucose may also be important in its anticancer effect [96, 97].

1.3: PROPOSED MECHANISMS OF ACTION OF METFORMIN IN CANCER

1.3.1: DIRECT VERSUS INDIRECT THEORY OF EFFECT

Despite intense investigation it is still not clear as to whether it is direct effect on cancer cells or rather an indirect modulation of the insulin axis that drives metformin's anticancer effect (**Figure 1.2**).

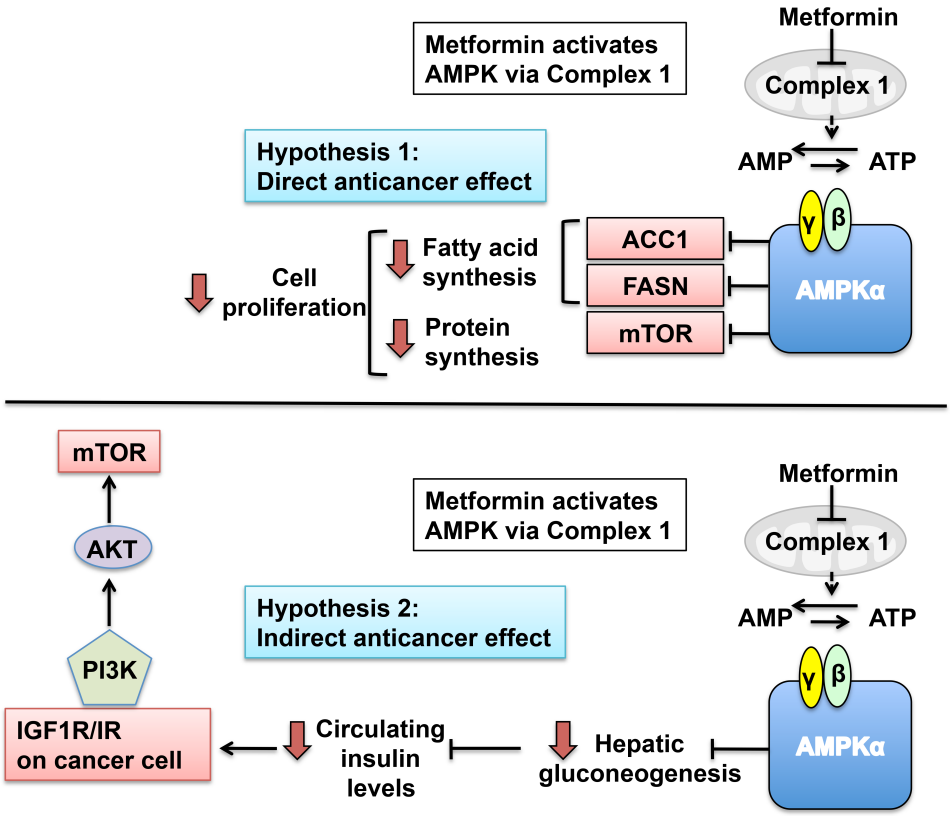


Fig 1.2: There are 2 hypotheses as to the mechanism behind metformin's anti-cancer effect. **Upper panel.** The direct effect in which metformin generates an energy stress in tumour cells via its inhibition of complex 1 and subsequent activation of AMPK leads to catabolic downstream effects and inhibition of cancer cell proliferation. **Lower panel.** The indirect effect in which AMPK activation in the liver results in reduced circulating insulin levels and subsequent inhibition of the IGF1/PI3K axis in tumour cells. ACC1, Acetyl CoA Carboxylase 1; FAS, Fatty acid synthase; IGF1, Insulin growth factor 1; IR, Insulin receptor.

1.3.1.1 DIRECT EFFECT

One school of thought is that metformin causes an energy stress secondary to complex 1 toxicity, directly in the cancer cell itself, resulting in activation of 5' adenosine monophosphate-activated protein kinase or AMPK, a serine/threonine kinase that is a key regulator of energy homeostasis in the cell. The subsequent downstream catabolic effects would be expected to be anticancer in nature (see *sections 1.3.2 and 1.3.3* for a detailed description of the mechanism and sequelae of AMPK activation and Complex 1 inhibition). In vitro studies of breast cancer cell lines have shown that the antiproliferative effects of metformin can be dependent on activation of AMPK [48, 98] and that the downstream target of AMPK, mammalian target of rapamycin (mTOR), can be inhibited by metformin [48, 59]. The inhibitory effect on mTOR has been implicated in metformin's suppression of cell growth [59] and Zhuang et al showed that cell cycle arrest is associated with the downregulation of the mTOR dependent cell cycle regulator, cyclin D1, resulting in the release of the cyclin-dependent kinases (CDKs), $p27^{Kip1}$ and $p21^{Cip1}$ [47]. Besides mTOR, another known target of AMPK, p53, has been implicated in metformin's anticancer effect. In mouse embryonic fibroblasts (MEFs) AMPK activation has been shown to phosphorylate p53 resulting in cell cycle arrest [99]. Buzzai et al showed that wild-type p53 colon cancer cells were resistant to metformin whilst p53-null cells were sensitive with the p53 deficient cells unable to adapt under energy stress conditions (in particular to upregulate glycolysis) [52]. Some investigators have also presented evidence that metformin can have direct effects on cells in the absence of AMPK activation that might be relevant to its anticancer effect. Kalender et al demonstrated that in MEFs, null for TSC2 or the α1 and α2 AMPK subunits, metformin could still activate mTOR

in a rag GTPase-dependent manner [100]. In rat hepatocytes metformin has been shown to inhibit hepatic gluconeogenesis in an AMPK independent manner [101].

1.3.1.2: INDIRECT EFFECT

Alternatively, it is postulated that metformin may exert an indirect anticancer effect by influencing the insulin axis. To date all the clinical data suggestive of metformin having an anticancer effect has been collected from diabetic patients that will have an abnormal metabolic state and it is known that obesity and type 2 diabetes are associated with cancer risk [89]. Insulin receptor (IR) and insulin growth factor-1 (IGF-1) signaling is upstream of the PI3K/AKT/mTOR signaling network and upregulated insulin and insulin-like growth factor-1 signaling may promote tumour growth [89]. AMPK activation by metformin in the liver will inhibit hepatic gluconeogenesis reducing serum glucose levels and subsequently circulating insulin. This effect would be likely to be especially prominent in obese metformin treated or diabetic individuals. An in vivo study using a triple negative breast cancer xenograft model fed a high energy diet suggested greater inhibitory effects on tumour growth by metformin in mice fed a high energy diet when compared to a standard diet [102]. Another in vivo study showed that metformin inhibited tumor growth and reduced insulin receptor activation in tumors of mice with diet-induced hyperinsulinemia in the absence of tumour LKB1 expression. However, in the absence of hyperinsulinaemia, LKB1 was required for antineoplastic activity [103]. As discussed below (see *section 1.3.2*), LKB1 is an upstream AMPK activator and cells lacking LKB1 have been shown to display reduced AMPK signaling [104]. One prospective clinical study has already linked, in breast cancers, a decrease in the proliferation

marker, Ki67, with a raised homeostasis model assessment (HOMA), a measure of insulin resistance (also see *section 1.5.2*) [105].

1.3.2: AMPK ACTIVATION

For some time the overall consensus has been that the anticancer effects of metformin are most likely driven via its activation of AMPK. This energy sensing/signaling protein is the control point for maintaining energy homeostasis in the cell and is activated under conditions of energy stress (**Figure 1.3**).

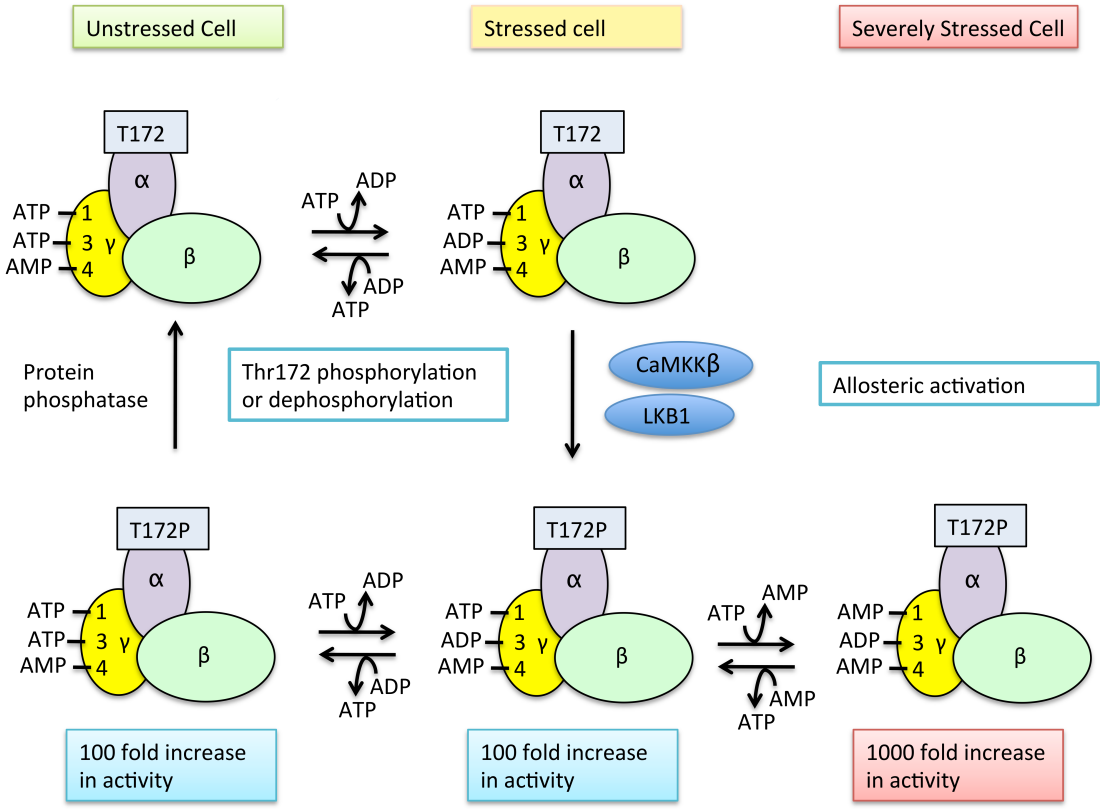


Fig 1.3: Activation of AMPK. The LKB1 complex is important in providing a high level of basal phosphorylation at Thr172 that can then be modulated by the binding of ADP, AMP or ATP to the γ-subunits. There are two key binding sites for these nucleosides: a) site 1 at which AMP may bind at times of severe stress leading to allosteric activation of AMPK and b) site 3 at which binding of ADP or AMP at times of moderate stress promotes phosphorylation of Thr172. Site 4 is consistently bound to AMP. Adapted from *Hardie et al, Nature Rev Mol Cell Biol, 2012;13(4):251-62*

Although all the minutiae of AMPK's regulation and activation are not fully understood it is now clear that upstream kinases (in particular the tumour suppressor LKB1) and the ratios of AMP/ATP and ADP/ATP all play a role in its activation via phosphorylation at the Thr172 residue. In this system the upstream LKB1 complex is important in providing a high level of basal phosphorylation at Thr172 that can then be modulated by the binding of ADP, AMP or ATP to the γ-subunits. There seem to be two key binding sites for these nucleosides: a) site 3 at which binding of ADP or AMP 'protects' against dephosphorylation at Thr172 and b) site 1 at which AMP may bind leading to allosteric activation of AMPK. Site 4 seems to be consistently bound to AMP [106]. A view gaining credence is that under normal conditions or those of moderate energy stress ADP plays a greater role in maintaining activation of AMPK given that its concentration in cells is generally greater than AMPK and that the affinity of ADP and AMP to their binding sites are similar. However amplification of AMPK activity by allosteric binding of AMP occurs under more extreme energy stress [107]. Alternatively phosphorylation of AMPK can be driven by greater calcium-calmodulin-dependent protein kinase (CAMMK) activity dependent on increased intracellular calcium. Activation can occur under these circumstances without changes in the ADP/AMP/ATP ratio [108].

In its activated, phosphorylated, state AMPK has a profound effect on cellular metabolism, increasing cellular ATP by inhibiting anabolic energy consuming pathways and activating ATP producing, catabolic pathways [109, 110]. Many of the downstream metabolic pathways of AMPK are known to be dysregulated in many cancer cells and are already important drug targets in their own right (**Figure 1.4**). For

example activation of AMPK inhibits the biosynthesis of proteins by downregulating the mammalian target of rapamycin (mTOR) signaling pathway through its inhibition of the key mTOR regulators TSC2 and RAPTOR [111]. Besides protein biosynthesis mTOR also phosphorylates RRN3 a transcription factor for RNA polymerase 1 resulting in the inhibition of ribosomal RNA synthesis [112]. AMPK's activation is associated with the inhibition of fatty acid and cholesterol synthesis and activation of fatty acid uptake and fatty acid β-oxidation. It has been shown to activate the tumour suppressor gene, p53, probably via phosphorylation of its ser-15 residue. p53 has many anticancer mechanisms, and plays a role in apoptosis, genetic stability, and the inhibition of angiogenesis [113]. AMPK activation also plays a key role in the

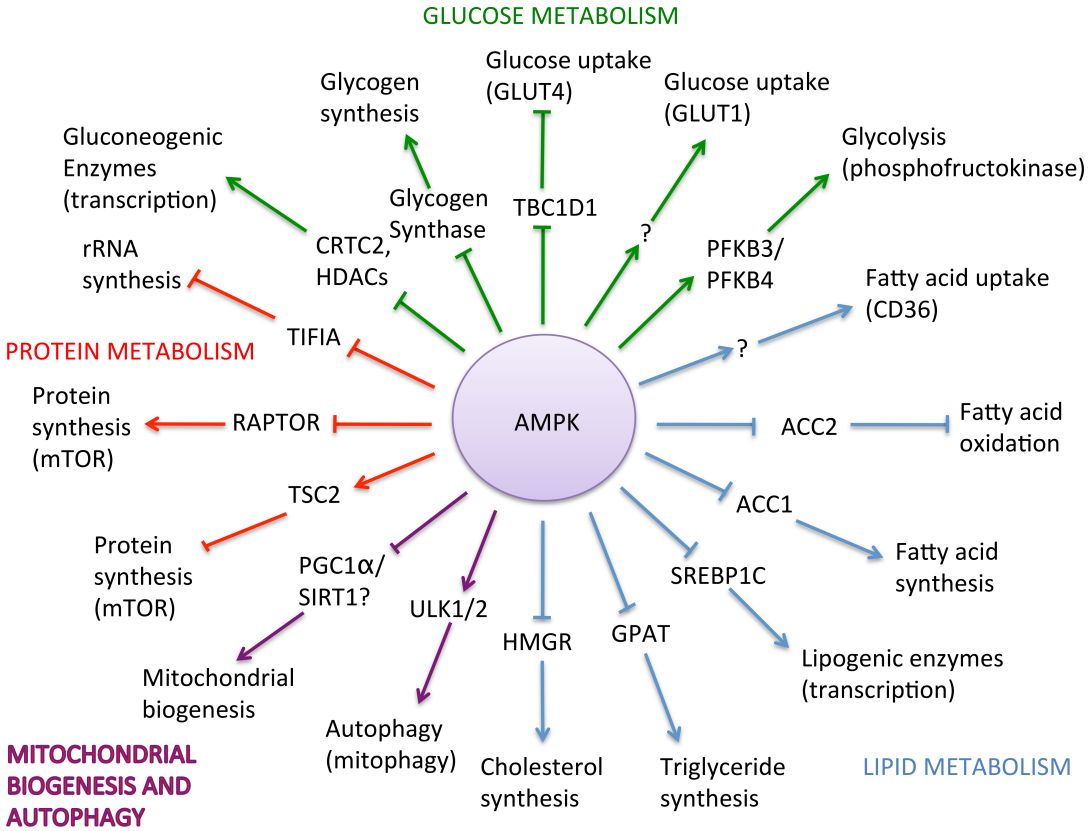


Figure 1.4: Key pathways regulated by AMPK. Adapted from *Hardie et al, Nature Rev Mol Cell Biol, 2012;13(4):251-62*

regulation of glucose metabolism including the stimulation of increased glucose uptake in contracting muscle, mediated via translocation of the GLUT4 receptor to the plasma membrane, and in liver and adipose cells mediated via activation of GLUT1 [114, 115]. It stimulates glycolysis via the indirect activation of the glycolytic enzyme 6-phosphofructo-1-kinase [116, 117]. Consistent with its catabolic nature both of the gluconeogenic enzymes phosphoenolpyruvate carboxykinase and glucose-6-phosphatase have been demonstrated to be downregulated after AMPK activation [118, 119].

The role of altered AMPK signaling in tumorigenesis has become of increasing interest since the discovery of metformin's anticancer effects. One histological study suggested that phosphorylation of AMPK is lower in breast cancer tissue when compared to normal breast epithelium and that reduced expression was significantly associated with higher histological grade and axillary node metastasis in breast cancer [120]. However, another study of AMPK activation in 718 cases of colorectal cancer did not demonstrate a correlation with improved survival [121].

1.3.3: INHIBITION OF MITOCHONDRIAL COMPLEX 1

The activation of AMPK by metformin is not understood to be due to a direct interaction between metformin and AMPK. Indeed, metformin does not stimulate AMPK activity or phosphorylation of AMPK by LKB1 in cell-free assays [122]. Rather, it is attributed to an increase in the ADP or AMP to ATP ratio resulting from inhibition of complex 1 of the electron transport chain (ETC) in the mitochondria. The inhibitory effect of metformin on complex 1 was described in a series of studies that showed that metformin treatment of rat hepatocytes led to the accumulation of

certain TCA cycle intermediates [122-124]. Consistent with the complex 1 theory, clinical studies using indirect calorimetry techniques have suggested some inhibition of fatty acid β-oxidation consistent with complex 1 and mitochondrial poisoning [125]. However, in contrast to these relatively 'crude' observations, studies of metformin's effects on cultured rat hepatocytes have either demonstrated either an increase in fatty acid β-oxidation (AMPK dependent) or no effect [32, 33, 126].

Mitochondrial complex 1 is a large membrane bound protein consisting of a hydrophobic unit anchored to the inner mitochondrial membrane and a hydrophilic arm protruding into the mitochondrial matrix (**Figure 1.5**). Its function is to accept electrons from NADH before donating them to Coenzyme Q for further shuttling down the ETC. Along with other members of the ETC the energy released by electron transfer facilitates the pumping of protons across the inner mitochondrial membrane to create an electrochemical gradient that allows ATP synthase to catalyse the conversion of ADP to ATP. The regulation of its catalytic activity is complex and still not fully understood but seems to be governed by a combination of the amount of functional Complex 1 protein, post translational modification via its phosphorylation or acetylation, its binding to proteins or lipids and the availability of substrate i.e. NADH. Complex 1 is also considered to be a major source of Reactive Oxygen Species (ROS) and ROS may also influence its catalytic function [127].

One study suggested that Complex 1 was not inhibited when isolated mitochondria are treated with metformin as opposed to intact cells. On the basis of this it was proposed that metformin may in fact act on mitochondria via some unidentified

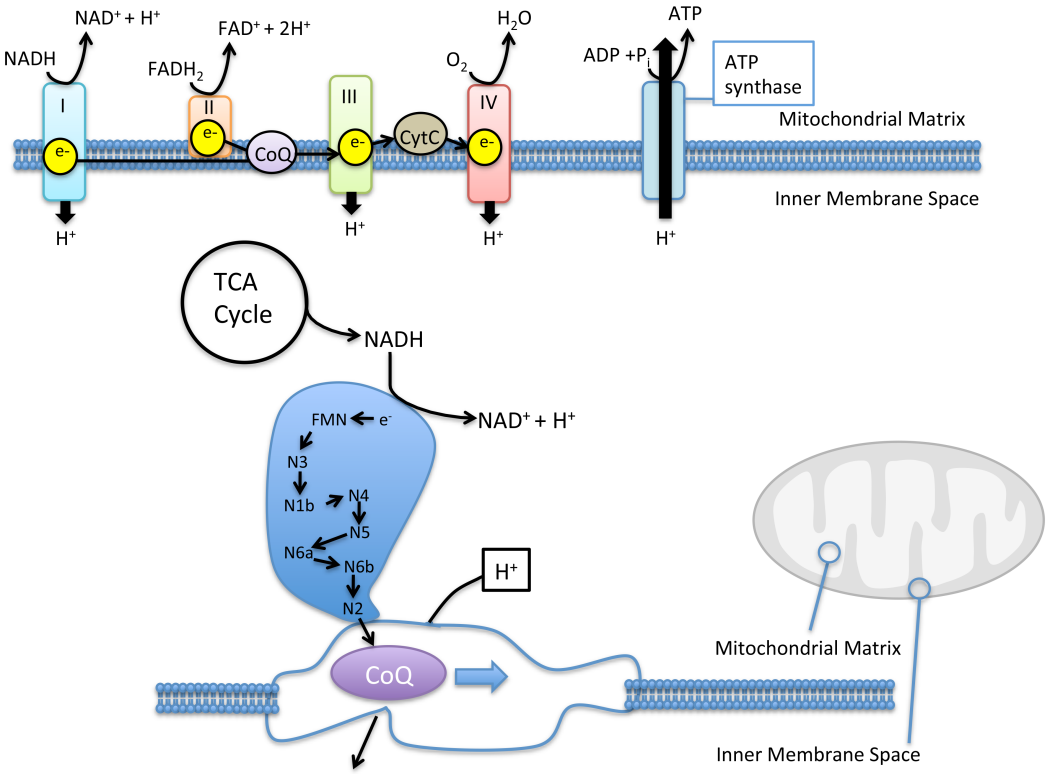


Fig 1.5: Complex 1 structure and function

Lower panel. Mammalian Complex 1 is an L-shaped protein with a hydrophobic domain anchored within the mitochondrial inner membrane and hydrophilic domain protruding into the mitochondrial matrix. Flavin mononucleotide (FMN) accepts electrons from NADH before transfer through 7 iron-sulphur clusters (N3, N1b, N4, N5, N6a, N6b and N2) to the electron carrier Coenzyme Q (CoQ). ***Upper panel.*** Coenzyme Q then shuttles electrons to the other members of the electron transport chain. The energy released by electron transfer facilitates the pumping of protons across the mitochondrial inner membrane creating an electrochemical gradient that facilitates the conversion of ADP to ATP synthase. Adapted from: *Koopman et al, Antioxid Redox Signal, 2010; 12(12):1431-70.*

cellular signaling pathway [124]. However, data from another group investigating metformin treatment of isolated mitochondria and small mitochondrial particles repudiated this finding [123]. Some leading investigators speculate that as the electron transport chain contains several large multiprotein complexes there would be many potential binding sites for drugs such as metformin and that the positive charge of the metformin molecule could lead to an accumulation of the drug in mitochondria [107, 128]. Although there is no clear data to show that metformin binds directly to complex 1 components recent work has suggested that interaction with copper ions may be crucial to its mitochondrial effect [129].

It has long been known that metformin increases mitochondrial mass in mammalian cells. This may be due to activation of AMPK (mitochondrial biogenesis being a known sequelae) or it has been proposed that oxidative stress resistance mechanisms subsequent to metformin induced reactive oxygen species lead to the upregulation of peroxisomal proliferation-activated receptor-α which is known to increase mitochondrial mass [130]. Recent in vitro studies have shown that metformin treatment can change mitochondrial morphology and that these changes may correlate with sensitivity [98].

1.3.4: LIMITATIONS OF PRECLINICAL MODELS

There is now a wealth of evidence from preclinical models to show that metformin has an anticancer effect. However, it is difficult to know whether this in vitro and in vivo data is relevant to the clinical setting. To date, all the epidemiological and retrospective clinical data suggestive of a clinical benefit has been derived from studies of diabetic patients. The complex effects of metformin on liver

gluconeogenesis and the insulin axis are impossible to model in the in vitro setting. In order to generate the antineoplastic effects in cell lines discussed above the doses of metformin used in vitro (typically 2 to 50 mM) have tended to be many times higher than that seen at therapeutic plasma level (2.8 to 15 μM) [131]. Where serum metformin levels have been measured for in vivo xenograft studies the levels have been between 2 - 45 times that of peak plasma level in humans but typically less than that used in vitro [131]. However, some studies in vivo have demonstrated antineoplastic effect with dosing comparable to therapeutic levels achieved in humans [60, 70]. Most in vitro studies of metformin have used culture media supplemented with glucose of between 10 and 25 mM and this is significantly greater than the plasma level seen in non-diabetic patients (typically 4-7 mM). Indeed within tumours themselves the glucose level is probably much less than this. A mass spectrometry study of metabolites in stomach and colon cancer tissue estimated the glucose concentration to be 13 times and 45 times less, respectively, than that of plasma [132]. However, these very low concentrations are very difficult to model in a closed in vitro system. Most media is supplemented with foetal calf serum (FCS) at concentrations of 5-10% and this will typically contain high amounts of insulin and growth factors. The in vitro combination of high glucose concentrations and FCS may be highly protective against the energy stress induced by metformin. Glucose withdrawal has been shown to cause massive apoptosis in some metformin treated breast cancer cell lines [133].

1.4: CANCER METABOLISM

1.4.1: OVERVIEW

Although cancer cells display a diverse aetiology and phenotype, certain features of their metabolism share common attributes that are peculiar to malignancy. It is now clear that this dysregulation of protein synthesis, lipogenesis and energy metabolism is vital for cancer cell survival and proliferation and over the past decade interest has grown exponentially in the potential to harness the altered metabolic pathways of the cancer cell for therapeutic value. Indeed, recognition of the importance of the reprogramming of energy metabolism in cancer cells led to this recently being designated an 'emerging hallmark of cancer' [134].

1.4.2: THE WARBURG EFFECT: GLUCOSE METABOLISM IN CANCER CELLS

In the 1920's Otto Warburg first noted that there was an alteration in the metabolism of cancer cells when he observed that an increase in glycolysis was maintained in conditions of high oxygen tension, leading to a rise in lactate production [135]. This is characterised by an increase in glucose uptake and consumption which for several years now has been exploited for clinical benefit in cancer imaging in the use of the positron emission tomography (PET) tracer, (18F)-fluoro-2-deoxy-D-glucose (FDG). Compared to oxidative phosphorylation, aerobic glycolysis is an energetically wasteful process (36 ATP molecules produced compared to 2 ATP for each glucose molecule). However, current consensus is that this increased rate of glycolysis acts as a source of glucose carbons for the synthesis of fatty acids, nucleotides and amino acids that are vital as building blocks for the proliferating cancer cell [136].

How cancer cells control the rate of glycolysis and direct the utilisation of the substrates produced is currently an area of great interest. The production of pyruvate provides the link between glycolysis and the TCA cycle and the synthesis of other metabolic intermediates. Under hypoxic conditions pyruvate is predominantly metabolised to lactate by lactate dehydrogenase but in normoxia is directed toward acetyl-CoA by pyruvate dehydrogenase (PDH), the first step in the TCA cycle [137]. PDH activity is regulated by two enzymes; inactivating pyruvate dehydrogenase kinase (PDK), which phosphorylates PDH and pyruvate dehydrogenase phosphatase, which dephosphorylates PDH to the active form [138]. Under hypoxic conditions the upregulation of PDK activity reduces pyruvate conversion to acetyl CoA and together with the increase in LDH-A diverts pyruvate into lactate prior to export from the cell by the monocarboxylate transporter MCT4 [139]. However, pyruvate under normoxic conditions may also be directed toward the mitochondria where it is used to generate ATP via oxidative phosphorylation or fed into synthesis pathways for fatty acids or amino acids (**Figure 1.6**) Pyruvate kinase converts phosphoenolpyruvate to pyruvate, the final rate-limiting reaction of glycolysis, and hence is also a key oncogenic control point for this pathway. There are 4 isoforms of pyruvate kinase (PK), PKL, PKR, PKM1 and PKM2, but the last is of particular interest as it is the predominant PK in proliferating cells and cancer cells. PKM2 exists as both dimer and tetramer that possess low and high levels of pyruvate kinase activity, respectively. Reduced PK activity results in the accumulation of upstream metabolites including 3-phosphoglycerate, shunted into serine synthesis, and phosphoenolpyruvate and glucose-6-phosphate, shunted into the pentose phosphate pathway. Hence there is a diversion of carbons toward macromolecular synthesis [140]. There is now good

evidence that PKM2's glycolytic activity is regulated by oncogenes and tumour suppressors [141, 142] and it has become a potential drug target in its own right.

As an inhibitor of oxidative phosphorylation and activator of AMPK, metformin might be expected to modulate the glycolytic rate and indeed in vitro studies have already shown that metformin treated cancer cell lines upregulate glycolysis with a subsequent increase in lactate production, glucose consumption and glucose uptake [52, 143]. Metformin induces an increase in the expression of the glucose transporter, GLUT-1, in cancer cell lines [144]. Inhibition of hexokinase, the enzyme that catalyses the first step of glycolysis, by 2-deoxyglucose (2DG), had a marked anticancer synergy with metformin in vitro and in xenograft models [145, 146].

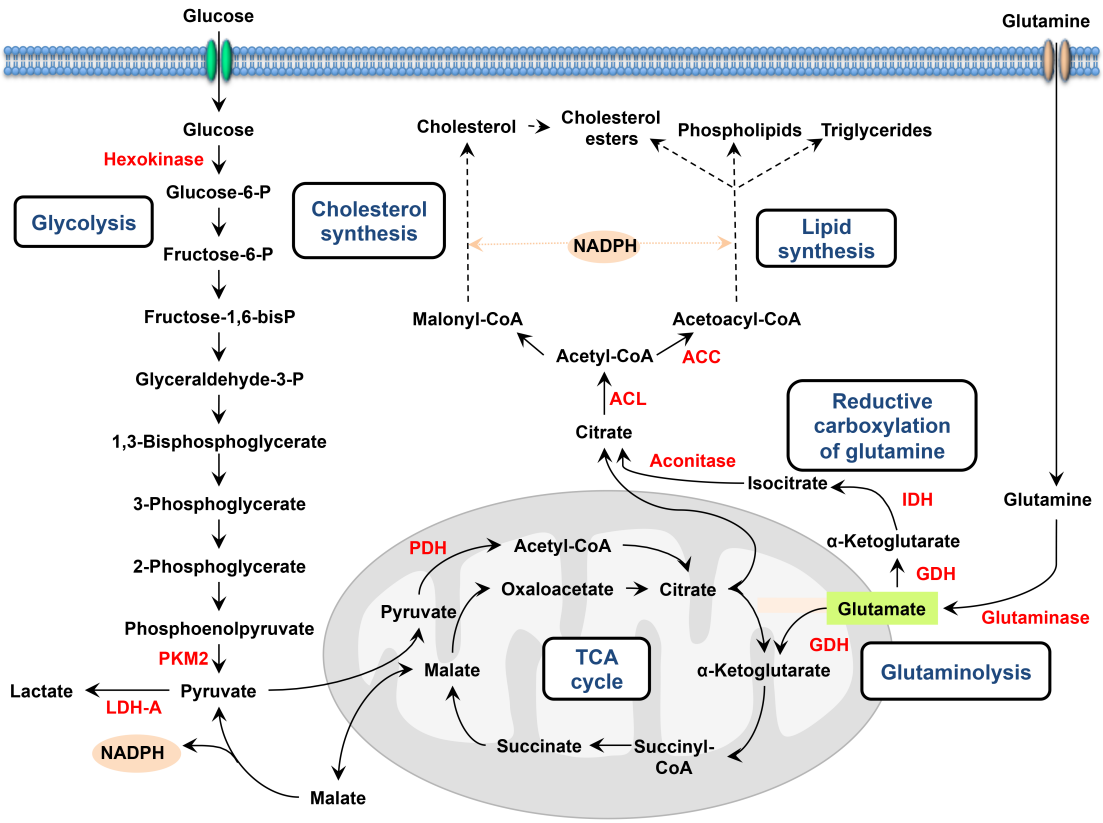


Fig 1.6: Predominant fates of glucose and glutamine in cancer cells. Glucose is converted to pyruvate via the glycolysis pathway. Pyruvate may then be converted to lactate by LDH-A or be taken up by the mitochondria for oxidative phosphorylation. Citrate from the TCA cycle may then be used as a precursor molecule for lipid synthesis. Glutamine may also feed into the TCA cycle via glutaminolysis or alternatively at times of hypoxia or mitochondrial stress be diverted away via the reductive carboxylation pathway toward citrate. ACC, Acetyl CoA Carboxylase; ACL, Acetyl Citrate Lyase; GDH, Glutamate Dehydrogenase; IDH, Isocitrate Dehydrogenase; LDH-A, Lactate Dehydrogenase-A; PDH pyruvate dehydrogenase; PKM2 Pyruvate kinase M2.

1.4.3: GLUTAMINE METABOLISM IN CANCER

Although it was first observed in the 1950's that cancer cells in culture are avid consumers of glutamine [147] it is only recently that the importance of this phenomenon has been revisited by cancer researchers. Glutamine is the most abundant amino acid in plasma [148] and is an important source of both nitrogen and carbon to the proliferating cell. Glutamine acts as a source of both amino and amido nitrogens in the synthesis of nucleotides, hexosamines and proteins. Hexosamines are amino sugars involved in protein posttranslational modification and are important in propagating cell growth signaling [149]. After loss of its amino and amido groups via glutaminolysis, the carbon skeleton of glutamine can also be fed into the tricarboxylic acid (TCA) cycle to generate ATP or alternatively its carbons may be directed toward macromolecular synthesis (**Figure 1.6**). This ability to feed glutamine carbons into the TCA cycle facilitates cell growth by maintaining anapleurosis as carbons are removed to supply biosynthetic pathways such as fatty acid synthesis. Recent work has highlighted the importance of glutamine as a carbon source for maintaining proliferation in cancer cells under conditions of mitochondrial interference or hypoxia. In particular, the reductive carboxylation pathway allows glutamine carbons to avoid the TCA cycle and still be fed into fatty acid synthesis [150, 151]. A key checkpoint in the glutaminolysis pathway is the deamidation of glutamine to glutamate catalysed by the enzyme glutaminase. Glutaminase is highly expressed in cancer and its activity has been shown to be important in maintaining tumour growth rates [152, 153]. The possibility of targeting the glutaminolysis pathway for therapeutic value has been investigated and an allosteric inhibitor of glutaminase, Bis-2-(5-phenylacetamido-1,3,4-thiadiazol-2-yl)ethyl sulfide (BPTES), has been shown to inhibit the growth of glioma and astrocytoma cells with mutant isocitrate

dehydrogenase-1, a key enzyme in the reductive carboxylation pathway [154]. Oncogenic signaling pathways have been shown to play an important role in regulating glutamine metabolism. It is now clear that besides its importance in regulating virtually all the glycolytic enzymes [155], the oncogenic transcription factor, Myc, also plays an important role in enhancing glutamine metabolism. Glutamine withdrawal has been shown to be more potent in triggering cell death in Myc transformed cells [156] and Myc has been shown to upregulate expression of glutaminase [152].

1.4.4: CANCER LIPID METABOLISM

1.4.4.1: OVERVIEW

The altered metabolism of cancer cells is predominantly directed toward enabling the production of metabolic intermediates that can be used to provide the precursors for cell growth and lipid metabolism (**Figure 1.7**). In normal cells fatty acid synthesis from carbohydrate substrate occurs as a consequence of the need to store energy and well-nourished individuals cells preferentially use exogenous circulating dietary fatty acids in the synthesis of new lipids. However labeling studies have shown that in cancer cells greater than 90% of fatty acids are derived from de novo fatty acid synthesis [157-160]. The bulk of these endogenously derived fatty acids are then converted to phospholipids and incorporated into cell membrane lipids, a vital activity for proliferating cells [158]. Besides phospholipid synthesis fatty acids are an important source of energy for cancer cells via β-oxidation. Lastly, fatty acids act as precursor molecules in the synthesis of signaling lipids, the dysregulation of which, in cancer cells, has been implicated in proliferation, angiogenesis and metastasis [161].

Several avenues are being explored in order to exploit the dysregulated lipid metabolism seen in cancer cells for therapeutic gain, in particular: inhibition of fatty acid synthesis; modulating fatty acid oxidation; and altering the ability for cancer cells to store lipid.

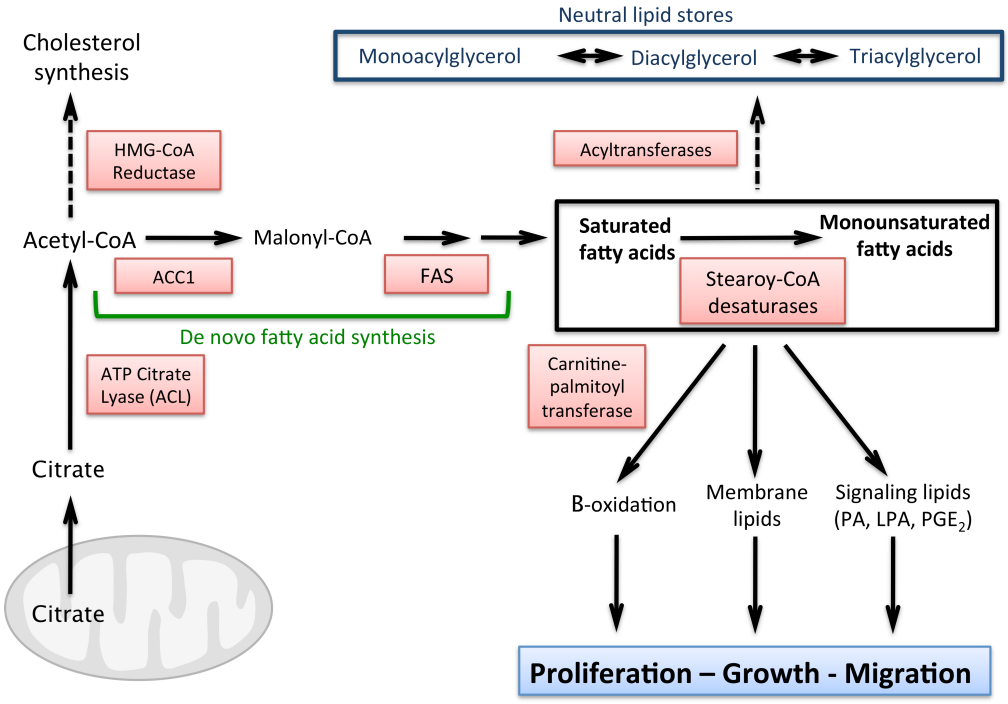


Fig 1.7: Altered lipid metabolism in cancer. Increased lipogenesis has been identified as a feature of cancer cell metabolism. Tumour cells require lipids to form membranes and intracellular signaling molecules and act as a source of energy via the β-oxidation pathway. ATP Citrate Lyase (ACL) catalyses the conversion of citrate into Acetyl CoA. Acetyl CoA can be used in the production of fatty acids via conversion to Malonyl-CoA by Acetyl CoA Carboxylase-1 (ACC1) or for cholesterol synthesis. The degradation of fatty acids via β-oxidation requires their transport across the mitochondrial membrane which is facilitated by Carnitine-palmitoyl Transferase (CPT). Stearoyl CoA desaturase (SCD) catalyses a rate limiting step in the synthesis of unsaturated fatty acids. The enzymes in red are commonly dysregulated in cancer. Dotted lines represent pathways with multiple steps. Adapted from: *Schug et al, Acta Oncologica, 2012;51(3):301-10.*

1.4.4.2: SUMMARY OF STRUCTURE AND FUNCTION OF LIPIDS

Fatty acid molecules have 2 components, a hydrophobic hydrocarbon chain and a carboxyl group. The carboxyl (-COOH) group is hydrophilic and behaves as an acid. Saturated fatty acids have hydrocarbon chains that have the maximum number of hydrogen atoms and hence no double bonds between carbon atoms (unlike unsaturated fatty acids). Most cellular lipids consist of fatty acids covalently bound to a polyalcohol backbone via an ester bond, the exception being the plasmalogens. The polyalcohol may be a glycerol in the case of triglyceride, diglyceride or 2-monoacyl-sn-glycerol (these lipids are particularly hydrophobic as they lack a polar head group). Other lipids include the phospholipids that are characterised by a glycerol molecule that is linked to 2 fatty acid chains but also a phosphate residue and a polar group such as choline. The polar head group forms a hydrophilic region and determines the type of phospholipid whilst in contrast the fatty acid side chains are hydrophobic, giving this type of lipid its 'amphiphilic' qualities. Many different types of phospholipid exist depending on the type of phosphoester moiety and alcohol, including phosphatidic acid (the simplest phospholipid), phosphatidycholine, phosphatidylserine and phosphatidylethanolamine. Glycolipids are another type of lipid that, instead of a phosphate residue, incorporate a single carbohydrate or a complex chain of up to 7 carbohydrate moieties. Lastly the cholesterols have unique structures with 4 linked hydrocarbon rings and both a hydrocarbon and hydroxyl tail.

The distribution of lipids within the cell is tightly controlled and dependent upon function. Triglyceride is mainly sequestered within lipid droplets in the cell and serves as an energy store. Phospholipids are the major constituents of membranes, the differential attraction to water of the polar head and acyl chains resulting in the

formation of the membrane bilayer. Phospholipids also act as cofactors in enzymatic reactions and can facilitate the active conformational structure of proteins. They also play an important role in signal transduction and are essential for the absorption and transport of lipids. Glycolipids are always found on the outer surface of the lipid bilayer and act as markers for cellular recognition. Cholesterols are especially abundant in the membranes of animal cells. They act as biosynthetic precursor molecules to steroid hormones, bile acids and vitamin D and also are involved in embryonic development, signal transduction and sperm development [162-164].

1.4.4.3: FATTY ACID SYNTHESIS IN CANCER CELLS

Fatty acids may either be taken up from the microenvironment or synthesised by the cell. All lipids are synthesised from the precursor molecule acetyl-CoA which is predominantly derived from glucose via glycolysis and the tricarboxylic acid cycle in mammalian cells. However, dependent upon whether the lipid is based on a sterol or fatty acid structure the synthesis pathway thereafter differs and for purposes of brevity this overview will focus on fatty acid synthesis or de novo lipogenesis (DNL). The initial step in fatty acid synthesis is the cleaving of citrate to form acetyl-CoA by ATP-citrate lyase (ACLY) after its export to the cytosol. Acetyl-CoA is then converted into malonyl-CoA by Acetyl-CoA carboxylase-1 (ACC1), a vital rate limiting step in de novo lipogenesis (DNL). Malonyl-CoA has its carbon chain then extended by fatty acid synthase (FAS) to form a 16-carbon fatty acid chain (palmitate or 16:0). Downstream of palmitate several desaturation and elongation enzymes work to produce a whole variety of fatty acids [162, 163]. Three key enzymes of the lipogenesis pathway have been shown to be commonly dysregulated in the cancer phenotype: ACLY, FAS and the ACCs.

ACLY has been shown to be upregulated in several types of cancer including breast cancer [165-167]. Its activity is understood to be mediated by direct phosphorylation of ACLY by AKT [168] and increased activity of SREBP-1 secondary to activation by mTOR [169]. The inhibition of ACLY by small molecule inhibitors or RNA interference has been shown to suppress cancer cell proliferation and there is interest in this enzyme as a therapeutic target [170-172]. However, its product, acetyl-CoA, is an important precursor metabolite for many molecules and hence the inhibition of ACLY could have disadvantageous and toxic consequences in normal tissues.

The ACCs are biotin-containing enzymes that catalyse the carboxylation of acetyl-CoA to form malonyl-CoA and both of these isoforms are inactivated by phosphorylation after AMPK activation. The 2 isoforms of ACC in humans, ACC1 and ACC2, are encoded by separate genes. ACC1 is found predominantly in lipogenic tissues (liver and adipose tissue) and catalyses the production of malonyl-CoA prior to long chain fatty acid synthesis by FAS. ACC2 is found mainly in the heart or skeletal muscle and its product, malonyl-CoA, here inhibits the enzyme carnitine palmitoyltransferase I (CPT1) whose function is to facilitate entry of long chain fatty acids into mitochondria for β-oxidation [173]. Both ACC1 and ACC2 have been found to be overexpressed in tumours when FAS is similarly overexpressed [165, 174] and mutations in the tumour suppressor, LKB1, have been linked to activation of ACC, almost certainly via AMPK suppression [175]. Mutations in another tumour suppressor, the Breast Cancer Susceptibility Gene 1 (BRCA1), have been associated with ACC1 activation and this scaffold protein has been shown to bind directly to ACC1 preventing its phosphorylation and inactivation [176]. In cultured prostate and

breast cancer cell lines, specific siRNA silencing of ACC1 has been shown to lead to growth inhibition and apoptosis [177, 178]. Similarly exposure of two cultured prostate cancer cell lines to the potent ACC1 and ACC2 inhibitor, Soraphen A, led to cell death whilst addition of the fatty acid, palmitic acid, rescued this effect. Of note, a premalignant cell line was far less affected suggesting that malignant cells are more dependent on ACC activation [179].

FAS catalyses the synthesis of long-chain fatty acids from malonyl-CoA for eventual storage as trigylcerides in liver and adipose tissue. Its expression has been found to be increased in many human cancers, including breast, colon, prostate, head and neck, ovary and bladder cancer [180]. Greater expression of FAS correlates with poor prognosis in many tumour types. For example, one study suggested that on multivariate analysis breast cancer patients with positive FAS staining on immunohistochemistry were 4 times more likely to relapse over 10 years than those with FAS negative tumours (HR 4.44, 95% CI 1.92-10.25, $p < 0.0001$) [181]. In breast cancer cell line models greater FAS expression correlates with increased HER-2 expression and vice-versa and FAS inhibition suppresses HER2 expression [182]. In vitro and in vivo observations have shown that inhibition of FAS using drug inhibition or RNA interference preferentially kills cancer cells [180, 183]. Although cancer cells rely on FAS mediated de novo synthesis of fatty acids it may in fact be the accumulation of malonyl CoA that is toxic [184]. Whether FAS is a practical drug target remains to be seen as some inhibitors of FAS have caused marked toxicity in animal models, including severe weight loss [185].

Targeting the master regulators of fatty acid synthesis is another therapeutic strategy of current interest. Activation of AMPK leads to inhibition of FAS and ACC and has been postulated to contribute to metformin's anticancer effect [186]. The transcription factor, SREBP-1, activates ACLY, ACC and FAS, in consequence upregulating fatty acid synthesis [187]. Upregulation of SREBP-1 expression has been linked to escape from anti-androgen therapy in a prostate cancer xenograft model [188]. Inhibition of activation of SREBP-1 by shRNA knockdown or the drugs 25-hydroxycholesterol, fatostatin, and FGH10019 has been shown to lead to apoptosis in cancer cell lines, in particular in those in which EGFR is constitutively activated [189, 190]. Lastly, metformin has been shown to downregulate SREBP-1 expression in a hepatocyte model secondary to activation of AMPK [33].

1.4.4.4: FATTY ACID UPTAKE INTO CANCER CELLS

As discussed above, cancer cells typically derive the bulk of their lipids from DNL rather than uptake from the microenvironment. However, it has been shown in a co-culture in vitro model that ovarian cancer cells can scavenge lipid from surrounding adipocytes with induction of lipolysis in the adipocytes and β-oxidation in the cancer cells. The importance of fatty acid binding protein-4 (FABP-4) has been implicated in ovarian cancer progression with high expression seen in clinical samples from omental metastases and reduced tumor burden seen in Fabp4−/− knockout mice compared to wild-type using an ovarian cancer xenograft model [191]. In vitro, a prostate cancer cell line when treated with FAS or ACLY inhibitors only demonstrated sensitivity with the withdrawal of lipoprotein (i.e. the source of exogenous lipid) from the media [192]. However, with the limited investigation to

date, it is not currently clear as to the importance of these mechanisms, in particular in vivo.

1.4.4.5: FATTY ACID DESATURATION IN CANCER CELLS

There are 2 isoforms of stearoyl-CoA desaturase (SCD) in human cells, SCD1 and SCD5. Their role is to regulate the composition of cellular lipids by desaturating fatty acids (predominantly palmitic acid and stearic acid from DNL) by introducing double bonds at the C9 position of saturated fatty acids. There is now growing evidence that altered regulation and activity of this process may play a role in malignant transformation and proliferation [193]. It is attractive as a target given that cancer cells preferentially rely on DNL derived lipid. The inhibition of this enzyme by RNA interference and small molecules has been shown to cause apoptosis in cancer cells in vitro and suppression of tumour growth in vivo probably due to build up of saturated fatty acids [194, 195]. SREBP-1 is an activator of SCD1 and hence its repression leads to a build up of saturated fatty acids. This has been suggested to be the driver behind the antiproliferative effect in cancer cells consequent to SREBP-1 inhibition [190].

1.4.5.5: FATTY ACID OXIDATION IN CANCER CELLS

The importance of fatty acid oxidation for the growth and survival of cancer cells is currently not clear. However, etomoxir, an inhibitor of CPT1 the key transporter for the transfer of fatty acids into the mitochondria prior to β-oxidation, has been shown to cause cancer cell death [196, 197]. Zaugg et al showed that an isoform of CPT1, CPT1C, normally found in brain tissue is commonly upregulated in lung cancers and that its increased expression is associated with increased β–oxidation and ATP

production, resistance to metabolic stress and nutrient deprivation or hypoxia [198]. Cytosolic NADPH has 2 main functions in the cell, to counter oxidative stress via its redox power and act as a coenzyme for anabolic enzymes. Fatty acid oxidation is an important source of NADPH and a recent study showed that in glioma cells when fatty acid oxidation was inhibited there was a profound decrease in NADPH levels and associated cell death [196]. AMPK is a key regulator of fatty acid oxidation via inactivation of ACC and under conditions of metabolic stress will promote fatty acid oxidation to maintain reserves of NADPH and ATP [199]. Peroxisome proliferator-activated receptor (PPAR) signaling has been shown to be regulated by the tumour suppressor, promyelocytic leukemia gene (PML) and PPARα is an important activator of fatty acid oxidation. However the complexity of PPARα signaling and its role in carcinogenesis and tumour progression is yet to be fully understood. Activation of PPARα signaling in rodents has been linked to the development of hepatocellular carcinoma but in contrast there is inhibition of tumour growth in other models [200].

1.4.5.6: STORAGE AND LIPOLYSIS OF LIPID IN CANCER CELLS

After synthesis, in large part, fatty acids are either used for membrane synthesis, broken down via β-oxidation or stored as neutral lipids, in particular triglyceride, in lipid droplets. In order to modify these lipids or access them for energy, triglyceride must then be broken down via the lipolysis pathway (**Figure 1.8**). The accumulation of lipid droplets has frequently been seen in cancer cells and this might reflect a response to cellular stress [201]. Given this observation, the potential of targeting the triglyceride storage mechanisms for cancer therapeutics is now being investigated.

The synthesis of most triglyceride in the cell occurs via the Kennedy or glycerol 3-phosphate pathway (**Figure 1.8**) in which fatty acids are condensed with glycerol 3-phosphate. It is catalysed by 4 key enzymes: glycerol-3-phosphate (GPAT), acylglycerophosphate acyltransferase (AGPAT), phosphatidic acid phosphohydrolase (PAP) and diacyglycerol acyltransferase (DGAT) [202]. First, GPAT esterifies sn-glycerol-3-phosphate with a fatty acid coenzyme A (FA CoA) ester to form lysophosphatidic acid (LPA). LPA is then in turn further esterified with a FA CoA to form phosphatidic acid (PA), a reaction catalysed by AGPAT. There are several isoforms of AGPAT and this may limit its potential as a therapeutic target. With regards to its role in cancer greatest interest has been directed toward the AGPAT2 isoform. AGPAT2 expression has been correlated with poor prognosis in ovarian cancer [203, 204] and several studies have demonstrated that AGPAT2 inhibitors can cause decreased cancer cell proliferation and increase apoptosis in vitro [205-209] and decrease tumour growth in xenograft models [208, 209]. The second step in this pathway involves the dephosphorylation of phosphatidic acid to 1,2-diacyl-sn-glycerol by PAP, of which there are 3 known mammalian isoforms: lipin-1, 2 and 3. Although PAP has recently been shown to be inhibited by mTOR and can activate SREBP its regulation and importance in malignant transformation is currently little understood [210]. The final step involves the acylation of 1,2-diacyl-sn-glycerol to tri-sn-glycerol or triglyceride by DGAT. There are 2 mammalian isoforms of DGAT, DGAT1 and DGAT2 and one study demonstrated that transformed lung fibroblasts overexpressing DGAT1 led to reduced phospholipid synthesis and cell growth rates [211].

Another mechanism by which the storage of lipid in cancer cells can be modulated is to target lipolysis of triglyceride to prevent release from lipid droplet stores. Three key enzymes are involved in catalyzing the lipolysis pathway, adipose triglyceride lipase (ATGL), hormone sensitive lipase (HSL) and monoacylglycerol lipase (MAGL). ATGL catalyses the conversion of triglyceride (TG) to diglyceride (DG) and HSL the subsequent conversion of (DG) to monoacylglycerol (MAG). No clear role for ATGL and HSL in malignant transformation has yet been elucidated although ATGL deficient mice have been shown to be resistant to cancer related cachexia compared to wild type in lung and melanoma xenograft models [212]. MAGL hydrolyses MAG to release the final fatty acid, leaving just the glycerol backbone. There has been recent interest in the oncogenic role of MAGL. A proteomic screen of a selection of aggressive cancer cell lines demonstrated that MAGL was especially highly expressed here. Overexpression of this protein led to increased migration, invasion and survival, but this phenotype was then reversed with pharmacological and short-hairpin RNA-mediated MAGL inhibition [213].

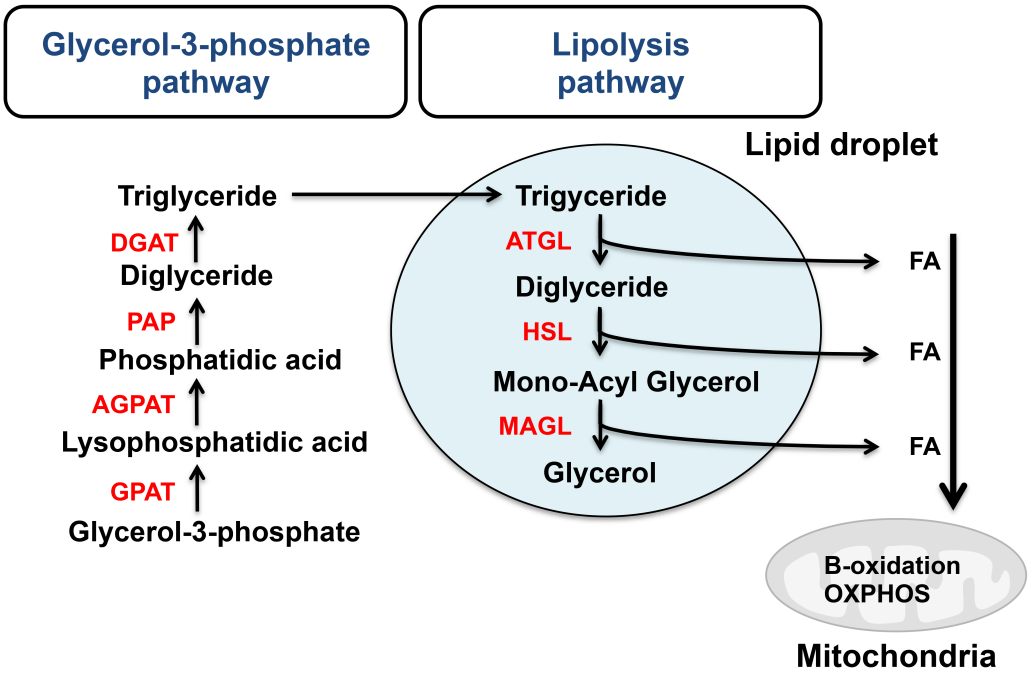


Fig 1.8: Triglyceride storage and breakdown. Triglyceride is synthesised from glycerol-3-phosphate via the glycerol-3-phosphate or Kennedy pathway. Several enzymes involved in catalyzing these steps are of interest as drug targets in their own right. Breakdown of triglyceride can occur via lipolysis or fatty acid oxidation. MAGL has been implicated in the oncogenic phenotype although the roles of HSL and ATGL are unclear. FA, fatty acid; OXPHOS, oxidative phosphorylation; GPAT, glycerol-3-phosphate acyltransferase; AGPAT, acylglycerophosphate acyltransferase; PAP, phosphatidic acid phosphohydrolase; DGAT, diacyglycerol acyltransferase; ATGL, adipose triglyceride lipase; HSL, hormone sensitive lipase; MAGL, monoacylglycerol lipase.

1.5: BIOMARKER TRIALS OF METFORMIN

1.5.1: OVERVIEW

Breast cancer is a heterogenous disease and this is reflected in the varying response to targeted anti-cancer drugs between patients, for example for ER and HER2 expression. There are now approximately 50 clinical trials worldwide investigating the clinical effects of metformin in the cancer setting many of which are assessing for evidence of clinical benefit in unselected cancer populations [52]. However, at an early stage of metformin's development as a cancer drug it is important that biomarkers are developed to select patients who may be suitable for metformin treatment and inform the design and interpretation of future trials. The history of cancer drug development is littered with examples of promising treatments tested in unselected patient populations in which clinical benefit could not be demonstrated. Already one phase 3 adjuvant study of metformin has completed recruitment in an unselected breast cancer population prior to satisfactory biomarker development, the primary endpoint being disease free survival [52]. There has been criticism of the way this trial has been developed prior to biomarker studies being carried out to help determine which patients may benefit most from metformin as a cancer therapy. In an unselected population no significant benefit may be seen when perhaps a subpopulation of breast cancer patients is especially responsive. Alternatively it may be that an overall benefit is seen in the unselected population but that an unknown proportion of the population is resistant to treatment leading to future unwarranted therapy for this group with clear quality of life and health economic implications. It is also vital that biomarkers generated from smaller studies can be prospectively tested in sub-studies within phase 3 trials to examine robustness, something that is too late to be assessed in this phase 3 study.

Window of opportunity studies in which a treatment of interest is given over a short period (typically 2-4 weeks) prior to conventional therapy are an ideal design to screen for potential biomarkers. Pharmacodynamic tests can be carried out before and after the study treatment to assess for changes in markers of interest. These trials can be carried out in 'pristine' untreated cancers giving an opportunity to study cancer cells that have not been selected for survival by one treatment or another. A recent detailed pharmacodynamic study of the early response of primary breast cancers to bevacizumab, in which dynamic magnetic resonance imaging was correlated with gene expression profiles has attempted to address this for anti-VEGF therapy and demonstrated a marked short term heterogeneity of response [214].

1.5.2: PUBLISHED WINDOW OF OPPORTUNITY STUDIES AND METFORMIN

The results of several clinical biomarker studies of metformin in the breast cancer setting have recently been published or were reported at the 2012 San Antonio Breast Cancer Symposium (**Table 1.3**) [105, 215-218]. Without exception these studies took place in a 2-4 week window between breast cancer diagnosis and surgery with the collection of tumour samples comprising of a pre-metformin biopsy sample and post-metformin surgical sample after an intervening short course of metformin. Diabetic patients were excluded from these trials and one study was enriched for obese patients, but otherwise the breast cancer population was unselected. All of these trials have focused on metabolic serum markers and changes in intratumoral proliferation (Ki67) or apoptosis (TUNEL) using immunohistochemistry. Results so far suggest that metformin may inhibit both cancer cell proliferation, measured by Ki67, and reduce insulin resistance in this non-diabetic population, as measured by the

homeostasis model assessment index or HOMA (a measure of insulin resistance calculated from the product of glucose (mmol/L) and insulin (mU/L) divided by 22.5). Correlation between immunohistochemical markers, in particular Ki67, has suggested a relationship between the metabolic syndrome and a greater effect for metformin in breast cancer. The largest study to date did not demonstrate a clear relationship between oestrogen or progesterone receptor status and Ki67 [105].

In addition one limited study examined for changes in gene expression using RNA microarray analysis of 14 paired pre- and post–metformin primary breast cancer samples. After metformin treatment, 34 gene sets were overexpressed and 60 underexpressed. In particular, this study identified both upregulation in the tumour necrosis factor receptor 1 (TNFR1) pathway and underexpression of p53 signaling, suggestive of an effect of metformin on key pathways known to regulate tumour cell proliferation, invasion and metastasis. There was also prominent downregulation of phosphodiesterase 3B (PDE3B) a known regulator of the lipolytic and glycogenlytic effects of insulin [215].

Of note, no published study has used functional imaging to determine metabolic response to metformin or assessed for intratumoral changes in metabolite concentrations.

Study	Enrolment and design	Population	Effect of metformin on serum metabolic markers	Effect of metformin on immunohistochemical markers
Bonnani et al & Cazzaniga et al	200 metformin (n=100), placebo (n=100)	Untreated breast cancer Non-diabetic	Decrease in CRP (-0.8mg/L, p=0.029) and total cholesterol (-9.4mg/dL, p=0.001). Decreased glucose (-2.8mg/dL, p=0.15) and trend toward reduced insulin (-0.2mU/L, p=0.92) if BMI>27.	10.5% mean proportional decrease in Ki67 relative to placebo if HOMA >2.8 (p=0.045). No effect on TUNEL.
Hadad et al	55 metformin (n=47), placebo (n=8)	Untreated breast cancer Non-diabetic	No significant change in serum insulin - note patients received intravenous glucose prior to post-metformin blood sampling.	3.4% decrease in mean absolute level of Ki67 (p = 0.027) and no change in control levels of Ki67, decrease in pAKT (p=0.04) and increase in pAMPK (p=0.04).
Kalinsky et al	35 no control arm	Untreated breast cancer Non-diabetic Enriched for obese women	Significant decrease in total cholesterol (-16.4mg/dl, p<0.01) and leptin (-2ng/ml, p=0.03). Trend toward decrease in insulin (-4.1 uIU/ml, p=0.06), HOMA (-1.0, p=0.06) and adiponectin (-388ng/dl, p=0.06). No significant change in glucose or IGF-BP3.	
Niraula et al	39 no control arm	Untreated breast cancer Non-diabetic	Decrease in glucose (-0.14mmol/l, p=0.045) and HOMA (-0.21, p=0.047) No significant change in insulin, leptin or CRP.	3.0% decrease in mean absolute level of Ki67 (p=0.016) and 0.5% increase in TUNEL (p=0.004).

Table 1.3: Neoadjuvant studies of potential metformin biomarkers of effect in breast cancer patients. HOMA, homeostasis model assessment index (an estimate of insulin resistance, HOMA formula: fasting blood glucose (mmol) x insulin (mU/L)/22.5); IGFBP3, insulin-like growth factor binding protein-3; TUNEL, terminal deoxynucleotidyl transferase dUTP nick end labeling [105, 215-218].

1.5.3: ROLE OF FUNCTIONAL IMAGING, GENE SEQUENCING AND METABOLOMICS IN CANCER DRUG DEVELOPMENT

1.5.3.1: FUNCTIONAL IMAGING

Functional imaging is already used in the determination of early drug response for cancer agents both within the clinical trial setting and routine clinical care [219]. With the advent of an era of cancer treatments that specifically target metabolism, it can be expected that these techniques will become more critical for this purpose. The most commonly used tracer for positron emission tomography (PET) imaging is 2-deoxy-2-(^{18}F)fluoro-D-glucose (^{18}F-FDG) a radiolabelled glucose analogue. As discussed above, in vitro investigation using cancer cell lines has demonstrated that a metformin induced energy stress leads to the upregulation of glycolysis and increased glucose uptake [143] and a recent xenograft model, using colon cancer cell lines confirmed increased intratumoral ^{18}F-FDG uptake 24 hours after intraperitoneal injection of metformin [220].

1.5.3.2: RNA SEQUENCING

The first cancer genome was sequenced by second generation technology only in 2008 and the reduction in cost of this technique and greater availability of it as a resource is likely to have a major impact on treatment, prognostics and our understanding of cancer biology in coming years [221]. Since this breakthrough in DNA sequencing, second generation RNA sequencing of the transcriptome has become a realistic tool in terms of cost and availability for more general use. RNA sequencing has many advantages over gene array technologies. In particular, there is a much improved ability to measure transcription levels across different genes, samples and platforms. Lastly there is greater sequencing depth, i.e. there is a greater ability to

detect a rare transcript or variant. However, due to the great increase in data generated from these techniques, bioinformatic processes to efficiently process these large datasets are still being developed [222].

Given its novelty, thus far little use for this technique has been made for drug biomarker discovery and there are challenges here. The transcriptional response to any treatment is likely to be highly variable between tumour samples. In order to overcome this with gene array data, several groups have previously used pathway analysis of genes associated with particular processes or tumour environments [214, 223, 224].

1.5.3.3: METABOLOMICS

Mass spectrometry has long been used as a tool for cancer drug biomarker discovery but mainly in carrying out proteomic screens. The use of stable isotope labeling for in vitro studies of cancer metabolism, in conjunction with nuclear magnetic resonance and mass spectrometry techniques, has been vital to a growing understanding of the intricacies of cancer cell substrate utilisation for key processes vital to proliferation, such as fatty acid and amino acid synthesis. Similarly, clinical studies using these techniques have also proved invaluable in investigating the altered metabolism associated with diabetes and obesity [225-227]. There is potentially an important place for this methodology to study the effect drugs targeting cancer metabolism have on intratumoral metabolites in clinical studies. Study participants can be given a stable isotope, for example, deuterated water or [U-13C] palmitic acid prior to recovery of tumour tissue to allow tracing of substrates through metabolic pathways.

1.5.4: POTENTIAL BIOMARKERS OF METFORMIN'S CLINICAL EFFECT IN BREAST CANCER

It is clear that under in vitro conditions there is a significant variability in the sensitivity to the effect of metformin on proliferation between different breast cancer cell lines. **Table 1.4** summarises a published screen of metformin's effects on cancer cell proliferation (measured by MTS assay) and colony formation (measured by clonogenic assay) [46, 49]. Dependent upon whether the direct or indirect effects of metformin on the cancer cell are key, several mechanisms of resistance have been proposed (**Table 1.5**).

Cell line	**Receptor status**	**Effect on proliferation as percentage of control (10mM metformin)**	**Effect on colony formation as percentage of control (1mM or 2mM metformin)**
MCF7	ER +ve, HER2 -ve	60%	60% (2mM)
MDA-MB-468	Triple negative	40%	90% (1mM)
BT20		30%	45% (1mM)
MDA-MB-231		50%	90% (1mM)
BT549		30%	30% (1mM)
BT474	ER +ve, HER2 +ve	50%	80% (2mM)
MCF7/713 (transfected with erbB2)		80%	100% (2mM)
SKBR3	ER -ve, HER2 +ve	60%	90% (2mM)

Table 1.4: Metformin's effects on cancer cell proliferation as measured by MTS assay and colony formation as measured by clonogenic assay. No clear relationship between ER and HER2 receptor status and sensitivity to metformin is demonstrated. Note that values are estimated from published figures and are not actual values [46, 49].

1.5.5: MECHANISMS OF RESISTANCE TO METFORMIN'S INDIRECT EFFECT

Mechanisms of resistance that are relevant to the proposed indirect effect of metformin's anticancer effect would be expected to relate to metformin's ability to modulate the host's insulin axis. As discussed above, early clinical prospective studies have already suggested that there may be a link between metformin's effects on breast

cancer cell proliferation as measured by Ki67 and the metabolic syndrome [105]. Hence, it is plausible that insulin secretion (either measured by fasting insulin or c-peptide), along with insulin resistance (as measured by HOMA) and BMI may all be important biomarkers of metformin's effect in cancer. Similarly, levels of free IGF-1 may also act as a biomarker. Uptake of metformin via the gut or into liver cells is also potentially vital to its physiological effect. Organic Cation Transporter 1 (OCT-1) is known to play an important role in the uptake of metformin into hepatocytes. Several polymorphisms of OCT-1 have been described that can influence the uptake of metformin, the most common being OCT1-420del the alleleic frequency of which is 20% in caucasian North Americans [27]. Lastly, with regard to the cancer cell, expression of the insulin receptor and degree of activation of the PI3K/mTOR axis may influence susceptibility to insulin axis host response to metformin.

Marker	Relevant to indirect effect	Relevant to direct effect
Host	+	
BMI	+	
Insulin secretion	+	
Insulin resistance	+	
Liver OCT-1 expression	+	
Cancer cell		
IR/IGF1R expression	+	
PI3K/mTOR pathway activation	+	+
Tumour OCT-1 expression		+
LKB1 expression		+
VEGF response		+
Myc expression		+
IDH1 expression		+
GLUT1 and GLUT4 expression		+
NRF2 expression		+
Complex 1 mutations		

Table 1.5: Potential mechanisms of resistance to metformin's anticancer effect relevant to direct and indirect anticancer effects of metformin. Adapted from: *Dowling et al, J Mol Endocrinol, 2012;48 (3):R31-R43.*

1.5.6: MECHANISMS OF RESISTANCE TO METFORMIN'S DIRECT EFFECT

In vitro and in vivo work has provided evidence of several potential cancer cell specific mechanisms of sensitivity/resistance to metformin. Firstly, the ability of metformin to modulate the AMPK axis in cancer cells may be important. Upstream of AMPK is the tumour suppressor gene LKB1. An inactivating mutation of LKB1 is responsible for the premalignant condition Peutz-Jegher's syndrome and this gene is also commonly mutated in sporadic lung cancers [228, 229]. Deletion of LKB1 in the livers of adult mice led to greatly reduced activation of AMPK, dephosphorylation of CRTC2 (a central regulator of gluconeogenesis) and the loss of effect on glucose levels by metformin and hence it may be important in mediating metformin's indirect effect [28]. However, shRNA knockdown of LKB1 of tumour cells in vitro led to increased sensitisation to metformin, possibly due to an inability of cells to react to the energy stress via activation of the AMPK axis. In vivo, tumour LKB1 expression was only essential for the in-vivo anticancer effect of metformin in mouse xenograft models that did not have diet-induced hyperinsulinemia [103]. Downstream of AMPK the dependence of a cancer cell on the activation of the mTOR and PI3K axes for growth by the cancer cell may be important.

The reliance of cancer cells on particular metabolic pathways and the ability to respond by using other energy or carbon sources may be critical to their sensitivity. For example the 'glycolysis reserve' may be dependent on their ability to upregulate glucose uptake. AMPK activation has previously been shown to upregulate glucose transporter expression via translocation of glucose transporter type 4 (GLUT4) from intracellular storage vesicles to the plasma membrane [230-232]. The flexibility of

cancer cells to utilise glutamine as an alternative carbon source is also likely to be important [143]. The glutamine reductive carboxylation pathway that allows metformin treated cancer cells to redirect glutamine carbons away from the TCA cycle and changes in expression of its regulators such as IDH are of interest [151]. The constitutive expression of the oncogene, myc, has been linked to 'addiction' of glutamine as a bioenergetic substrate [233] and overexpression of this transcription factor has been associated with increased sensitivity to metformin [234]. Additionally, mutations in the mitochondrial genome and, in particular, genes encoding for constituents of complex 1 may also be key markers of resistance or sensitivity.

One study suggested that metformin may increase the expression of VEGF, a neoangiogenic signal, and hence promote angiogenesis and tumour survival. Using xenograft models several different cancer cell lines were treated with metformin. Three of the cell lines had suppression of tumour growth but MDA-MB-435 cells (a melanoma cell line) had increased expression of VEGF in an AMPK dependent manner and demonstrated tumour progression [144].

The ability of cancer cells to take up metformin may be important. One study has shown that in 2 ovarian cancer cell lines siRNA knockout of OCT-1 results in resistance to metformin both in terms of its inhibitory effects on cancer cell proliferation and AMPK activation [235].

High levels of NRF2, a transcription factor that acts as the master regulator of an array of genes that promote the antioxidant response, has been associated with chemo-resistance in endometrial cancer models [236]. Metformin has been shown to increase

ROS production in mammalian cells and greater expression of NRF2 is known to correlate with metformin induced improved lifespan in nematodes [130, 237].

1.6: SUMMARY AND AIMS

1.6.1: SUMMARY

There is now a wealth of evidence that metformin reduces the cancer incidence in patients with type 2 diabetes and in vitro and in vivo cancer cell line studies suggest metformin has an antiproliferative and anticarcinogenesis effect. However there are concerns over the validity of the preclinical models with regard to their relevance to the human clinical setting and substantial questions still remain as to the mechanism of its anticancer effect. In order to understand which cancer patient populations should be targeted for metformin treatment and aid the development of future, similarly metabolically active drugs, further study of metformin's biological effect in cancer needs to be undertaken. In particular, investigation needs to focus on clinical samples.

1.6.2: AIMS

Hence the overall aims of this DPhil project were to:

a) further examine the effect of metformin on breast cancer metabolism using in vitro cell line models to gain greater insight into its anticancer mechanism of action;
b) develop an understanding of pathways that might be targeted to synergise with metformin's anticancer effect;
c) set up a 'window of opportunity' clinical trial to study metformin's effects on breast cancer metabolism to develop potential biomarkers of its metabolic effect and further investigate its in vivo mechanism of action.

CHAPTER 2: MATERIALS AND METHODS

2.1: MATERIALS

2.1.1: CELL LINES

The MCF7, MDA-MB-468, MCF7, T47D, MDA-MB-157 and BT474 cells were obtained from the American Type Culture Collection (LGC standards, UK). The MCF7 and MDA-MB-231 cells expressing mitochondrial red fluorescent protein were provided by Francisco Iborra [238].

2.1.2: CHEMICALS

For all laboratory studies metformin was obtained from Calbiochem and AICAR and rotenone purchased from Sigma Aldrich. The source of all other chemicals is specified in the text.

2.1.3: ANTIBODIES

Rabbit anti- pAMPK monoclonal (thr172 residue), rabbit anti- AMPK polyclonal, rabbit anti- pACC (ser79 residue) polyclonal, rabbit anti- ACC polyclonal, rabbit anti- pS6 (Sr235/236 residues) polyclonal, rabbit anti- pEIF4-BP1 polyclonal, and rabbit anti- SCD1 polyclonal antibodies were obtained from Cell Signaling. Rabbit anti- SCD5 polyclonal antibody was obtained from Novus biological and mouse anti- Ki67 monoclonal antibody from DAKO. All HRP-conjugated antibodies were obtained from DAKO. For Western blot loading control, HRP conjugated monoclonal Anti- Bactin from Sigma was used.

2.2: CELL CULTURE AND IN VITRO TECHNIQUES

2.2.1: CELL CULTURE

All cell lines were cultured in Dulbecco's Modified Eagle Medium (DMEM) (Invitrogen) supplemented with 10% foetal bovine serum (FBS), 100 U/ml penicillin, and 100 μg/ml streptomycin at 37 °C and 5% CO_2, in sterile flasks (Corning) in a humidified incubator. Cells were passaged when they reached 80% confluency by treating with trypsin-EDTA (Invitrogen) to detach after a PBS wash. The cells were then spun in a centrifuge at 1000 rcf for 5 minutes prior to reseeding at 1 in 10.

2.2.2: HYPOXIC EXPOSURE

Incubation under hypoxic conditions was performed at 0.1% oxygen (5% CO_2) using an INVIVO$_2$ 400 hypoxic chamber (Pro-Lab Diagnostics).

2.2.3: RNA INTERFERENCE

AMPKα1 (PRKAA1 On-TAplus SMART pool duplex, Dharmacon) and AMPKα2 (PRKAA2 On-TAplus SMART pool duplex, Dharmacon) were used for AMPK siRNA knockdown. On-TAplus non-targeting pool (Dharmacon) was used as a negative control. In summary, siRNAs diluted in Opti-MEM^{TM} reduced serum media were transfected into MCF7 cells at 20 nM using Lipofectamine RNAiMax and then cultured in antibiotic free media for 8 hours prior to media change (it was at this point that metformin was added.) This assay was carried out either in T175 flasks (Corning) seeded at 2 x 10^6 cells per flask, for the mass spectrometry experiments, or 6 well plates (Corning) seeded at 1 x 10^5 cells per well, for the FACS experiments.

2.3: CELL GROWTH ASSAYS

2.3.1 CELL COUNTING

A 20 μl aliquot of each sample was taken and then a cell count obtained using the Cellometer Auto T4 Cell Counter (Nexcelom Bioscience).

2.3.2 CELL NUMBER ASSAYS

100,000 cells per well were plated on to 6 well plates and the following day the media replaced with DMEM media containing drug concentrations as specified in the text. The media was supplemented with 5 mM or 25 mM glucose with or without 4 mM glutamine. Cell number was counted daily to 96 hours. To maintain a more consistent glucose, glutamine and lactate concentration the media was replaced on a 24 hourly basis for all assays.

2.3.3: SPHEROID FORMATION AND VOLUME QUANTIFICATION

Spheroids were grown in vitro by plating 5000 cells with matrigel per well in non-adherent 96-well plates and then centrifuging at 1000 G for 10 minutes. After 24 hours metformin at varying concentrations as specified in the text was added. Images were taken of spheroids at baseline and days 2, 4 and 7 using a Zeis Axiovert 135 microscope and AxioCam digital camera. Spheroid volume was estimated using image analysis software (ImageJ).

2.3.4: PROLIFERATION ASSAYS

2.3.4.1 SULFORHODAMINE B (SRB) ASSAY

Dependent upon the cell line 1500-3000 cells were plated on a 96 well plate and the following day the metformin at varying concentrations as specified in the text was added. After 48 hours the cells were then fixed with 10% trichloroacetic acid and stained with 0.04% SRB. After 3 washes with 1% acetic acid and the addition of 10 mM Tris, the absorbance was measured at 540nm on a colorimetric microplate reader.

2.3.4.2 CYQUANT^{TM} ASSAY

Dependent upon the cell lines 1000-2000 cells were seeded per well on a 96 well plate and left to recover overnight prior to media change with drugs added at varying concentrations as specified in the text. Cyquant mastermix was made up with 8.8 ml deionised water, 2.2 ml of 5x Hank's balanced salt solution and 22 μl Cyquant NF dye. After 96 hours the media was removed and 50 μl of the Cyquant mastermix added prior to measuring the fluorescence intensity using a fluorescence microplate reader with excitation at 485 nm and emission detection at 530 nm.

2.4: ASSAYS OF CELLULAR METABOLISM

2.4.1: GLUCOSE AND LACTATE MEASUREMENT

Cells were seeded at 1 x 10^6 per 10 cm dish and after recovery overnight were treated either with or without 2mM metformin in 10 ml of 25 mM DMEM for 24 hours. At this timepoint 1ml of media was collected after 24 hours. Glucose and lactate concentration were then measured using a GEM Premier3000 (Instrumentation Laboratory, Lexington, MA). Note this assay was carried out with help from Dr Jenny Collins.

2.4.2: OXYGEN CONSUMPTION AND EXTRACELLULAR ACIDIFICATION EXPERIMENTS

Dependent upon the cell lines 17,500-20,000 cells were seeded per well on a 96 well plate and left to recover for 24 hours prior to a media change with metformin added at varying concentrations as specified in the text. After metformin treatment overnight the cells were assayed using the XF96 extracellular flux analyser (Seahorse Bioscience). This analyser uses solid state probes only 200 μm above the cell monolayer to measure oxygen consumption and proton extrusion in real time. Compounds can be then be pneumatically injected into the assay plate wells to assess specific mitochondrial and glycolysis parameters (Oligomycin, Mesoxalonitrile 4-trifluoromethoxyphenylhydrazone (FCCP), Actinomycin A, rotenone and 2-DG). Please see Chapter 3 for further discussion of the role of these compounds and the mitochondrial and glycolysis parameters assessed. Note this assay was carried out with help from Dr Simon Wigfield.

2.4.3: ATP ESTIMATION

Cells were seeded on 96 well white opaque plates overnight prior to treatment for 24 hours with 0, 2 or 10 mM metformin treatment with or without 100 μM etomoxir. ATP levels were then measured using the Enzylight^{TM} ADP/ATP ratio assay kit (ELDT-100). Briefly, for each 96-well plate, 95 μL of assay buffer was mixed with 1 μL of substrate, 1 μL of cosubstrate and 1 μL of ATP Enzyme. The media was then removed and 90 μL ATP Reagent was added to each well prior to mixing on a plate shaker. After 1 min, the luminescence was read on a luminometer. ATP levels were adjusted for cell proliferation as measured using the Cyquant^{TM} assay.

2.4.4: ESTIMATION OF OLEATE OXIDATION

$1.5x10^6$ cells were plated overnight prior to 48hr treatment with 0, 2 or 10mM metformin treatment with or without 100μM etomoxir. The media was changed after 24 hours. After a PBS wash cells were then incubated at 37ºC for 1hr, in a radiolabelled oleic acid solution (glucose-free RPMI, supplemented with 3mM glucose and containing 0.5mM oleic acid and 0.55μCi [1-14C] oleic acid at 53mCi/mmol; Amersham). At the end of the incubation, glass "boats" containing 1ml of 3M KOH were inserted inside the flasks and the caps were sealed tightly with parafilm. Cells were incubated for a further 2hr at 37°C. To liberate CO_2 in the medium, 1ml of 60% perchloric acid was injected through the cap of the flask using a syringe. The caps were resealed with parafilm and the flasks were placed on a shaker at room temperature for 2hr. The boats were then removed from the flasks and the KOH was collected and added to scintillation vials containing 7ml of OptiPhase 'HighSafe' 3 scintillation fluid (Perkin Elmer). The trapped $^{14}CO_2$ was measured by liquid scintillation counting on a Beckman LS6500 scintillation counter. Another set of flasks was set up simultaneously for cell counts to adjust for cell number between conditions. Note that this assay was performed with help from Ms Ulrike Harjes.

2.4.5: MEASUREMENTS OF TOTAL LIPOLYSIS, HSL AND ATGL ACTIVITY

6 x T175 flasks were seeded with $2 x10^6$ cells overnight prior to 48hr treatment with or without 2mM metformin treatment. The media was changed after 24 hours. At endpoint the cells were washed with PBS prior to freezing at -80°C.

ATGL and HSL activity was then measured by our collaborator's team, Prof Hoeffler, on samples provided, as previously described by Das et al [212] and corrected for

protein. In brief, (description provided by Prof Hoeffler's team) the cell samples were rinsed in phosphate- buffered saline (PBS) containing 1 mM ethylene diamine tetraacetic acid (EDTA) and homogenized in lysis buffer (0.25 M sucrose, 1 mM EDTA, 1 mM dithiothreitol (DTT), 20 μg/ml leupeptin, 2 μg/ml antipain, 1 μg/ml pepstatin, pH 7.0) using a Magna Lyser (Roche Diagnostics GmbH, Mannheim, Germany). This cell lysate was then centrifuged at 100,000 G for 1 h at 4 °C. The lipid-free infranatant (cytosolic fraction) was collected and used for TG hydrolase assays. The substrate for determining lipase activity contained non-labeled triolein and [9,10-3H(N)-triolein] (NEN Life Science Products, Boston, MA) as a radioactive tracer that was emulsified with phosphatidylcholine/phosphatidylinositol using a conventional ultrasound sonicator. The cytosolic fractions with or without the specific HSL inhibitor 76-0079 (NNC 0076- 0000-0079, Novo Nordisk, Bagsværd, Denmark) were incubated at 37 °C for 60 min under constant shaking. The reaction was terminated by the addition of methanol/chloroform/heptane (10:9:7), 0.1 M potassium carbonate and 0.1 M boric acid (pH 10.5). After centrifugation at 800 G for 20 min the radioactivity in 1 ml of the upper phase was determined by liquid scintillation counting in a LS 6500 Multi-Purpose Scintillation Counter from Beckman Coulter (Fullerton, CA). For this experiment liver and adipose tissue were used as controls and the assumption was made that lipolysis activity not accounted for after this addition of the HSL inhibitor was secondary to ATGL.

2.5: RT-PCR

2.5.1: RNA EXTRACTION

Cells were washed with PBS and then lysed with 1 ml Tri Reagent (Sigma) prior to chloroform/ethanol extraction. 200 µl of chloroform was added to each sample per 1 ml of Tri reagent. These samples were then shaken vigorously for 15 seconds prior to incubation at room temperature for 5 minutes. After centrifugation at 12,000G for 10 minutes at 4^{o}C the aqueous phase was transferred to a fresh RNAse free eppendorf tube and 500uL of isopropanolol added. The samples were incubated for a further 5 minutes at room temperature before centrifugation at 20,000 G for 5 minutes at 4 ^{o}C. The supernatant was carefully removed without disturbing the pellet and 1ml of 75% ethanol added. After centrifugation at 12,000 G for 5 min the ethanol was removed. The RNA pellet was air dried for 5 minutes prior to being dissolved in 50 µl of DEPC treated water and stored at -80 ^{o}C. Using the Nanodrop ND 1000 Spectrophotometer (Nanodrop technologies) the quantity and quality of RNA was then assessed.

2.5.2: cDNA SYNTHESIS

cDNA synthesis was carried out using the High Capacity cDNA Archive Kit (Applied Biosystems and reverse transcription completed on a thermal cycler (PTC-2000, MJ systems) for 10 minutes at 25^{o}C followed by 120 minutes at 37^{o}C and 85^{o}C for 5 seconds. Each reaction contained 2 µg of RNA, reverse transcription buffer (1x), random primers (1x), 4 mM dNTPs, and 5 units of multiscribe, made up with DEPC treated water to a final volume of 20 µl. Post reaction the cDNA was diluted with DEPC treated water to 200 µl.

2.5.3: QUANTITATIVE PCR (qPCR)

After cDNA synthesis change in mRNA expression was assessed by real-time reverse transcription PCR using the Taqman PCR Master Mix kit (Abgene, Epsom, UK) and 7900HT Fast real time PCR system (Applied Biosystems). The mastermix for each reaction was made up of 2 µl cDNA and 1x Taqman primers made up to a final volume of 10 µl with DEPC treated water. Conditions for the PCR reaction were as follows: 2 minutes at 50 ^{o}C, 10 minutes at 10^{o}C after which there were 50 cycles, each consisting of 15 seconds at 95 ^{o}C and 1 minute at 60 ^{o}C.

2.5.4: QUANTIFICATION OF GENE EXPRESSION

For all qPCR assays the gene expression was normalized to the expression of HRPT1. Expression was quantified using the comparative CT method (Δ CT method), as per the formula below:

Target quantity = 2^ - ((CT RNA of interest) – (CT control RNA))

Comparisons were made between the number of cycles necessary for the level of fluorescence to reach a threshold that lay in the logarithmic phase. This method makes the assumption that the expression of the gene of interest and control gene are identical. Data is presented as fold change, compared to untreated at the earliest timepoint.

2.6: PROTEIN EXTRACTION AND ANALYSIS

2.6.1: PROTEIN EXTRACTION

Cells seeded onto 10 cm dishes were washed with ice cold PBS prior to lysis with 300 µl RIPA buffer (sigma). For every 10 mls of RIPA buffer prepared, 1x protease inhibitor tablet (Roche), 200 ul phosphatase cocktail 2 (Sigma) and 100 ul phosphatase inhibitor cocktail 3 (Sigma) were added. After scraping the 10 cm dish with a cell scraper the cell lysate was stored at -20 ^{o}C. Protein quantification was undertaken using the BioRad system (BioRad) in which absorbance was measured at 690 nm using a colorimetric plate reader for each sample in quadruplicate. Absorbance values were then compared to a standard curve generated from samples containing known concentrations of BSA.

2.6.2: PROTEIN ELECTROPHORESIS AND ANTIBODY DETECTION

Samples were spun down prior to use at 10,000 G for 10 minutes at 4 ^{o}C. NuPAGE® sample buffer (Invitrogen) was then added to each 30 µg protein sample (1:3) and the protein heat denatured at 95 ^{o}C for 5 minutes. Proteins were separated on precast NuPAGE® Bis-Tris gels by electrophoresis at 200 V for 50 minutes (1x NuPAGE® MOPS running buffer). Semi-dry transfer to a methanol activated PVDF membrane was then undertaken at 130mAmp per gel for 60 mins (1x NuPAGE® transfer buffer). After blocking with either low fat milk or 5% BSA in wash buffer (25 mM Tris, 150 mM sodium chloride, 2.8 mM potassium chloride and 0.05% Tween-20) the membranes were then incubated overnight at 4^{o}C with the primary antibody diluted appropriately again in wash buffer with either 5% low fat milk or 5% BSA. The following day the membranes were washed 3 times with wash buffer for 5 minutes and the appropriate HRP-conjugated secondary antibody was added for a 1 hour

incubation at room temperature. After 3 further washes with wash buffer, immunoreactivity was detected using ECL™ chemiluminescent reagent (Amersham) and visualised using the ImageQuant LAS 4000 digital imaging system (GE Healthcare).

2.7: IN VIVO EXPERIMENTS

All protocols were carried out under Home Office regulations. 6 - 8 week old female Balb-C nu/nu mice were injected into the mammary fat pad with 25 μl Matrigel (BD Bioscience) and 2.5 x10^6 MDA-MB-468 cells suspended in 25 μl serum free medium. Once greater than 50% of xenografts had reached a size greater than 150 mm^3 half the mice were treated with metformin in the drinking water (750 mg/kg/day). Tumour volume was calculated from the formula $V = L \times W \times H \times \pi/6$ (L = length, W = width, and H = height). Once tumors reached 1.44 cm^3, mice were sacrificed by cervical dislocation.

2.8: FLOW CYTOMETRY

2.8.1: BODIPY UPTAKE ANALYSIS

Prior to BODIPY uptake measurements, cells were seeded in 6 well plates, left to recover overnight, and then treated with metformin for 24 hours. At endpoint the cells were treated with the fluorescent palmitate analogue, 4,4-Difluoro-5,7-Dimethyl-4-Bora-3a,4a-Diaza-s-Indacene-3-Hexadecanoic Acid (BODIPY® FL C16, Invitrogen) for 15 minutes and then washed with PBS. After harvesting with trypsinisation the cells were fixed with 4% paraformaldehyde prior to re-suspension in PBS and then analysed using a FACSCalibur flow cytometer (BD Biosciences) and Cellquest software (BD Biosciences).

2.9: ELECTRON MICROSCOPY TECHNIQUES

Cells were harvested by trypsin digestion and fixed in 2.5% glutaraldehyde in phosphate buffer. After spinning down, pellets were washed, post-fixed in 1% osmium tetroxide, pre-embedding stained with 2% uranyl acetate, dehydrated and embedded in Spurr's resin (all from Agar Scientific, UK). Ultrathin sections were cut onto nickel grids, contrast enhanced with 2% uranyl acetate and lead citrate and viewed using a Joel 1010 electron microscope. Please note that after the initial sample preparation, images were taken by Prof David Ferguson.

2.10: GAS CHROMATOGRAPHY AND MASS SPECTROMETRY TECHNIQUES

2.10.1: PREPARATION OF SAMPLES

At experiment endpoint, cells were trypsinised and washed with PBS 3 times before being aliquotted in a 0.75 ml PBS cell suspension to pyrex 10 ml tubes. The number of cells per sample was counted using the Nexcelom Cellometer at this point in order to adjust results for cell number. Extraction of total lipids using the Folch solvent extraction method was the undertaken as follows. 7.5 ml of chloroform; methanol (2:1) was added to all tubes and 20 µl of diluted internal standard to all tubes. A blank tube was also treated as above using 0.75 ml 0.9% saline in place of cell suspension.

The tubes were then shaken vigorously by hand for 2 minutes prior to mixing on a rotary mixer for a further 15 minutes. Afterward 1.5 ml of 1 M sodium chloride was added to each tube and mixed before centrifugation for 10 minutes at 2000 rpm at 14 °C. The top aqueous phase was aspirated and discarded before the solvent phase was

transferred to another glass tube and evaporated to dryness in a concentration evaporator (Zymark) at 50 °C under nitrogen. 1 ml of chloroform was added to the dry lipid extract and the sample pulse vortexed to dissolve.

Separation of the triglyceride and phospholipid fractions of the lipid extract was then undertaken using pre-washed (with 2 x 1 ml acetone and then with 2 x 1 ml of chloroform) solid phase extraction aminopropyl columns (Varian Ltd, Oxford, UK). After the initial elute had dripped through into a glass collection tube a further 2 x 1ml chloroform was added, drawn through by suction. This elute was contained TG fatty acids and cholesteryl esters. Using a fresh collection tube 2 ml of 3:2 chloroform; methanol was drawn through by suction. This elute was used to analyse the non-acidic PL fraction from cells. These two different elutes were then dried down in the concentration evaporator (Zymark) at 50 °C under nitrogen.

The TG fatty acid/cholesteryl ester fraction was then separated by dissolving in 1 ml hexane and passing it through a new solid phase extraction column into a collection tube (pre-washed with 4 x 1 ml hexane). A further 2 washes of the extraction column with hexane were carried out. This elute contained cholesteryl esters. Using a new round bottomed 10 ml collection tube, the TG fatty acid fraction was eluted with 2 x 1 ml hexane:chloroform; ethyl acetate (100:5:5) under vacuum. The TG elute was then dried down in the concentration evaporator at 50 °C under nitrogen.

Methylation of the TG fraction was then carried out. 400 µl of toluene was added to each dried fraction prior to pulse vortexing after which 800 µl of 1.5% H_2SO_4 in methanol was added (6% H_2SO_4 in methanol for phospholipids). Samples were then

placed in a waterbath at 80°C for 1 hour (or 2 hours if phospholipids) after which they were removed and allowed to cool. Then 2 ml of neutralising solution (0.025 M potassium hydrogen carbonate and 0.025 M potassium) was added to each sample followed by 2 ml of cyclohexane. After mixing on a rotary mixer for 15 minutes the samples were centrifuged for 10 minutes at 2000 rpm at14 °C. Using a glass pipette, the upper solvent phase was transferred into a new glass tube dried down in the concentration evaporator at 50 °C under nitrogen.

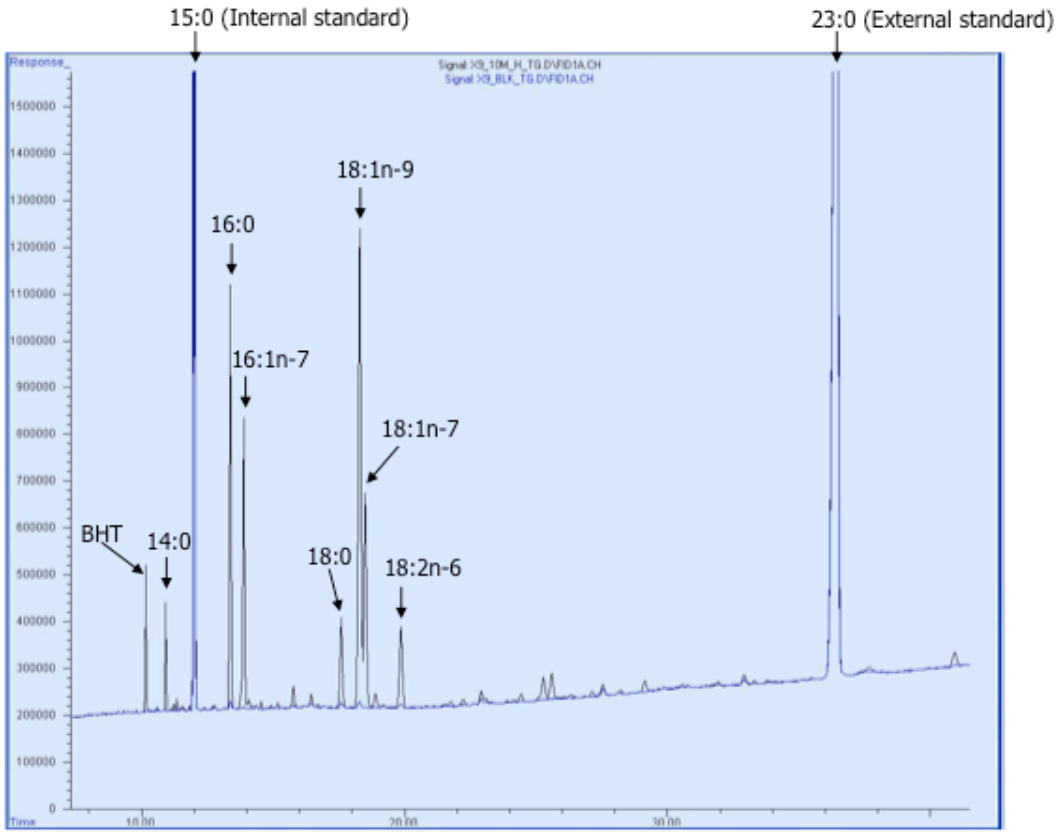


Figure 2.1: Example of a chromatogram. Chromatogram taken from a TG fatty acid profile of untreated MCF7 cells. Different peaks represent different fatty acids. The internal standard (C15:0 TG, 1mg/ml) and external standard (C17:0 TG, 1mg/ml) are marked.

2.10.2: GAS CHROMATOGRAPHY

Fatty acid methyl esters (FAMEs) of the isolated triglyceride fatty acids were prepared by incubating the samples for 1 hour at 800 ^{o}C with methanolic sulfuric acid. In order to allow quantification of fatty acids a 50 μg internal standard (C15:0 TAG) was added to each sample prior to Folch extraction whilst an external standard (50 μg C23:0 FAME) was added to each sample just before GC analysis. GC and mass spectrometry analysis was carried out using the Agilent 6890 system and individual fatty acid peaks identified by reference to known FAMEs from the internal standard. The addition of both an internal and external standard allowed the calculation of the percentage recovery of fatty acids (i.e. estimation of the loss of fatty acid during extraction.) The amount of fatty acid for each sample was then expressed in μg per 4 x 10^6 cells based on the cell count prior to extraction. An example of a chromatogram of triglycerides extracted from MCF7 cells is shown in **Figure 2.1**. **Please note that after initial sample collection, the preparation and running of the Gas Chromatography samples was carried out by Dr Jennifer Collins at the Oxford Centre for Diabetes, Endocrinology and Metabolism (OCDEM).** The figures in this thesis that include data obtained from these chroamtograms are Fig 3.8A & B, 4.1, 4.3B, 4.4A & B, 4.5A & B, 4.6 A, B &D, 4.7C, 4.9A, 4.10A, B &D and 4.11A.

2.10.3: USE OF STABLE ISOTOPES AND MASS SPECTROMETRY

Dulbecco's Modified Eagle's Medium was made up from powder to contain deuterated water to a total concentration of 0% or 5%. In separate experiments [U-13C] glucose (to 25 mM) or [U-13C] glutamine (to 4 mM) (both CK Gas) were added to media lacking these components. After extraction of triglyceride derived fatty acids (as above) GC-mass spectrometry using the Agilent 6890 system coupled to a 5973N

mass spectrometer (also from Agilent) was carried out. The mass to charge ratios were then measured using selected ion monitoring (i.e. only a limited range of the spectrum was analysed). Based on a method published by Lee et al, by calculating the relative abundance of each mass isoptomer (for each fatty acid) from the mass spectrum and correcting for the fact that only 5% of the water was deuterated, we were able to estimate the fraction of triglyceride that had deuterium atoms incorporated and hence was derived from de novo lipogenesis [239]. The fraction of TG fatty acid that did not have any deuterium atoms incorporated is described as 'exogenous' in the text. For the ^{13}C labeled glutamine, glucose and lactate experiments as all of the substrate within the media was labeled the assumption could be made that any ^{13}C containing TG was derived from the substrate in question. Note that after sample collection, the preparation and running of these samples was carried out by our collaborators at OCDEM.

2.11: LD540 STAINING

2.11.1: LD540 STAINING OF CELLS IN VITRO

MCF7 cells were seeded on sterile cover slips in 6 well plates overnight prior to treatment for 48 hours with 2mM metformin treatment. The cover slips were then removed and washed x3 in PBS after which they were incubated in the dark for 15 minutes with the LD540 (concentration dependent upon batch). After a 3 further washes with PBS the cover slips were mounted on slides using Vectashield mounting medium with DAPI. Z-stack images were then created with laser scanning confocal microscopy (Zeiss LSM510 Meta). To act as controls some untreated samples were placed in hypoxia for 48 hours and others had oleic acid to a concentration of 0.8μM

added for 24 hours prior to microscopy. See acknowledgments with regards to the sourcing of LD540.

2.8.2: LD540 STAINING OF XENOGRAFT SECTIONS

Tumours were then snap frozen in liquid nitrogen. Frozen sections were cut from xenografts and mounted on slides by Mr Graham Steers. The slides were then incubated in the dark for 15 minutes with LD540 (concentration dependent upon batch). After the slides were washed 3 times with PBS, cover slips were mounted onto the slides using Vectashield mounting medium with DAPI. A Zeiss Axio Observer Z1 inverted epifluorescence microscope was used to capture images of the (less necrotic) periphery of the tumour. The area staining for lipid with LD540 was then defined as a percentage of the area staining for DAPI using image analysis software (Image J). See acknowledgments with regards to the sourcing of LD540.

2.12: IMMUNOHISTOCHEMISTRY TECHNIQUES FOR CLINICAL STUDY

2.12.1: CELL PELLET GENERATION FOR VALIDATION AND CONTROLS

In order to validate the antibodies to be used for immunohistochemistry in the clinical study treated cell pellets were generated to a) determine the optimum conditions for each antibody and b) act as controls for each staining run with the clinical samples. To generate the cell pellets, the MCF7 (for pAMPK and pS6) and SKBR3 (for pEIF4-BP1) breast cancer cell lines was treated in vitro with conditions designed to either upregulate or downregulate expression of the antigen of interest. Briefly, 3 x 10^6 MCF7 cells were seeded on 10 cm dishes and left to recover overnight. The following

morning the media was changed to contain either 250 μM AICAR, 20 μM Compound C, or 10/100 nM everolimus. After 24 hours the cells were washed with PBS, trypsinised and washed with PBS again before being fixed in 4% paraformaldehyde and left overnight. The following day the cells were embedded in paraffin wax in the Oxford University Hospitals Department of Histopathology.

2.12.2: SUMMARY OF IMMUNOHISTOCHEMISTRY ANTIBODY OPTIMISATION

The protocols for immunohistochemical staining were adapted from previously published studies [120, 240]. Using protein lysates generated under the same conditions as the cell pellets western blotting was carried out to demonstrate the appropriate effect on protein expression in the same cell lines **(Figure 2.2 – 2.4)**. Once this had been demonstrated, sections cut from the cell pellets were tested on a Leica Bond-max autostainer by Ms Leticia Campo in the GCP laboratory, Department of Pharmacology, University of Oxford under various staining conditions – see below for the different conditions tested for each antibody. Once the antibody had been optimised in this way it was tested on a tissue microarray which included examples of normal breast tissue and sections from different breast cancers in order to ensure that there was differential staining between clinical breast samples. The quality of immuno-staining was reviewed throughout this process by myself, Dr Helen Turley and Dr Cameron Snell.

During the final staining run the cell pellets generated during the antibody optimisation process were used as controls along with one section stained with a non-

immune immunoglobulin of the same isotype. For the Ki67 staining, tonsil samples were used as controls.

2.12.3: VALIDATION OF pAMPK ANTIBODY

The antibody of interest was Phospho-AMPKα (Thr172) (Cell signaling #2535). MCF7 cells were treated with either 20 μM Compound C (negative control) or 250 μM AICAR (positive control) for 24 hours prior to harvesting and generation of a formalin fixed, paraffin embedded cell pellet block. After sections were cut the following conditions were tested on the Leica Bond-max autostainer:

Primary antibody dilutions tried: 1 in 25 to 1 in 4000

Antigen retrieval times: 20 minutes vs 40 minutes

Antigen retrieval pH: pH6

Optimised conditions chosen see **(Figure 2.2A-C)**:

Antigen retrieval: **ph6, for 40 mins**

Primary antibody: **1 in 200, for 1 hour**

2.12.4: pS6 STAINING VALIDATION

The antibody of interest was Phospho-S6 Ribosomal protein (Sr235/236) (Cell signaling #2211). MCF7 cells were treated either with 100 nM Everolimus (negative control) or were left untreated for 24 hours prior to harvesting and generation of a formalin fixed, paraffin embedded cell pellet block. After sections were cut the following conditions were tested on the Leica Bond-max autostainer:

Primary antibody dilutions tried: 1 in 100 to 1 in 4000

Antigen retrieval times: 20 minutes vs 40 minutes

Antigen retrieval pH: pH9

Optimised conditions chosen **(Figure 2.3A-C)**:

Antigen retrieval: **ph9, 40 mins**

Primary antibody: **1 in 600, for 1 hour**

2.12.5: pEIF4-BP1 STAINING VALIDATION

The antibody of interest was Phospho-4E-BP1 (Th70) Antibody (Cell signaling #9455). SKBR3 cells were treated with 10 nM Everolimus (negative control) or were left untreated for 24 hours prior to harvesting and generation of a formalin fixed, paraffin embedded cell pellet block. After sections were cut the following conditions were tested on the Leica Bond-max autostainer:

Primary antibody dilutions tried: 1 in 100 to 1 in 3200

Antigen retrieval times: 40 minutes

Antigen retrieval pH: pH6 vs pH9

Optimised conditions chosen **(Figure 2.4A-C)**:

Antigen retrieval: **pH6 40 mins**

Primary antibody: **1 in 100, for 1 hour**

2.12.6: KI67 STAINING

This antibody had previously had had the optimum conditions determined in the GCP laboratory.

2.12.7: COLLECTION OF BIOPSIES FOR IMMUNOHISTOCHEMISTRY AND HANDLING

After biopsy, breast tumour samples were immediately placed in a cassette and submerged in 30 – 50 mls of 10% formalin in a standard biopsy pot and then left at RT for 24-72 hours. The biopsy sample was then removed from the formalin and placed in 70% ethanol. Samples were then transferred to the GCP laboratory, Department of Pharmacology, University of Oxford where the biopsy was immediately embedded in a paraffin block. After sections were cut staining was carried out on a Leica Bond-max autostainer.

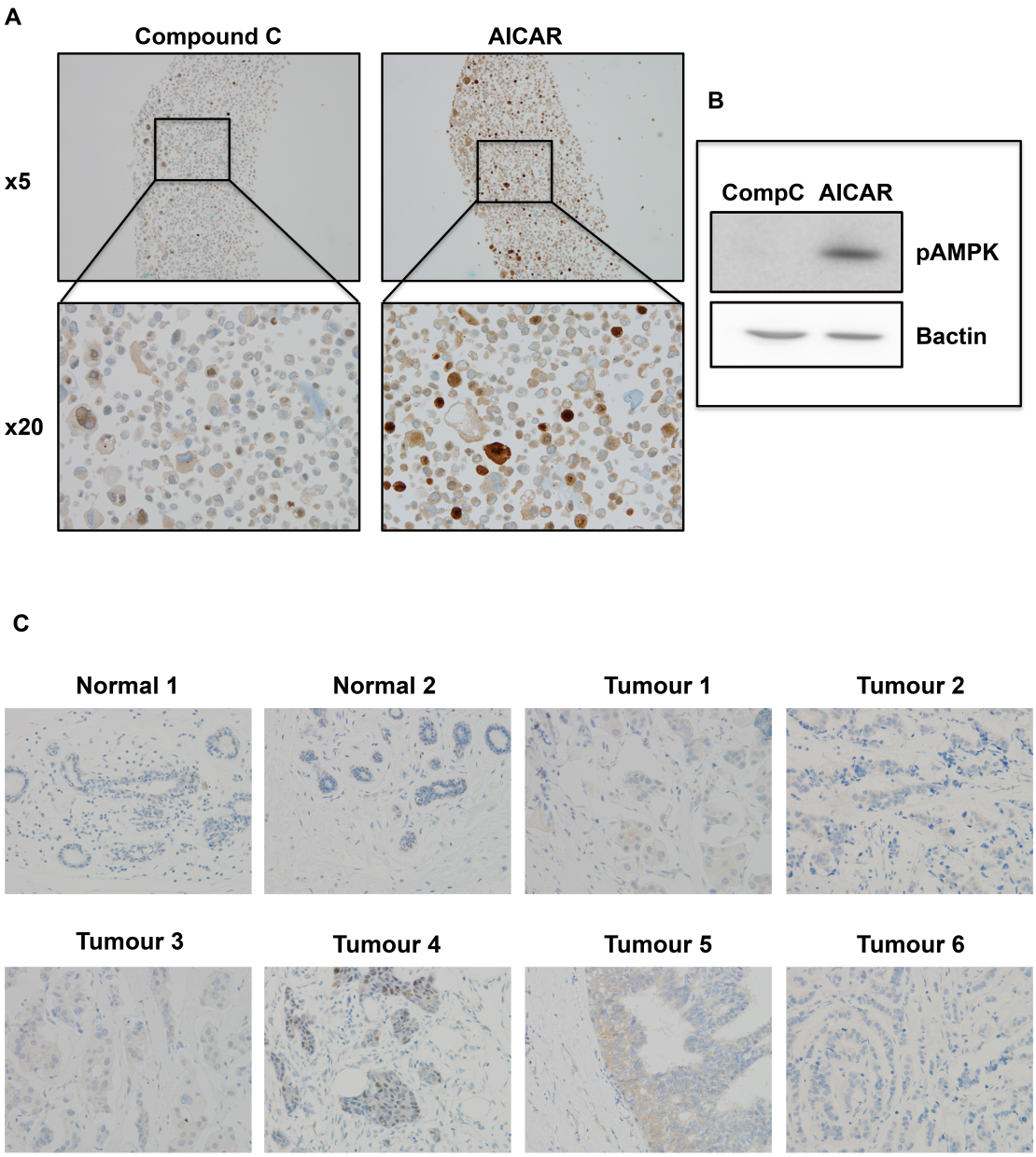


Figure 2.2A: Example of pAMPK staining of Compound C and AICAR treated MCF7 cell pellets. **B:** Western blot of MCF7 cell lysate to confirm activation of AMPK with AICAR treatment **C:** Staining of normal and breast cancer tissue TMA to confirm differential staining between tissue.

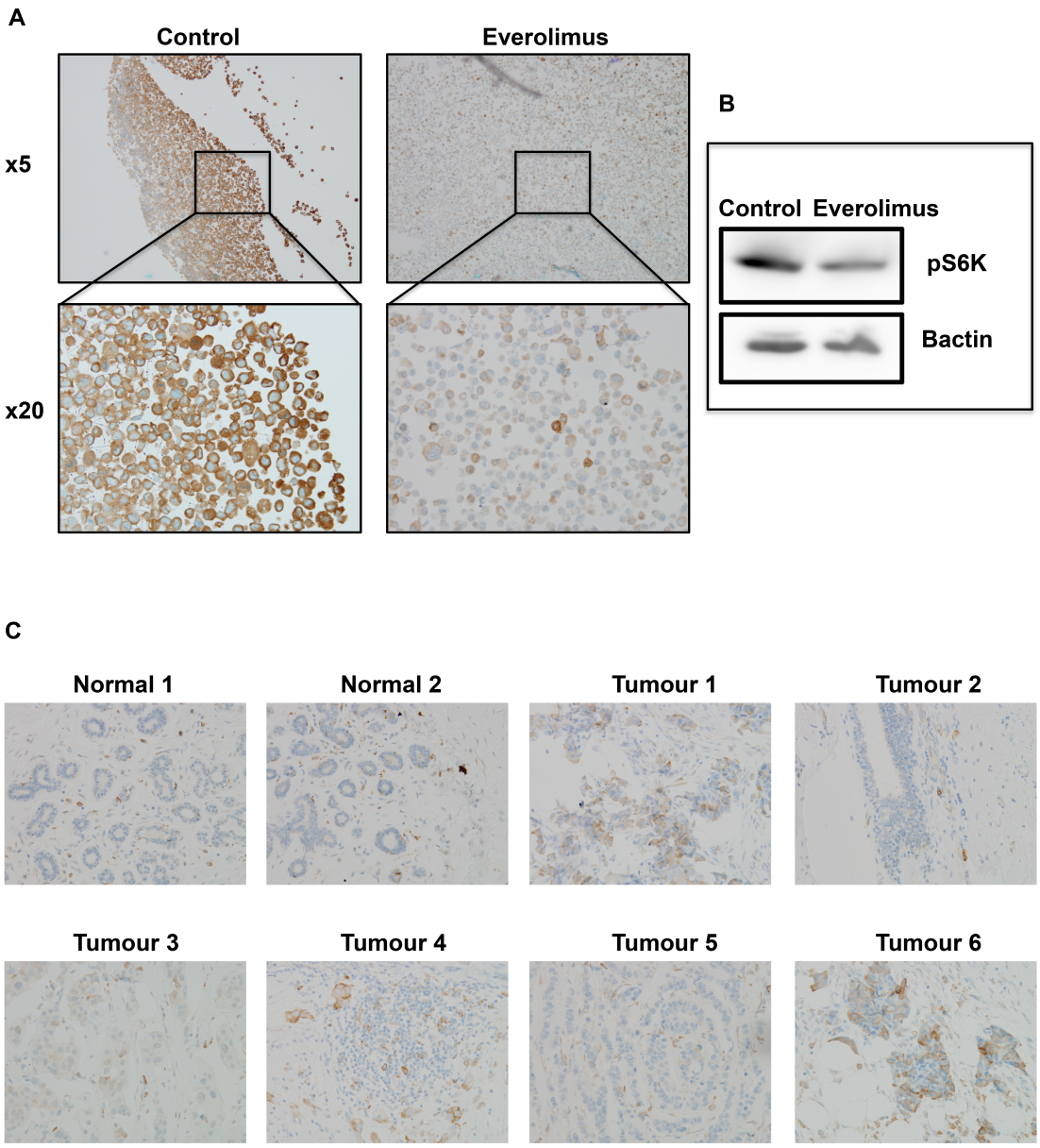


Figure 2.3A: Example of pS6 staining of Control and Everolimus treated MCF7 cell pellets. **B:** Western blot of MCF7 cell lysate to confirm inhibition of phosphorylation of S6 with Everolimus treatment **C:** Staining of normal and breast cancer tissue TMA to confirm differential staining between tissue.

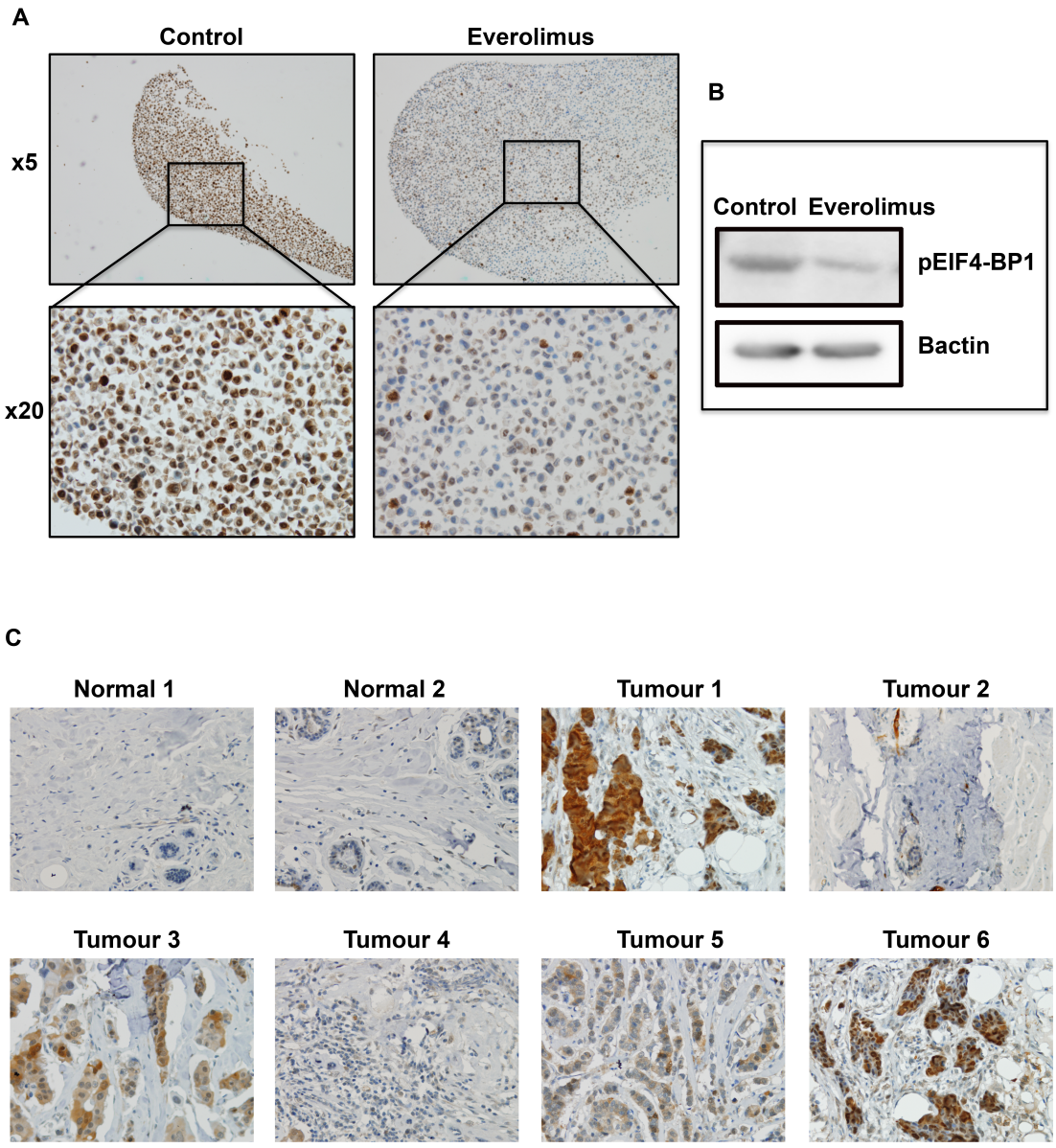


Figure 2.4A: Example of p4E-BP1 staining of Control and Everolimus treated SKBR3 cell pellets. **B:** Western blot of SKBR3 cell lysate to confirm inhibition of phosphorylation of 4E-BP1 with Everolimus treatment **C:** Staining of normal and breast cancer tissue TMA to confirm differential staining between tissue.

2.13: ANALYSIS OF ^{18}[F]-FDG PET-CT SCANS

2.13.1: PET-CT PROTOCOL

The PET-CT tracer, 2-deoxy-2-(18F)fluoro-D-glucose (^{18}[F]-FDG), was used for all examinations. Prior to scanning, patients were fasted overnight for at least 8 hours but could drink water. The patient's blood glucose was checked just prior to the scan with a portable blood glucose monitor to ensure it was <7mmol/L. All scans (for the preliminary analysis presented in this thesis) took place on a General Electric Discovery 690 STE 16-slice PET-CT system. Patients had a cannula sited in their antecubital fossa and lay supine in the PET-CT scanner. A dynamic acquisition of the breast tumour (and any lymph nodes within the field of view) was initiated, followed by injection of ^{18}[F]-FDG (3 MBq/kg, up to a maximum of 400 MBq) and scanning for a further 45 minutes. 50 minutes after injection, a 30 minute static scan was performed from skull base to mid-thigh, with the expectation that the primary breast cancer was scanned at 60 minutes post injection (**Table 2.1**). A 3D acquisition was carried out using filter back projection for the dynamic scan and an iterative reconstruction for the static scan. Attenuation CT scans were performed for both the dynamic and static PET acquisitions.

Patient preparation	
Patient preparation	Fasted for 8 hours plus, good hydration, no water preceding 60 min, voided just beforehand. Patient arms down on scanner for both dynamic and static scans.
CT	
CT parameters	Ultra-low-dose CT purely for attenuation correction (120 kV, 30 mA)
PET	
Radiopharmaceutical	^{18}[F]-FDG
Coverage	Dynamic PET volume to cover tumour only. Static PET volume from skull base to mid-thigh (start at skull base).
Injected Activity	3 MBq/kg (Up to a maximum of 400 MBq) 6 ml volume injected as bolus over 30s 30 seconds post dynamic PET acquisition start
Uptake time	Dynamic study: minimum of 45 minutes Static study: starts at 50 min post injection so that tumour is scanned at 60 min
Dynamic frames	List mode used prior to rebinning Series Name: AIF 1 x 30 sec 60 x 1 sec 12 x 10 sec Series: Kinetic 1 x 30 sec 12 x 5 sec 6 x 10 sec 5 x 30 sec 10 x 1 min 6 x 5 min
Static acquisition	4 minute acquisitions
Fields of view	50cm
Reconstruction parameters	2 iterations 24 subsets Matrix size 128 x 128

Table 2.1: Summary of ^{18}[F]-FDG PET-CT protocol for both static and dynamic scans

2.13.2: ANALYSIS OF STATIC PET-CT

The static PET-CT images were examined independently by 2 radiologists. After a volume of interest (VOI) was drawn around the primary tumour or metastasis, the standardized uptake value (SUV) was calculated using Hermes Medical Solutions® software. This value ($SUV = Q \times W/Q_{inj}$) is a semi-quantitative measure of ^{18}[F]-FDG uptake derived from the volume of interest activity (Q), injected activity (Q_{inj}) and body weight (W). It represents the ratio of image derived radioactivity concentration found in the VOI at a particular point in time relative to the radioactivity distributed across the entire body. For the static scans, SUV_{max} was used in which the image voxel with the highest activity in the VOI is taken as the measure of ^{18}[F]-FDG uptake. This has the advantage in assessing treatment response of minimising operator variability in determining the VOI.

Lean body mass (LBM) was used to determine 'W' as this has been shown to give less variation in calculating the SUV than using the patient's weight [241]. LBM was determined using the following equations:

LBM = 0.32810 x Weight + 0.33929 x height – 29.5336 (for male)

LBM = 0.295669 x Weight + 0.41813 x height – 43.2933 (for female)

2.13.3 ANALYSIS OF DYNAMIC PET-CT

Kinetic modeling in which the rate of glucose uptake and phosphorylation over time (usually expressed as Bq/ml or Bq/cc) is determined is a more quantitative method of assessing ^{18}[F]-FDG dynamics. For a fully quantifiable kinetic analysis to be performed an estimation of the delivery of ^{18}[F]-FDG to the tumour site via the

arterial supply needs to be made, known as the arterial input function (AIF). The most rigorous method of determining the AIF is by arterial blood sampling allowing measurement of blood ^{18}[F]-FDG concentrations during the scanning period. Given the burden of investigations for participants involved in this study and hence the ethical and the logistical considerations of arterial blood sampling an alternative, non-invasive, method was used to calculate the AIF. This involved drawing VOIs over the left ventricle on the images themselves i.e. an image-derived input function. In generating the arterial input function it is important to use as large a vascular volume as possible as this reduces noise and spillover effects due to the finite resolution of the detector. The dynamic study was carried out at the same sitting as the static study with the uptake of ^{18}[F]-FDG into the primary breast cancer (and any metastatic lymph nodes at the same level) measured over a 45 minute period (**Table 2.1**). After the VOI had been defined by Dr Neel Patel for each frame using Hermes Medical Solutions® software and modeling by Dr Dan Liu, an ^{18}[F]-FDG time activity curve (TAC) was calculated (example - **Figure 2.5**). Further modeling allowed for the calculation of kinetic parameters including K_1 (an estimate of ^{18}[F]-FDG influx rate from carrier blood to tumour cells), k_2 (an estimate of ^{18}[F]-FDG efflux from tumour intracellular pool back to blood), k_3 (an estimate of ^{18}[F]-FDG phosphorylation rate in tumour cells), k_4 (an estimate of ^{18}[F]-FDG dephosphorylation rate in tumour cells) and Vb (an estimate of the fractional blood volume in the tumour VOI). The rate of FDG transfer from the blood through to intracellular phosphorylation can be approximately described using the compound parameter, Ki (or flux) determined by the following equation: (K1 * k3) / (k2 + k3).

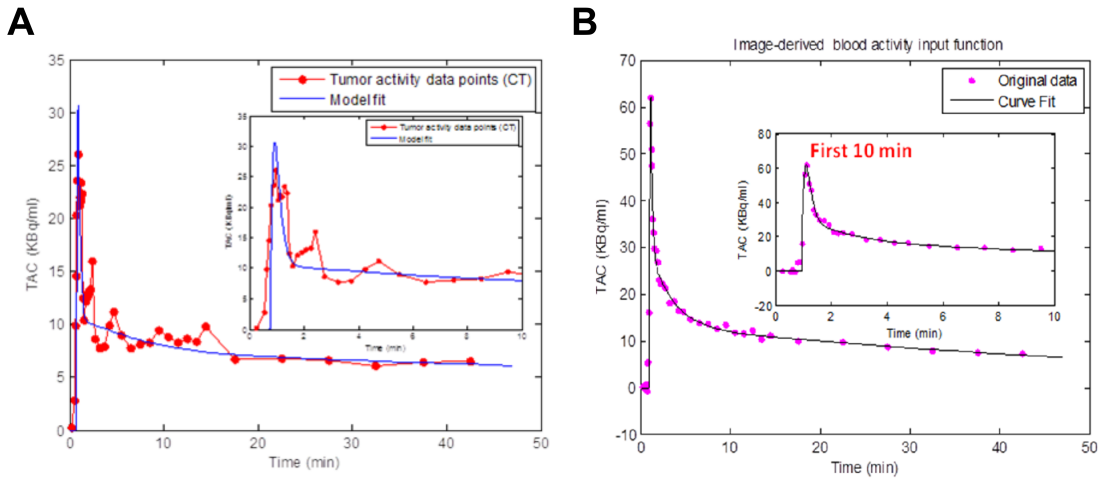


Figure 2.5A: Example of a dynamic PET-CT ^{18}[F]-FDG time activity curve (both the 10 and 45 minute time frames shown). **B:** Example of an arterial input function curve (both the 10 and 45 minute time frames shown).

2.14: GENE SEQUENCING OF BREAST BIOPSY SAMPLES

2.14.1: COLLECTION OF BIOPSIES AND HANDLING

After biopsy, breast tumour samples were immediately placed in RNAlater™ and then left at 4 °C for 24-72 hours prior to the sample being removed from RNAlater™ and placed in a new cryovial. Samples were then stored at -80 °C until time of RNA extraction and processing.

2.14.2: RNA PREPARATION FROM BIOPSY SAMPLES

Stored cryovials were thawed on ice prior to the biopsy sample being placed on a sterile petri dish (on ice). The sample was then cut up as small as possible using a sterile RNase free scalpel and the pieces of tumour placed in 1ml of Tri reagent (Sigma) in a 50ml tube (Corning) on ice and homogenised using a hand held Turrax T8 homogeniser probe (Ika). In order to remove RNases the homogenisor probe had been prewashed via 2 x 10 second pulses in 1 M sodium hydroxide preceeding 3

further washes in DEPC treated water. Following homogenisation Tri reagent/tumour samples were then transferred to RNase free 1.5 ml microfuge tubes, left for 10 minutes at room temperature, before being spun at 10,000 G in a centrifuge for 10 minutes at 4 °C and the supernatant removed and placed in a new 1.5 ml microfuge tube, leaving the cellular debris. RNA extraction was then carried out as per *section 2.5.1* and samples stored at -80 °C until analysis.

2.14.4: QUANTIFICATION AND QUALITY CONTROL OF SAMPLES

A Nanodrop ND 1000 Spectrophotometer (Nanodrop technologies) was used to quantify the RNA. The RNA integrity number (RIN) was also assessed as a measure of the RNA quality using the RNA 6000 Nano-chip system (Agilent technologies) and Agilent 2100 Bioanalyser (Agilent technologies). **Figure 2.2A** shows the typical spectrophotometer trace obtained and **Figure 2.2B** the spread of RNA quality obtained for the first 24 paired samples analysed.

2.14.5: NEXT GENERATION SEQUENCING OF SAMPLES

After RNA extraction, for each sample, 14 µl of RNA was prepared at a concentration of 250 ng/µl with each sample aliquotted into the wells of a fully skirted 96-well plates (Thermo Scientific) sealed with a thermo PCR adhesive seal (Thermo Scientific). Next generation sequencing of 'Poly (A) targeted' mRNA, including library preparation, was then carried out by the Oxford Genomics Centre core facility at the Welcome Trust Centre for Human Genetics as a service. The NEBNext mRNA Library Prep Master Mix Set (New England Biolabs) was used for preparation of the expression libraries and the Illumina HiSeq 2000 system used to carry out the sequencing.

2.15: CLINICAL SERUM METABOLIC MARKERS

All blood samples were taken in the morning after an overnight fast (8 hours) and the samples handled as per the following protocols:

2.15.1: SERUM SAMPLE FOR GLUCOSE, INSULIN, IGF-1, IGF-2, IGF-BP-3, C-PEPTIDE, LACTATE AND LEPTIN

1. 20 mL of blood in 2 appropriately labelled 10 ml serum tubes was collected and the tubes gently inverted 8 times to mix the contents.
2. Sample processing:
    a. After allowing 30 to 120 minutes for the blood to clot at room temperature the sample was centrifuged at 2000 G for 10 minutes.
    b. The separated serum was immediately transferred to a 15 ml conical tube with a disposable pipette and then aliquotted (500 µl) into cryovials prior to freezing at -80 ^{o}C.

2.15.2: EDTA SAMPLE FOR HDL, TOTAL CHOLESTEROL AND TRIGLYCERIDES

1. 30mL of blood in 3 appropriately labelled 10ml EDTA tubes was collected and the tubes gently inverted 8 times to mix the contents.

2. Sample processing:

a. Within 30 minutes of taking the blood sample the sample was centrifuged at 1000G at room temperature for 10 minutes.

b. The separated clear plasma was immediately transferred to a 15ml conical tube with a disposable pipette and then aliquotted (500µl) into cryovials prior to freezing at -80^{o}C.

2.15.3: PROCESSING OF SERUM AND EDTA SAMPLES

According to local protocols the glucose, insulin, C-peptide, lactate, HDL, total cholesterol and triglyceride assays were carried out at the John Radcliffe Hospital, Department of Clinical Biochemistry. The IGF-1, IGF-2 and IGF-BP-3 assays were carried out at the BMS2 SAS Peptide Hormone Section, Clinical Laboratory, Royal Surrey County Hospital and the leptin assay at the Core Biochemical Assay Laboratory, Clinical Biochemistry, Cambridge University Hospitals NHS Trust.

2.16: STATISTICAL METHODOLOGY

2.16.1: DATA FROM IN VITRO AND IN VIVO MODELS

The Prism™ software package was used for all analyses. All error bars represent the standard error of the mean unless stated. An unpaired T-test was used in all cases unless stated.

2.16.2: BIOINFORMATIC ANALYSIS OF GENE SEQUENCING DATA

Analysis of the mRNA gene sequencing data was carried out by Dr Francesca Buffa as described below. FASTQC (http://www.bioinformatics.babraham.ac.uk) quality control was performed. FastQC provides summary statistics and quality control checks on raw sequence data. Total sequences and sequence quality scores were

considered as the main criteria, with default thresholds for rejection; when residual adaptor sequences were detected they were clipped using Trimmomatic (http://www.usadellab.org). Mapping and alignment were done using Bowtie2 and TopHat2 (http://tophat.cbcb.umd.edu/). TopHat2 is a fast splice junction mapper for RNA sequencing reads; specifically, it aligns the reads to mammalian-sized genomes using the short read aligner Bowtie2, and then analyzes the mapping results to identify splice junctions between exons. Paired pre- and post-treatment samples for each patient were processed using Cuffdiff (http://cufflinks.cbcb.umd.edu) for transcript assembly and quantification of gene expression changes. Ensemble gene IDs were used as reference. Genes were ranked by their differential gene expression as estimated by Cuffdiff; rank product was used to merge samples from different patients and to call the significantly up- and down-regulated genes over the patient cohort. False discovery rate was estimated using the Bioconductor *rankprod* package (http://www.bioconductor.org/packages/2.13/bioc/html/RankProd.html) and a false discovery of 5% was considered as threshold to call a gene significantly up- or down-regulated. The rank product non-parametric approach was chosen because it has been previously shown to be effective and robust relative to other parametric approaches, particularly in cases where the sample size (i.e. the size of the clinical cohort) is not large. However, the effect size (i.e. the level of differential expression) in this approach is lost and it does not provide a general framework where covariates can be included. Further work on both the analyses and methods is ongoing to address these issues, although the size of the cohorts limits the number of covariates that can be considered in this specific case.

Pathway analyses were then performed using the Genecodis 3.0 (http://genecodis.cnb.csic.es/) program that identifies those annotations that are overrepresented within a group of genes with respect to a reference set of genes (e.g. those relevant to the glycolysis pathway) [242-244]. The hypergeometric distribution method was chosen to compute the p values in the Genecodis analysis. The universe was set to Ensembl genes and a false discovery rate of 5% was chosen as the threshold to call the enrichment in a specific pathway/annotation significant.

2.16.3: IMMUNOHISTOCHEMISTRY DATA

Quantitative scoring of the staining of complete tumour sections was evaluated using high power fields and carried out by Dr Russell Leek. For Ki67 the percentage of cells with nuclear staining in at least 3 separate areas of a section were assessed and the mean taken. For the pAMPK, pS6 and p4E-BP1 antibodies the intensity of the immunostaining was classified into 4 categories: 0, no immunostaining present; 1, weak staining; 2, moderate staining; and 3, strong staining and the percentage of positive cells at each intensity was then classified into 4 groups; 1 (0-10% positive cells), 2 (11% to 50% positive cells), 3 (51% to 80% positive cells) or 4 (81 to 100% positive cells). The H-score of immunoreactivity was obtained by multiplying the intensity and percentage scores. Paired ‘pre-metformin’ and ‘post-metformin’ samples were analysed using the paired t-tests.

CHAPTER 3: METFORMIN ALTERS SUBSTRATE UTILISATION IN BREAST CANCER CELLS

3.1: INTRODUCTION

3.1.1: CURRENT UNDERSTANDING OF METFORMIN'S DIRECT (INSULIN INDEPENDENT) EFFECTS ON CANCER CELLS

A series of papers published a decade ago presented good evidence that metformin inhibits Complex 1 of the mitochondrial respiratory chain [123, 124, 245]. The energy stress subsequent to TCA cycle interference has been shown, in both in vitro and in vivo models, to activate AMPK and this activation has been linked to its anticancer effect [48]. In generality, AMPK activation leads to the upregulation of catabolic ATP-generating pathways, such as glycolysis and fatty acid oxidation, and the inhibition of anabolic ATP-consuming pathways, for example fatty acid and protein synthesis [107]. In cancer cells metformin has been shown to inhibit mTOR signalling leading to a net reduction in global protein synthesis and this has been associated with its anti-proliferative effect [59].

3.1.2: GLUCOSE, GLUTAMINE AND THE CANCER PHENOTYPE

The best characterised metabolic change in malignant cells is the 'Warburg effect' i.e. increased aerobic glycolysis, despite the presence of ample oxygen. Glycolysis generates ATP with lesser efficiency than oxidative phosphorylation but at a faster rate and it had previously been hypothesised that this faster rate might be beneficial to

proliferating cancer cells. Alternatively, mitochondrial dysfunction in cancer cells had been postulated as the primary reason for this phenotype. However, many studies have now suggested that mitochondria are the primary source of ATP in cancer cells [246] and it is not currently thought that somatic mutations of mitochondrial DNA are critical for tumorigenesis [247]. Rather, it seems that it is the need of cancer cells to feed glucose carbons toward the biosynthesis of fatty acids, nucleotides, amino acids and NADPH that drives the glycolytic rate [136]. An oxidative/mitochondrial stress toward the TCA cycle is therefore liable to disrupt this flow of glucose carbons [150, 151] (**Figure 3.1**).

It has long been known that tumour cells metabolise glutamine at significantly greater rates than any other amino acid [147] but interest in the role of glutamine in supporting cancer cell proliferation and the potential of glutamine metabolism is relatively recent. Much of this interest has stemmed from the discovery that the proto-oncogene Myc plays a role in the regulation of glutamine metabolism. Myc transformed cells have been shown to be especially sensitive to glutamine withdrawal [156] and subsequently it has been demonstrated that Myc induces the gene expression of several enzymes involved in glutamine metabolism [233]. The importance of glutamine in supporting cancer cell proliferation and providing carbon for lipid synthesis has been shown to be of greater importance at times of mitochondrial stress with the reductive carboxylation pathway allowing glutamine to bypass the TCA cycle in its conversion to citrate [151]. Two key enzymes of the glutaminolysis pathway, glutaminase and glutamate dehydrogenase, have been shown to be potential therapeutic targets in cancer cells [248, 249] (**Figure 3.1**).

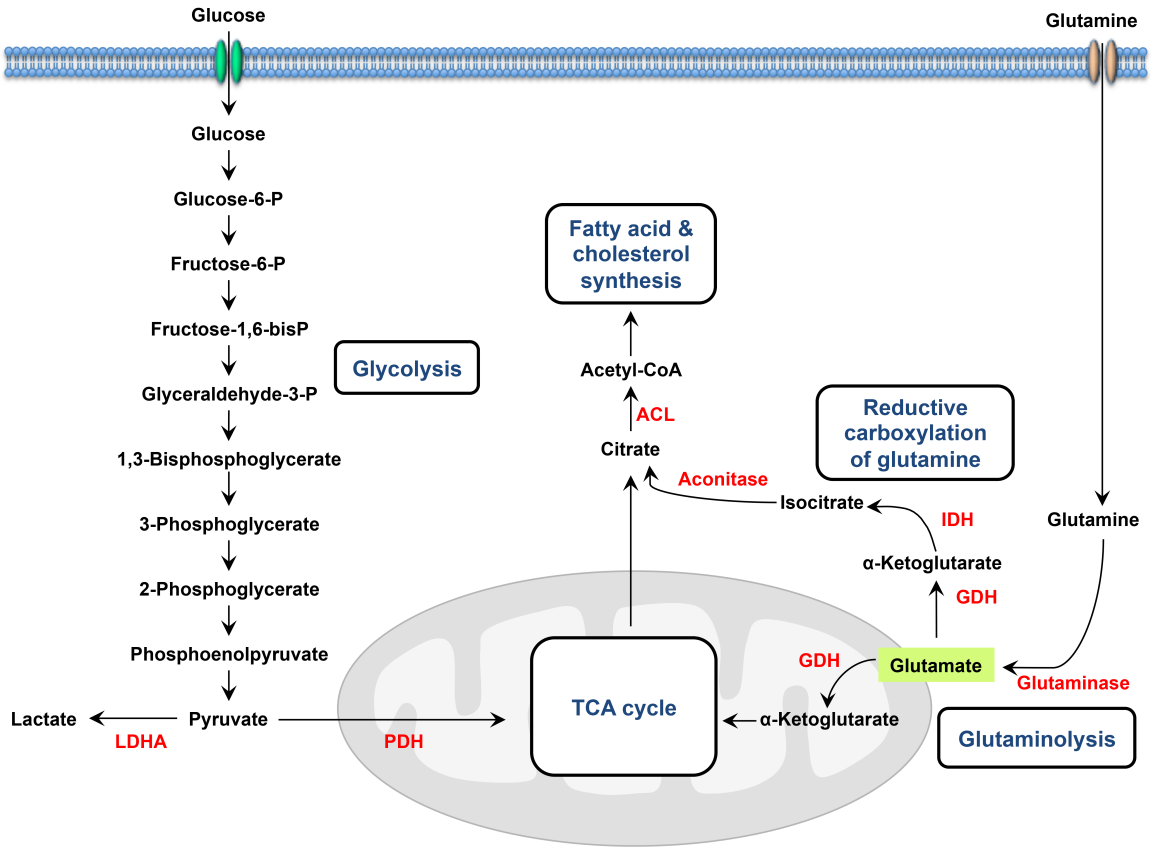


Fig 3.1: Overview of how glucose and glutamine carbons feed into the TCA cycle and subsequently lipid and cholesterol synthesis. A mitochondrial insult will disrupt the TCA cycle and consequently aerobic glycolysis becomes more essential for the generation of ATP. Glutamine's role as a substrate for lipid biosynthesis increases as it can be shunted via the reductive carboxylation pathway away from the TCA cycle and to citrate. Abbreviations: ACL, ATP citrate lyase; GDH, Glutamate dehydrogenase; IDH, Isocitrate dehydrogenase; LDHA, Lactate dehydrogenase A; PDH, Pyruvate dehydrogenase.

3.1.3: AIMS

At the outset, the focus of this DPhil project was to develop a neoadjuvant clinical study of metformin's effects on breast cancer metabolism. Laboratory work was designed to be carried out along side this so that the observed in vitro effects of metformin on breast cancer cell metabolism could be later correlated in the clinical samples. Hence the initial aim of the in vitro project was to: a) develop an in vitro breast cancer model and check that it functioned in a similar vein to that already described in the literature; b) assess metformin's effect on substrate utilisation and its relevance to breast cancer cell proliferation, and c) explore potential therapeutic strategies dependent on the above that might be taken forward in future clinical studies.

3.2: RESULTS

3.2.1: EFFECT OF METFORMIN ON THE PROLIFERATION OF A PANEL OF BREAST CANCER CELL LINES

As discussed in the introduction, many published studies using cell lines from different cancer types have demonstrated an anti-proliferative effect for metformin in vitro. As a first step, in order to determine a working dose, the proliferation of 2 breast cancer cell lines (MCF7 and MDA-MB-468) that had been demonstrated in the literature to be especially sensitive to metformin and one particularly resistant (MDA-MB-231) was investigated. After exposure to progressively inccreasing doses of metformin up to 400mM in DMEM supplemented with 25mM glucose and 4mM glutamine over 48 hours an SRB assay was carried out. Dose response curves were generated and it was apparent that in the MCF7 (IC50 = 35mM) and MDA-MB-468 (IC50 = 9mM) cell lines inhibition of proliferation in vitro occurred from doses of metformin of approximately 1mM and in the MDA-MB-231 cell line (IC50 = 118mM), 10mM (**Figure 3.2A**). These doses were consistent with previously published data [46, 60].

To further assess heterogeneity of response between different cell lines the effect on proliferation by metformin at doses of 2mM and 10mM on a panel of 6 different breast cancer cell lines was investigated using cell counts taken at the 96 hour timepoint. This panel of cell lines included 3 ‘triple receptor negative’ cell lines and 3 oestrogen receptor positive cell lines. Again this experiment was carried out using DMEM supplemented with 25mM glucose and 4mM glutamine and the media was changed on a 24 hourly basis

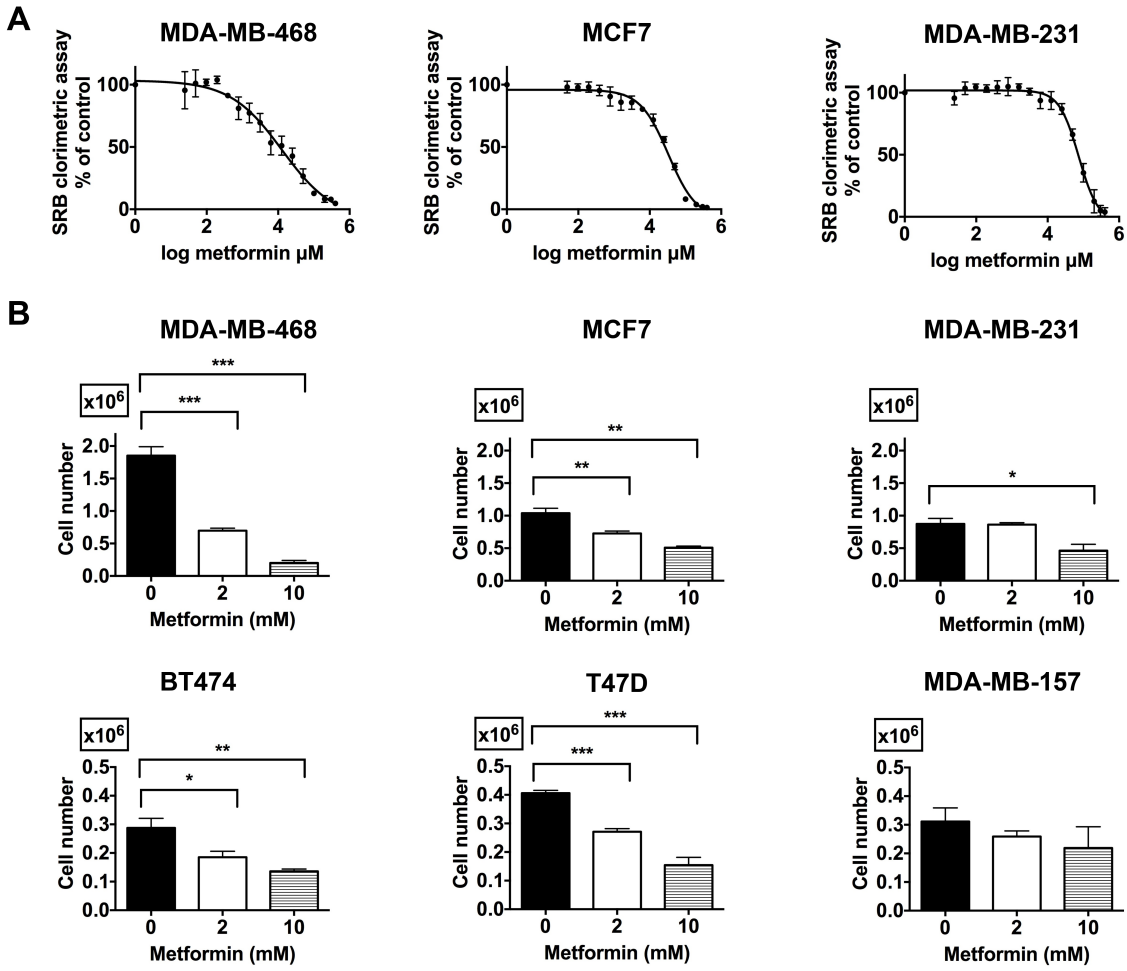


Fig 3.2A: SRB dose response curves to establish working doses of metformin in the MDA-MB-468 (IC50 9mM), MCF7 (IC50 35mM) and MDA-MB-231 (IC50 118mM) cell lines (n=4). **B:** Effect of 2mM and 10mM metformin on cell number at 96 hours in 2D in vitro culture (n=4). Data shown are mean ± SEM *p < 0.05; **p < 0.01; ***p < 0.001.

in order to avoid the media becoming nutrient deplete. Consistent with the SRB IC50 data, metformin's effect on proliferation, at the 2mM dose, was greatest in the MDA-MB-468 cell line (3 fold decrease, $p < 0.001$), but also significantly inhibited the growth of the MCF7, BT474, and T47D cell lines whilst there was no effect in the two most resistant cell lines, MDA-MB-231 and MDA-MB-157. At a concentration of 10mM metformin there was a statistically significant inhibitory effect on the proliferation of all 6 cell lines except for MDA-MB-157 (**Figure 3.2B**). There was no clear relationship between oestrogen receptor positivity and response.

In summary, for this panel of breast cancer cell lines there was a range of sensitivities to metformin in terms of the antiproliferative effect. In view of these findings 3 cell lines were chosen for further study: the sensitive MCF7 and MDA-MB-468 cell lines and the resistant MDA-MB-231 cell line.

3.2.2: METFORMIN AND ACTIVATION OF AMPK IN MCF7 CELLS

Metformin has been shown to activate AMPK in MCF7 cells in a dose dependent manner with activation seen from metformin concentrations of 5mM [59]. Given that effects on proliferation had been seen at a dose less than this (2mM), and in order to confirm that the MCF7 model in this study conformed to the literature, MCF7 cells were treated with 2mM and 10mM metformin for 6 to 24 hours in DMEM supplemented with 10% FCS and 25mM glucose under normoxic conditions. Immunoblotting of protein after cell lysis at the 6, 24 and 48 hour timepoints revealed increased phosphorylation of AMPK with 10mM metformin but not at the 2mM metformin dose, but solely at the 6 hour timepoint (**Figure 3.3A**). A commonly used surrogate marker of AMPK activation is its downstream target, phosphorylated Acetyl CoA Carboxylase (pACC), and a corresponding increased expression of this marker was observed again at the 10mM dose but again not for 2mM metformin at the 6 hour timepoint (**Figure 3.3A**).

In vitro culture conditions are not typical of the tumour microenvironment where a lack of nutrients and oxygen would, one might expect, give metformin a greater chance of generating an energy stress that would induce activation of AMPK. Hence activation of AMPK after 24 hours treatment with 2mM metformin was also assessed in 'more physiological' conditions of 5mM glucose (**Figure 3.3B**). The reality is that the level of glucose in the tumour microenvironment is still likely to be markedly less than 5mM but this is difficult to model as, in a closed in vitro system without a 'continuous infusion set up', glucose in the media will quickly deplete to 0mM. However, when MCF7 cells were treated with metformin under conditions of 0.1% hypoxia, activation of AMPK was seen at doses down to 0.1mM (**Figure 3.3C**). This

observation gives some weight to the theory that the doses of metformin that have been typically required to generate an anticancer effect in vitro are significantly higher than might be required ‘in vivo’.

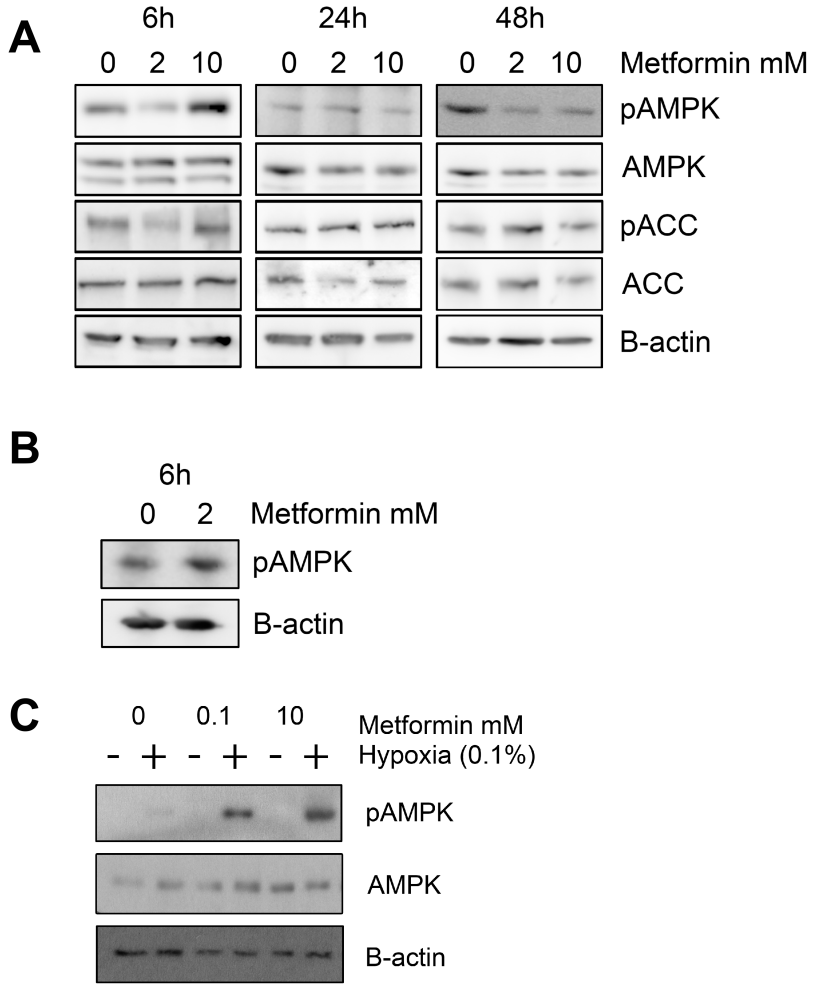


Fig 3.3A: Effect of 2mM and 10mM metformin on phosphorylation of AMPK at 6, 24 and 48 hour timepoints in MCF7 cells cultured in DMEM supplemented with 25mM glucose. Activation of AMPK was only seen at the 6 hour timepoint when treated with 10mM metformin **B:** Effect of 2mM metformin on phosphorylation of AMPK at the 6 hour timepoint in MCF7 cells cultured in DMEM supplemented with 5mM glucose. No clear evidence of activation. **C:** Effect of 0.1mM and 10mM metformin on phosphorylation of AMPK at the 24 hour timepoint with and without hypoxia (0.1% oxygen) in MCF7 cells cultured in DMEM supplemented with 25mM glucose. Under hypoxic conditions metformin activated metformin at doses as low as 0.1mM. Replicates, n=2.

3.2.3: METFORMIN INHIBITS MITOCHONDRIAL RESPIRATION AND DEPLETES CELLULAR ATP

The data presented above shows that there is significant heterogeneity in terms of metformin's effect on proliferation in vitro between different breast cancer cell lines. In view of the substantial published evidence supporting metformin's role as an inhibitor of mitochondrial Complex 1 it was important to assess its effect using mitochondrial assays. The Seahorse^{TM} Bioenergetics assay allows the realtime measurement of the oxygen consumption rate (OCR) using solid state sensor probes that are placed in the media just above the cell monolayer. The OCR was adjusted for cell proliferation using the Cyquant^{TM} DNA assay. In order to compare the dose response curves for MCF7 and MDA-MB-231 cells the OCR was measured after plating cells overnight in media containing progressively decreasing doses of metformin (0.01mM to 20mM). The basal OCR was greater in untreated MCF7 cells compared to MDA-MB-231 cells (129.2 ± 10.3 pMoles/min/Cyquant vs 47.9 ± 7.2 pMoles/min/Cyquant ($p = 0.003$), respectively). Metformin reduced the basal OCR in both the MCF7 and MDA-MB-231 cell lines compared to control in a dose-dependent manner consistent with mitochondrial toxicity. Surprisingly, given their differing sensitivity with regards to effect on proliferation, both cell lines demonstrated similar sensitivity to metformin with the OCR almost completely abrogated from a dose of 1mM metformin (**Figure 3.4A and B**).

By delivering different drugs that act as 'mitochondria stressors' into the media using automated drug injection ports during the assay it is possible to measure key parameters of mitochondrial function (**Figure 3.4B**). The addition of oligomycin blocks ATP synthase and any subsequent fall in the OCR should therefore correlate

with ATP production. Using this surrogate measurement, from a dose of 1mM metformin, there was evidence of a fall in ATP production compared to control in both cell lines but no clear difference between them. Mesoxalonitrile 4-trifluoromethoxyphenylhydrazone (FCCP) is capable of depolarizing plasma and mitochondrial membranes and is an uncoupler of oxidative phosphorylation in mitochondria. The addition of this agent allows one to measure the maximum respiration feasible under a particular condition, and hence the difference between maximal respiration and basal respiration i.e. spare capacity or ability to respond to ATP demand. Again there was similarity between both cell lines with spare capacity beginning to fall from the 5mM dose. Lastly the addition of Actinomycin A and Rotenone will inhibit mitochondrial activity and hence it is possible to estimate the non-mitochondrial OCR i.e. superoxide production or proton leak. For both cell lines the addition of metformin reduced this parameter from a dose of 1mM metformin upwards. In summary there was little difference between these 2 cell lines in terms of OCR response even when put under conditions of mitochondrial stress suggesting that resistance, at least for MDA-MB-231 cells, is not at the mitochondrial level.

Although the Seahorse assay allows for the putative indirect measurement of ATP levels, these were also measured directly using the Enzylight^{TM} ADP/ATP fluorescence assay. Here 2mM metformin treatment was shown to significantly decrease ATP levels in MCF7 cells and MDA-MB-468 cells but not MDA-MB-231 cells (fold difference in luminescence compared to control; 0.80 ± 0.01, 0.66 ± 0.03 and 0.91 ± 0.04, for MCF7, MDA-MB-468 and MDA-MB-231 cells respectively).

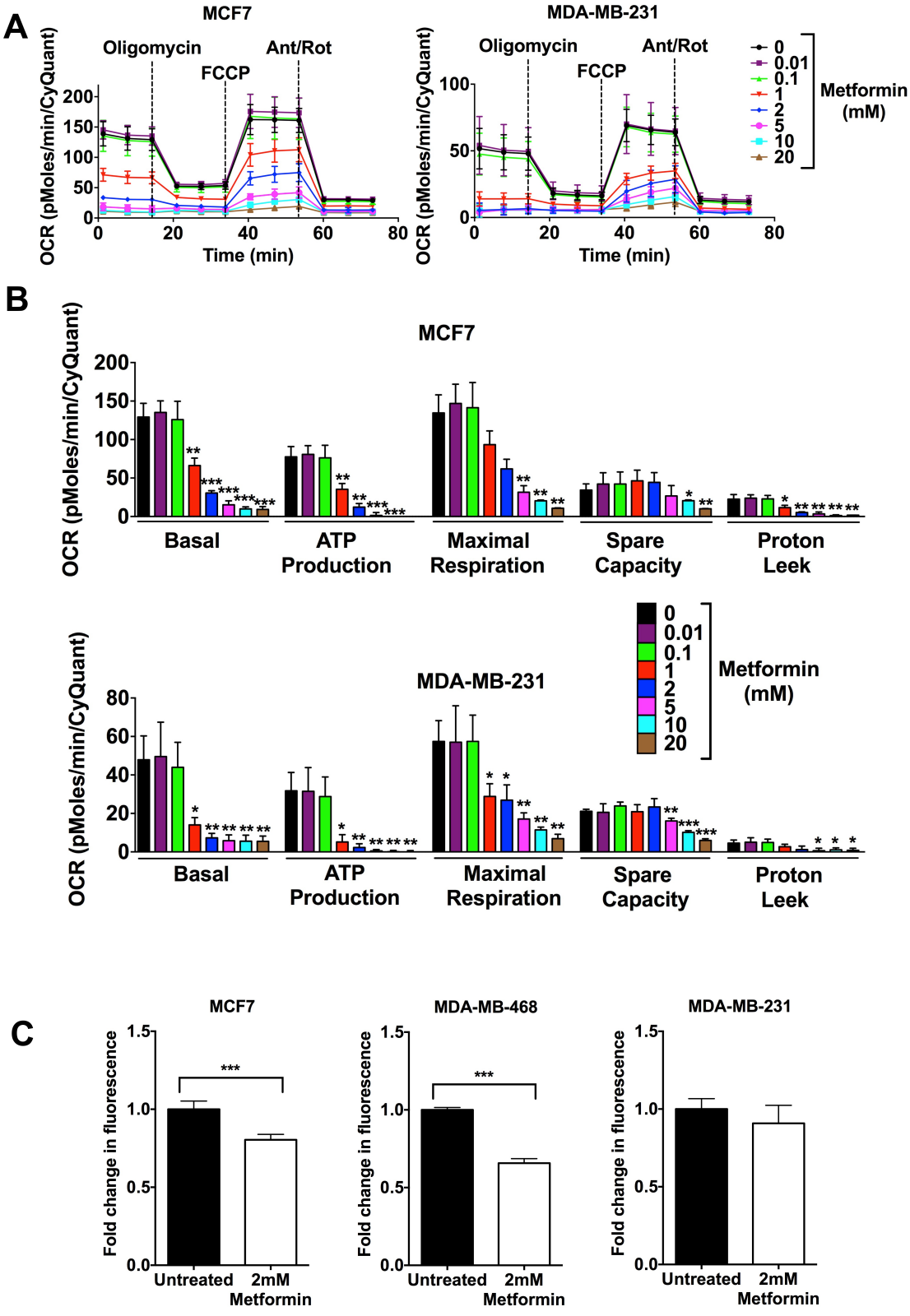


Fig 3.4A: See previous page. Effect of 0-20mM metformin on oxygen consumption in MCF7 and MDA-MB-231 cells (n=3) **B:** Parameters of mitochondrial function determined from the same experiment as in Fig 3.4A. Prior to the addition of mitochondrial stressor agents the affect of

metformin on basal respiration can be assessed. The addition of oligomycin blocks ATP synthase and any subsequent fall in the OCR should therefore correlate with ATP production. FCCP depolarizes the plasma and mitochondrial membranes uncoupling oxidative phosphorylation in mitochondria allowing one to measure maximum respiration. The spare capacity is the difference between maximal respiration and basal respiration. Rotenone will inhibit mitochondrial activity and hence it is possible to estimate the non-mitochondrial OCR i.e. superoxide production or proton leak. There was no clear difference in the dose response between MCF7 cells and MDA-MB-231 cells with regard to these parameters **C:** Effect of 2mM metformin on ATP levels at 24 hours in MCF7, MDA-MB-468 and MDA-MB-231 cells (n=3). Metformin treatment led to the depletion of ATP in MCF7 and MDA-MB-468 cells but not MDA-MB-231 cells. Data shown are mean ± SEM, *p < 0.05; **p < 0.01; ***p < 0.001.

3.2.4: METFORMIN ALTERS MITOCHONDRIAL MORPHOLOGY IN MCF7 CELLS BUT NOT MDA-MB-231 CELLS

Another method of comparing the effect of metformin on the mitochondria of the MCF7 and MDA-MB-231 cell lines is to assess for changes in mitochondrial morphology. Using these two cell lines, that had been stably transfected with a red fluorescent protein that is tagged to the cytochrome c oxidase subunit VIII of the mitochondria, live cell imaging using confocal microscopy was carried out to assess for changes in mitochondrial morphology after 48 hours of 2mM metformin treatment. While there were no significant changes seen in the mitochondrial morphology of the MDA-MB-231 cells in response to metformin, metformin induced mitochondrial rounding in the MCF7 cells (**Figure 3.5A**). Image analysis software (ImageJ) was used to quantify this change in morphology. Mitochondrial circularity was significantly increased in metformin-treated MCF7 cells but not MDA-MB-231 cells (**Figure 3.5B**). Electron microscopy of metformin treated metformin treated cells confirmed this differential effect with metformin-treated MCF7 cells showing

enlarged mitochondria that lacked clearly defined cristae but again no effect in MDA-MB-231 cells (**Figure 3.5C**). The differential response of the mitochondria in terms of morphology but not oxygen consumption is puzzling. Mitochondria are dynamic entities continually changing their shape through fission and fusion but the physiology of mitochondria shape change and link between form and function is poorly understood [250]. Decreased intracellular ATP concentration has been implicated in mitochondrial shape change secondary to the abolition of fusion events [251]. It is possible that the greater capacity for MDA-MB-231 cells to maintain ATP levels might provide an explanation for the pattern of mitochondrial response to metformin.

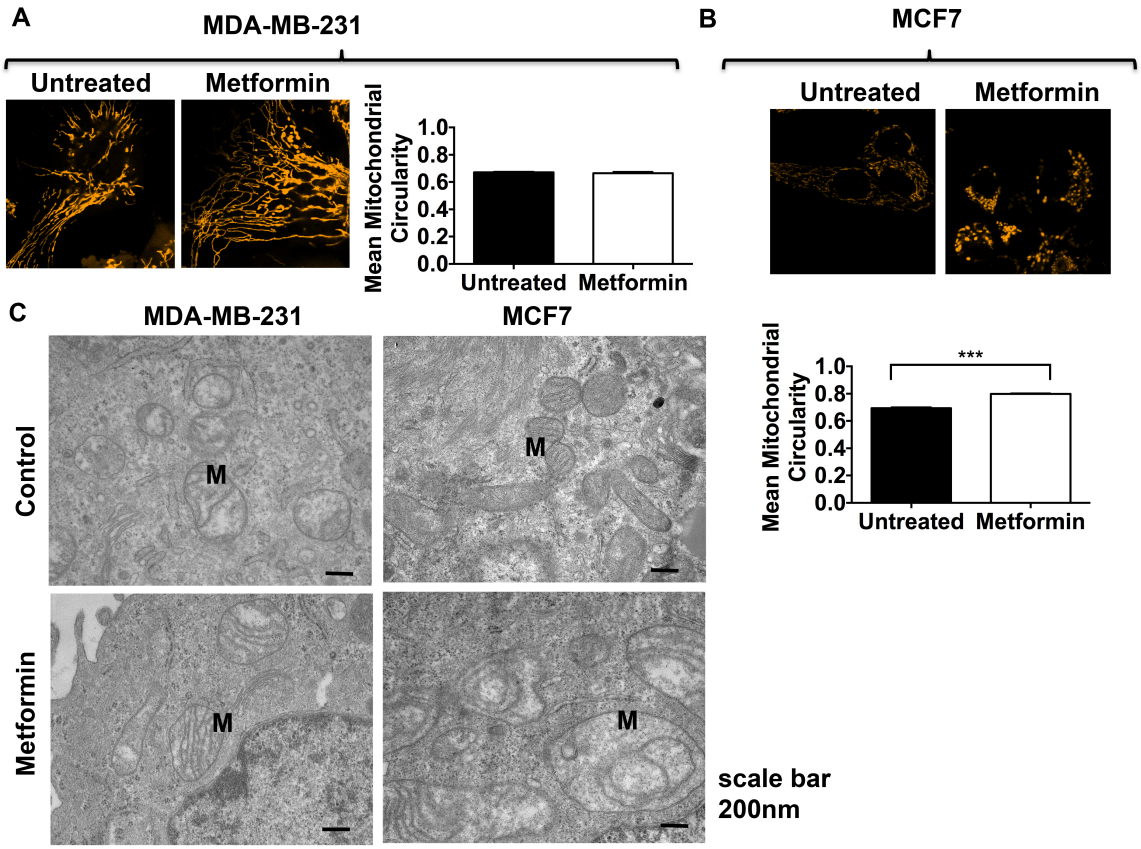


Fig 3.5A and B: Effect of metformin on the mitochondrial morphology of MDA-MB-231 and MCF7 cells that had been stably transfected with a red fluorescent protein that is tagged to the cytochrome c oxidase subunit VIII of the mitochondria. Live cell imaging using confocal microscopy was carried out to assess for changes in mitochondrial morphology after 48 hours of 2mM metformin treatment. Image analysis software (ImageJ) was used to quantify this change in morphology by assessing for changes in mitochondrial circularity. A circularity value of 1.0 indicates a perfect circle but as the value approaches 0.0, it indicates an increasingly elongated polygon. Circularity = $4\pi(\text{area}/\text{perimeter}^2)$. 2mM metformin had no effect on mitochondrial rounding of MDA-MB-231 cells (**A**) but did induce a significant conformational change in MCF7 cells (**B**) (n = 3 for both). **C:** Electron microscopy revealed that in MCF7 cells, after 48 hours of 2mM metformin treatment, there was enlargement of the mitochondria, lacking well-defined cristae. Mitochondrial morphology in MDA-MB-231 cells was unaffected by metformin treatment. Data shown are mean ± SEM, ***$p < 0.001$.

3.2.5: METFORMIN TREATMENT LEADS TO AN INCREASE IN THE GLYCOLYTIC RATE IN BREAST CANCER CELL LINES

It has previously been described that metformin increases glucose consumption and lactate production in cancer cell lines [234]. To determine whether this 'glycolytic response' applied to all of the above breast cancer cell lines, the media concentration of lactate and glucose was measured after 48 hours treatment with 2mM metformin. For all 6 cell lines, including the resistant MDA-MB-231 cell line, there was a decrease in media glucose concentration and an increase in lactate concentration consistent with an increase in the glycolytic rate (**Figure 3.6A and B**).

The effect of metformin on the glycolytic rate can also be assessed in realtime using the Seahorse Bioenergetics assay by measuring the extracellular acidification rate (ECAR). Here dose response was compared for the MCF7 and MDA-MB-231 cell lines (**Figure 3.6C and D**). The ECAR was adjusted for cell proliferation using the Cyquant^{TM} DNA assay. The cells were initially incubated in glycolysis stress test medium without glucose during which the basal ECAR could be measured i.e. that related to non-glycolytic acidification. Glucose at 10mM was then injected which is taken up by the cells and utilized in the glycolytic pathway producing ATP and protons leading to an increase in the ECAR. By subtracting the maximal increase in ECAR from the basal ECAR it is possible to estimate the rate of glycolysis. The rate of glycolysis in untreated MCF7 cells was comparable to MDA-MB-231 cells (35.7 ± 2.1 mpH/min/Cyquant vs 35.2 ± 0.84 mpH/min/Cyquant, respectively). Metformin increased the rate of glycolysis in both the MCF7 and MDA-MB-231 cell lines compared to control but there was little difference in the ECAR response between the 2 cell lines. For example at the 5mM metformin dose MCF7 cells demonstrated a

71% increase in the ECAR compared to a 64% increase for MDA-MB-231 cells (35.7 ± 2.1 mpH/min/Cyquant vs 61.1 ± 6.9 mpH/min/Cyquant ($p = 0.03$) and 35.2 ± 0.8 mpH/min/Cyquant vs 57.9 ± 6.1 mpH/min/Cyquant ($p = 0.02$) for untreated and 5mM metformin treated MCF7 and MDA-MB-231 cells, respectively). Hence it seems that the ability, of these 2 cell lines at least, to increase their glycolytic rate at times of mitochondrial stress is not key to their sensitivity to metformin.

During the above assay, the injection of drugs into the assay media was used to assess other parameters of glycolytic function (**Figure 3.6E and F**). The injection of the ATP synthase inhibitor, oligomycin, inhibits mitochondrial ATP production with the subsequent increase in ECAR being a measure of maximum glycolytic capacity. Although metformin reduced the glycolytic capacity from a dose of 5mM metformin upward in both cell lines again there was little difference in the dose response between the 2 cell lines. The difference between the glycolysis rate and glycolysis capacity is the 'glycolysis reserve' and again there was little difference in the dose response between the 2 cell lines. The glucose analog, 2-deoxyglucose, is an inhibitor of hexokinase, the first enzyme in the glycolytic pathway, and its use in this assay confirmed that any change in ECAR was secondary to a change in the glycolytic rate.

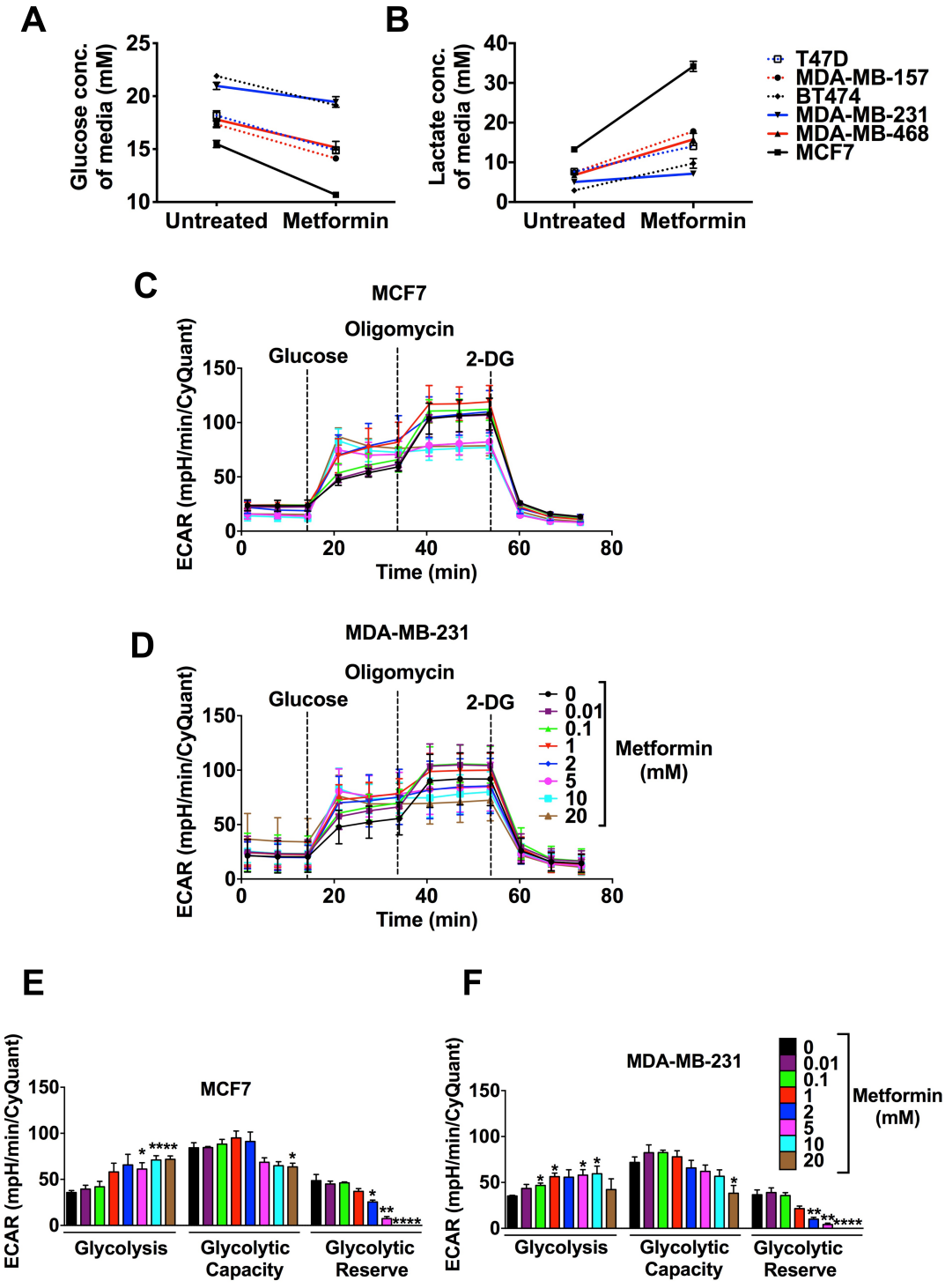

A
Glucose conc. of media (mM)
25
20
15
10
Untreated
Metformin
B
Lactate conc. of media (mM)
40
30
20
10
0
Untreated
Metformin
T47D
MDA-MB-157
BT474
MDA-MB-231
MDA-MB-468
MCF7
C
MCF7
Oligomycin
Glucose
2-DG
ECAR (mpH/min/CyQuant)
150
100
50
0
0
20
40
60
80
Time (min)
D
MDA-MB-231
Oligomycin
Glucose
2-DG
0
0.01
0.1
1
2
5
10
20
Metformin (mM)
ECAR (mpH/min/CyQuant)
Time (min)
E
MCF7
ECAR (mpH/min/CyQuant)
Glycolysis
Glycolytic Capacity
Glycolytic Reserve
F
MDA-MB-231
Metformin (mM)
ECAR (mpH/min/CyQuant)
Glycolysis
Glycolytic Capacity
Glycolytic Reserve

Fig 3.6A: See previous page. Effect of metformin on glucose depletion from the media after 2mM metformin treatment at 48 hours in 6 different cell lines. **B:** Effect of metformin on lactate production in the media after 2mM metformin treatment at 48 hours in 6 different cell lines. **C, D, E and F:** Effect of metformin on glycolysis parameters using the Seahorse Bioscience assay. There was little difference between the MCF7 and MDA-MB-231 cell lines in terms of dose response to metformin on glycolysis, glycolytic capacity or glycolytic reserve (n=3). Data shown are mean ± SEM. **p < 0.01; ***p < 0.001.

3.2.6: DEPLETION OF GLUCOSE ENHANCES THE ANTI-PROLIFERATIVE EFFECT OF METFORMIN IN SENSITIVE BREAST CANCER CELL LINES

The observation that metformin leads to an increase in the glycolytic rate in cultured breast cancer cells raised the question as to whether altering the availability of glucose would alter sensitivity in terms of the anticancer effect. Given that routine cell culture is usually carried out at unphysiological concentrations of glucose, as were the above proliferation assays (in this case 25mM), it was important to examine the effect of metformin at a lower glucose concentrations. In this assay a glucose concentration equivalent to that in human serum, 5mM, was used. The reality is that glucose concentrations in the tumour microenvironment are likely to be significantly lower than this [132] but without continuous media exchange and nutrient replenishment lower concentrations are difficult to model. At this 'more physiological' level of environmental glucose both the MCF7 and MDA-MB-231 cell lines, but not MDA-MB-468 cells, had greater proliferation rates when not exposed to metformin. Indeed hyperglycaemia has been shown to have an inhibitory effect on cell growth in some cancer cell lines possibly due to secondary oxidative stress [252]. However there was evidence of an increased inhibitory effect on cell proliferation for MCF7 and MDA-MB-468 cells treated with 2mM metformin in the presence of 5mM glucose (p = 0.06

and p = 0.02, respectively) and at the10mM dose for MCF7 cells (p = 0.02) whereas the inverse effect was seen in MDA-MB-231 cells (p=0.04) (**Figure 3.7A)**. Hence, for the more 'sensitive' MCF7 and MDA-MB-468 cells it is seems that hyperglycaemia is protective against metformin in vitro. These results are consistent with the increased glucose requirements expected after upregulation of glycolysis in response to metformin's mitochondrial toxicity.

Spheroid models offer the opportunity to assess the effects, in vitro, of nutrient and oxygen gradients on the effectiveness of a particular treatment [253]. Given the increased sensitivity to metformin shown by MCF7 cells with decreased concentrations of glucose in the media one could hypothesise that one might see greater effects of metformin on 3-dimensional spheroid growth. However, the MCF7 and MDA-MB-231 spheroid models demonstrated similar sensitivity to that observed in standard 2-D culture (**Figure 3.7B**).

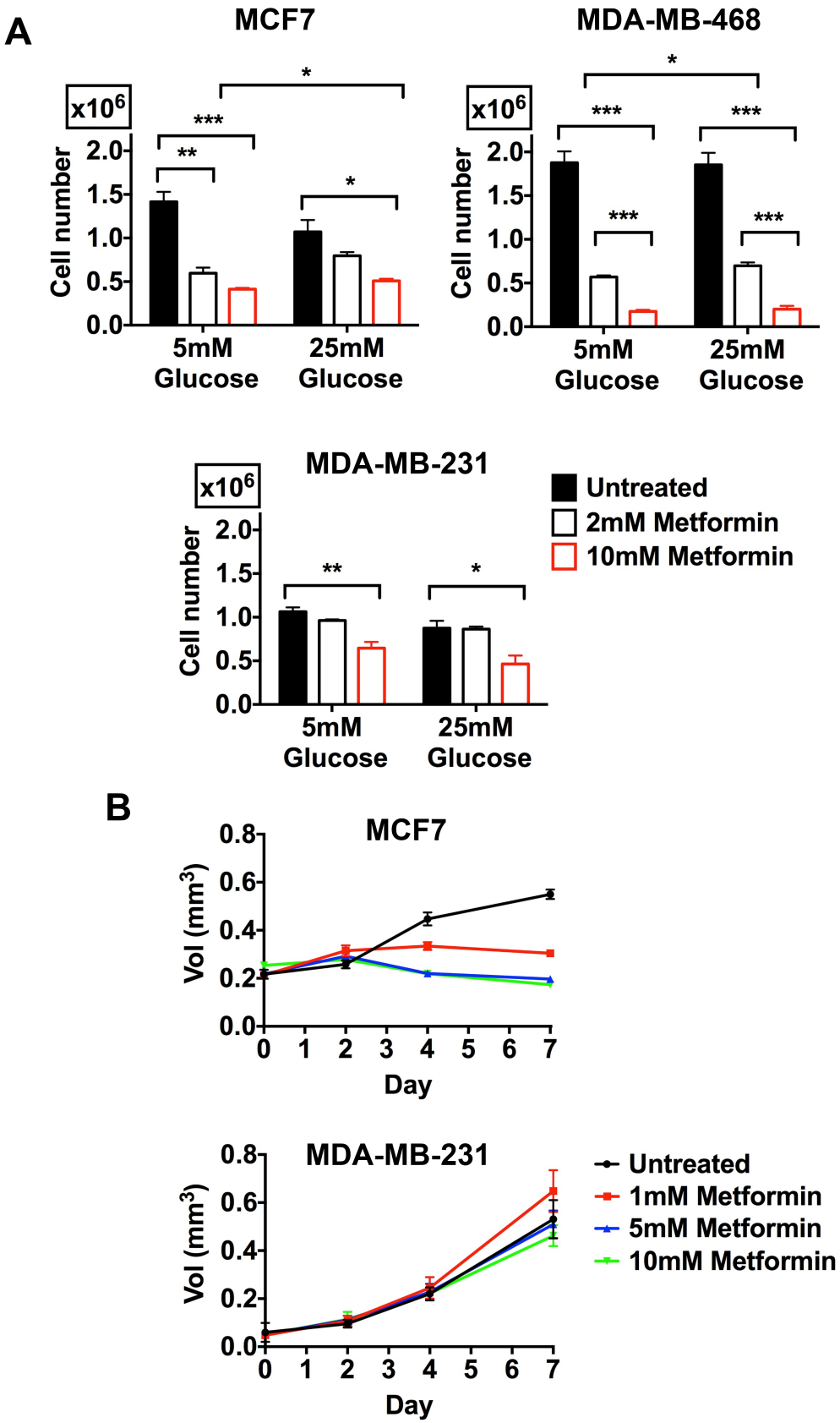


Fig 3.7A: See previous page. The effect of differing media glucose concentrations (5mM and 25mM) on 2-D cell proliferation was compared at 96 hours with increased sensitivity of MCF7 and MDA-MB-

468 cells to metformin treatment seen for 5mM glucose supplementation. No clear difference in effect was seen for MDA-MB-231 cells (n = 4). **B:** 3-D spheroid growth of MCF7 and MDA-MB-231 cells demonstrated a similar sensitivity to the 2-D cell proliferation assay (n = 4). Data shown are mean ± SEM *p < 0.05; **p < 0.01; ***p < 0.001.

3.2.7: EFFECT OF METFORMIN ON THE INDIVIDUAL CONTRIBUTIONS OF GLUCOSE, GLUTAMINE AND LACTATE AS SUBSTRATES FOR DE NOVO LIPOGENESIS IN MCF7 CELLS

The observations above that, a) metformin stimulated an increase in the rate of glycolysis and, b) a reduction in the concentration of glucose in the media increased the sensitivity of some cell lines to metformin (in terms of effect on proliferation), drew attention to the effect of metformin on how breast cancer cells utilised different anabolic substrates. Investigation was focused on 3 substrates for de novo lipogenesis (DNL), glucose, glutamine and lactate. Mitochondrial stress has recently been demonstrated to increase the utilisation of glutamine as a substrate for DNL via the reductive carboxylation pathway with this amino acid having been shown to become more important than glucose in the supply of carbons to newly synthesised fatty acids provided that stress is great enough [150, 151]. Lactate was also of interest as studies have shown that cancer cells can, not only take up lactate as a ‘fuel’ source, but may also do this preferentially over glucose. After conversion by lactate dehydrogenase to pyruvate, carbons from lactate can be funneled into the citric acid cycle and subsequently DNL [254].

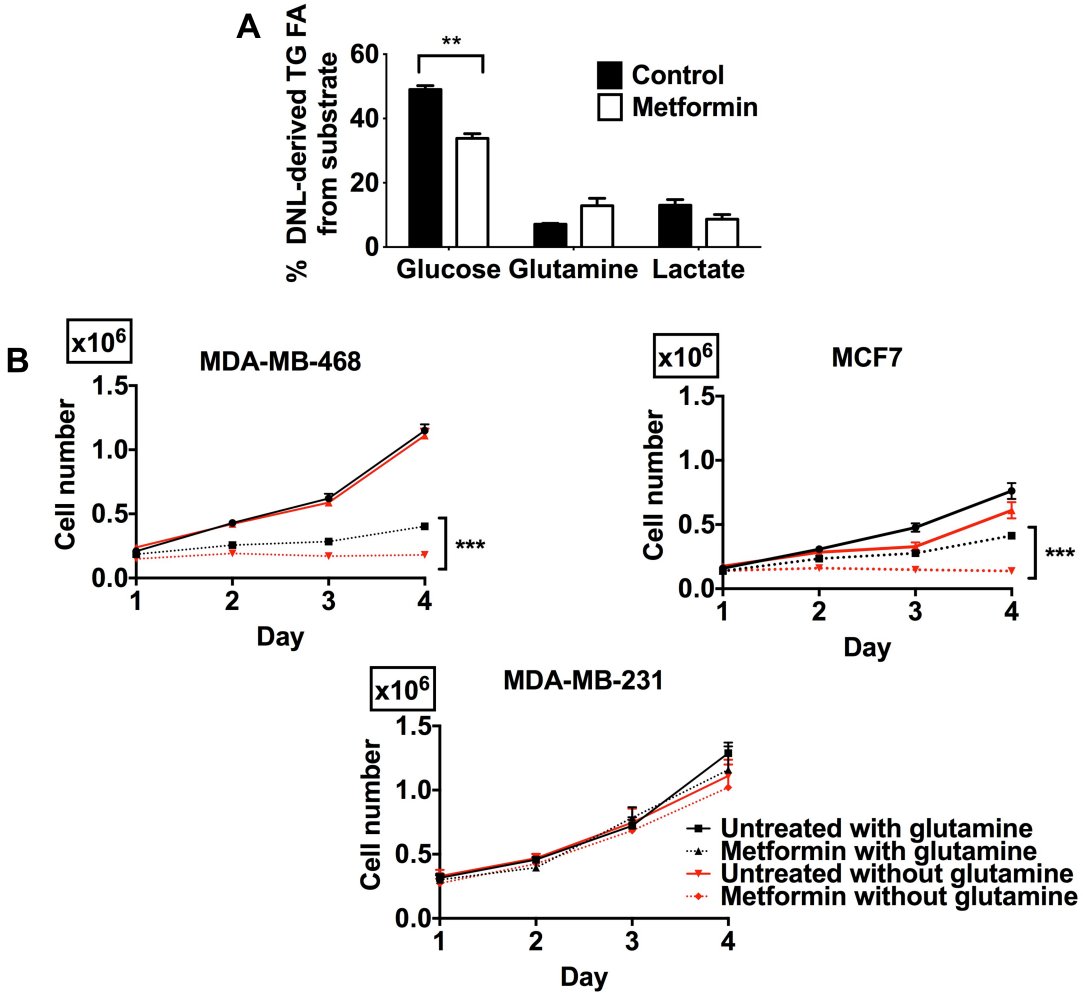


Fig 3.8A: See previous page. The effects of metformin on glutamine, glucose and lactate as substrates toward DNL-derived TG fatty acid in MCF7 cells was calculated and showed a shift in the proportions of substrates used for DNL (expressed as a percentage of the total amount of DNL-derived TG fatty acid in control and metformin treated MCF7 cells) (n=3). **B:** MCF7 and MDA-MB-468 cells were more sensitive to metformin treatment under conditions of glutamine deprivation bit there was no effect in MDA-MB-231 cells. Cells were treated with 2mM metformin versus untreated for up to 96 hours in media supplemented with 25mM glucose with or without 4mM glutamine prior to cell counting (n=4). Data shown are mean ± SEM. **p < 0.01; ***p < 0.001.

Using mass spectrometry techniques and [U-^{13}C] labeling, the effect of metformin on the individual contributions of [U-^{13}C] glucose, glutamine and lactate as substrates for DNL could be assessed. **Figure 3.8A** shows that after treatment of MCF7 cells for 48 hours with 2mM metformin there was a shift in substrate utilisation for de novo lipogenesis (DNL). Without metformin glucose was the main substrate for fatty acid synthesis in control cells, contributing to 49.0% ± 1.2% of total synthesised fatty acid, while glutamine was a minor substrate, only contributing 7.2% ± 0.2% of newly synthesised TG fatty acid. Lactate contributed to 13.2% ± 1.8% of synthesised TG fatty acid. Metformin treatment altered the proportion of each substrate used for DNL: there was a 30% reduction in glucose-derived DNL TG fatty acid (to 33.8% ± 1.4% as a proportion of synthesised fatty acid, $p = 0.001$) and a 33% reduction in use of lactate (8.7% ± 1.4%, $p = 0.11$), while glutamine-derived TG fatty acid increased by 82% (12.9% ± 2.3%, $p = 0.06$). It is important to note that lactate produced by glycolysis from the cells (which, as above will increase with metformin treatment) will have diluted the [U-^{13}C] lactate and, therefore, the calculation of lactate as a substrate for DNL is likely to have been underestimated. Hence we see that the utilisation of glucose and glutamine as substrates for DNL was changed reciprocally by metformin. This observation is consistent with published data describing the effect of an insult to the mitochondrial electron transport chain on utilisation of glutamine as a substrate for DNL [151]. **Please see Chapter 4 regarding further discussion and results for the investigation into the effects of metformin on lipid metabolism.**

3.2.8: WITHDRAWAL OF GLUTAMINE ENHANCES THE ANTI-PROLIFERATIVE EFFECT OF METFORMIN IN SENSITIVE BREAST CANCER CELL LINES

In view of the increased importance of glutamine as a substrate for DNL, how important was the presence of glutamine in continuing to support growth in metformin treated cells? To answer this question MCF7, MDA-MB-468 and MDA-MB-231 cells were treated with 2mM metformin for 96 hours in DMEM supplemented with 10% FCS and 25mM glucose with and without 4mM glutamine. In order to ensure against marked nutrient depletion the media was changed daily. The removal of glutamine from the media had no effect on the growth of untreated MDA-MB-468 or MDA-MB-231 cells although there was some evidence of a small effect on inhibition of proliferation of untreated MCF7 cells. The removal of glutamine from the media had a profound effect on the proliferation of metformin treated MDA-MB-468 and MCF7 cells with virtually complete inhibition of growth after 96 hours. However, MDA-MB-231 cells displayed no increase in sensitivity with glutamine withdrawal (**Figure 3.8B**). It is therefore clear that a source of glutamine is vital in maintaining the proliferation of sensitive breast cancer cells treated with metformin in culture presumably to maintain anapleurosis, firstly by providing substrate for de novo lipogenesis via the reductive carboxylation pathway [151] but potentially also by feeding carbons into a disrupted citric acid cycle.

3.2.9: A SCREEN OF INHIBITORS OF KEY MODULATORS OF GLUTAMINE METABOLISM IN COMBINATION WITH METFORMIN REVEALS PROMISING SYNERGY

The importance of glutamine as a carbon source in metformin treated breast cancer cells raised the possibility of potential synergy between metformin and other agents that more specifically modulated glutamine metabolism. After a literature search to identify potential drugs that would inhibit different steps of the glutaminolysis and reductive carboxylation pathways, 8 different compounds were investigated for synergy (**Figure 3.9**). In order to determine a suitable dose for each compound, a dose response curve was initially generated using the Cyquant^{TM} assay by exposing MCF7 cells to progressively decreasing doses of each agent in DMEM supplemented with 25mM glucose and 4mM glutamine over 96 hours (**Figure 3.10**). Once a suitable dose had been established (i.e. that at which a small effect on proliferation was observed) the MCF7, MDA-MB-468 and MDA-MB-231 cell lines were treated with 2mM metformin alone, the agent of interest or combination treatment again in DMEM supplemented with 25mM glucose and 4mM glutamine for 96 hours. The media was changed on a 24 hourly basis prior to cell counting.

L-γ-glutamyl-p-nitroanilide (GPNA) is an inhibitor of solute carrier family 1 member 5 (SLC1A5), a high affinity L-glutamine transporter [255]. SLC1A5 is a member of the sodium dependent ASC system of amino acid transporters that are the most commonly expressed amino transporters in tumour cells [256-258]. In a lung cancer model SLC1A5

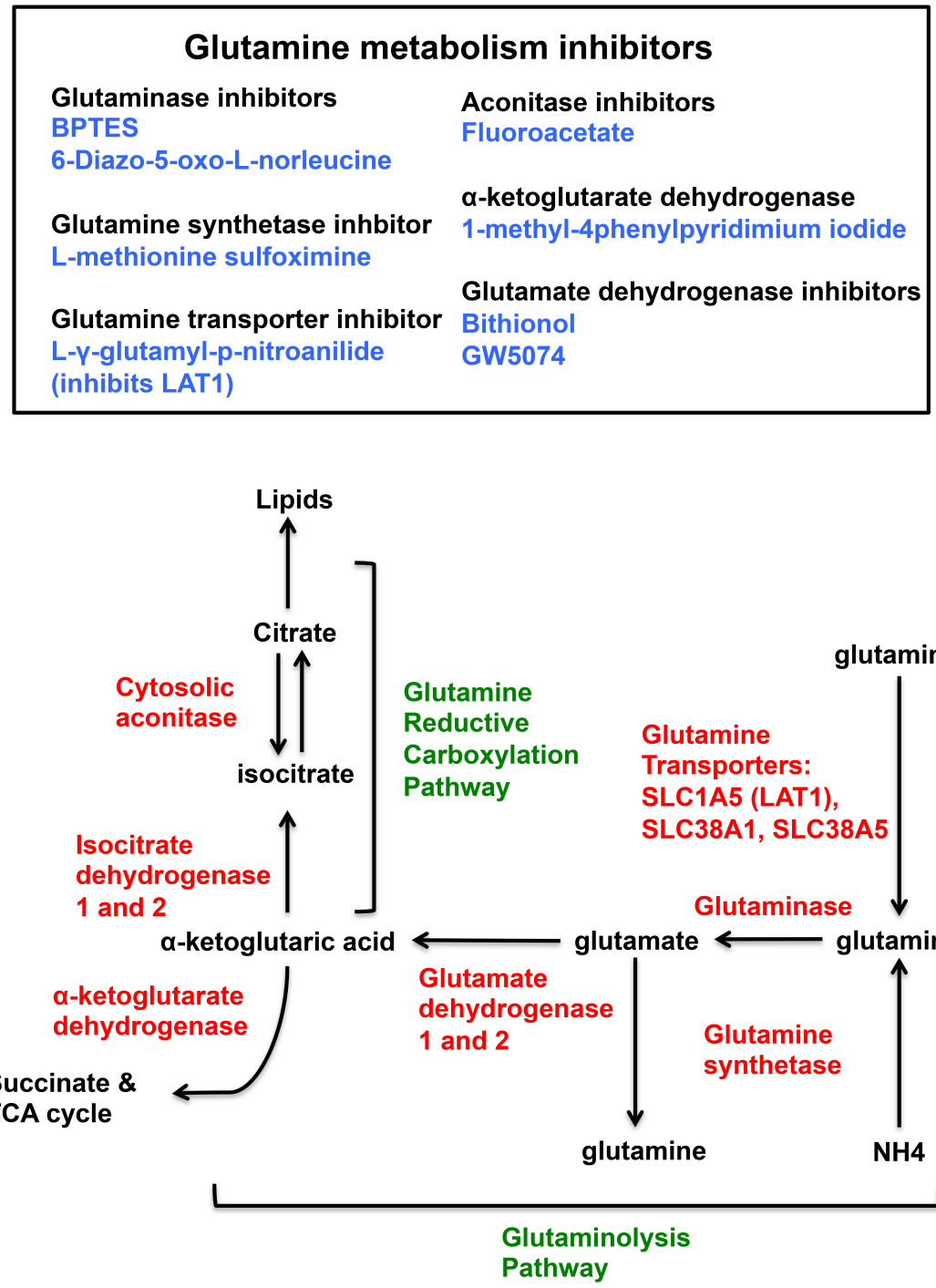


Fig 3.9: The glutaminolysis and reductive carboxylation pathways. Eight compounds that targeted different steps in these pathways were investigated for synergy with metformin.

has been shown to mediate glutamine transport required for cell proliferation and survival [259]. The Cyquant assay did not demonstrate any effect on MCF7 cell growth even at a dose of 1mM (the highest concentration soluble in water.) Despite the Cyquant result, using cell counting there was a 26% and 29% decrease in proliferation for the MCF7 ($p = 0.03$) and MDA-MB-468 ($p = 0.006$) cell lines, respectively, when treated with GPNA alone compared to control, but no significant effect in MDA-MB-231 cells. In combination with metformin there was no clear evidence of synergy for MCF7 and MDA-MB-231 cells but MDA-MB-468 cells demonstrated approximately a further 2 fold decrease in proliferation ($p = 0.015$) when compared to metformin treatment alone (**Figure 3.11A**).

Glutamine synthetase is an enzyme that catalyses the condensation of glutamate with ammonia to form glutamine and ammonia has been shown to support proliferation of transformed cells under conditions of glutamine deprivation [260]. L-methionine sulfoximine is phosphorylated by glutamine synthetase resulting in an irreversible, non-covalent, inhibition of the enzyme [261]. Treatment with 12.5mM L-methionine sulfoximine alone had no significant effect on the proliferation of MCF7 or MDA-MB-231 cells, but MDA-MB-468 cells were very sensitive with a 75% decrease in cell growth ($p < 0.001$). However, there was no evidence of synergy with metformin in any of the 3 cell lines (**Figure 3.11B**).

Bis-2-(5-phenylacetamido-1,3,4-thiadiazol-2-yl)ethyl sulfide (BPTES) and 6-Diazo-5-oxo-L-norleucine (DON) are both inhibitors of glutaminase, the enzyme that catalyses the conversion of glutamine to glutamate in the glutaminolysis pathway. BPTES has already been shown to have a synergistic effect with metformin on cancer cell growth

in a prostate cancer cell model [143]. DON is a diazo analogue of L-glutamine which has shown anticancer activity in human xenograft models and has been studied in combination with chemotherapy in clinical trials [262]. In all 3 cell lines treated with 12.5μM BPTES there was a reduction in cell proliferation when compared to untreated cells: for MCF7 cells this was 35% ($p = 0.008$), MDA-MB-468 cells, 64% ($p < 0.001$) and MDA-MB-231 cells, 53% ($p = 0.005$). In the MCF7 and MDA-MB-468 cell lines there was evidence of synergy with metformin (42% decrease in cell growth ($p = 0.003$) and 55% ($p = 0.003$) when compared with metformin alone, respectively). This was not the case in the MDA-MB-231 cell line (**Figure 3.11C**). DON alone when compared to untreated cells also had an anti-proliferative effect in all 3 cell lines: for MCF7 cells there was a 61% reduction in cell growth ($p = 0.004$), MDA-MB-468 cells, 65% ($p = 0.001$) and MDA-MB-231 cells, 56% ($p = 0.03$). However, there was no clear evidence of synergy between DON and metformin (**Figure 3.11D**).

Bithionol and GW5074 were recently shown to be inhibitors of glutamate dehydrogenase, the enzyme that catalyses the conversion of glutamate to α-ketoglutaric acid, in a high throughput screen [263]. Bithionol is licensed for the treatment of helminthic infections in humans and has been shown to reduce MDA-MB-231 and melanoma cell line migration in vitro via inhibition of the motility stimulating factor, autotaxin [264]. GW5074 is a RAF inhibitor with known anticancer effects [265]. Bithionol at a dose of 20μM when used alone had an anti-proliferative effect in both the MCF7 and MDA-MB-468 cells (29% ($p = 0.02$) and 29% ($p = 0.01$) reduction in cell growth, respectively) but no clear effect for the MDA-MB-231 cell line. In all 3 cell lines there was evidence of synergy between

metformin and bithionol when compared to metformin alone: for MCF7 cells there was a 48% reduction in growth ($p < 0.001$), MDA-MB-468 cells, 64% ($p < 0.001$) and MDA-MB-231 cells, 48% ($p = 0.002$). Notably synergy existed in the MDA-MB-231 cells when no significant effect on proliferation was seen with either drug alone (**Figure 3.11E**). MDA-MB-468 cells exhibited sensitivity to GW5074 alone (43% reduction in cell growth compared to untreated cells ($p = 0.001$)) and in combination with metformin there was further cell growth inhibition (37% reduction in cell growth compared to metformin treated cells ($p = 0.045$)). However in MCF7 cells and MDA-MB-231 cells there was no clear effect on cell proliferation for this agent (**Figure 3.11F**).

In order to feed α-ketoglutaric acid into the TCA cycle, this metabolite must be dehydrogenated to succinate by α-ketoglutarate dehydrogenase. This step may be inhibited by the compound 1-methyl-4 phenylpyridimium iodide (MPP) by competitive inhibition with respect to NAD^+ [266]. For MDA-MB-468 cells there was a 29% reduction in cell growth after MPP treatment alone compared to untreated cells ($p = 0.004$) and in combination metformin there was further cell growth inhibition (35% reduction in cell growth compared to metformin treated cells ($p = 0.024$)). MCF7 cells and MDA-MB-231 cells demonstrated no clear evidence of sensitivity for this drug (**Figure 3.11G**).

The reductive carboxylation pathway has been shown to be important for the funneling of glutamine carbons toward lipid synthesis and supporting cancer growth when there is loss of efficiency of the TCA cycle, for example secondary to mitochondrial toxins or under hypoxic conditions [150, 151]. Aconitase and isocitrate

dehydrogenase are the catalytic enzymes of the reductive carboxylation pathway. There are no known specific inhibitors of isocitrate dehydrogenase but the 5-fluorouracil breakdown product, fluoroacetate (FA), inhibits aconitase via its metabolite 4-hydroxy-trans-aconitate binding tightly to the enzyme [267]. MDA-MB-468 cells demonstrated sensitivity to FA alone (34% decrease in cell growth compared to untreated cells ($p = 0.002$)) and there was a trend toward an effect on MCF7 cells too (25% decrease in cell growth compared to untreated cells ($p = 0.066$)). There was evidence of synergy between metformin and FA in MCF7 cells (28% decrease in cell growth compared to metformin treated cells ($p = 0.044$)) but not the other 2 cell lines (**Figure 3.11H**).

It is clear that in this '2-D' in vitro breast cancer model several different agents targeting different aspects of the glutaminolysis pathway have synergy with metformin. Besides demonstrating a potential treatment strategy this reaffirms the importance of glutamine in maintaining the growth of metformin treated cells. Of particular note, for some compounds synergy with metformin existed in the otherwise resistant MDA-MB-231 cell line.

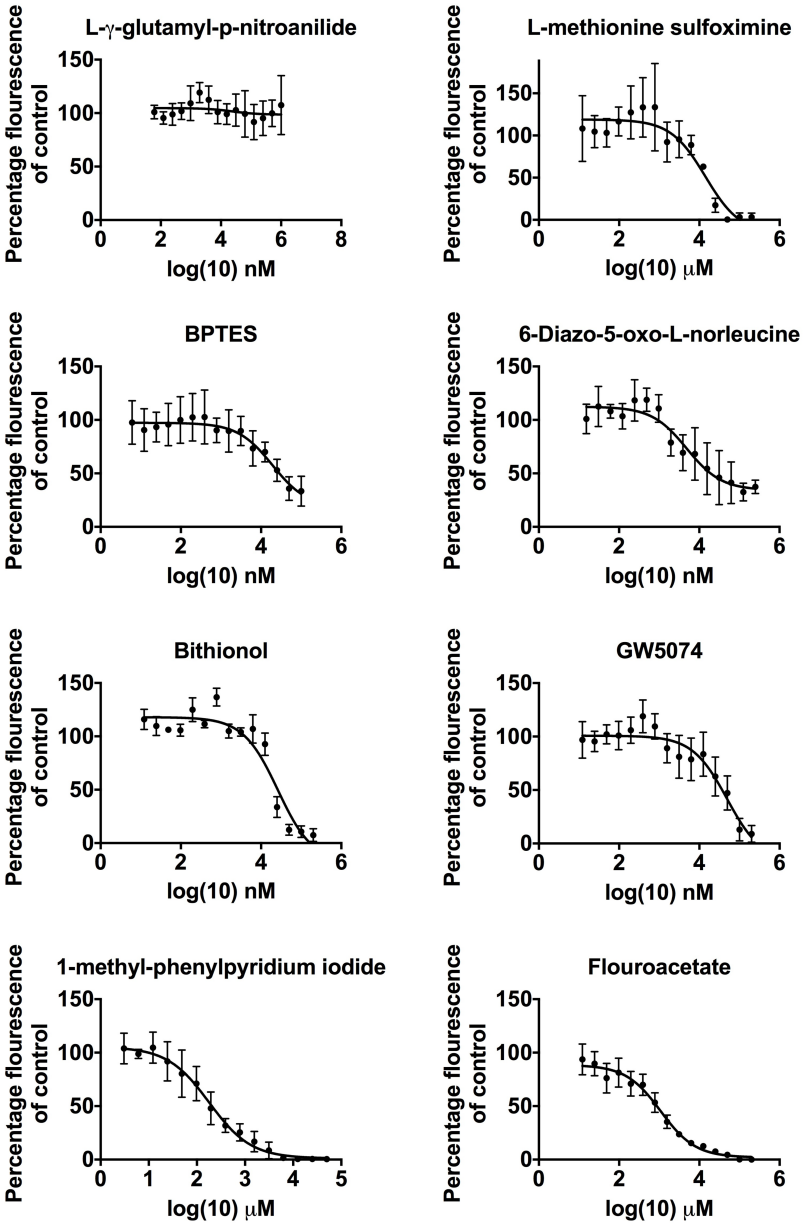


Fig 3.10: Cyquant dose response curves in MCF7 cells for compounds that targeted glutamine metabolism: L-γ-glutamyl-p-nitroanilide (no effect at soluble doses), L-methionine sulfoximine (IC50 14.2mM), BPTES (IC50 19.2μM), 6-Diazo-5-oxo-norleucine (IC50 4.8μM), Bithionol (IC50 26.2μM), GW5074 (IC50 49.2μM), 1-methyl phenylpyridium iodide (IC50 180.7μM) and Fluoroacetate (IC50 1.1mM) (n=4). Data shown are mean ± SEM.

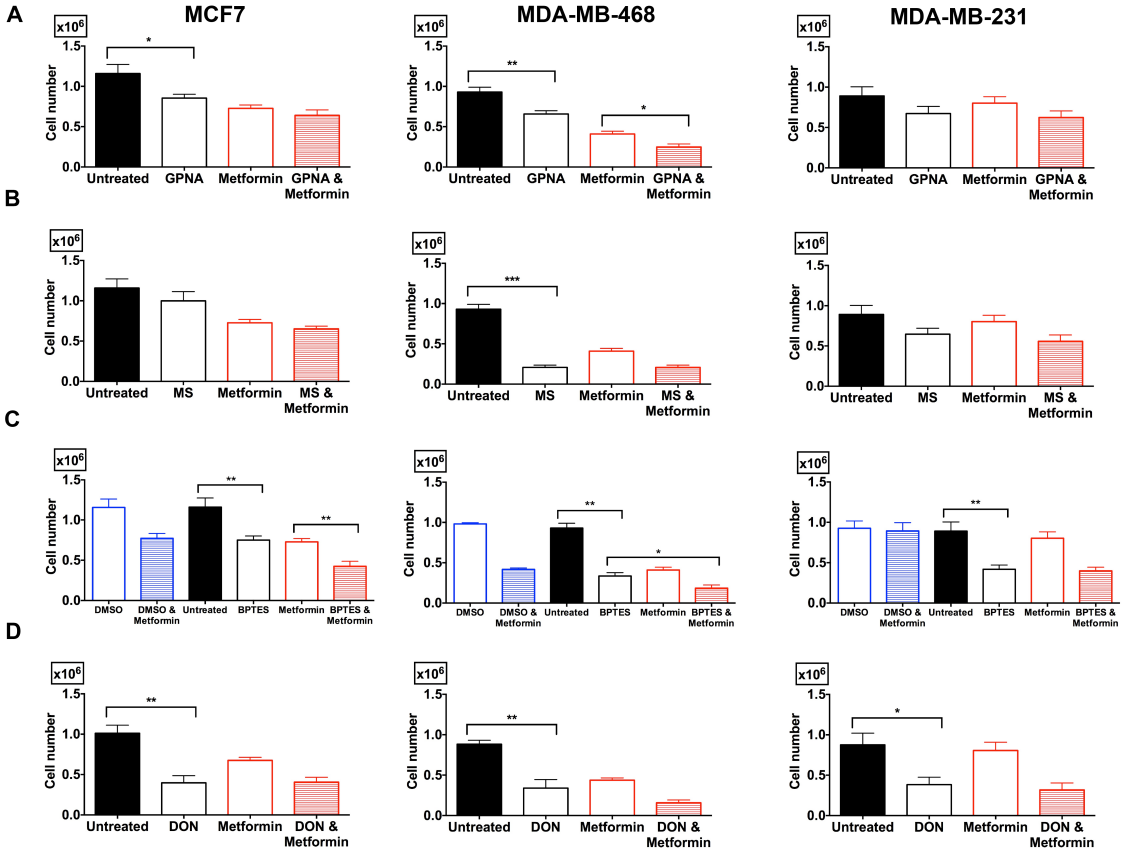


Fig 3.11A-D: Effect of metformin on cell number in 3 different cell lines after 96 hours treatment in 2-D culture with and without 8 different compounds that target glutamine metabolism. **A:** L-γ-glutamyl-p-nitroanilide (GPNA), **B:** L-methionine sulfoximine (MS), **C:** BPTES, **D:** 6-Diazo-5-oxo-norleucine (DON). Data shown are mean ± SEM *p < 0.05; **p < 0.01; ***p < 0.001.

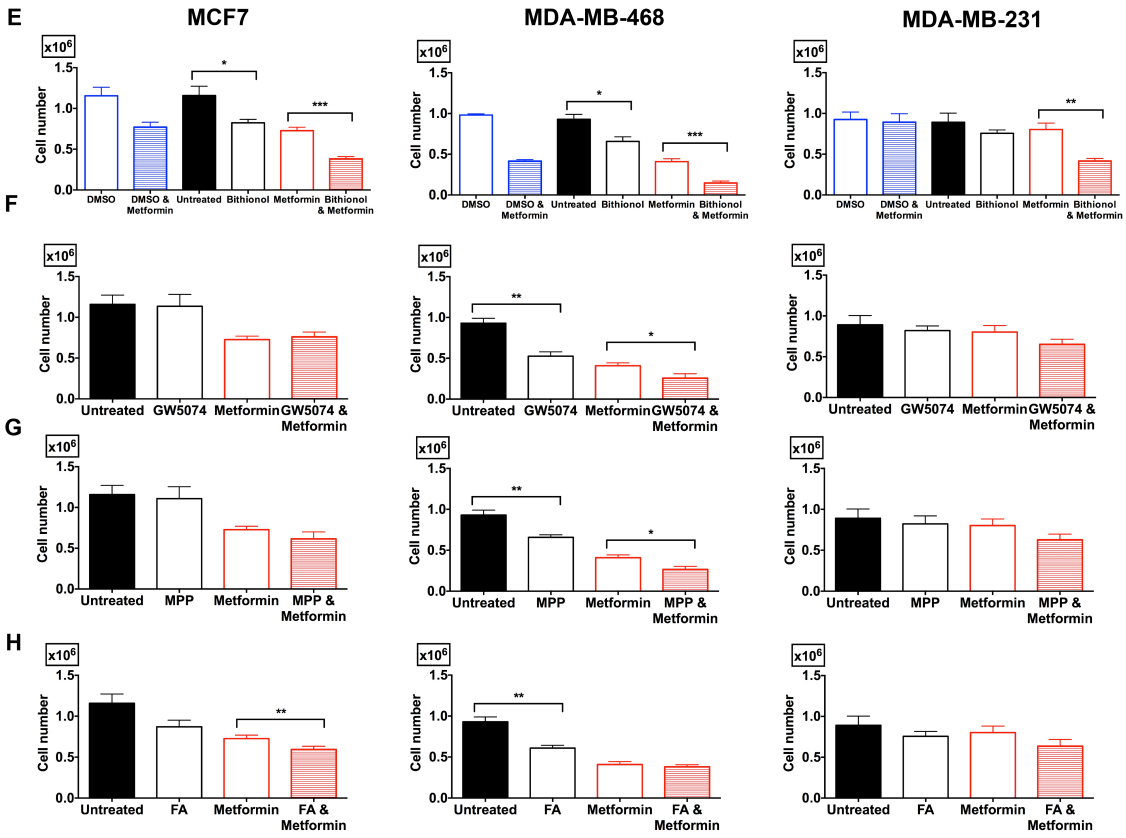


Fig 3.11E-H: Effect of metformin on cell number in 3 different cell lines after 96 hours treatment in 2-D culture with and without 8 different compounds that target glutamine metabolism. **E:** Bithionol, **F:** GW5074, **G:** 1-methyl-phenylpyridium iodide (MPP) and **H:** Fluoroacetate (FA) (n=6). Data shown are mean ± SEM *p < 0.05; **p < 0.01; ***p < 0.001.

3.3: DISCUSSION

3.3.1: SENSITIVITY TO METFORMIN BETWEEN CANCER CELLS IS NOT DETERMINED BY MITOCHONDRIAL RESISTANCE OR THEIR CAPACITY TO UPREGULATE GLYCOLYSIS

The inhibition of oxygen consumption in MCF7 and MDA-MB-231 cells and alteration of the morphology of mitochondria seen in MCF7 cells shown above is consistent with metformin's known toxicity toward Complex 1 of the mitochondrial respiratory chain. The fact that the dose of metformin at which oxygen consumption starts to decrease (1mM) is the same in both the MCF7 and MDA-MB-231 cells lines suggests that it is not the direct effect on the mitochondria that is responsible for lack of sensitivity or otherwise. Similarly the ability of these cell lines to upregulate glycolysis to compensate for inefficiency of the TCA cycle does not differ. Although there is this similarity in the effect of metformin between these 2 cell lines, one difference in particular stands out. Metformin in MCF7 cells depletes ATP but not in MDA-MB-231 cells. This suggests that some other process, such as fatty oxidation, is compensating for the metabolic stress incurred by metformin in MDA-MB-231 cells, but not MCF7 cells – *see chapter 4*.

3.3.2: METFORMIN ACTIVATES AMPK AT LOWER DOSES UNDER HYPOXIC CONDITIONS

It is notable that at the 2mM dose, which clearly inhibits the growth of the 'sensitive' MCF7 breast cancer cell line, there was no evidence of AMPK activation on immunoblotting under normoxic conditions. However, when an additional stress was placed on oxidative respiration i.e. hypoxia AMPK activation, AMPK activation became apparent at significantly lower doses of metformin (0.1mM). Although the

aim of this study was not to specifically assess the importance of AMPK activation with regard to metformin's anticancer effect, as this has previously been extensively investigated, this data suggests that in the oxygen poor tumour microenvironment metformin may activate AMPK at much lower doses than most of the in vitro studies to date.

3.3.3: SYNERGY BETWEEN INHIBITORS OF GLUTAMINE METABOLISM AND METFORMIN OFFERS A PROMISING CANCER TREATMENT STRATEGY

This data shows that targeting the glutaminolysis pathway in combination with metformin represents a promising strategy for cancer treatment. During the course of this project several papers were published identifying the importance of glutamine in maintaining cancer cell growth at times of mitochondrial stress [143, 150, 151]. The reductive carboxylation pathway allowing the cytosolic feeding of carbons from glutamine toward lipid synthesis [151] and our data and others [143] which demonstrates glutamine's increased role as a substrate for lipid synthesis confirms the importance of this pathway as a cancer resistance mechanism to metformin treatment. Anapleurosis of the TCA cycle may also be an important role for glutamine in maintaining the growth of metformin treated cancer cells. It was notable that, in generality, MDA-MB-468 was the most sensitive cell line to agents that modulated glutamine metabolism and MDA-MB-231 the least. Glutamine has been shown to be important for ROS control especially in triple negative breast cancer cell lines [268] and it is possible that MDA-MB-468 cells are especially sensitive to ROS induced either by electron transport chain interference (metformin) or a lack of glutamine metabolites (secondary to drug targeting of the glutamine pathway).

The observation that bithionol has anticancer effects alone and in combination with metformin is of significant interest. Although bithionol is known to have anticancer effects via its inhibition of autotaxin regulated cancer cell migration [264] the fact that such synergy was seen with metformin here does suggest that its inhibition of glutamine dehydrogenase is also important. The in vitro doses at which an anticancer effect is observed are approximately 15 times less than those measured at peak plasma level in clinical studies [269]. This drug is already licensed for use in humans in many countries and is generally well tolerated [269]. Hence clinical evaluation of this drug in the cancer setting would potentially be relatively straightforward and cost effective.

3.3.4: FUTURE WORK

There are of course limitations to in vitro cancer models. It would be feasible to assess the effects of metformin on utilisation of [U-13C] labelled glucose and glutamine in vivo by giving the animals these substrates shortly before sacrifice and using NMR or mass spectrometry techniques to trace the labeled carbons. PET imaging techniques using radiolabelled glucose or glutamine to assess the effects of metformin on xenograft uptake of these substrates might aid the search for synergistic drugs and biomarker development.

Beyond metformin, given recent observations regarding the importance of glutamine as a carbon source for cancer cells at times of metabolic stress, further investigation of the anticancer potential of bithionol and also glutamate dehydrogenase, in general, as a therapeutic target, would be a sensible next step. It would be key first of all to confirm that bithionol at the 20μM dose is having an effect on glutamine metabolism

in these cell lines. NMR techniques and [U-13C] tracing with labeled glutamine offers the most effective approach here. It would be intriguing to see if α-ketoglutaric acid could rescue the growth of bithionol treated cells (with and without metformin). Lastly it would be important to confirm the synergy of bithionol with metformin in vivo using xenograft cancer models.

CHAPTER 4: EFFECT OF METFORMIN ON BREAST CANCER LIPID METABOLISM

4.1: INTRODUCTION

4.1.1: METFORMIN AND ITS EFFECTS ON LIPID METABOLISM

It has long been established that metformin changes the dynamics of lipid metabolism in diabetes patients. It has been shown that metformin significantly decreases serum fasting total and LDL-cholesterol and circulating triglycerides (TG) in diabetic patients [270-272]. Another study suggested that serum metformin levels inversely correlate with these effects on the lipid profile [273]. Basal lipid oxidation when measured using indirect calorimetry in type 2 diabetics treated with metformin may be lowered [125, 274] and patient studies using ^{14}C labeled-palmitate have suggested metformin induces a reduction free fatty acid turnover and again fatty acid oxidation [274]. In contrast to these indirect measurements of fatty acid oxidation in patients laboratory based studies have to date focused on mouse embryonic fibroblasts (MEFs), hepatocytes, and cardiac and skeletal muscle cells. In these models metformin has been shown to increase fatty acid oxidation in an AMPK dependent manner with a resultant decrease in cellular lipid content [32, 33, 52, 275-277]. For example in primary rat hepatocytes metformin has been shown to activate AMPK, reduce ACC activity, reduce the expression of the transcription factor sterol regulatory element-binding protein 1 (SREBP-1) which regulates the expression of many lipogenic enzymes and decrease fatty acid oxidation [33]. Lastly metformin has been shown to reduce gene expression of the fatty acid desaturating enzyme stearoyl CoA desaturase-1 (SCD1) in the livers of mice in an AMPK dependent manner [34].

4.1.2: ARE METFORMIN'S EFFECTS ON LIPID METABOLISM A POTENTIAL LINK TO ITS ANTICANCER EFFECT?

The activation of AMPK and subsequent downstream modulation of lipid metabolism is a possible link to its anticancer effects. Activation of AMPK has been shown to inhibit cholesterol, fatty acid, and TG synthesis, and also increase fatty acid oxidation and fatty acid uptake [278, 279]. Phosphorylation by AMPK of two key substrates, 3-hydroxy-3-methylglutaryl-co-enzyme A reductase (HMG-CoA reductase) and acetyl-CoA carboxylase (ACC), which are the rate-limiting enzymes in cholesterol and fatty acid biosynthesis, respectively, results in their inactivation [280, 281]. Expression of fatty acid synthase (FAS), another key enzyme involved in catalysing de novo lipogenesis (DNL), has also been shown to be reduced by AMPK activation [282]. Several studies have shown that FAS is constitutively upregulated in cancer [180, 283] and that in prostate cancer cells SREBP mediates upregulation of the lipogenic pathway by androgens [284]. The inhibition of FAS leads to selective cancer cell death and has become a drug target in its own right. Xenograft cancer models when treated with the FAS inhibitor C75 showed evidence of fatty acid synthesis inhibition, apoptosis, and inhibition of tumour growth [180]. Inhibition of cholesterol synthesis may also be important in driving AMPK's anticancer effect, although no firm link has yet been demonstrated. Statins, commonly used in the treatment of hypercholesterolaemia and which inhibit HMG-CoA reductase, have been reported from studies using in vitro and xenograft models and in case controlled population studies to have anticancer effects [285].

Recently published work has suggested a link between metformin's effects on lipid metabolism and its anticancer effect in the absence of AMPK activation. This study demonstrated a decrease in expression of the lipogenic enzymes fatty acid synthase (FASN) and ATP citrate lyase (ACLY) in the livers of mice treated with metformin. In addition, although metformin protected mice against diethylnitrosamine induced hepatocellular tumours, restoring lipogenic gene expression by ectopic expression of the lipogenic transcription factor SREBP1c rescued metformin-mediated 'anti-carcinogenesis'. The effects of metformin in this model seemed to occur in the absence of AMPK activation [286].

4.1.2: AIMS

Hence the aim of this part of the project was to describe metformin's effects on breast cancer lipid metabolism and in particular to: a) compare metformin's effect on breast cancer cells with the observations in the literature made in other in vitro and in vivo models; b) assess whether effects by metformin on lipid metabolism in breast cancer cells were driven by AMPK activation and c) whether any effects on lipid metabolism were important with regard to driving or predicting metformin's anticancer effect. The outcome of this investigation could potentially be a catalyst for metformin relevant biomarker development in cancer and future development of other similarly metabolically targeted drugs.

4.2: RESULTS

4.2.1: METFORMIN TREATMENT OF BREAST CANCER CELL LINES LEADS TO AN ACCUMULATION OF TRIGLYCERIDE AND LIPID DROPLET FORMATION IN VITRO AND IN VIVO

Initially in order to establish whether metformin modulated breast cancer cell lipid metabolism, GC analysis of changes to total triglyceride in the oestrogen receptor positive cell line, MCF7, was carried out. Both 2 and 10mM metformin significantly increased total TG fatty acid in MCF7 cells and the effect was dose dependent (25.5 ± 1.5 versus 63.3 ± 3.4 versus 77.4 ± 13.3 μg/4 x 10^6 cells in control, 2mM metformin, $p < 0.001$, and 10mM metformin, $p = 0.018$, treated MCF7 cells, respectively) (**Figure 4.1**).

To assess whether metformin induced triglyceride accumulation in all breast cancer cell lines gas chromatography techniques were used in a further 5 breast cancer cell lines: estrogen/progesterone receptor (ER/PR) positive MCF7 and T47D, HER2/neu positive BT474, and triple negative (lacking ER, PR and HER2) MDA-MB-231, MDA-MB-468 and MDA-MB-157 cells. This showed that in vitro, after 48 hours of 2mM or 10mM metformin treatment, there was a marked accumulation of triglyceride (TG) fatty acid in 2 cell lines out of 6 investigated. Hence cell lines were categorised as either sensitive (MCF7 and MDA-MB-468), or resistant to metformin (T47D, MDA-MB-157, BT474 and MDA-MB-231 cells) based on the increase in triglyceride fatty acid content (**Figure 4.1**). In this small sample of cell lines there was no clear relationship between response and oestrogen receptor status.

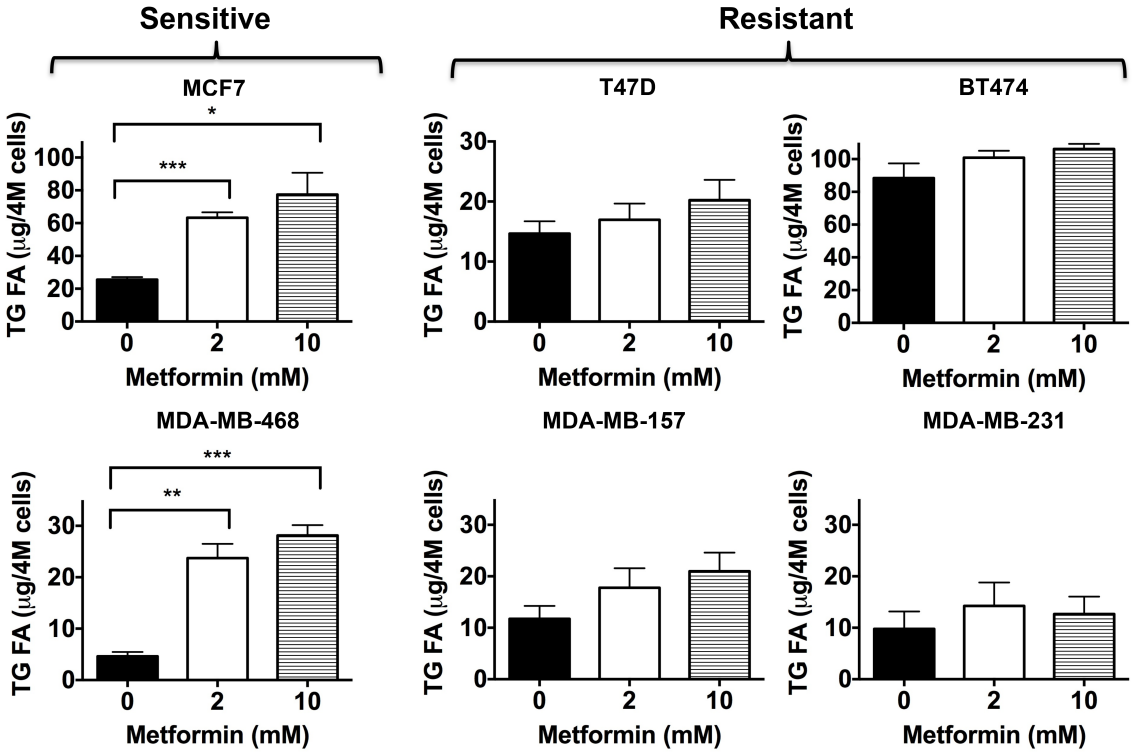


Fig 4.1: Effect of metformin on intracellular TG fatty acid accumulation in a panel of breast cancer cell lines. Cells were treated with either 2 or 10mM metformin versus control (no metformin) for 48 hours and TG fatty acid measured using gas chromatography (GC). The greatest fold change in accumulation occurred in MCF7 and MDA-MB-468 cells (n = 3). Data are expressed as mean total triglyceride FA (µg/4 x 10^6 cells) ± SEM *p < 0.05; **p < 0.01; ***p < 0.001.

The observed metformin-induced increase in cellular TG accumulation was further confirmed by LD540 staining showing a marked increase in lipid droplets in MCF7 cells after 48 hours incubation with 2mM and 10mM metformin (**Figure 4.2A**). LD540 staining of metformin treated MDA-MB-468 xenografts also demonstrated a marked increase in lipid accumulation compared to controls (percentage of DAPI staining area: 8.9% ± 2.8% versus 26.6% ± 6.3% in control and metformin treated xenografts respectively, $p = 0.03$) (**Figure 4.2B-D**). Tumour growth rate was decreased in the metformin treated MDA-MB-468 xenografts although this difference did not reach statistical significance (**Figure 4.2E**).

Based on these findings further investigation was focused the effects of metformin on lipid metabolism in breast cancer cells mainly on 3 cell lines: the sensitive MCF7 cells and MDA-MB-468 cells, and resistant MDA-MB-231 cells.

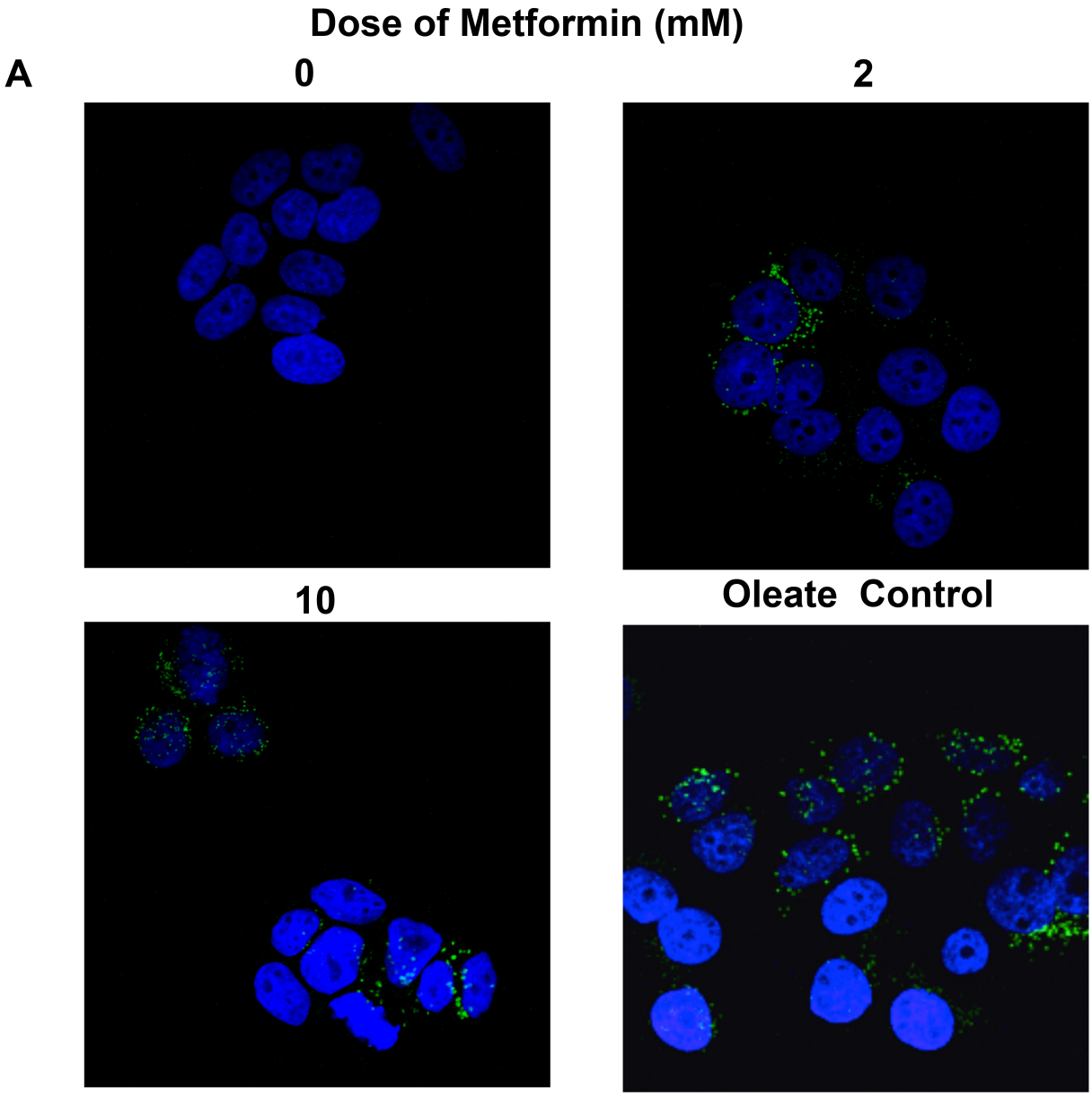


Fig 4.2A: LD540 staining of lipid droplets (green) in MCF7 cells treated with 0, 2 and 10mM metformin. DAPI-stained nuclei are seen in blue. 250µM oleate was also added to MCF7 cells as a control. Metformin treatment led to an accumulation of lipid droplets.

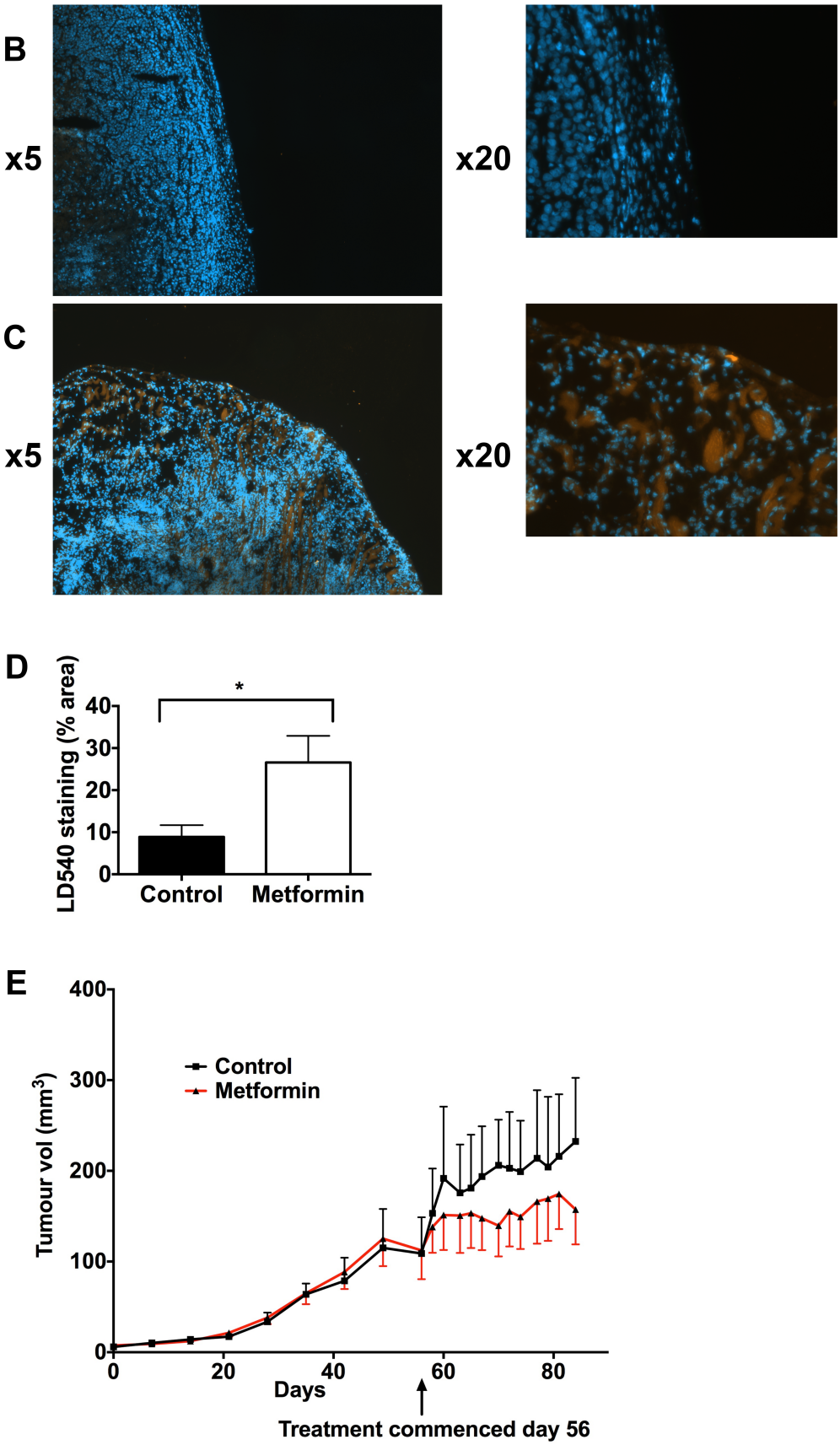


Fig 4.2B and C. See previous page: LD540 staining of control (B) and metformin treated (C) MDA-MB-468 xenografts. An increase in LD540 staining was seen in the metformin treated xenografts. **D:**

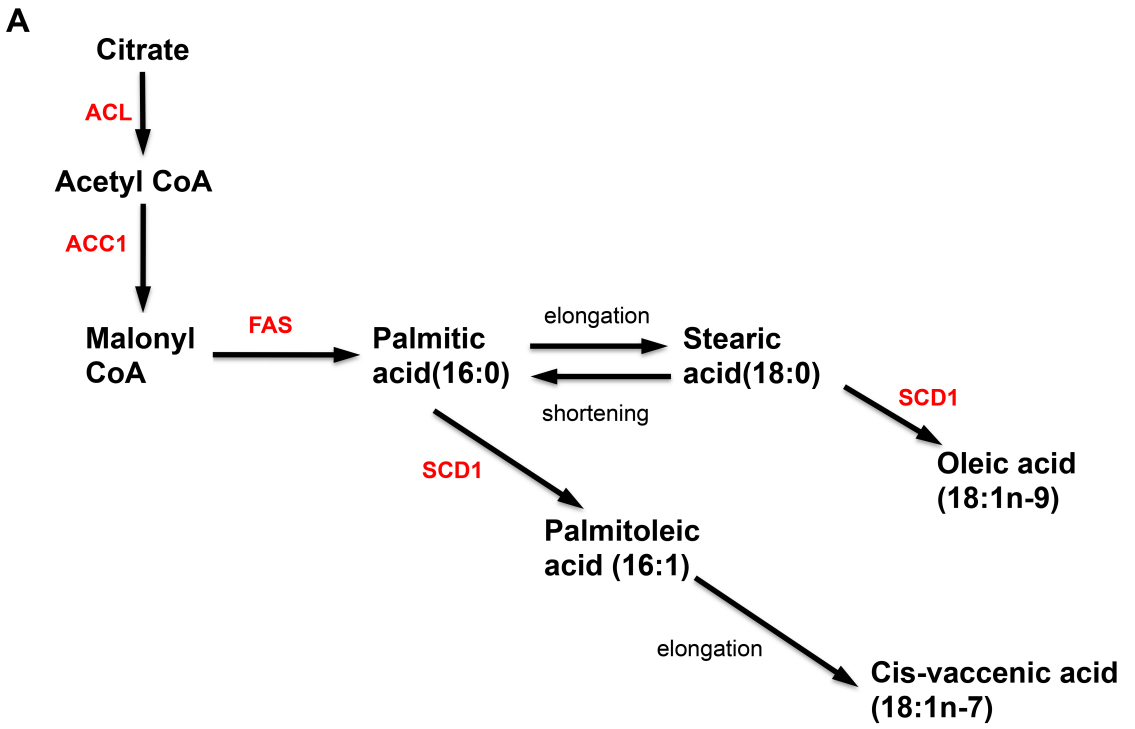
Image analysis quantification of the LD540 staining in the xenografts expressed as a percentage of the area staining for DAPI (n = 6, each group). **E:** Effect of metformin on tumour growth rates of MDA-MB-468 xenografts. Although the metformin treated xenografts had lower growth rates this did not reach statistical significance. Data shown are mean ± SEM *p < 0.05.

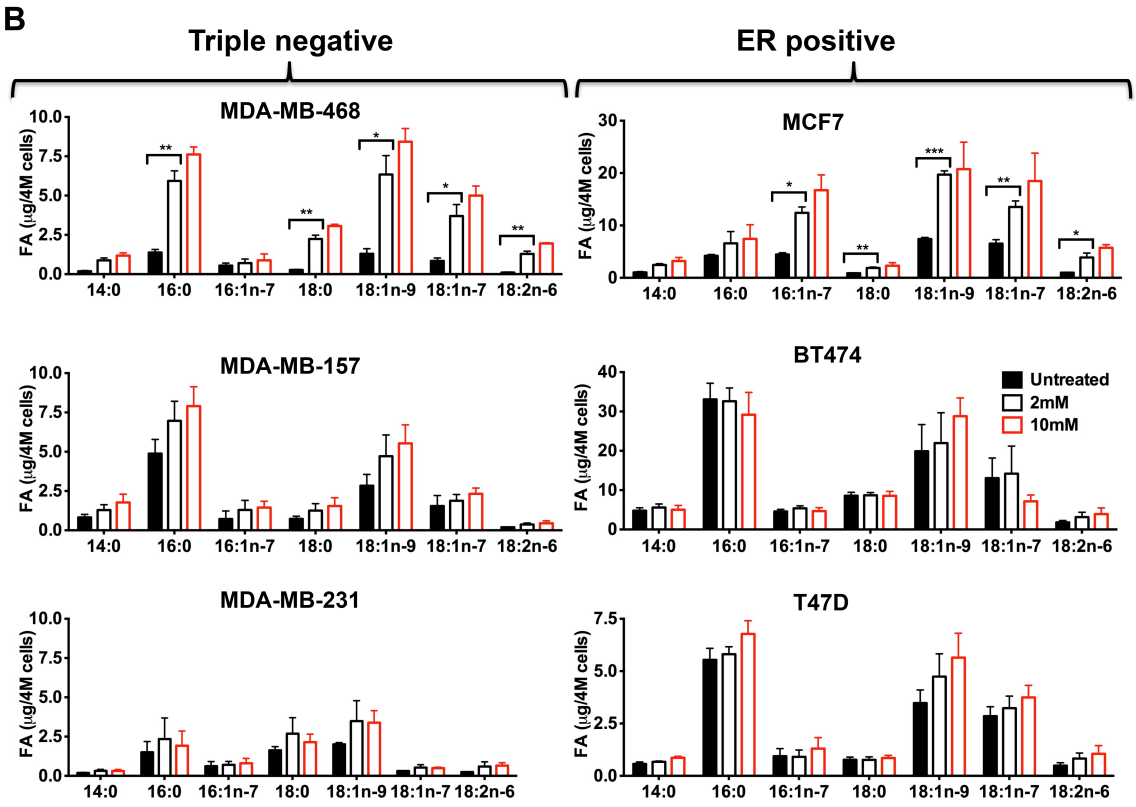
4.2.2: EFFECT OF METFORMIN ON FATTY ACID DESATURATION AND ELONGATION

A more detailed look at the amounts of individual fatty acids per cell further confirmed heterogeneity between cells lines with regard to the lipid metabolism response after exposure to 2mM metformin for 48 hours. **Figure 4.3A** shows the place of these fatty acids in the early steps of de novo lipogenesis. For example levels of stearic acid, 18:0 (p=0.012), palmitoleic acid, 16:1 (p=0.013), oleic acid, 18:1n-9 (p=0.003), cis-vaccenic acid, 18:1n-7 (p=0.003) increased 3-4 fold with metformin treatment in (responsive) MCF7 cells but there was no significant change in (resistant) MDA-MB-231 cells. Of note in sensitive MCF7 cells (p=0.007) and MDA-MB-468 cells (p=0.002) there was an increase in the level of the essential fatty acid, linoleic acid, (p=0.03). Given that linoleic acid cannot be generated via de novo lipogenesis, this was early evidence that there might be an increase in fatty acid uptake (**Figure 4.3B**).

The SCD and elongase indexes are proxy measures of SCD and elongase activity and are calculated using product-to-precursor ratios, that is, 16:1n-7/16:0 and 18:0/16:0. Metformin increased the SCD index but not the elongase index in MCF7 cells (product to precursor ratio 0.68 ± 0.08 versus 1.03 ± 0.09 μg/4 x 10^6 cells, p = 0.019 and 0.34 ± 0.01 versus 0.32 ± 0.02, for the SCD and elongase index, respectively) (**Figure 4.4A**). The ratio of 18;1n-9 to 18:0 was also consistent with an increase in

SCD activity (product to precursor ratio 6.33 ± 0.44 versus 7.84 ± 0.50 μg/4 x 10^6 cells, p = 0.051).


A
Citrate
ACL
Acetyl CoA
ACC1
Malonyl CoA
FAS
Palmitic acid(16:0)
elongation
shortening
Stearic acid(18:0)
SCD1
Oleic acid (18:1n-9)
SCD1
Palmitoleic acid (16:1)
elongation
Cis-vaccenic acid (18:1n-7)


B
Triple negative
ER positive
MDA-MB-468
MCF7
MDA-MB-157
BT474
MDA-MB-231
T47D
FA (μg/4M cells)
14:0
16:0
16:1n-7
18:0
18:1n-9
18:1n-7
18:2n-6
Untreated
2mM
10mM

See previous page. Fig 4.3A: Early steps of synthesis of fatty acids. Citrate from the TCA cycle is converted to Acetyl CoA by ATP citrate lyase (ACL). Acetyl CoA is then converted to Malonyl CoA by Acetyl CoA carboxylase 1 (ACC1). Palmitic acid is then produced from a reaction catalysed by fatty acid synthase. Further desaturation and elongation steps enable conversion to other fatty acids. **B:** Changes in the fatty acid profiles in a panel of breast cancer cell lines (n = 3). Data are expressed as mean total triglyceride FA (µg/4 x 10^6 cells) ± SEM *p < 0.05; **p < 0.01; ***p < 0.001.

The incorporation of [U-^{13}C] palmitate into the TG lipid fraction can be measured with GC MS. After 48 hours of 2mM metformin treatment there was an increase in SCD-mediated desaturation of [U-^{13}C] palmitate for both the MCF7 and MDA-MB-468 cells lines (percentage of TG fatty acid in the desaturated fraction: 21.6% ± 3.0% versus 39.0% ± 3.1%, p = 0.007, in control and metformin-treated MCF7 cells, and 17.2% ± 0.7% versus 46.2% ± 1.7%, p < 0.001, in control and metformin-treated MDA-MB-468 cells, respectively). There was also an increase in elongation of the exogenous fatty acids (39.2% ± 4.5% versus 55.9% ± 2.5% of TG fatty acid in the elongated fraction, in control and metformin-treated MCF7 cells, p = 0.018, and 18.9% ± 1.6% versus 50.4% ± 1.2%, p < 0.001, in control and metformin-treated MDA-MB-468 cells, respectively) (**Figure 4.4B**). Note that when measured for the entire TG pool there was no evidence of any change in elongation activity (see section 4.2.2) so this effect seems specific solely for exogenous fatty acid.

Stearoyl CoA desaturase (SCD) is the enzyme that catalyzes the formation of monounsaturated fatty acids from saturated fatty acids. There are 2 isoforms of SCD in humans, SCD1 (ubiquitously expressed in human tissue) and SCD5 (limited expression). Given the observed increase in the SCD index RT-PCR to assess for the change in gene expression of SCD1 and SCD5 was carried out. However there was no

clear evidence of a change in SCD1 or SCD5 mRNA expression at 24, 48, 72 or 96 hours (**Figure 4.4C and D**). Similarly, western blotting did not demonstrate any clear increase in protein expression of SCD1 or SCD5 at 24, 48 or 72 hours (**Figure 4.4E and F**). Although, evidence to date suggests that SCD1 activity is predominantly down to its rate of transcription, there is some evidence of post-transcriptional modulation that may at least in part be ubiquitin proteosome dependent [193]. This might provide an explanation as to why there was evidence of an increase in SCD activity despite there not being an increase in gene or protein expression.

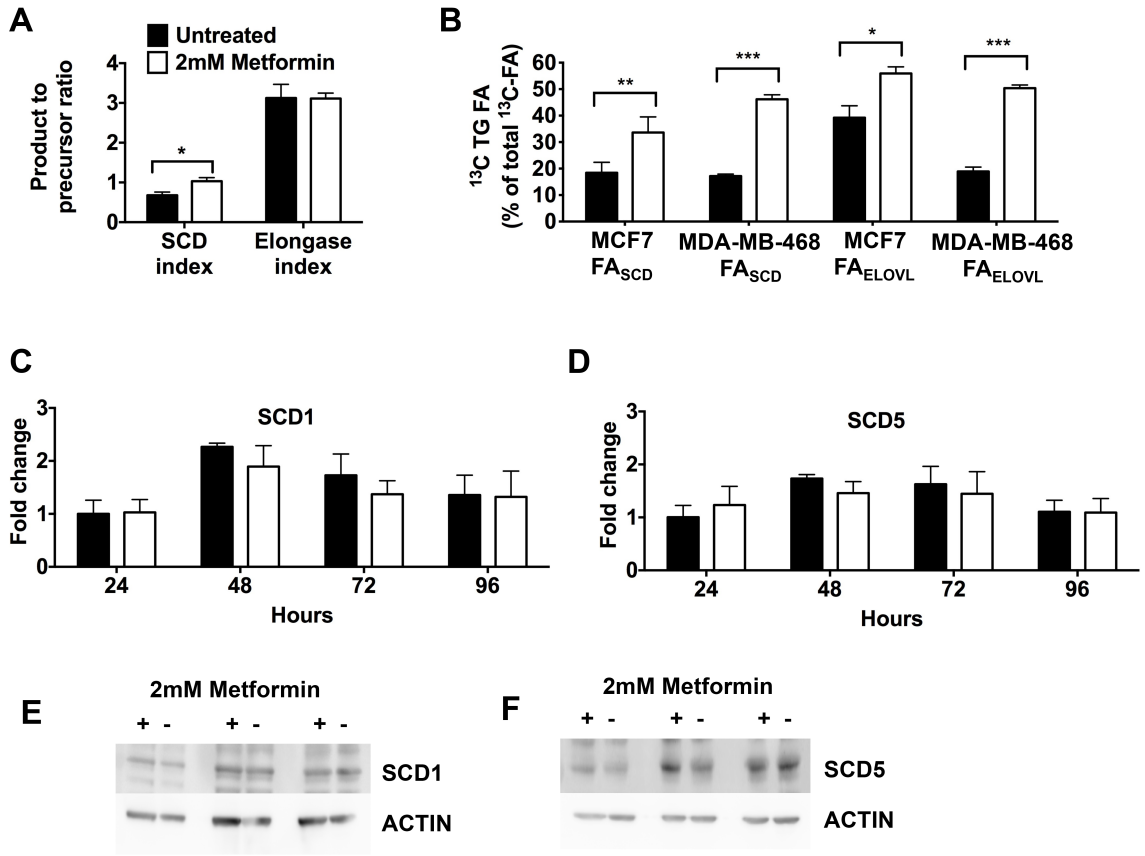


Fig 4.4A: The fatty acid SCD and elongation indexes were calculated as described above and the SCD index (16:1n-7/16:0) increased after 24 hours of 2mM metformin treatment for all cellular TG fatty acid. However there was no effect on the elongation index (n = 5). **B:** Effect of metformin on desaturation and elongation of fatty acids in the exogenous TG fatty acid fraction. Here there was evidence of both increased desaturation and elongation **C, D, E and F:** Effect of metformin on fold change in RNA expression of SCD1 (C) and SCD5 (D) as determined by RTPCR (n=3) and protein expression as determined by western blot (E and F) (n=2). There was no evidence of increased SCD1 or SCD5 mRNA transcription or protein expression. Data shown are mean ± SEM, *p < 0.05; **p < 0.01; ***p < 0.001.

4.2.3: METFORMIN REDUCES THE PROPORTION OF TRIGLYCERIDE FATTY ACID DERIVED FROM DE NOVO LIPOGENESIS (DNL)

Malignant transformation is associated with a greater proportion of fatty acids being derived from DNL rather than exogenous sources (i.e. fatty acid uptake). Given the accumulation of triglyceride that had been observed in sensitive breast cancer cell lines an obvious question arose as to whether this was down to upregulation of DNL. Using mass spectrometry techniques the stable isotope, deuterated water ($^2H_20$), may be traced into fatty acids and hence an estimation of proportion of fatty acid derived from DNL may be made. In these experiments DMEM media was made up with 5% $^2H_20$ as greater proportions of $^2H_20$ in the media were noted to have an inhibitory effect on proliferation. After 48 hours of metformin treatment there was an accumulation of DNL-derived TG fatty acid (7.9 ± 0.5 versus 12.3 ± 1.0 μg/4 x 10^6, p = 0.015 in control and metformin-treated MCF7 cells, and 2.4 ± 0.2 versus 11.9 ± 0.7 μg/4 x 10^6, p <0.001 cells in control and metformin-treated MDA-MB-468 cells, respectively) (**Figure 4.5A**). However the proportion of fatty acids synthesised by DNL within the cellular TG pool in the MDA-MB-468 cell line fell (from 36.9% ± 5.4% to 29.7% ± 0.2%, p <0.001). For MCF7 cells there was a trend (although not statistically significant) toward a reduction in the proportion of fatty acids synthesised by DNL (from 68.6% ± 0.4% to 59.0% ± 1.9%, p = 0.17) (**Figure 4.5B**). Hence, although there was an accumulation of TG fatty acid derived from DNL it seemed likely that another process was important in driving the more general accumulation of TG fatty acid.

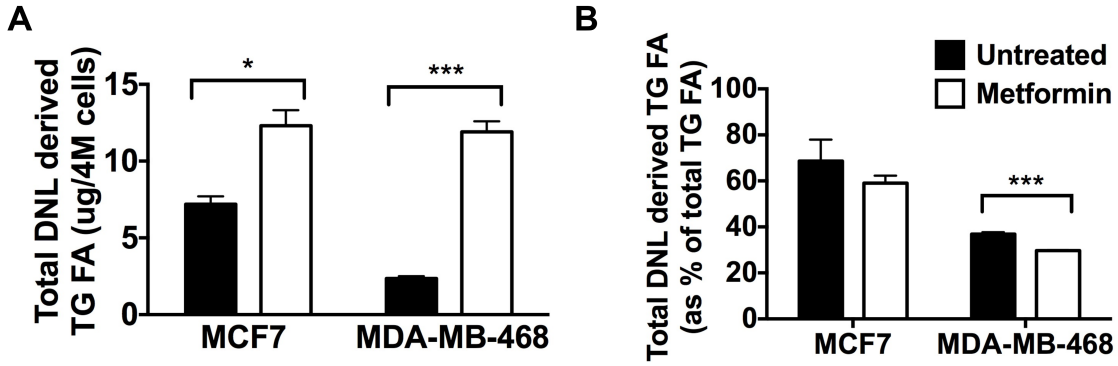


Fig 4.5A: Effect of 48 hours of 2mM metformin treatment on amount of intracellular DNL-derived fatty acid (estimated from ^2H_2O enrichment of TG fatty acid) expressed as total TG fatty acid (μg/4 x 10^6 cells) in MCF7 and MDA-MB-468 cells. Metformin treatment led to an accumulation of DNL-derived fatty acid in both cell lines. **B:** However as a percentage of total TG fatty acid metformin treatment reduced the proportion that was derived from DNL in MCF7 and MDA-MB-468 cells. Data shown are mean ± SEM, *$p < 0.05$; ***$p < 0.001$.

4.2.4: METFORMIN INCREASES FATTY ACID UPTAKE IN MCF7 AND MDA-MB-468 CELLS

As noted above metformin increased the total amount of the linoleic acid within MCF7 and MDA-MB-468 cells. However there was also evidence for an increase in linoleic acid as a proportion of the total TG fatty acid (4.0% ± 0.5% vs 6.4% ± 1.2%, $p = 0.14$, in control and metformin-treated MCF7 cells, and 2.2% ± 0.16% vs 6.1% ± 0.2%, $p < 0.001$, in control and metformin-treated MDA-MB-468 cells, respectively) (**Figure 4.6A**). As an essential fatty acid, linoleic acid could only have been taken up from the media and not synthesised via DNL. Also given that as a proportion of total TG fatty acid, DNL-derived fatty acid decreased, one could speculate that fatty acid uptake was predominantly responsible for the observed TG accumulation of TG fatty

acid in metformin-treated cells. Hence, the effects of metformin on cellular fatty acid uptake were examined.

BODIPY or boron-dipyrromene is a class of flourescent dye that can be tagged to a variety of molecules including fatty acids. 4,4-Difluoro-5,7-Dimethyl-4-Bora-3a,4a-Diaza-s-Indacene-3-Hexadecanoic Acid or BODIPY® FL C16 is an analogue of palmitate and using FACS techniques its uptake into cells can be traced. Consistent with an increase in fatty acid uptake, after 48 hours of treatment with 2mM metformin there was increased uptake of BODIPY® FL C16 in MCF7 cells compared with untreated cells (fold difference in fluorescence 1.42 ± 0.07, $p < 0.001$). Metformin (2mM) also stimulated uptake of BODIPY® FL C16 into MDA-MB-231 cells but the effect was less pronounced (fold difference in fluorescence 1.21 ± 0.07, $p = 0.008$) (**Figure 4.6B**).

Another method of tracing the passage of exogenous fatty acid into cells is to use ^{13}C labeling of fatty acids and determine any change in the proportion of the cellular TG fatty acid pool that is ^{13}C labeled using mass spectrometry techniques. MCF7 and MDA-MB-468 cells were incubated for 48 hours with or without 2mM metformin, in the presence of 50μM [U-^{13}C] palmitate. Using GC total TG fatty acid was measured and then via GC-MS the total isotopic enrichment of the TG fatty acid was measured. **Figure 4.6C** shows that metformin increased incorporation of exogenous palmitate into TG fatty acids in both MCF7 and MDA-MB-468 cells (^{13}C-labelled TG fatty acid: 4.5 ± 1.1 versus 13.5 ± 1.1 ug /4 x 10^6 cells, in control and metformin-treated MCF7 cells, $p = 0.008$ and 6.6 ± 1.0 versus 37.4 ± 2.0 μg /4 x 10^6 cells, $p < 0.001$, in control and metformin-treated MDA-MB-468 cells, respectively).

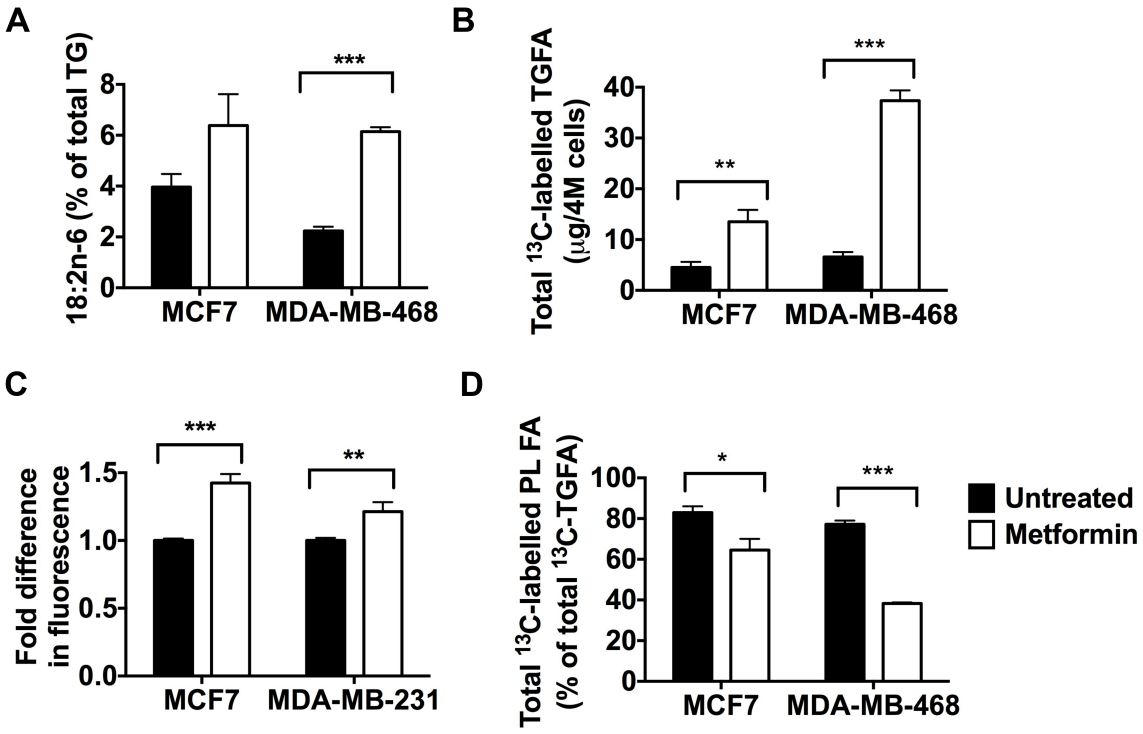


Fig 4.6A: 48 hours of 2mM metformin treatment increased the amount of linoleic acid (18:2n-6) as a proportion of total TG fatty acid in MCF7 and MDA-MB-468 cells (n=3). **B:** 48 hours of incubation with 2mM metformin and 50μM [U-^{13}C] palmitate resulted in an accumulation of (exogenous) ^{13}C-labelled TG fatty acid in MCF7 and MDA-MB-468 cells (n=3). **C:** 2mM metformin (after 48 hours treatment) increased the uptake of the fluorescent palmitate analogue BODIPY® FL C16 into MCF7 and MDA-MB-231 cells (n=3). **D:** 48 hours of 2mM metformin in the presence of 50μM [U-^{13}C] palmitate treatment led to a decrease in the proportion of ^{13}C-labelled PL fatty acid (as a proportion of total ^{13}C-labelled TG fatty acid) in MCF7 and MDA-MB-468 cells (n=3). Data shown are mean ± SEM. *$p < 0.05$; **$p < 0.01$; ***$p < 0.001$.

In contrast to [U-^{13}C] palmitate, BODIPY® FL C16 is only incubated with a cancer cell line for 15 minutes just prior to preparation for FACS analysis. Hence this technique only measures short-term uptake of fatty acid by the cell limiting the potential for cellular metabolism and secretion so that its measurement should be directly proportional to uptake. The degree of [U-^{13}C] palmitate incorporation into TG fatty acid might be altered by any downstream effect TG fatty acid breakdown e.g. by lipolysis or fatty acid oxidation.

4.2.5: METFORMIN REDUCES THE PROPORTION OF EXOGENOUS FATTY ACID DIRECTED TOWARD CELLULAR PHOSPHOLIPID

By measuring ^{13}C enrichment of PL fatty acids in the same samples that were used to measure enrichment of TG fatty acids from exogenous ^{13}C-palmitate it was observed that while metformin increased incorporation of exogenous fatty acid into intracellular TG, there was reduced incorporation into PL fatty acids (^{13}C-labelled PL as a percentage of total ^{13}C-labelled TG fatty acid: 83.0% ± 3.1% versus 64.5% ± 5.5%, in control and metformin-treated MCF7, $p = 0.019$, and 77.2% ± 1.9% versus 39.0% ± 1.9%, $p < 0.001$, in control and metformin-treated MDA-MB-468 cells, respectively) (**Figure 4.6D**). This suggested that in response to metformin exogenous fatty acids taken into the cells were stored as TG fatty acid rather than used for PL synthesis.

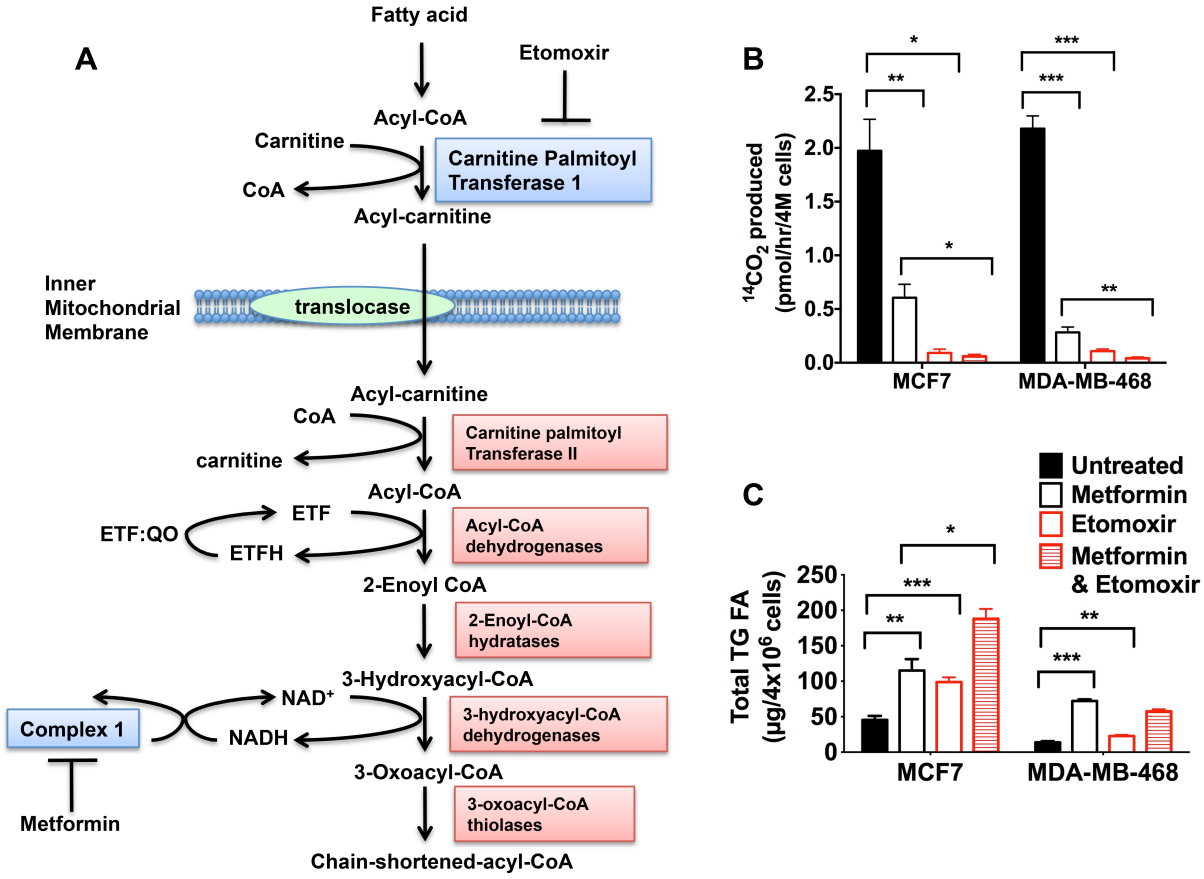


Fig 4.7A: Key steps of the fatty acid oxidation pathway. Carnitine palmitoyl transferease-1 transports long-chain fatty acids from the cytosol into the mitochondria and is inhibited by etomoxir. Complex 1 catalyses the second dehydrogenation step of the fatty acid oxidation pathway via its production of NAD^+ and this step is inhibited by metformin. Electron transfer flavoprotein (ETF) and ETF:coenzyme Q oxidoreductase (ETF-QO) are mitochondrial enzymes that are involved in fatty acid oxidation indirectly by accepting accepting electrons from FAD-dependent acyl-CoA dehydrogenases. **B:** Rate of oleate oxidation in MCF7 and MDA-MB-468 cells after 48hrs treatment with 0, 1mM (MDA-MB-468) or 2mM (MCF7) metformin and/or 100µM etomoxir (n = 3 for both cell lines). Metformin reduced markedly reduced oleate oxidation and further suppression was seen with the addition of etomoxir. **C:** Both 48 hours of metformin (2mM) and etomoxir (100µM) treated resulted in an accumulation of total TG fatty acid (n = 4 for MCF7s and n = 6 for MDA-MB-468s). Data shown are mean ± SEM *p < 0.05; **p < 0.01; ***p < 0.001.

4.2.6: METFORMIN REDUCES FATTY ACID OXIDATION IN MCF7 AND MDA-MB-468 CELLS

Metformin has been shown to both inhibit mitochondrial Complex 1 and activates AMPK. Complex 1 catalyses the second dehydrogenation step of the fatty acid oxidation pathway via the oxidizing power of NAD^+ [287] and hence its inhibition would be expected to downregulate fatty acid oxidation (**Figure 4.7A**). In contrast AMPK activation has been shown to increase fatty acid oxidation by decreasing malonyl-CoA concentrations and increasing expression of PPARα and PGC-1 expression [288]. Using [1-^{14}C]oleate as a tracer to measure fatty acid oxidation, ^{14}C-labelled CO_2 was captured and the rate of oleate oxidation could be estimated. Metformin treatment reduced fatty acid oxidation in MCF7 and MDA-MB-468 cells 3 and 8 fold respectively (1.97 ± 0.29 and 0.61 ± 0.13 pmol CO_2/h/4 x 10^6 cells in control and metformin-treated MCF7 cells, respectively, $p < 0.001$ and 2.18 ± 0.12 and 0.28 ± 0.04 pmol CO_2/h/4 x 10^6 cells in control and metformin-treated MDA-MB-468 cells, respectively, $p < 0.001$). Etomoxir is an inhibitor of carnitine palmitoyltransferase-1 (CPT-1) an enzyme that is responsible for the transport of long-chain fatty acids from the cytosol into the mitochondria, a rate limiting step for fatty acid oxidation. Used alone etomoxir reduced fatty acid oxidation approximately 20 fold in MCF7 cells ($p < 0.001$) and 40 fold in MDA-MB-468 cells ($p < 0.001$) and the combination of 100μM etomoxir and metformin further reduced fatty acid oxidation in both cell lines (**Figure 4.7B**).

This inhibition of fatty acid oxidation in MCF7 and MDA-MB-468 cells by metformin, provided a possible explanation for the observed accumulation of TG fatty acid in these cell lines. We repeated the experiments measuring incorporation of [U-

^{13}C]palmitate (50μM) into intracellular fatty acid and added 100μM etomoxir to inhibit fatty acid oxidation in both MCF7 and MDA-MB-468 cells. Etomoxir treatment, in a similar fashion to metformin, resulted in total TG fatty acid accumulation in both cell lines (45.6 ± 5.6 versus 98.9 ± 6.7 μg/4 x 10^6 cells, in control and metformin-treated MCF7 ($p < 0.001$) and 13.9 ± 1.6 versus 22.8 ± 1.7 μg/4 x 10^6 cells in control and metformin-treated MDA-MB-468 cells, respectively ($p = 0.005$)) (**Figure 4.7C**). This implies that the TG accumulation in response to metformin in MCF7 and MDA-MB-468 cells is at least partly dependent on reduced fatty acid oxidation. In MCF7 cells, but not in MDA-MB-468, the combination of etomoxir and metformin led to an increased accumulation of TG fatty acid compared to metformin treatment alone despite in both cell lines there being a further inhibition of fatty acid oxidation with the addition of etomoxir. The reason for this is unclear, but different cancer cell lines may have different capacities for lipid storage.

4.2.7: ETOMOXIR AND METFORMIN HAVE AN ADDITIVE EFFECT IN SUPPRESSING THE GROWTH OF BREAST CANCER CELLS IN VITRO

If metformin was suppressing fatty acid oxidation in sensitive breast cancer cell lines, was this effect important for its inhibition of cancer cell proliferation? Etomoxir (100μM) had a small but statistically significant inhibitory effect on the proliferation of MCF7 cells (6.8 ± 3.7 x10^5 cells versus 5.8 ± 3.1 x10^5 cells at 96 hours, for untreated and etomoxir treated cells, respectively ($p=0.04$)) when used alone and there was a trend toward an inhibitory effect in the MDA-MB-468 (1.3 ± 1.3 x10^6 cells versus 1.1 ± 0.9 x10^6 cells at 96 hours, for untreated and etomoxir treated cells, respectively ($p=0.20$)) and MDA-MB-231 cell lines (1.4 ± 0.2 x10^6 cells versus 1.2 ± 0.1 x10^6 cells at 96 hours, for untreated and etomoxir treated cells, respectively

(p=0.14)). There was also evidence of an additive antiproliferative effect for etomoxir and metformin in all 3 cell lines (5.8 ± 3.1 $x10^5$ cells and 5.9 ± 0.5 $x10^5$ cells versus 4.5 ± 0.4 $x10^5$ cells at 96 hours, for etomoxir (p = 0.014) and 2mM metformin (p = 0.037) versus combination treated MCF7 cells, respectively; 1.1 ± 0.1 $x10^6$ cells and 0.9 ± 0.03 $x10^6$ cells versus 0.6 ± 0.04 $x10^6$ cells at 96 hours, for etomoxir (p = 0.001), 1mM metformin (p=0.019) versus combination treated MDA-MB-468 cells, respectively; 1.2 ± 0.2 $x10^6$ cells and 0.9 ± 3.1 $x10^6$ cells versus 0.9 ± 0.1 $x10^6$ cells at 96 hours, for etomoxir (p < 0.001) and 10mM metformin (p=0.005) versus combination treated MDA-MB-231 cells, respectively). This suggests that the suppression of fatty acid oxidation and subsequent induced energy stress is important in promulgating metformin's anticancer effect (**Figure 4.8A**).

Both metformin and etomoxir treatment alone decreased ATP levels in MDA-MB-468 cells, with further ATP depletion observed upon combination treatment (fold difference in luminescence for untreated, 1.00 ± 0.02; metformin 0.66 ± 0.03; etomoxir 0.86 ± 0.01; and combination, 0.56 ± 0.001, respectively). That etomoxir alone also reduced ATP levels but to a lesser extent compared to metformin suggests that it is metformin's effect in combining the inhibition of glucose oxidation and fatty acid oxidation that induces an especially marked energy stress (**Figure 4.8B**).

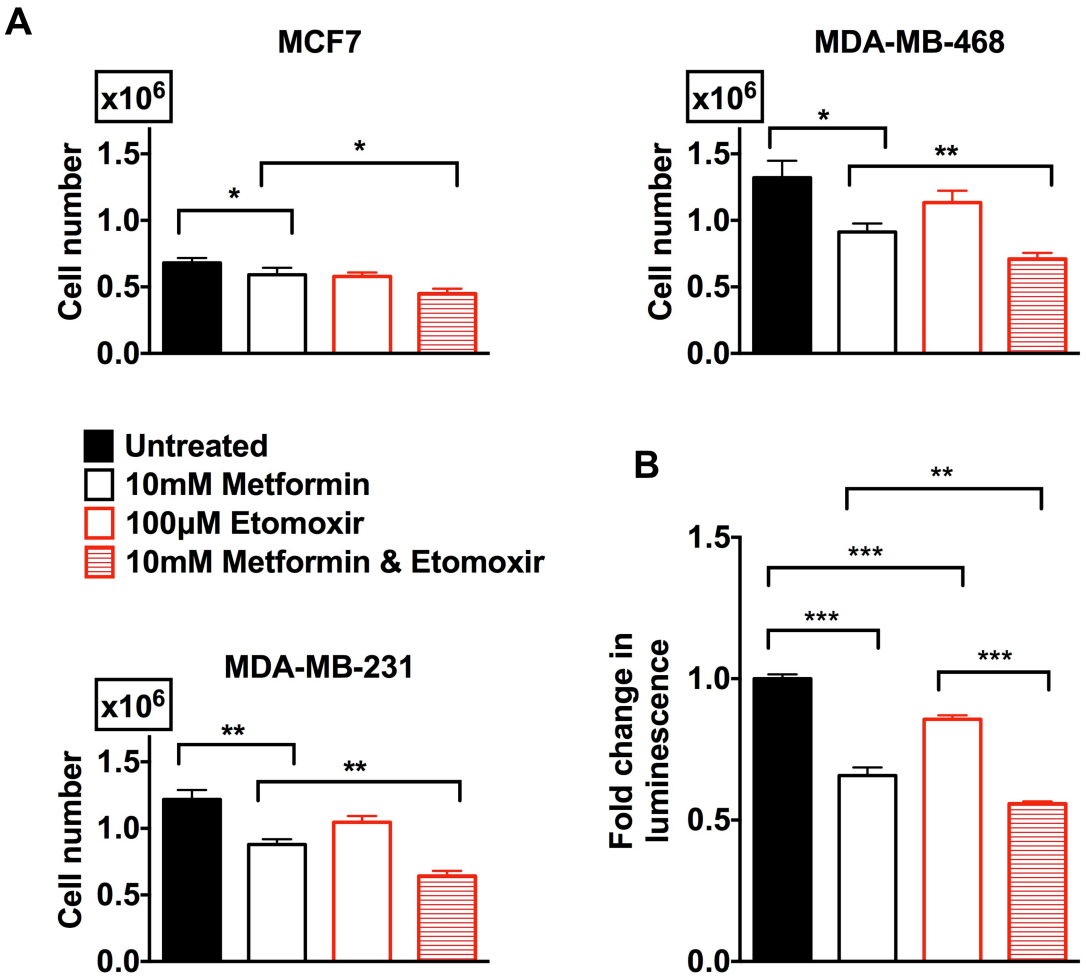


Fig 4.8A: MCF7, MDA-MB-468 and MDA-MB-231 cells were treated with 2mM metformin and/or 100μM etomoxir versus control for up to 96 hours and cell number measured (n=12 for all cell lines) In all 3 cell lines there was evidence of synergy between metformin and etomoxir with regard to antiproliferative effect. **B:** Both metformin and etomoxir alone reduced ATP levels in MDA-MB-468 cells and there was further depletion in combination (n = 4). Data shown are mean ± SEM *$p < 0.05$; **$p < 0.01$; ***$p < 0.001$.

4.2.8: METFORMIN TREATMENT DOES NOT AFFECT LIPOLYSIS

Another hypothesis that might explain the accumulation of TG fatty acid observed was inhibition of breakdown of TG to diglyceride (DG) i.e. lipolysis. One indirect method of measuring lipolytic activity is to calculate the ratio of DG to TG. Metformin-treated MCF7 cells had a significantly reduced ratio ($p = 0.005$), suggesting that metformin may down-regulate lipolysis (**Figure 4.9A**).

Adipose triglyceride lipase (ATGL) is the enzyme that catalyses the lipolysis of TG to DG and indirect measurements of its activity were made (please note that this work was undertaken on samples I provided to a collaborator, Prof Hoefler's group at the University of Graz and this assay was performed by Ms Pooja Jha). ATGL activity was measured as previously described by Das et al [212] using the radiolabelled triglyceride [9,10-3H(N)-triolein]. After incubation with or without the specific hormone sensitive lipase (HSL) inhibitor, 76-0079, lipolytic activity could be estimated by measuring the radioactivity of the free fatty acid fraction using a liquid scintillation counter. ATGL activity could then be assessed by making the assumption that any lipolytic activity that occurred in the presence of the HSL inhibitor was due to ATGL. Using this assay 48 hours of 2mM metformin treatment had no effect on ATGL or HSL enzyme activity in MCF7 cells (**Figure 4.9B**). ATGL is thought to be subject to post-translational regulation that is still not fully understood [289] but is thought to be activated, at least in part, via its phosphorylation. It has been shown that this is regulated by AMPK [289]. Certainly, when measured by RT-PCR, metformin had no effect on the expression of *PNPLA2* (ATGL's encoding gene) (**Figure 4.9C**). In summary, in our in vitro model there was no clear evidence of metformin having an effect on lipolytic activity.

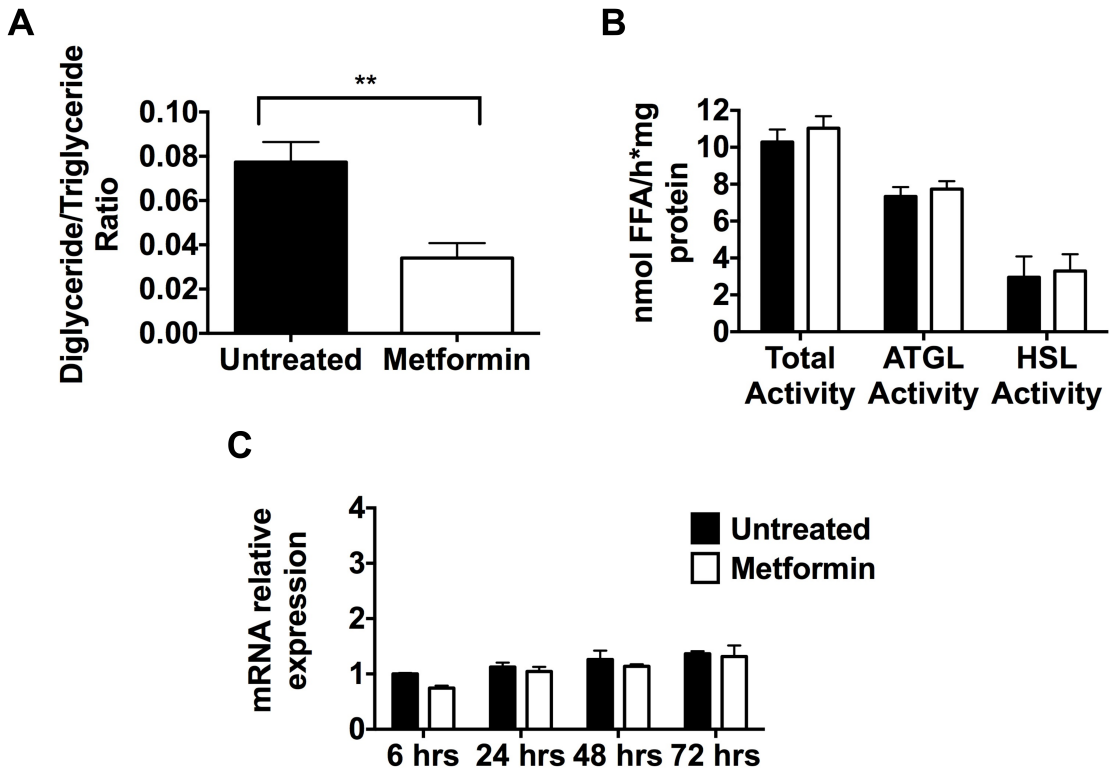


Fig 4.9A: 48 hours of 2mM metformin significantly reduced the diglyceride to triglyceride ratio in MCF7 cells (n=5). **B:** Adipose Triglyceride Lipase (ATGL) activity, an enzyme that plays a key role in triglyceride breakdown and lipid droplet degradation, was not affected by metformin. Hormone sensitive lipase (HSL) activity was also not affected by metformin (n=3). **C:** 2mM Metformin had no clear effect on the expression of PNPLA2 (ATGL's encoding gene) (n=3). Data shown are mean ± SEM. **P < 0.01.

4.2.9: ACTIVATION OF AMPK DOES NOT MEDIATE METFORMIN'S EFFECTS ON TRIGLYCERIDE ACCUMULATION

There have been many studies that have linked metformin, activation of AMPK and its subsequent phenotypic effects on cancer cells. The finding that metformin inhibited fatty acid oxidation, rather than stimulating it, already suggested that at least some of metformin's effects on lipid metabolism were independent of AMPK but rather secondary to its more direct mitochondrial effect. In order to further investigate whether AMPK activation was important in the effect on TG fatty acid accumulation, the effect of other compounds that modulate AMPK activation and siRNA inactivation of AMPK were examined.

AICAR or ZMP is an activator of AMPK via its mimicry of AMP [290]. Using GC chromatography accumulation of TG fatty acid in MCF7 cells was measured after 48 hours with and without 0.25mM AICAR. However, AICAR treatment had no significant effect on TG accumulation or percentage synthesis (**Figure 4.10A and B**). The effects of AMPK knockdown on DNL and exogenous fatty acid accumulation in metformin-treated MCF7 cells were then investigated. Using AMPK-targeted siRNA to the PRKAA1 and PRKAA2 subunits of AMPK, approximately 70 to 80% knockdown was achieved (as determined using qPCR) and abrogation of phosphorylation of AMPK at 72 hours (**Figure 4.10C**). **Figure 4.10D** shows that total TG fatty acid increased with metformin treatment but was unaffected by AMPK silencing (control Scr and AMPK knockdown = 13.7 ± 1.8 and 12.6 ± 2.6 µg/4 x 10^6 cells, respectively, and metformin Scr and AMPK knockdown = 23.4 ± 3.5 and 21.7 ± 4.2 µg/4 x 10^6 cells, respectively). Silencing of AMPK also had no effect on DNL-derived TG fatty acid accumulation as a percentage of total TG fatty acid in either

control or metformin-treated cells when measured by $^{2}H_20$ enrichment (control Scr and AMPK knockdown = 39.8% ± 1.0% and 39.3% ± 1.5%, respectively, and metformin Scr and AMPK knockdown = 33.7% ± 1.0% and 34.1% ± 0.7%, respectively).

AMPK knockdown in MCF7 cells did lead to a reduction in BODIPY uptake both in control cells (fold difference in fluorescence compared with scrambled control 0.82 ± 0.03, p=<0.001) and metformin treated cells (fold difference in fluorescence compared with scrambled control from 1.52 ± 0.05 to 1.27 ± 0.02 after knockdown, p=0.002) (**Figure 4.10E**). However, the fact that that accumulation of exogenous TG fatty acid (as defined by all TG fatty acid minus DNL-derived fatty acid) as measured in the $^{2}H_2O$ experiment above was not affected by AMPK knockdown in either the control or metformin treated cells does suggest that any impact on TG FA accumulation by an AMPK induced increase in fatty acid uptake is insignificant with regard to driving the accumulation of TG fatty acid (control Scr and AMPK knockdown = 5.91 ± 0.72 and 10.98 ± 1.59 µg/4 x 10^6 cells, respectively, and metformin treated Scr and AMPK knockdown = 5.56 ± 1.12 and 10.32 ± 1.93 µg/4 x 10^6 cells, respectively). Consistent with known sequelae of AMPK activation AICAR did modestly increase fatty acid oxidation (12.7 ± 0.3 versus 13.9 ± 0.2 pmol CO_2/h/4 x 10^6, p = 0.015, in control and AICAR-treated MCF7 cells, respectively) (**Figure 4.10F**).

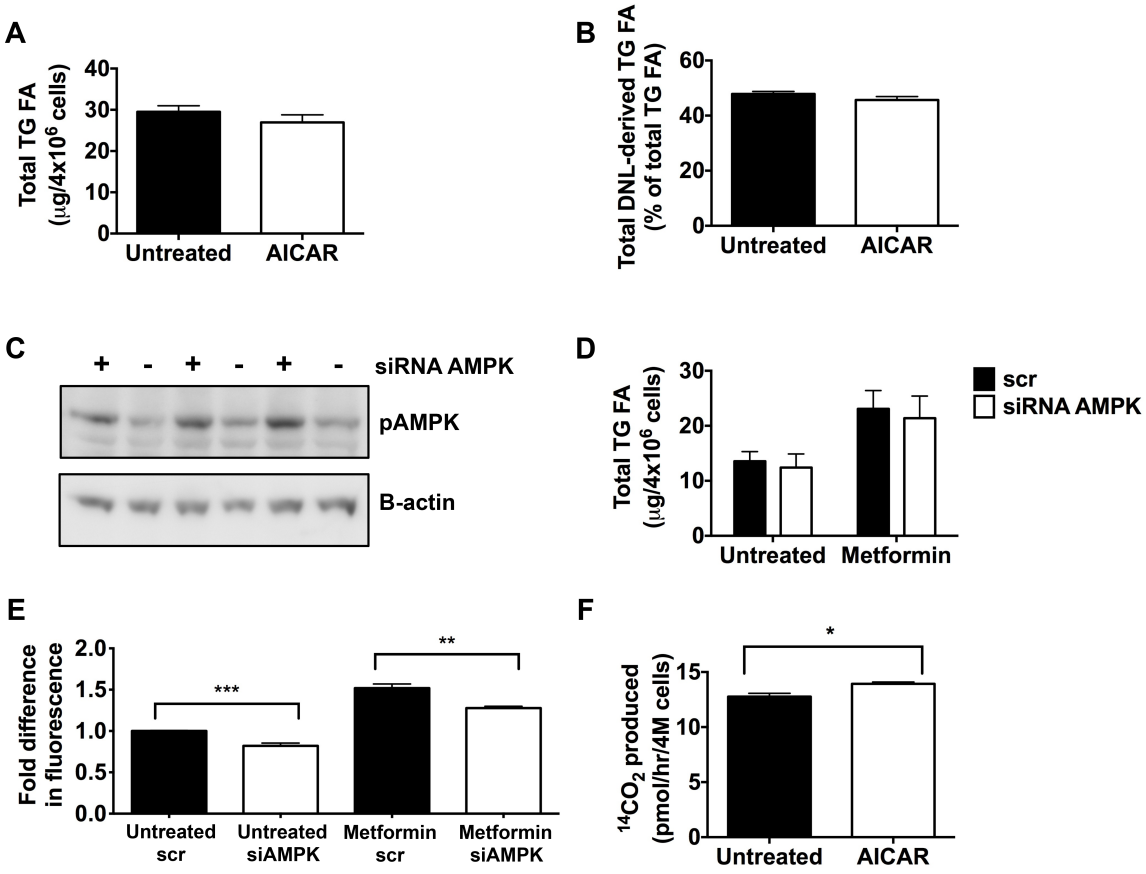


Fig 4.10A: Treatment of MCF7 cells with 0.25mM AICAR for 48 hours had no clear effect on intracellular TG fatty acid content (n = 3). **B:** Treatment of MCF7 cells with 0.25mM AICAR for 48 hours had no clear effect on the proportion of intracellular DNL-derived fatty acid (estimated from $^{2}H_2O$ enrichment of TG fatty acid) expressed as total TG fatty acid (μg/4 x 10^6 cells) in MCF7 cells (n = 3). **C and D:** AMPK knockdown of MCF7 cells (AMPK k/d) had no significant effect on TG fatty acid accumulation in metformin treated MCF7 cells compared with scrambled siRNA (Scr) (n = 3). **E:** AMPK knockdown of MCF7 cells resulted in reduced uptake of the fluorescent palmitate analogue BODIPY® FL C16 in both untreated and metformin treated cells (n = 3). **F:** Treatment of MCF7 cells with 0.25mM AICAR for 48 hours led to a small increase in fatty acid oxidation (n = 3). Data shown are mean ± SEM *p < 0.05; **p < 0.01; ***p < 0.001.

4.2.10: ROTENONE MIMICS METFORMIN'S EFFECTS ON TRIGLYCERIDE ACCUMULATION

Rotenone is another inhibitor of mitochondrial Complex 1 and hence was of interest as a comparator to metformin in terms of effects on lipid metabolism. Consistent with our findings for metformin, rotenone treatment led to an accumulation of TG fatty acid (26.9 ± 2.7 versus 39.6 ± 2.9 μg/4 x 10^6 cells in control and rotenone-treated MCF7 cells, respectively, p = 0.032) (**Figure 4.11A**). Furthermore, rotenone treatment significantly reduced oleate oxidation (8.1 ± 0.3 versus 4.9 ± 0.1 pmol CO_2/h/4 x 10^6, p < 0.001 in control and rotenone-treated MCF7 cells, respectively) (**Figure 4.11B**). These findings taken together with the results from the AICAR and AMPK knockdown experiments, are good evidence that metformin's effects on lipid metabolism are driven by its more direct mitochondrial toxicity but independent of AMPK activation in breast cancer cells.

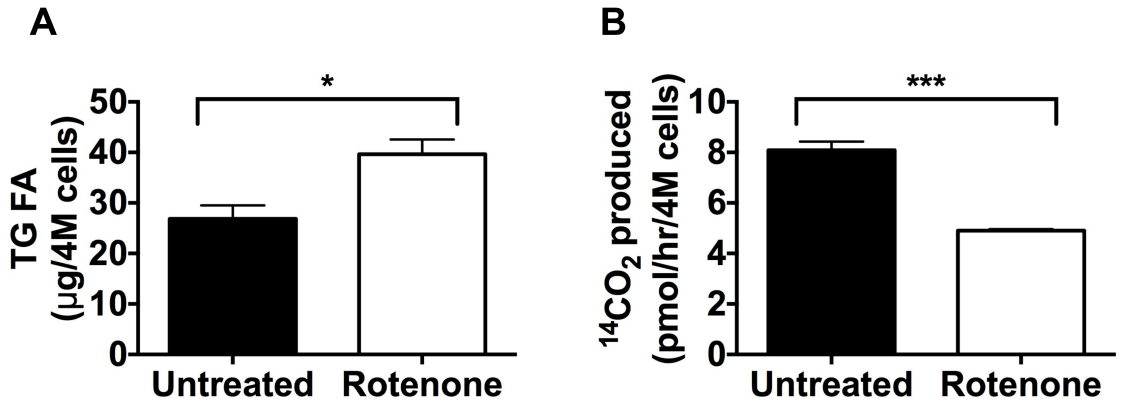


Fig 4.11A: Treatment of MCF7 cells with 100nM rotenone for 48 hours led to an increase in intracellular TG fatty acid content (n = 3). **B:** Treatment of MCF7 cells with 100nM rotenone for 48 hours led to a decrease in fatty acid oxidation (n = 3). Data shown are mean ± SEM *p < 0.05; ***p < 0.001.

4.2.11: ADDITION OF PALMITIC ACID AND OLEIC ACID DOES NOT ALTER METFORMIN'S EFFECT ON BREAST CANCER CELL LINE PROLIFERATION

As the accumulation of TG fatty acid was observed most strongly in the MCF7 and MDA-MB-468 cell lines, which were also the most sensitive cell lines in terms of effects on proliferation, a further question was whether this accumulation of TG fatty acid was also contributing to metformin's anticancer effects. In order to assess this hypothesis the fatty acids, palmitic acid and oleic acid, were added at different concentrations to MCF7 cells with and without 2mM metformin for 96 hours. However, the addition of either of these fatty acids had no effect on MCF7 proliferation suggesting that the accumulation of TG FA was not toxic in itself (**Figure 4.12A and B**). Note that marked lipid droplet formation was seen with the addition of 250μM oleic acid alone to MCF7 cells on confocal microscopy (**Figure 4.2A**) and doses of up to 500μM were used in this experiment.

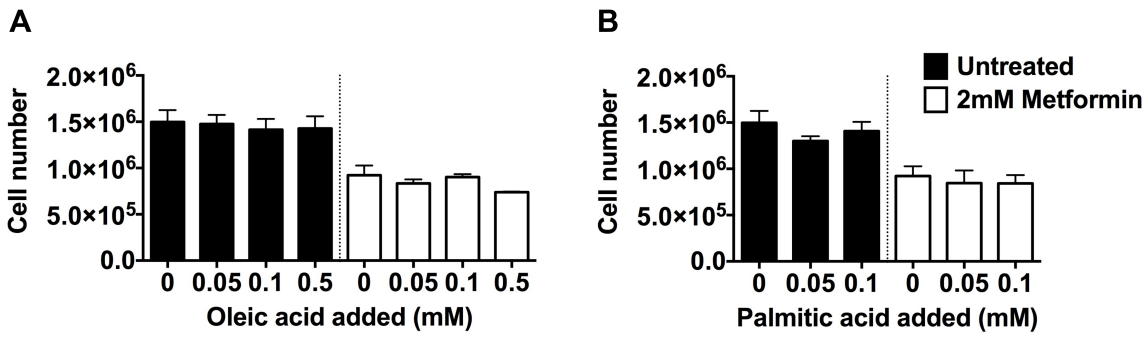


Fig 4.12A: Addition of 0.05, 0.1mM or 0.5mM oleic acid had no effect on MCF7 cell proliferation at 96 hour timepoint. **B:** Addition of 0.05 or 0.1mM palmitic acid had no effect on MCF7 cell proliferation at 96 hour timepoint. Data shown are mean ± SEM.

4.3: DISCUSSION

4.3.1: METFORMIN'S INHIBITION OF FATTY ACID OXIDATION IS IN CONTRAST TO PREVIOUS STUDIES AND IS A NOVEL EXPLANATION FOR ITS ANTICANCER EFFECT

As summarised in section 4.1.1 above, most in vitro studies of metformin's effects on lipid metabolism have been undertaken in non-cancer models. To date, the evidence has suggested that metformin decreases TG accumulation by inhibiting DNL and increasing fatty acid oxidation in an AMPK dependent fashion [32, 33, 276, 277]. However, the observation in this study was that in breast cancer cells metformin has the opposite effect, increasing TG accumulation and inhibiting fatty acid oxidation in an AMPK independent fashion. It is unclear as to why the effects are so different in these cell types although it may be that in hepatic, as a consequence of the liver's key role in metabolic homeostasis, activation of AMPK occurs more readily and overrides metformin's more direct mitochondrial effects. Similarly, in muscle cells, activation of AMPK may occur more readily to cope with more regular energy stresses.

The observed metformin-induced increase in total cellular TG seems to be due to 2 separate observed effects: a) decreased fatty acid oxidation, and b) increased exogenous fatty acid uptake; (**Figure 4.13**). Given that siRNA AMPK inactivation had no effect on TG accumulation and that the Complex 1 inhibitor, rotenone, in contrast to the AMPK activator, AICAR, mimicked metformin's effects, it is clear that in this breast cancer model metformin's more direct effect on complex 1 is the driver of changes to lipid metabolism rather than subsequent AMPK activation. The reduced proportion of fatty acid directed toward phospholipid synthesis as a ratio to stored TG fatty acid seems unlikely to be as a result of a direct effect of metformin on

this process but rather due to the build up of unusable fatty acid in a non-proliferating cell (i.e. a cell that does not require a comparative increase in phospholipid synthesis).

Is there a link between metformin's modulation of lipid metabolism and its anti-proliferative effect? It is notable that the most sensitive cell line to metformin both in terms of the anti-proliferative effects and TG accumulation response was MDA-MB-468 and the most resistant in terms of both parameters, the MDA-MB-231 cell line. The accumulation of TG fatty acid in itself does not seem to be toxic to cells, at least in the short term context of these in vitro experiments. Rather the link seems to be in regard to the ability of cells to utilise this lipid at times of metabolic stress. The finding that etomoxir has an additive antiproliferative effect with metformin suggests that suppression of fatty acid oxidation and the subsequent induced energy stress is important in driving metformin's anticancer effect. This seems especially to be the case when the cell is undergoing a concomitant energy stress as etomoxir had only a small effect when used alone in the MDA-MB-468 and MDA-MB-231 cell lines. Metformin has been shown to inhibit glucose oxidation and deplete ATP in cancer cells [143, 234] and the requirement of fatty acid oxidation for ATP production in cancer cells at times of metabolic stress has been shown in several different models. Zaugg et al showed that the overexpression of the mitochondrial fatty acid transporter, carnitine palmitoyltransferase 1 (CPT1) promoted tumour progression, resistance to mTOR inhibitors and enabled rescue from hypoxia or glucose deprivation [198]. Similarly, the ability of the promyelocytic (PML) protein to upregulate fatty acid oxidation promotes cell survival under conditions of metabolic stress [291, 292]. Metformin, selectively targets cancer stem cells and recently a link has been has been

made to active fatty acid oxidation and cancer stem cell maintenance and function [197, 293].

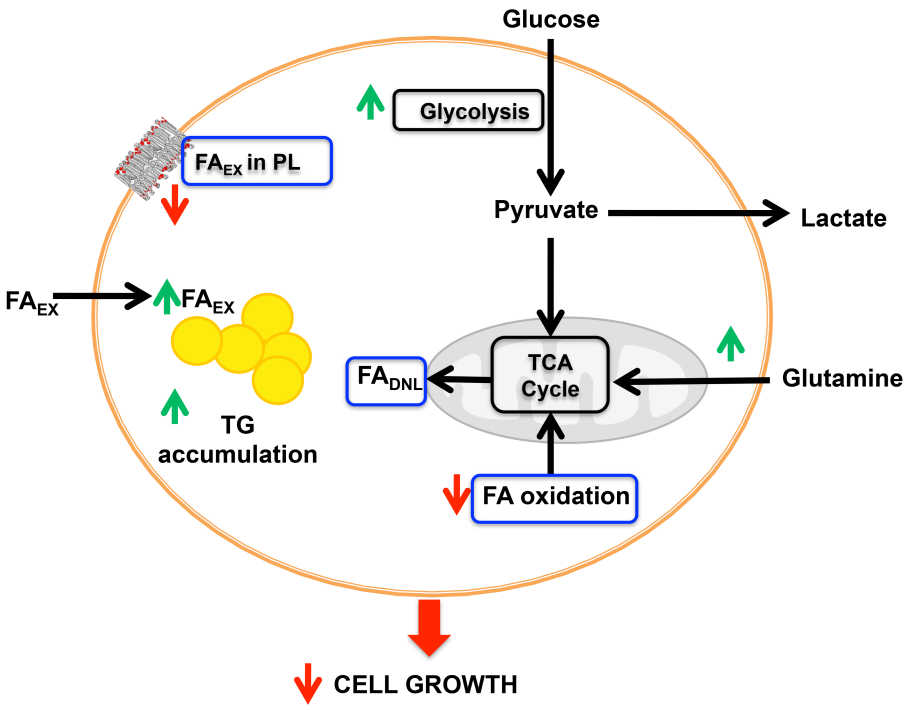


Fig 4.13: Summary of metformin's effects on lipid metabolism in breast cancer cells. Metformin treatment of breast cancer cells leads to an accumulation of exogenous and DNL-derived fatty acid. Accumulation of TG is secondary to reduced FA oxidation and increased fatty acid uptake. Flux of glucose towards DNL (still the main substrate for this process) is reduced whilst glutamine utilisation for fatty acid synthesis increased as a proportion. Metformin's predominant effects on lipid metabolism in breast cancer cells are via an AMPK-independent pathway and secondary to its more direct mitochondrial effect on Complex 1. In summary the inability of the cell to upregulate fatty acid oxidation in response to ATP depletion induced by the impaired oxidation of glucose leads to a further inhibitory effect on breast cancer cell proliferation.

Lastly, dependence on glutamine as a substrate for DNL and for proliferation (see Chapter 3) suggests there is a particular importance with regard to DNL in supporting growth in metformin treated cancer cells. Given that in the nutrient starved tumour microenvironment the concentration of glutamine will be very much less than that of DMEM (4mM) [132] this dependence may be an 'Achilles heal' for metformin treated cancer cells.

These findings provide an insight into metformin's mechanism of action and may have important clinical implications. This modulation of cancer lipid metabolism may prove a useful biomarker of anti-cancer effect, for example, the degree of accumulation of intracellular lipid or changes in lipid relevant gene and protein expression might define early metabolic response. Development of other drugs that target fatty acid oxidation should be explored and the combination of metformin with other modulators of lipid metabolism, such as FAS inhibitors or SCD inhibitors might result in synergistic lethality.

4.3.2: METFORMIN'S EFFECT ON TRIGLYCERIDE ACCUMULATION NEEDS FURTHER ASSESSMENT IN VIVO – FUTURE WORK

As with regard to the work described in chapter 3 ideally this data should be correlated with that obtained from an in vivo xenograft model. By giving the animals stable isotopes, for example deuterated water, ^{13}C glucose or ^{13}C glutamine, one could feasibly tease out the effect of metformin on DNL and confirm the effects on substrate utilisation for lipid synthesis in vivo. Effects on fatty acid oxidation might be assessed in a xenograft model using ^{14}C oleate. The lipid metabolism effects seen in vitro could also be validated by carrying out metabolomics, using biophysics

techniques, on clinical samples from the neoadjuvant metformin study discussed in later chapters. The investigation of metformin's effects on the lipid metabolism on cancer stem cells would be an especially interesting avenue of investigation. Lastly the combination of metformin with FAS and SCD inhibitors should be explored using in vitro and in vivo models.

CHAPTER 5: CLINICAL STUDY

5.1: INTRODUCTION

5.1.1: METFORMIN AND ITS PLACE IN THE BREAST CANCER CLINIC

It is still not clear as to the role of metformin in the oncology clinic and to date, in the cancer setting, no randomised prospective study with clinical benefit as an endpoint has been completed. One phase 3 clinical trial that randomises women with breast cancer to adjuvant treatment post surgery either placebo or metformin for 5 years and has relapse free survival as its primary outcome measure has recently completed the recruitment of 3649 patients [275]. However, this study recruited from an essentially unselected early breast cancer population and was designed prior to significant efforts toward biomarker development. Hence, it is possible that evidence of clinical benefit will be masked due to poor patient selection.

5.1.2: FOCUS OF PUBLISHED BIOMARKER STUDIES TO DATE

As discussed in Chapter 1 several assays have been proposed as possible biomarkers of metformin's clinical effect. However, most of these markers have been derived from in vitro and animal model studies rather than clinical data. In the past 2 years a series of neoadjuvant clinical studies have now been published that examine the effect of metformin on breast cancer in the 2-4 week 'window of opportunity' prior to surgery or primary chemotherapy. To date the focus in these studies has been put on the immunohistochemical measure of proliferation, Ki67, and serum metabolic markers, in particular, insulin and glucose levels. Although one such study has suggested that in patients with evidence of insulin resistance (as determined by a HOMA index >2.8) there may be a fall in Ki67 with metformin treatment, its promise

as a biomarker in breast cancer, at least over a short treatment period, seems limited [105]. One particular stumbling block for the development of robust biomarkers of metformin's clinical effect is that there is still much debate as to the drug's precise mode of action. Hence there remains a need for a detailed study of metformin's metabolic effect in breast cancer using clinical samples.

5.1.3: AIMS

The aim of this part of the project was to describe metformin's effects on breast metabolism and assess for evidence of anticancer effect in the clinical setting. In particular to: a) investigate whether metformin altered ^{18}[F]-FDG uptake into the primary breast cancer and any metastases b) assess whether change in mRNA expression pre- and post-metformin could shed light on its metabolic effect in the clinical setting c) assess the effect of metformin on serum metabolic markers in a non-diabetic breast cancer population d) assess metformin's effect on proliferation, AMPK activation and mTOR activation using immunohistochemical markers and e) assess effect of metformin on metabolite profile of tumour using detailed mass spectrometry metabolomic techniques (results not described in this thesis as work incomplete). Potential biomarkers of interest developed from this study would then need to be taken forward into large scale clinical trials in order to then correlate with definitive endpoints of clinical benefit. Note that in this thesis only the preliminary results of this study are presented.

5.2: STUDY DESIGN

This was a multicentre early phase, single arm, non-randomised, open label investigator-led study. In total 41 patients with early breast cancer and suitable for neoadjuvant chemotherapy were approached and recruited from the oncology clinic at 3 cancer centres: Oxford, Mt Vernon/Luton and Dundee. 37 of the 41 patients were recruited in Oxford and all but one patient had their PET-CT scans carried out in this centre. In order to ensure that the primary tumour was assessable on the research PET-CT scan, tumours had to be at least 2cm in the longest dimension. Of particular note, diabetic patients were excluded from this study in order that only tumours from patients with a 'normal metabolism' were studied. Please see **Table 5.1** below for a summary of all inclusion/exclusion criteria. Participants received a 13-20 day course of metformin shortly after diagnosis in the 'window of opportunity' before any other treatment had been given. Before and after a minimum of 13 days of metformin participants underwent a series of pharmacodynamic tests as detailed below:

- Administration of oral deuterated (heavy) water on evening prior to first and second research biopsy.
- Research PET-CT scan
- 3 research breast core biopsies
    - for immunohistochemistry
    - for next generation RNASeq analysis for messenger and small RNAs
    - for metabolomic analysis using mass spectrometry
- Fasting blood and urine samples

Over the first 6 days the metformin dose was increased stepwise from 500mg to 1500 mg daily in order to reduce the risk of significant side effects. Study participants then had the option of continuing to take metformin off study throughout their neoadjuvant chemotherapy after all formal study tests were completed. See **Figure 5.1** for summary of study schema.

Inclusion criteria	Exclusion criteria
Women with a histology proven in situ primary breast cancer ≥2 cm in diameter	Radiotherapy, major surgery, significant traumatic injury, endocrine therapy, immunotherapy, chemotherapy or experimental therapy during four weeks prior to starting or during trial
ECOG performance status 0-1	Pregnancy or breast feeding
Age ≥18 years	History of type 1 or type 2 diabetes
Fasting or random serum glucose less than 7.0 mMol/L	Treatment with metformin in the past year
No prior treatment for breast cancer and scheduled to commence neoadjuvant chemotherapy in ≤3 weeks time	Estimated glomerular filtration rate (eGFR) <45ml/min
Have given written informed consent and are capable of cooperating with protocol	Acute or chronic metabolic acidosis
Adequate bone marrow, renal and liver function	Known hypersensitivity to metformin

Table 5.1: Inclusion/exclusion criteria for clinical study

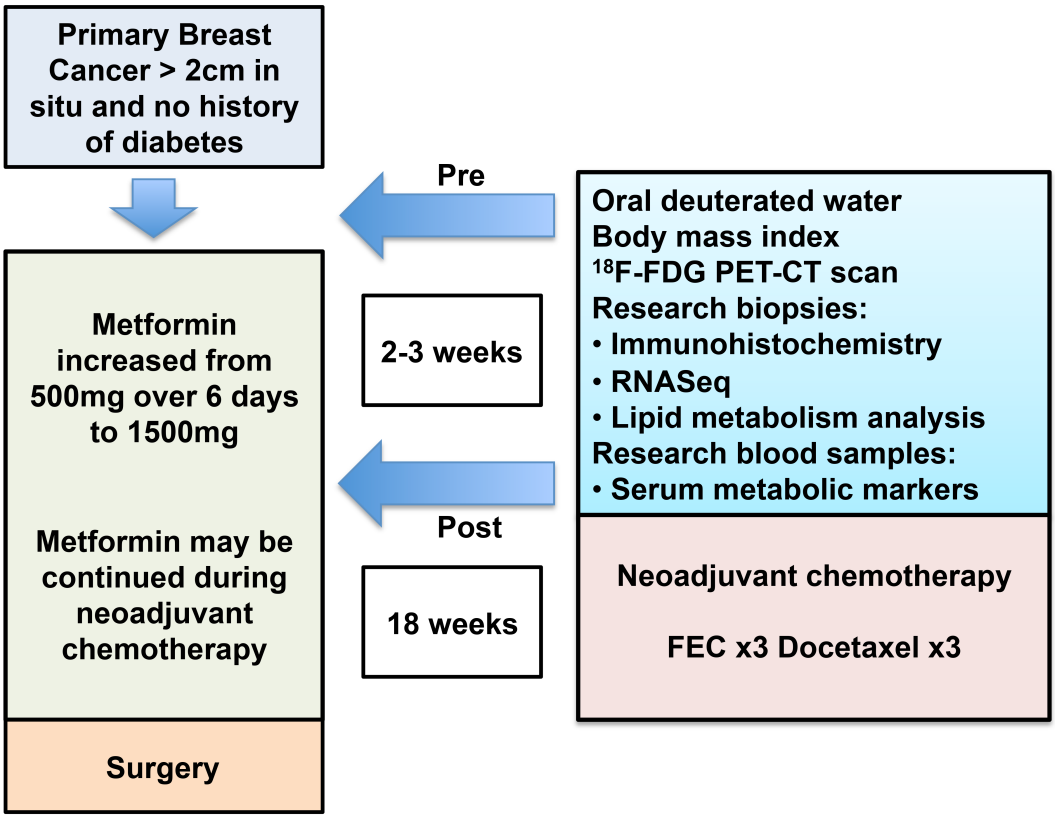


Fig 5.1: Schema for 'window of opportunity' clinical study of metformin's metabolic effects in breast cancer.

Centres	UK	Oxford, Dundee and Mt Vernon/Luton
Assays	Static and dynamic ^{18}[F]-FDG PET-CT	Assess for change in ^{18}[F]-FDG uptake into primary tumour and any metastases
Assays	Immunohistochemistry	Assess for change in protein expression of Ki67, pAMPK, pS6 and p4E-BP1
	Next generation RNASeq and small RNASeq	Assess for change in gene expression in relevant metabolic pathways
	Metabolomics: Liquid chromatography – mass spectrometry (LC-MS)	Assess for change in TCA cycle/glycolysis/glutamine intermediates and fatty acid profile, triglyceride accumulation and incorporation of deuterated water into triglyceride fatty acid
	Serum metabolic markers	Metformin, glucose, lactate, insulin, c-peptide, IGF1, IGF2, IGF-BP3, leptin, triglyceride, HDL and total cholesterol

Table 5.2: Summary of clinical study assays

As summarised in **Table 5.2** the pharmacodynamic tests were designed to detect drug induced metabolic changes in the primary breast cancer with a focus on glucose, glutamine and lipid metabolism. The role of the static and dynamic ^{18}[F]-FDG PET-CT scans was to detect changes in the flux of glucose into the primary tumour and any metastases. Immunohistochemical analysis was designed to detect changes in markers of signaling within the AMPK pathway and proliferation. Whole cancer genome sequencing analysis focused on changes in gene expression of pathways relevant to mitochondrial and oxidative phosphorylation metabolism and glucose, glutamine and lipid metabolism. Metabolomic analysis using liquid chromatography mass spectrometry techniques will assess for changes in glycolysis, TCA cycle and glutaminolysis intermediates. Lipidomic analysis will focus on the effect of

metformin on triglyceride accumulation, SCD flux and changes in the incorporation of deuterated water into fatty acids (reflective of an altered rate of fatty acid synthesis). Note this metabolomic work is ongoing and no preliminary data is available to be presented in this thesis. Lastly changes in serum metabolic markers relevant to the glucose/insulin axis and lipid metabolism were measured. Future correlation of change in these serum markers with change in the intratumoral assays should allow assessment of the importance of 'host' metabolic effects on the tumour.

5.3: PATIENT AND CLINICAL CHARACTERISTICS

In total 41 patients were recruited to the study over a period of 30 months. The clinical characteristics are summarised in **Table 5.3** and reflect the fact that these patients were recruited from a group referred to the medical oncology clinic with a view to neoadjuvant chemotherapy. Hence the young median age at diagnosis (49 years) and larger size of the tumours (median = 53mm). Only 20% of tumours were triple receptor negative and 71% oestrogen receptor positive, consistent with an unselected breast cancer population. However, given the young age of patients and larger size of tumours it might have been expected that a greater proportion were oestrogen receptor negative.

The body mass index of patients entering this study (27 SI) was the same as the UK average [294]. Under current WHO classifications, 39% of patients were of normal weight (BMI < 25), 24% overweight (BMI 25 – 30) and 37% obese (BMI ≥ 30).

Post chemotherapy, of those that had MRI assessment virtually all had a response to chemotherapy. However, only 4 patients (13%) had a pathological complete response

to chemotherapy, lower than might be expected in a cohort undergoing modern anthracycline and taxane based neoadjuvant chemotherapy. However this figure may well be coincidental due to the small sample size.

Recruitment	Total	41
Patient characteristics	Age at study entry	Median 49 (range 27-67)
	Body mass index	Median 27 (range 20-45) < 25, n = 16 (39%) 25 - 30, n = 10 (24%) ≥ 30, n = 15 (37%)
ER/HER2 status	ER positive	n = 31 (76%)
	ER negative	n = 10 (24%)
	HER2 positive	n = 8 (20%)
	Triple negative	n = 8 (20%)
Tumour type	Ductal carcinoma	n = 32 (78%)
	Lobular carcinoma	n = 7 (17%)
	Other	n = 2 (5%)
	Grade	G1 n=2 (5%), G2 n=24 (58%), G3 n=15 (37%)
	Tumour size	Median 53mm (range 30-147mm)
Clinical response	MRI radiological response post chemotherapy (out of n = 33)	PR n = 26 (79%), CR n = 5 (15%), SD n = 2 (6%)
	Pathological complete response (pCR) post chemotherapy (out of n = 31)	n = 4 (13%)

Table 5.3: Patient and clinical characteristics; ER, oestrogen receptor; MRI, magnetic resonance imaging; PR, partial radiological response; CR, complete radiological response; SD, stable disease.

5.4: ^{18}[F]-FDG PET-CT ANALYSIS

5.4.1: ANALYSIS OF STATIC ^{18}[F]-FDG PET-CT

An ^{18}[F]-FDG PET-CT scan was carried out before and after 13 days of metformin treatment. Study participants were asked to fast overnight prior to their scan and in virtually all cases it was carried out between 8am and 10am. For the second scan participants were asked to take their metformin that morning prior to the study test. As discussed in Chapter 2, two scanning protocols were carried out, static PET-CT and dynamic PET-CT. The static scan allowed the assessment of changes in ^{18}[F]-FDG uptake in the whole body whilst the dynamic scan only assessed uptake at the level of the primary breast tumour (which usually included axillary lymph node metastases). **Figure 5.2** is an example of a static PET scan in the same patient pre- and post-metformin (without the CT component). In this case it is evident that the left sided axillary lymph nodes that were not visible pre-metformin are now ^{18}[F]-FDG avid. **Figure 5.3A** plots the change in SUV_{Max} for 40 of the 41 patients that entered the study. Although there is no clear direction of change for this variable it is notable that for those primary tumours where there is an increase or decrease in SUV_{Max} greater than or equal to 1 KBq/ml the baseline SUV_{Max} was at least 3.4 KBq/ml or greater. Hence baseline SUV_{Max} may be a marker of response to metformin and should be correlated with other assays in this study (once a greater sample size is available for these assays). **Figure 5.3B** plots the change, post-metformin, in the SUV_{Max} for both the primary tumour alongside the change in SUV_{Max} for lymph node metastases and any distant metastases. Patients are ranked in order of change of SUV_{Max} of the primary tumour. In this limited sample size there was some evidence

of a correlation between the change in SUV_{Max} in the primary tumour and any metastases.

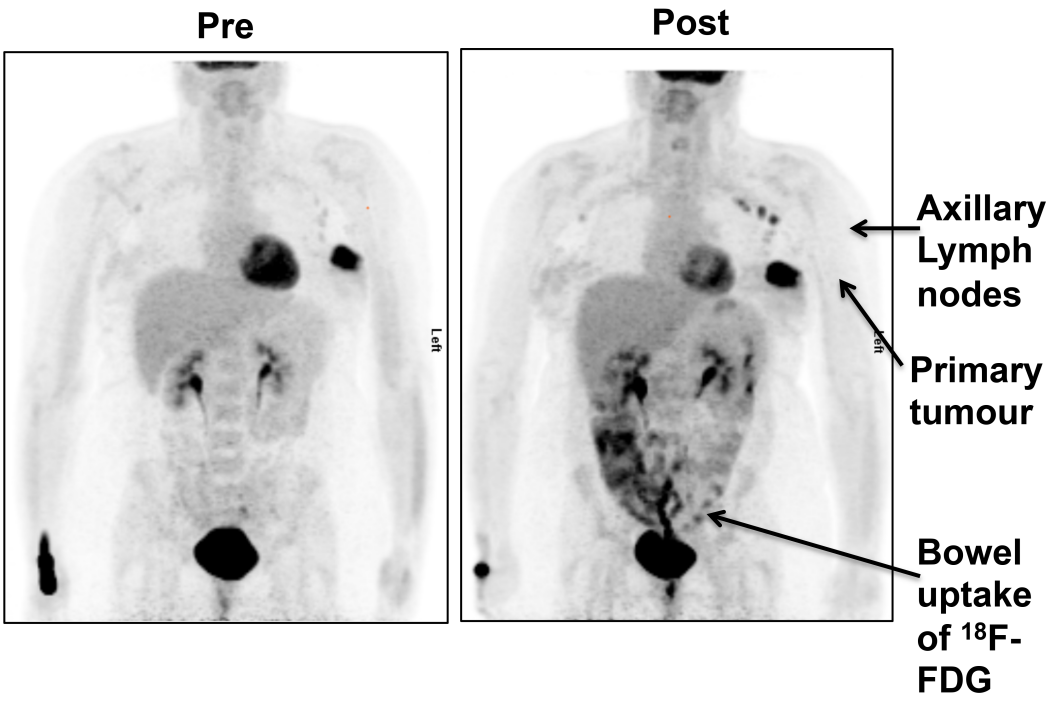


Fig 5.2: Example of coronal PET scan images pre- and post-metformin. Note increased uptake of ^{18}[F]-FDG in left sided axillary lymph nodes and small and large bowel post-metformin.

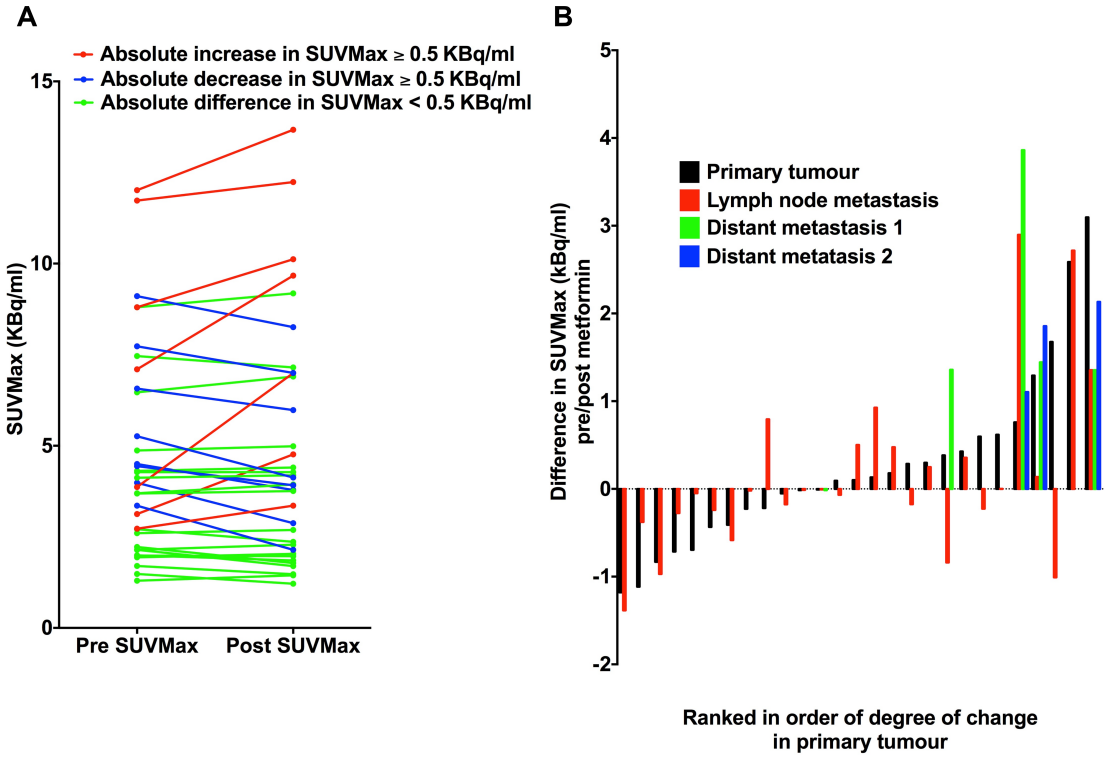


Fig 5.3A: Baseline and post-metformin SUV_{Max} (KBq/ml) for each primary breast cancer (n = 35). **B:** Change in SUV_{Max} (KBq/ml) for primary tumour (black), axillary metastases (red) and primary metastases (green and blue) in order of degree of change for each primary tumour for those patients that have metastases present (n = 27).

5.4.1.2: BOWEL UPTAKE OF ^{18}[F]-FDG

Previous studies have shown that diabetic patients taking metformin have an increased uptake of ^{18}[F]-FDG into the small bowel and colon. Indeed, this can mask locoregional cancers [21]. This has been put down to the local exposure to metformin the gut will experience in view of the drug's oral delivery as high concentrations of the metformin are observed in the small intestine in rodents [295]. In this study, in a non-diabetic cancer population this phenomenon was also observed (**Figure 5.4A and B**). It is possible that the degree of change in bowel uptake may correlate with metformin's bioavailability and possibly the activity. Certainly bowel uptake of ^{18}[F]-FDG is a good marker of medication compliance in this study.

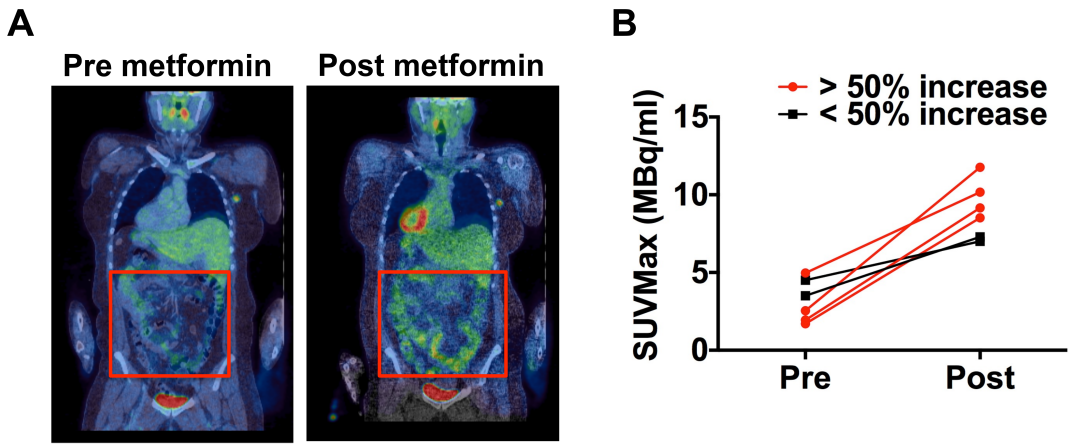


Fig 5.4A: Example of coronal PET-CT scan images pre- and post-metformin. Note increased uptake of ^{18}[F]-FDG in small and large bowel post-metformin. **B:** Baseline and post-metformin SUVMax (KBq/ml) for each area of bowel (n = 6).

5.4.2: ANALYSIS OF DYNAMIC ^{18}[F]-FDG PET-CT

Dynamic ^{18}[F]-FDG PET-CT scanning assesses the uptake of ^{18}[F]-FDG over time (in this case 45 minutes) and is a more sensitive and quantitative method than static PET-CT scanning. In this thesis data from the first 17 paired scans is presented for the dynamic study.

2-tissue compartment models with 3 rate-constants (3k) and four rate-constants (4k) model were compared using the Akaike Information Criterion (AIC). [296] The 4k model was found to describe the data more effectively with lower AIC scores and hence was chosen for the analysis. This allowed for the calculation of the kinetic parameters including K_1 (an estimate of the ^{18}[F]-FDG influx rate from carrier blood to tumour cells), k_2 (an estimate of the ^{18}[F]-FDG efflux from tumour intracellular pool back to blood), k_3 (an estimate of the ^{18}[F]-FDG phosphorylation rate in tumour cells) and k_4 (an estimate of the ^{18}[F]-FDG dephosphorylation rate in tumour cells) (**Figure 5.5A**). Flux (or Ki) of ^{18}[F]-FDG should correlate closely to the SUV_{Max} (essentially a measure of late ^{18}[F]-FDG uptake into the tumour). This correlation is a useful way to validate the robustness of the model and there was a strong correlation between flux (i.e. rate of ^{18}[F]-FDG uptake) and SUV_{Max} in our dataset (Pearson test, $p < 0.001$) (**Figure 5.5B**). There was no difference in the mean flux between the pre- and post-dynamic scans (**Figure 5.5C**) although there were marked increases or decreases in flux post-metformin for some primary tumours (greatest increase from baseline, 67%; greatest decrease, 47%) (**Figure 5.5D**).

To date, in the limited number of studies carried out, the K_1 and k_3 variables have been used to determine response in dynamic ^{18}[F]-FDG studies pre- and post-

treatment [297]. However, in this study there was no evidence of a particular direction of change for these variables, although again there were marked increases or decreases in these variables post-metformin for some primary tumours (**Figures 5.6A and C**, respectively). However, for the k_2 and k_4 variables, there was a trend toward a decrease post-metformin but again with much variability between paired scans (0.70 ± 0.11 vs 0.51 ± 0.05 ($p = 0.14$) and 0.052 ± 0.016 vs 0.030 ± 0.026 ($p = 0.20$) for k_2 and k_4, respectively) (**Figures 5.6B and D**, respectively). It is unclear what effect of metformin on tumour tissue this might represent but it could possibly indicate an alteration in cancer cell membrane permeability (at least with respect to k_2). Alternatively, metformin's effect on the dynamics of serum glucose concentration may impact on the K_i, K_1, k_2, k_3 and k_4 rate-constants and could provide an explanation for this finding. Certainly, one might expect it to via competitive inhibition of ^{18}[F]-FDG phosphorylation. Future modeling will involve including the serum glucose level as a model factor in order to examine this effect. It should be noted however that in this non-diabetic population there was no clear effect on serum glucose levels by metformin. Similarly, the kinetics of ^{18}[F]-FDG uptake and efflux is likely to be affected by the circulating serum insulin level and again this should be examined within the model. Previously published data however has suggested that high insulin levels (rather than low levels) would be expected to decrease dephosphorylation (k_4) [298].

Intriguingly, there was a significant correlation between the degree of decrease in k_2 and a greater BMI at baseline suggesting that this the 'pre-metabolic' state of the patient may influence the metformin response with regards to this variable (Pearson test, $p = 0.002$) (**Figure 5.7C**). Again, a differential response in terms of metformin's

effect on serum glucose and insulin levels in these patients may explain this and needs to be examined further. No correlation was found between baseline BMI and flux or the K_1, k_3 and k_4 variables (**Figures 5.7A, B, D, and E**, respectively).

Figures 5.7A, B, C D, and E suggest that there may be a link between oestrogen receptor (ER) status and response for the flux (**A**), K_1 (**B**), k_2 (**C**) and k_3 (**D**) variables. There were especially prominent increases in flux and K_3 and decreases in K_1 and k_2 for the ER negative patients. However as there were only 4 patients with ER negative disease in the initial cohort of dynamic scans modeled, the remaining number of pre- and post-scans will be necessary before more definitive correlation can carried out.

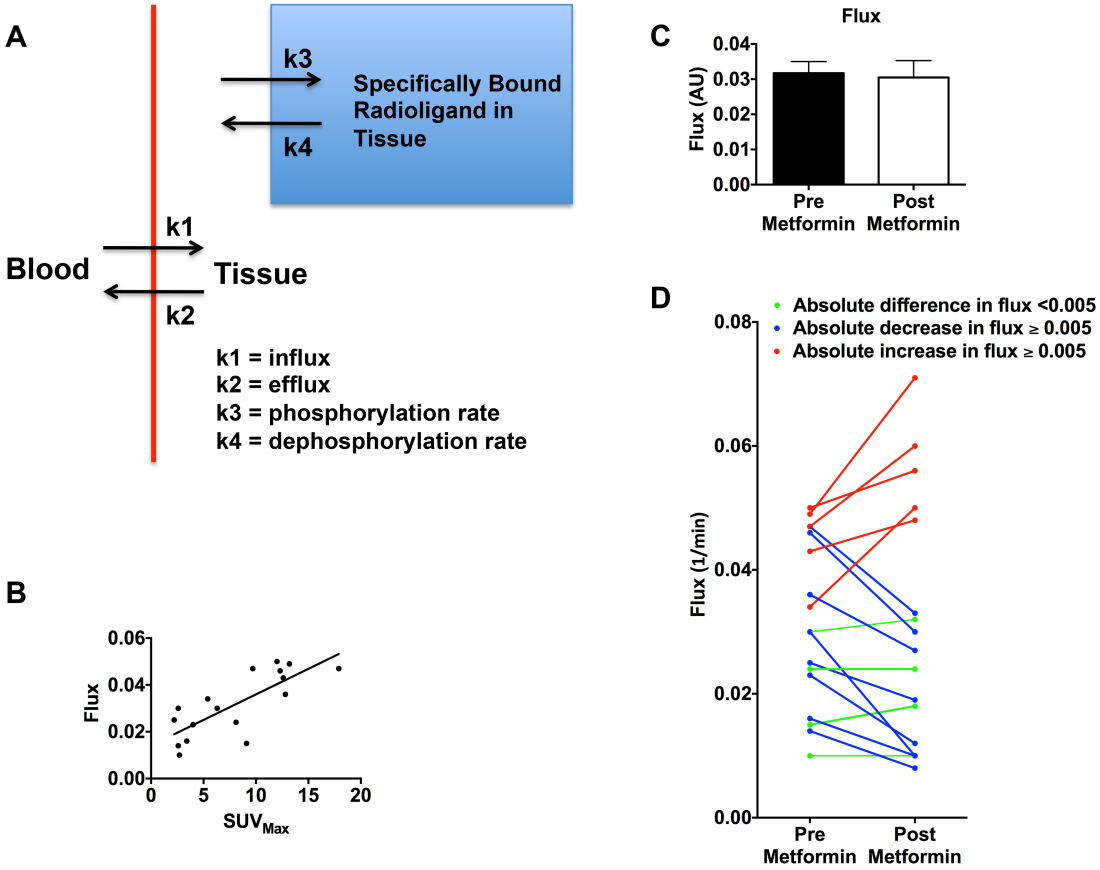


Fig 5.5A: Modeling of the dynamic ^{18}[F]-FDG PET-CT scan data allowed for the calculation of kinetic parameters including K_1 (an estimate of ^{18}[F]-FDG influx rate from carrier blood to tumour cells), k_2 (an estimate of ^{18}[F]-FDG efflux from tumour intracellular pool back to blood), k_3 (an estimate of ^{18}[F]-FDG phosphorylation rate in tumour cells) and k_4 (an estimate of ^{18}[F]-FDG dephosphorylation rate in tumour cells). **B:** Flux versus SUV_{Max} in each primary breast cancer. **C:** Mean baseline and post-metformin flux, data shown are mean ± SEM **D:** Baseline and post-metformin flux for each individual primary breast cancer (in all cases, n = 17).

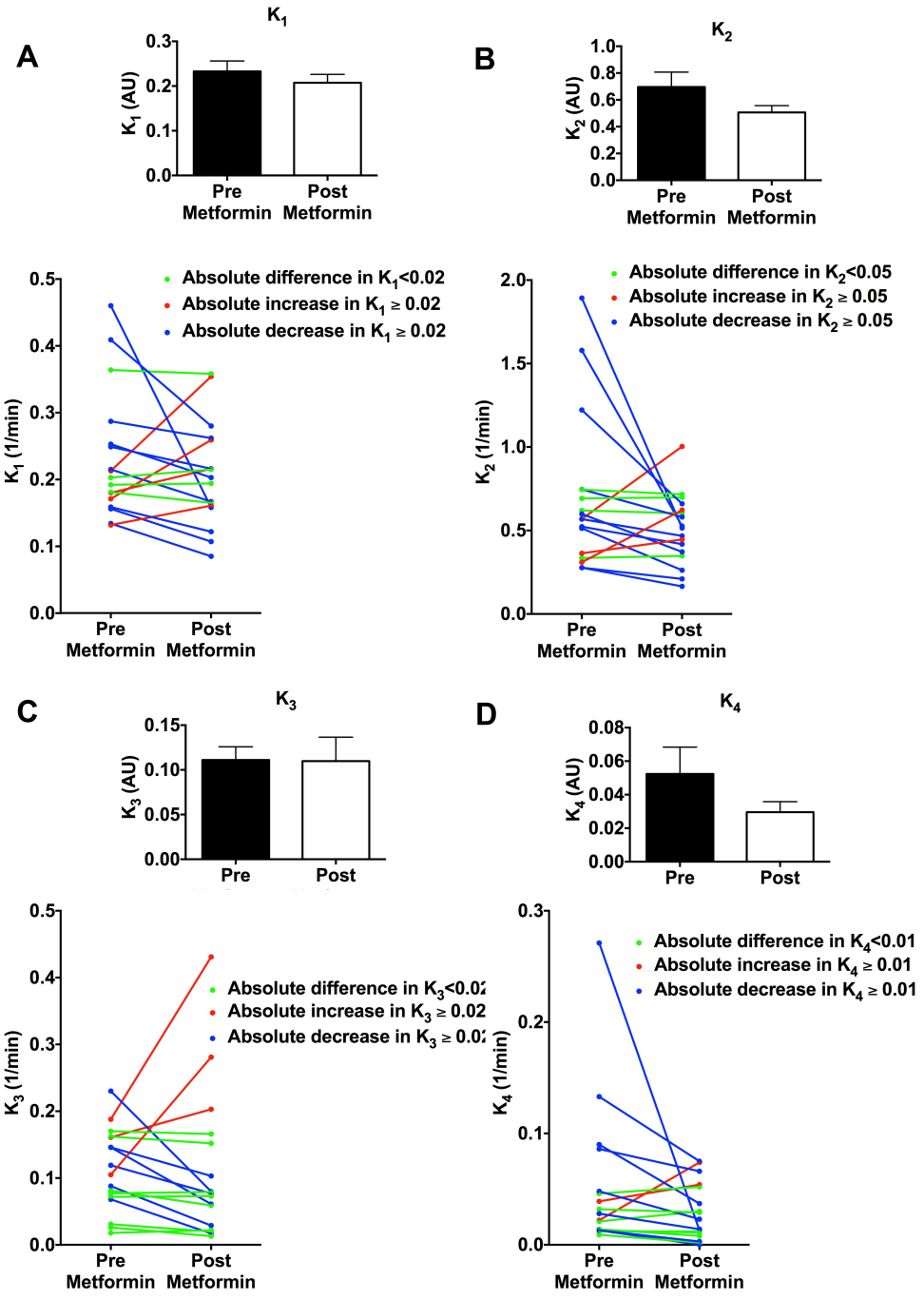


Fig 5.6A: Upper panel: Mean baseline and post-metformin K_1. **Lower panel:** Baseline and post-metformin K_1 for each individual primary breast cancer. **B: Upper panel:** Mean baseline and post-metformin k_2. **Lower panel:** Baseline and post-metformin k_2 for each individual primary breast cancer. **C: Upper panel:** Mean baseline and post-metformin k_3. **Lower panel:** Baseline and post-metformin k_3 for each individual primary breast cancer. **D: Upper panel:** Mean baseline and post-metformin k_4. **Lower panel:** Baseline and post-metformin k_4 for each individual primary breast cancer (in all cases, n = 17). Data shown are mean ± SEM.

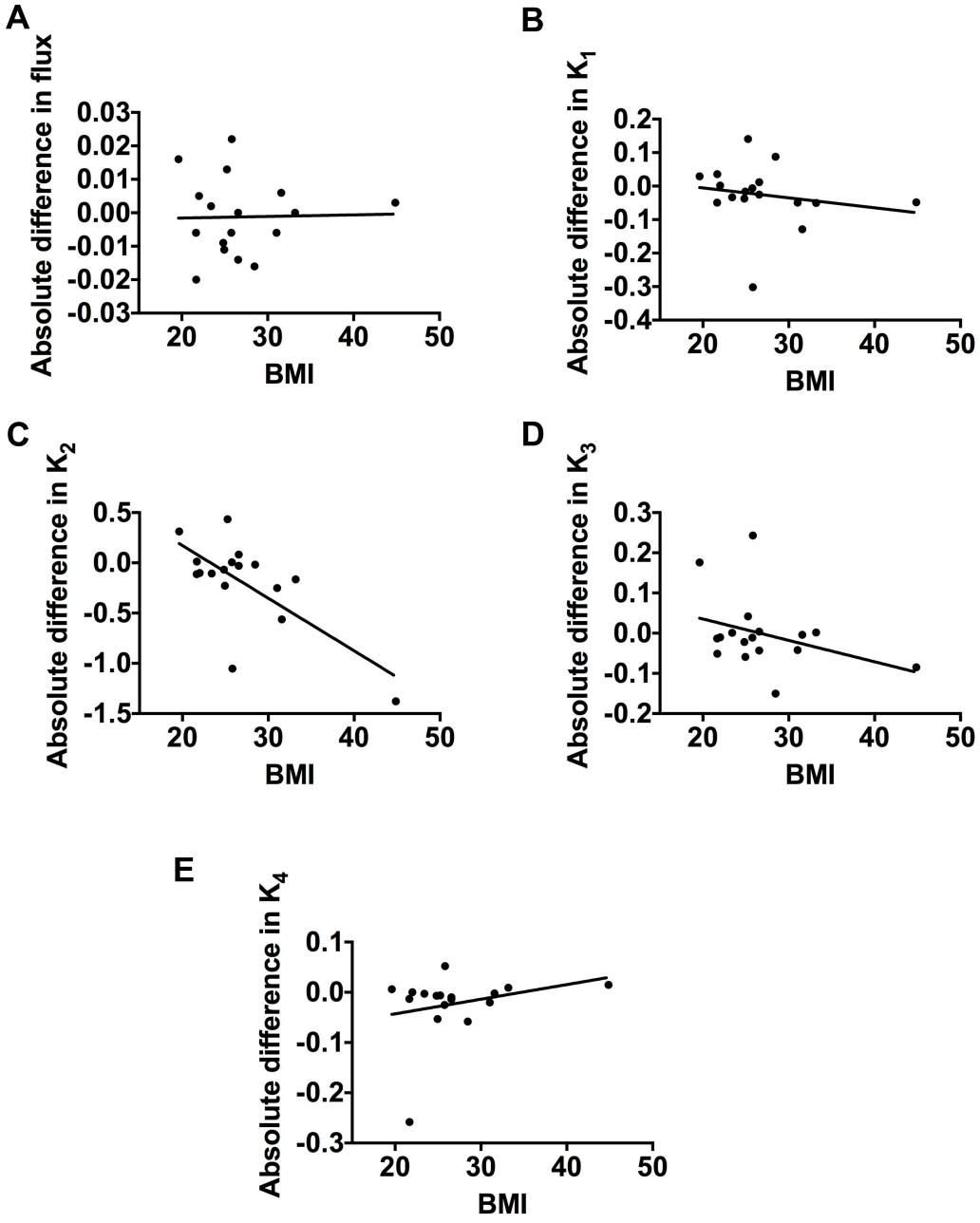


Fig 5.7: Absolute difference in flux (**A**), K_1 (**B**), k_2 (**C**), k_3 (**D**) and k_4 (**E**) in each primary breast cancer versus patient's BMI (n = 17).

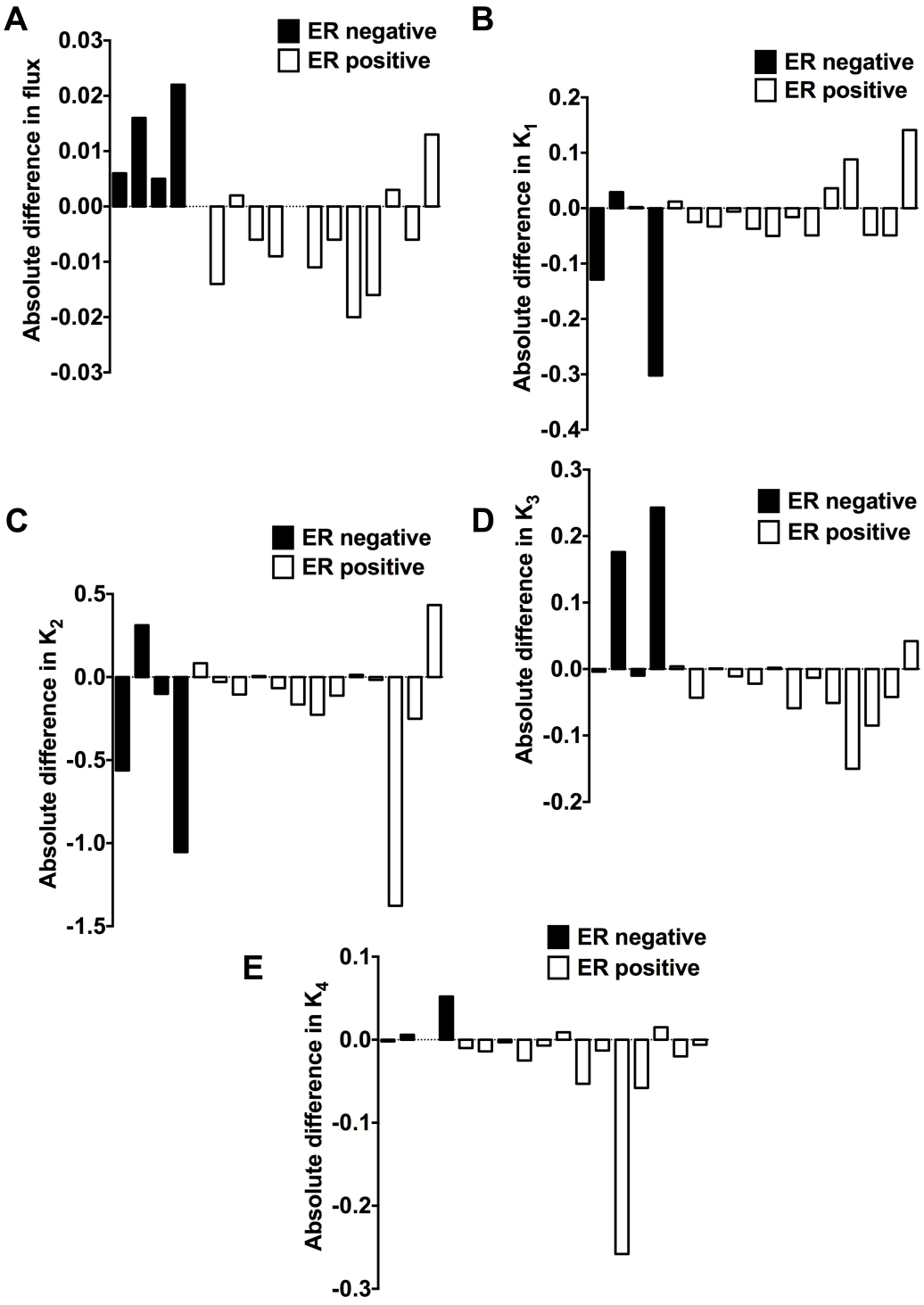


Fig 5.8: Absolute difference in flux (**A**), K_1 (**B**), k_2 (**C**), k_3 (**D**) and k_4 (**E**) for each ER negative and ER positive primary breast cancer (n = 17).

5.5: NEXT GENERATION RNA SEQUENCING

5.5.1: OVERVIEW

Core biopsies were taken from the primary breast cancer before and after 13 days of metformin treatment under ultrasound guidance by an experienced radiologist and then immediately placed in RNA later and processed as described in Chapter 2. After RNA extraction and quality control (see Chapter 2) 21 paired biopsies were determined to have RNA of sufficient quantity and quality for RNA sequencing. After next generation sequencing of 'Poly (A) targeted' mRNA, bioinformatic optimisation of the data set was carried out and genes were ranked by p-value based on the probability distribution of rank product. Pathway analysis was then performed using the Genecodis 3.0 program by inserting the ranked list of upregulated or downregulated genes into the program analysis tool (again see chapter 2 for full details). Individual genes pertinent to pathways of interest for metformin from our and other published in vitro and in vivo data were then also more specifically examined.

Below in tables 5.4 and 5.5 are listed the top pathways ranked by statistical significance (using Kegg pathway lists of annotated genes) that were upregulated and downregulated compared to baseline, respectively, after 2 weeks of metformin treatment. Pathways specifically relevant to metabolism are picked out in red. The statistically most significantly upregulated pathway was the cell cycle pathway with 60 out of 123 annotated genes upregulated. These genes include the cyclin dependent kinases (CDKs), Cyclin-CDK inhibitors (CKIs) and p53 pathway relevant genes. The significance of this finding is uncertain at this stage and will require further analysis and bioinformatic correlation once the full datasets have been generated. In the context of this thesis focus is placed on changes in metabolic pathways.

Oxidative phosphorylation was the 16th most upregulated Kegg pathway with 44 out of 130 genes upregulated and the TCA cycle the 35th with 15 out of 30 genes in the input list. Please see *sections 5.5.2 and 5.5.3* for the differential expression of individual genes and further discussion with regard to these pathways. Notably, pathways involved in Huntingdon's disease, Alzheimer's disease and Parkinson's disease all come near the top of the list upregulated pathways. These are all diseases that are associated with mitochondrial dysfunction.

Rank	Number of annotated genes in reference list	Number of annotated genes in input list	Hypergeometric p-value	Pathway
1	123	60	6.8e-20	Cell cycle
2	159	60	1.5e-13	Protein processing in endoplasmic reticulum
3	180	63	1.2e-12	Huntington's disease
4	163	57	1.7e-11	Alzheimer's disease
5	35	23	2.1e-11	DNA replication
6	118	46	2.5e-11	Spliceosome
7	110	44	2.4e-11	Oocyte meiosis
8	86	37	9.9e-11	Ribosome
9	71	33	9.5e-11	Adherens junction
10	145	51	9.1e-11	RNA transport
11	76	34	1.4e-10	Peroxisome
12	129	45	1.8e-09	Parkinson's disease
13	324	83	4.8e-09	Pathways in cancer
14	73	31	4.7e-09	Ribosome biogenesis in eukaryotes
15	41	22	6.6e-09	Nucleotide excision repair
16	130	44	6.8e-09	Oxidative phosphorylation
17	149	48	7.2e-09	Wnt signaling pathway
18	79	32	8.1e-09	mRNA surveillance pathway
19	158	49	1.8e-08	Purine metabolism
20	130	43	1.9e-08	Tight junction
21	88	33	3.9e-08	Prostate cancer
22	23	15	7.0e-08	Mismatch repair
23	86	32	7.7e-08	Progesterone-mediated oocyte maturation
24	62	26	1.0e-07	Colorectal cancer
25	21	14	1.3e-07	Biosynthesis of unsaturated fatty acids
26	93	33	1.6e-07	Pyrimidine metabolism
27	36	18	6.0e-07	Cysteine and methionine metabolism
28	193	52	7.8e-07	Endocytosis
29	44	20	8.1e-07	Valine, leucine and isoleucine degradation
30	70	26	1.5e-06	Pancreatic cancer
31	66	25	1.6e-06	RNA degradation
32	209	54	1.7e-06	Regulation of actin cytoskeleton
33	19	12	2.7e-06	Steroid biosynthesis
34	73	26	3.5e-06	Chronic myeloid leukemia
35	30	15	5.8e-06	Citrate cycle (TCA cycle)
36	262	62	5.9e-06	MAPK signaling pathway
37	133	38	6.1e-06	Insulin signaling pathway
38	133	38	6.1e-06	Hepatitis C
39	54	21	7.1e-06	Arginine and proline metabolism
40	124	36	7.2e-06	Neurotrophin signaling pathway
41	87	28	1.1e-05	ErbB signaling pathway
42	33	15	2.2e-05	Base excision repair
43	41	17	2.3e-05	Tryptophan metabolism
44	70	23	5.7e-05	Renal cell carcinoma
45	40	16	7.2e-05	Proteasome
46	40	16	7.2e-05	Aminoacyl-tRNA biosynthesis
47	32	14	7.0e-05	Propanoate metabolism
48	32	14	7.0e-05	Alanine, aspartate and glutamate metabolism
49	49	18	8.1e-05	Lysine degradation
50	53	18	0.0002	Non-small cell lung cancer

Table 5.4: Top 50 upregulated KEGG pathways on Genecodis analysis. Metabolism pathways in red.

Rank	Number of annotated genes in reference list	Number of annotated genes in input list	Hypergeometric p-value	Pathway
1	84	38	3.9e-13	ECM-receptor interaction
2	197	62	1.6e-12	Focal adhesion
3	259	74	1.2e-12	Cytokine-cytokine receptor interaction
4	83	35	1.8e-11	Hematopoietic cell lineage
5	128	44	1.2e-10	Axon guidance
6	324	80	3.5e-10	Pathways in cancer
7	186	53	3.1e-09	Chemokine signaling pathway
8	84	32	2.8e-09	Rheumatoid arthritis
9	126	41	3.0e-09	Osteoclast differentiation
10	193	54	3.2e-09	Endocytosis
11	123	40	4.1e-09	Toxoplasmosis
12	125	39	2.7e-08	Cell adhesion molecules (CAMs)
13	172	48	2.8e-08	Tuberculosis
14	92	32	2.8e-08	Fc gamma R-mediated phagocytosis
15	102	34	3.2e-08	Amoebiasis
16	121	36	3.8e-07	Lysosome
17	107	33	4.84e-07	T cell receptor signaling pathway
18	113	34	5.9e-07	Vascular smooth muscle contraction
19	22	13	5.8e-07	Glycosaminoglycan biosynthesis
20	209	51	9.4e-07	Regulation of actin cytoskeleton
21	42	18	1.4e-06	ABC transporters
22	175	44	2.6e-06	Calcium signaling pathway
23	75	25	2.8e-06	VEGF signaling pathway
24	77	25	4.9e-06	Fc epsilon RI signaling pathway
25	262	57	9.2e-06	MAPK signaling pathway
26	70	22	4.2e-05	Bacterial invasion of epithelial cells
27	75	23	4.0e-05	B cell receptor signaling pathway
28	124	32	4.8e-05	Glutamatergic synapse
29	113	30	4.8e-05	Leukocyte transendothelial migration
30	76	23	4.7e-05	Phosphatidylinositol signaling system
31	153	37	4.6e-05	Jak-STAT signaling pathway
32	130	33	4.5e-05	Measles
33	125	32	5.0e-05	Natural killer cell mediated cytotoxicity
34	98	27	5.4e-05	GnRH signaling pathway
35	44	16	6.6e-05	Intestinal immune network for IgA production
36	85	24	0.0001	Salivary secretion
37	372	13	0.0001	Olfactory transduction
38	137	33	0.0001	Phagosome
39	57	18	0.0002	Acute myeloid leukemia
40	78	22	0.0002	Protein digestion and absorption
41	53	17	0.0002	Arachidonic acid metabolism
42	84	23	0.0002	Small cell lung cancer
43	15	8	0.0003	Glycosphingolipid biosynthesis - ganglio series
44	98	25	0.0004	Melanogenesis
45	46	15	0.0005	Staphylococcus aureus infection
46	67	19	0.0006	Epithelial cell signaling in H. pylori infection
47	57	17	0.0006	NOD-like receptor signaling pathway
48	149	33	0.0007	Wnt signaling pathway
49	48	15	0.0008	Malaria
50	86	22	0.0009	Apoptosis

Table 5.5: Top 50 downregulated KEGG pathways on Genecodis analysis. Metabolism pathways in red.

Also upregulated was the insulin signaling pathway and several pathways involved in amino acid metabolism: the alanine, aspartate and glutamate metabolism pathway, the cysteine and methionine metabolism pathway, the valine, leucine and isoleucine degradation pathway, the arginine and proline metabolism pathway, the tryptophan metabolism pathway and the alanine, aspartate and glutamate metabolism pathway. In view of our and other group's data highlighting the importance of glutamine metabolism at times of mitochondrial stress, focus in this chapter is put on the glutamine pathway in *section 5.5.4*.

5.5.2: ELECTRON TRANSPORT CHAIN

The number of genes that were differentially expressed that code for components in the electron transport chain was especially striking (**Table 5.6** and **Figure 5.9)**. In particular 21 genes were differentially expressed out of a possible 47 annotated genes that code for the proteins that make up Complex 1 (NADH dehydrogenase). This provides the first good evidence that Complex 1 and the electron transport chain in cancer cells is targeted by metformin at clinical doses. Given that this, as far as is known, is the primary target of metformin, correlation of the degree of change in this pathway between tumours with other assays, once the full dataset has been established, will be of great interest.

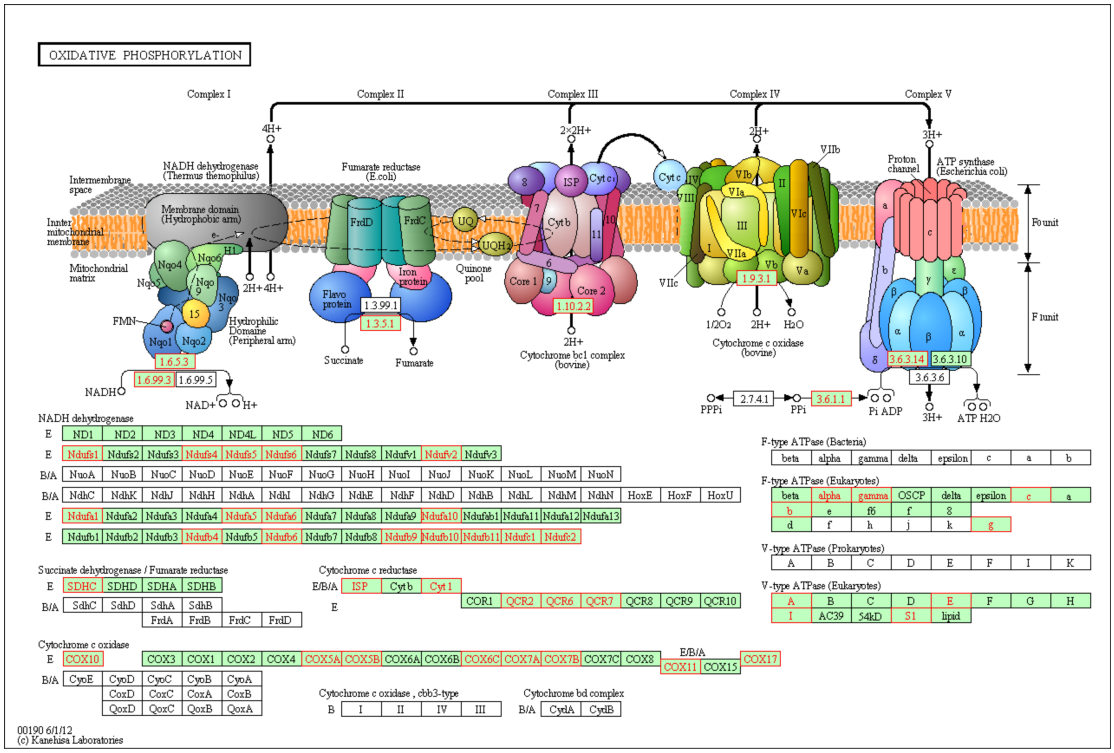


Fig 5.9: Genecodis KEGG pathway map of genes encoding mitochondrial components of the electron transport chain (significantly upregulated ($p < 0.05$), red; not significantly upregulated, green; white, prokaryotic genes) ($n = 21$).

ETC component	Protein	Gene	Mean differential expression (Log2)	P value
Complex 1 (21 genes from input list in reference list of 47 genes)	NADH Dehydrogenase (Ubiquinone) Fe-S Protein 1	NDUFS1	0.13	0.01
	NADH Dehydrogenase (Ubiquinone) Fe-S Protein 4	NDUFS4	0.08	0.004
	NADH Dehydrogenase (Ubiquinone) Fe-S Protein 5	NDUFS5	0.23	0.008
	NADH Dehydrogenase (Ubiquinone) Fe-S Protein 6	NDUFS6	0.14	0.005
	NADH Dehydrogenase (Ubiquinone) Fe-S Protein 7	NDUFS7	-0.05	0.03
	NADH Dehydrogenase (Ubiquinone) Fe-S Protein 8	NDUFS8	-0.01	0.04
	NADH Dehydrogenase (Ubiquinone) 1 Alpha Subcomplex, 1	NDUFA1	0.16	0.02
	NADH Dehydrogenase (Ubiquinone) 1 Alpha Subcomplex, 5	NDUFA5	0.16	0.006
	NADH Dehydrogenase (Ubiquinone) 1 Alpha Subcomplex, 6	NDUFA6	0.17	0.004
	NADH Dehydrogenase (Ubiquinone) 1 Alpha Subcomplex, 10	NDUFA10	0.11	0.02
	NADH Dehydrogenase (Ubiquinone) 1 Alpha Subcomplex, 11	NDUFA11	-0.05	0.004
	NADH Dehydrogenase (Ubiquinone) 1 Beta Subcomplex, 1	NDUFB1	-0.11	0.0003
	NADH Dehydrogenase (Ubiquinone) 1 Beta Subcomplex, 4	NDUFB4	0.12	0.03
	NADH Dehydrogenase (Ubiquinone) 1 Beta Subcomplex, 5	NDUFB5	-0.02	0.005
	NADH Dehydrogenase (Ubiquinone) 1 Beta Subcomplex, 6	NDUFB6	0.09	0.008
	NADH Dehydrogenase (Ubiquinone) 1 Beta Subcomplex, 9	NDUFB9	0.10	0.04
	NADH Dehydrogenase (Ubiquinone) 1 Beta Subcomplex, 10	NDUFB10	0.09	0.02
	NADH Dehydrogenase (Ubiquinone) 1 Beta Subcomplex, 11	NDUFB11	0.10	0.05
	NADH Dehydrogenase (Ubiquinone) 1, Subcomplex Unknown, 1	NDUFC1	0.14	0.004
	NADH Dehydrogenase (Ubiquinone) 1, Subcomplex Unknown, 2	NDUFC2	0.14	0.02
	NADH Dehydrogenase (Ubiquinone) 1 Alpha Subcomplex, 4-Like 2	NDUFA4L2	-0.24	0.02
Complex 2 (2 genes of 4)	Succinate Dehydrogenase Complex, Subunit C	SDHC	0.24	0.005
	Succinate Dehydrogenase Complex Assembly Factor 1	SDHAF1	-0.12	0.03
Complex 3 (7 genes from input list in reference list of 11 genes)	Ubiquinol-Cytochrome C Reductase, Rieske Iron-Sulfur Polypeptide 1	UQCRFS1	0.09	0.04
	Cytochrome C-1	CYC1	0.09	0.03
	Ubiquinol-Cytochrome C Reductase Core Protein 2	UQCRC2	0.13	0.02
	Ubiquinol-Cytochrome C Reductase Hinge Protein	UQCRH	0.19	0.006
	Ubiquinol-Cytochrome C Reductase Binding Protein	UQCRB	0.15	0.008
	Ubiquinol-Cytochrome C Reductase, Complex III Subunit VII	UQCRQ	0.03	0.07
	Ubiquinol-Cytochrome C Reductase, Complex III Subunit XI	UQCR11	-0.07	0.04

Complex 4 (12 genes from input list in reference list of 24 genes)	Cytochrome C Oxidase Subunit IV Isoform 1	COX4I1	0.04	0.04
	Cytochrome C Oxidase Subunit Va	COX5A	0.06	0.02
	Cytochrome C Oxidase Subunit Vb	COX5B	0.08	0.02
	Cytochrome C Oxidase Subunit VIc	COX6C	0.18	0.006
	Cytochrome C Oxidase Subunit VIIa Polypeptide 1	COX7A1	-0.32	0.001
	Cytochrome C Oxidase Subunit VIIa Polypeptide 2	COX7A2	0.15	0.02
	Cytochrome C Oxidase Subunit VIIb	COX7B	0.18	0.05
	Cytochrome C Oxidase Subunit VIIc	COX7C	-0.03	0.04
	Cytochrome C Oxidase Subunit VIIIA	COX8A	-0.04	0.04
	Cytochrome C Oxidase Assembly Homolog 10	COX10	0.14	0.03
	Cytochrome C Oxidase Assembly Homolog 11	COX11	0.12	0.05
	Cytochrome C Oxidase Copper Chaperone	COX17	0.19	0.007
Complex 5 (21 genes from input list in reference list of 41 genes)	ATP Synthase, H+ Transporting, Mitochondrial F1 Complex, Alpha Subunit 1, Cardiac Muscle	ATP5A1	0.16	0.02
	ATP Synthase, H+ Transporting, Mitochondrial F1 Complex, Delta Subunit	ATP5D	-0.18	0.003
	ATP Synthase, H+ Transporting, Mitochondrial F1 Complex, Epsilon Subunit	ATP5E	-0.08	0.008
	ATP Synthase, H+ Transporting, Mitochondrial F1 Complex, Gamma Polypeptide 1	ATP5C1	0.08	0.01
	ATP Synthase, H+ Transporting, Mitochondrial Fo Complex, Subunit C1	ATP5G1	0.14	0.02
	ATP Synthase, H+ Transporting, Mitochondrial Fo Complex, Subunit C2	ATP5G2	0.09	0.03
	ATP Synthase, H+ Transporting, Mitochondrial Fo Complex, Subunit C3	ATP5G3	0.05	0.03
	ATP Synthase, H+ Transporting, Mitochondrial Fo Complex, Subunit B1	ATP5F1	0.23	0.004
	ATP Synthase, H+ Transporting, Mitochondrial Fo Complex, Subunit G	ATP5L	0.19	0.02
	ATPase, H+ Transporting, Lysosomal 70kDa, V1 Subunit A	ATP6V1A	0.15	0.04
	ATPase, H+ Transporting, Lysosomal 56/58kDa, V1 Subunit B2	ATP6V1B2	-0.12	0.01
	ATPase, H+ Transporting, Lysosomal 31kDa, V1 Subunit E1	ATP6V1E1	0.13	0.03
	ATPase, H+ Transporting, Lysosomal 9kDa, V0 Subunit E1	ATP6VOE1	-0.23	0.002
	T-Cell, Immune Regulator 1, ATPase, H+ Transporting, Lysosomal V0 Subunit A3	TCIRG1	-0.44	0.0001
	ATPase, H+ Transporting, Lysosomal V0 Subunit A1	ATP6V0A1	-0.11	0.03
	ATPase, H+ Transporting, Lysosomal V0 Subunit A2	ATP6V0A2	-0.14	0.03
	ATPase, H+ Transporting, Lysosomal V0 Subunit A4	ATP6V0A4	0.24	0.004
	ATPase, H+ Transporting, Lysosomal 38kDa, V0 Subunit D1	ATP6V0D1	-0.16	0.009
	ATPase, H+ Transporting, Lysosomal 13kDa, V1 Subunit G2	ATP6V1G2	-0.06	0.05
	ATPase, H+ Transporting, Lysosomal 50/57kDa, V1 Subunit H	ATP6V1H	-0.21	0.02
	ATPase, H+ Transporting, Lysosomal Accessory Protein 1	ATP6AP1	0.06	0.03

Table 5.6 – see over: Differential expression of significantly differentially expressed genes encoding members of the electron transport chain: complex 1 (NADH dehydrogenase); complex 2 (succinate dehydrogenase / fumarate hydratase); complex 3 (cytochrome c reductase); complex 4 (cytochrome c oxidase); complex 5 (ATP synthase). P-value determined by probability distribution of rank product. Colour coding: red, upregulated; blue, downregulated.

5.5.3: TCA CYCLE

Consistent with electron transport chain interference by metformin was the differential expression seen for every gene coding for the enzymes involved in the TCA cycle (**Table 5.7** and **Figure 5.10)**. Notably this included the upregulation of 2 enzymes that have been shown to be important for anapleurosis of the TCA cycle in cancer cells, glutamate dehydrogenase and pyruvate carboxylase [249, 299]. One might expect a close link between the effects of metformin on the expression of components of the electron transport chain and TCA cycle enzyme expression and so again, correlation of the degree of change in these 2 pathways between tumours, once the full dataset has been established, will be of great interest.

Protein	Gene	Mean differential expression (log2)	P value
Pyruvate Dehyrogenase Phosphatase Catalytic Subunit 2	PDP2	0.19	0.02
Pyruvate Dehydrogenase Phosphatase Regulatory Subunit	PDP3	0.13	0.03
Pyruvate Dehydrogenase (Lipoamide) Alpha 1	PDHA1	0.25	0.009
Pyruvate carboxylase	PC	0.16	0.02
Glutamine dehydrogenase 1	GLUD1	0.18	0.05
Glutamate dehydrogenase 2	GLUD2	0.28	0.0008
Malate Dehydrogenase 1	MDH1	0.30	0.002
Malate Dehydrogenase 2	MDH2	0.25	0.007
Aconitase 2 (mitochondrial)	ACO2	0.21	0.03
Isocitrate Dehydrogenase 3 subunit Gamma	IDH3G	0.05	0.06
Isocitrate Dehydrogenase 3 subunit beta	IDH3B	-0.08	0.03
Fumarate hydratase	FH	0.32	0.001
Succinate Dehydrogenase Complex, Subunit C	SDHC	0.24	0.005
Succinate Dehydrogenase Complex Assembly Factor 1	SDHAF1	-0.12	0.03
Succinate-CoA Ligase, GDP-Forming, Beta Subunit	SUCLG2	0.16	0.01
Succinate-CoA Ligase, ADP-Forming, Beta Subunit	SUCLA2	0.11	0.02

Table 5.7: Differential expression of significantly differentially expressed genes encoding regulators of the TCA cycle. P value determined by probability distribution of rank product. Colour coding: red, upregulated; blue, downregulated; blue underlined in red, different subunits both up and down regulated.

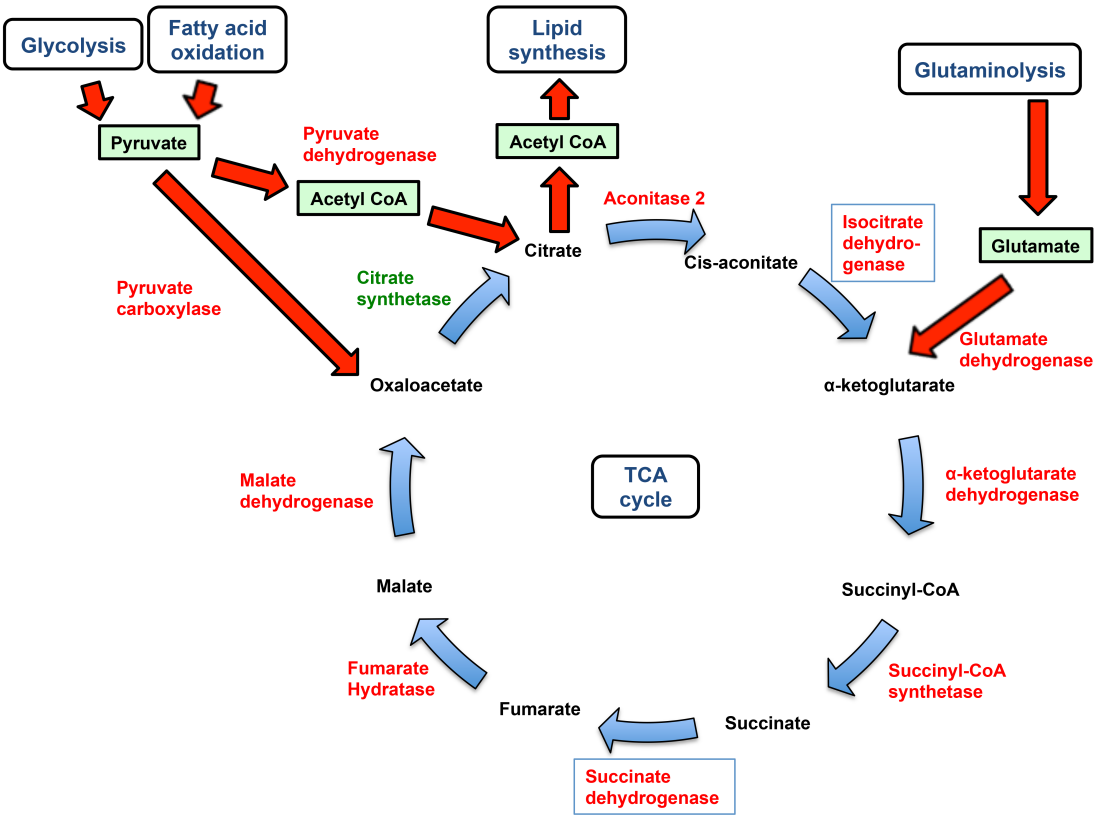


Fig 5.10: Significantly ($p < 0.05$) upregulated (red) and downregulated genes (blue) involved in regulation of the TCA cycle. Genes with different isoforms that are upregulated and downregulated are red surrounded by a blue box and genes that have no significant change in differential expression are in green ($n = 21$).

5.5.4: GLYCOLYSIS AND GLUCOSE UPTAKE

All but 2 of the genes coding for enzymes catalyzing the steps of the glycolysis pathway were differentially expressed (**Table 5.8** and **Figure 5.11)**. Of the GLUT transporters only one was upregulated, GLUT1, but this was one of the genes with the greatest upregulation as determined by the rank product significance (159th in the ranking). The upregulation of this pathway is once again consistent with a mitochondrial stress toward the cancer cell. The expression of GLUT1 has previously been shown to highly correlate with the degree of ^{18}F-FDG uptake on PET-CT [300-302] and future correlation between the change in glucose uptake seen on the PET-CT scans and change in GLUT1 mRNA expression will be of great interest (as will be correlation with glycolysis pathway gene expression).

Protein	Gene	Mean differential expression (log2)	P value
Solute Carrier Family 2 (Facilitated Glucose Transporter), Member 1 (GLUT1)	SLC2A1	0.61	<0.00001
Hexokinase 1	HK1	-0.05	0.04
Hexokinase 3	HK3	-0.09	0.02
Phosphoglucose isomerase	GPI	0.21	0.002
Phosphofructokinase (platelet)	PFKP	0.02	0.03
Glyceraldehyde phosphate dehydrogenase	GAPDH	0.12	0.02
Phosphoglycerate kinase	PGK1	0.08	0.02
Phosphoglycerate mutase	PGAM1	0.11	0.04
Enolase	ENO1	0.17	0.003
Lactate dehydrogenase	LDHA	0.19	0.005

Table 5.8: Differential expression of significantly up and down regulated genes encoding regulators of the glycolysis pathway. P value determined by probability distribution of rank product. Colour coding: red, upregulated; blue, downregulated.

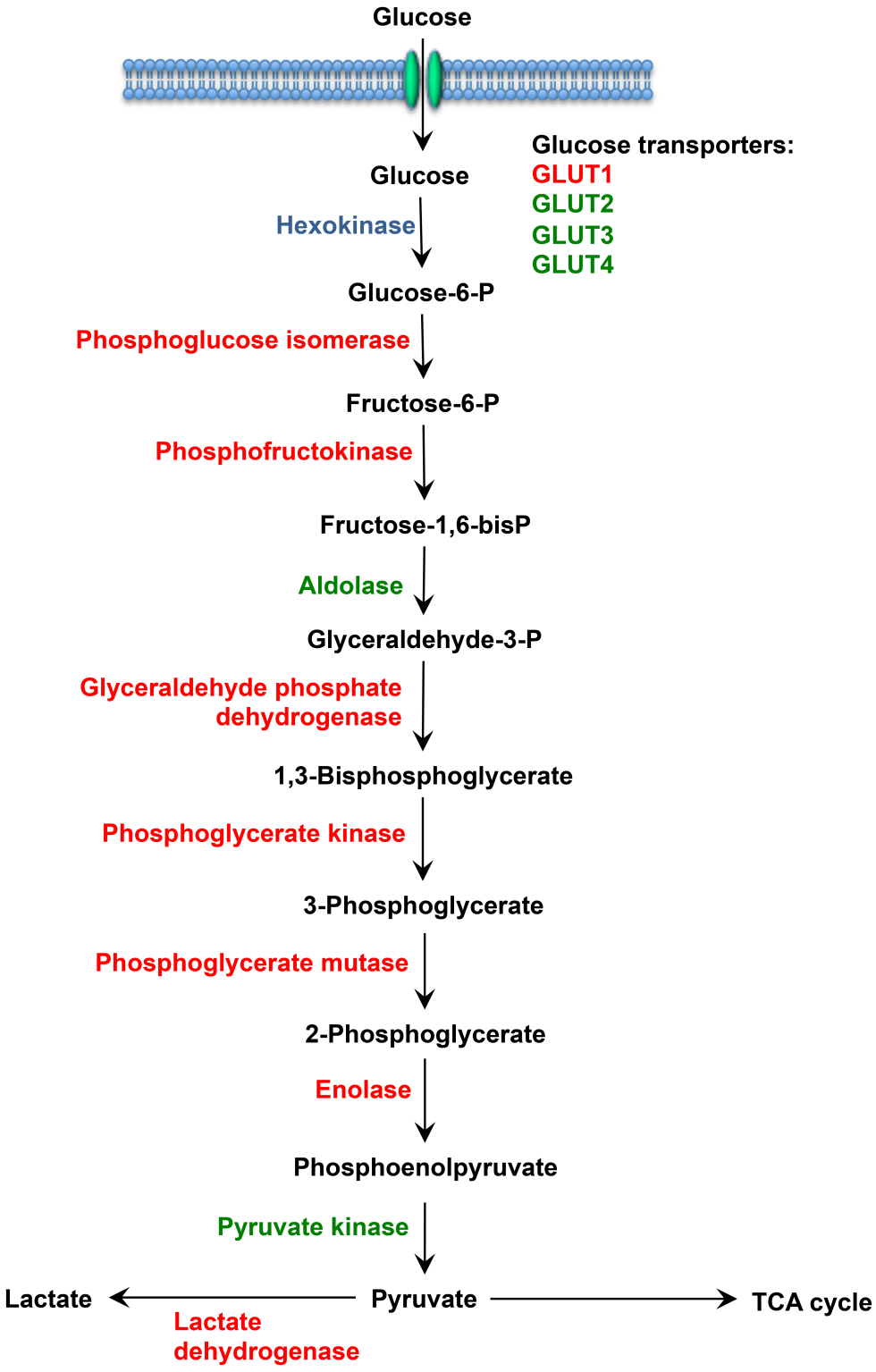


Fig 5.11: Significantly ($p < 0.05$) upregulated (red) and downregulated genes (blue) involved in regulation of the glycolysis pathway. Genes with different isoforms that are upregulated and downregulated are red surrounded by a blue box and genes that have no significant change in differential expression are in green (n = 21).

5.5.5: GLUTAMINE METABOLISM

As discussed in Chapter 3, evidence from in vitro and xenograft work shows that metformin treated cancer cells, at least in these models, turn to glutamine as an alternative source of carbon both to replenish the TCA cycle and as a substrate for lipid synthesis. Virtually all the genes encoding the key proteins involved in glutaminolysis, reductive carboxylation and glutamine uptake were upregulated (**Table 5.9** and **Figure 5.12)**. Glutamate dehydrogenase is also the target for bithionol (see chapter 3) adding to the potential of clinical synergy between these 2 drugs.

Protein	Gene	Mean differential expression (log2)	P value
Solute Carrier Family 38, Member 1	SLC38A1	0.35	<0.00001
Solute Carrier Family 38, Member 2	SLC38A2	0.23	0.003
Solute Carrier Family 38, Member 5	SLC38A5	-0.32	0.001
Glutamine synthetase	GLUL	0.27	0.002
Glutamine dehydrogenase 1	GLUD1	0.18	0.05
Glutamate dehydrogenase 2	GLUD2	0.28	0.0008
α-ketoglutarate dehydrogenase	OGDH	0.18	0.006
Isocitrate dehydrogenase 1	IDH1	0.002	0.02
Isocitrate dehydrogenase 2	IDH2	0.34	0.003
Cytosolic aconitase	ACO1	0.07	0.003

Table 5.9: Differential expression of significantly differentially expressed genes encoding regulators of the glutaminolysis and reductive carboxylation pathway. P value determined by probability distribution of rank product. Colour coding: red, upregulated; blue, downregulated.

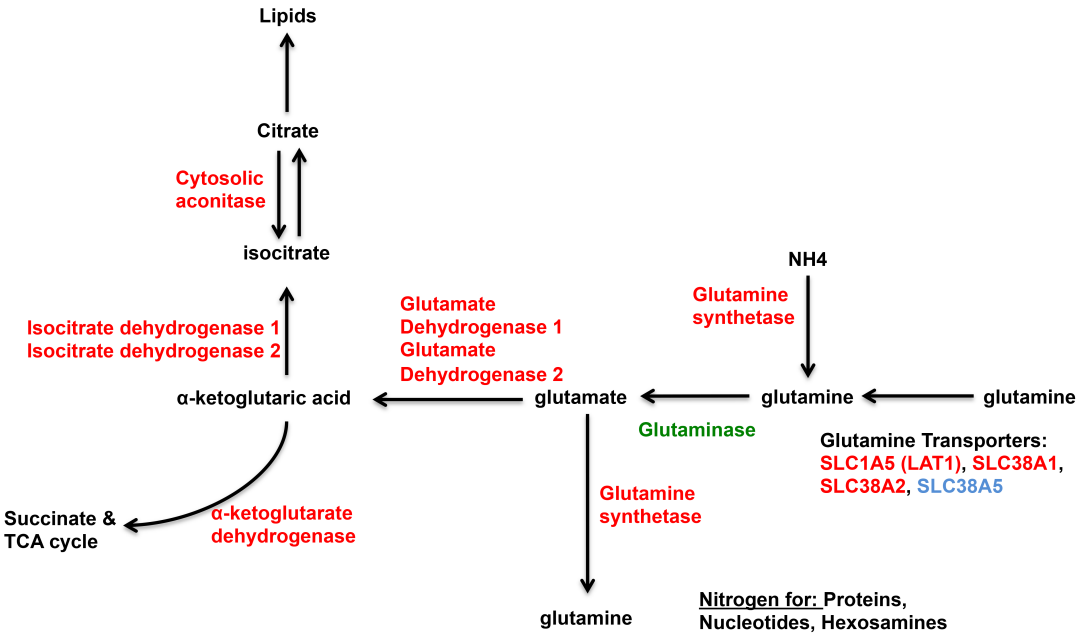


Fig 5.12: Significantly ($p < 0.05$) upregulated (red) and downregulated genes (blue) involved in regulation of the glutaminolysis and reductive carboxylation pathways. Genes with different isoforms that are upregulated and downregulated are red surrounded by a blue box and genes that have no significant change in differential expression are in green (n = 21).

5.5.6: LIPID METABOLISM

Consistent with the in vitro work presented in chapter 4 several of the genes encoding key enzymes involved in fatty acid oxidation were upregulated possibly reflecting a response to the inhibition of this pathway. Of note, none of the genes encoding the lipolysis enzymes ATGL, HSL or MAGL were differentially expressed. However, again consistent with the in vitro work presented in chapter 4 there was evidence of upregulation of the desaturase SCD1 and the elongases, ELOVL5 and ELOVL7 (**Table 5.10** and **Figure 5.13)**.

Protein	Gene	Mean differential expression (Log2)	P value
Acetyl-CoA Carboxylase Beta	ACACB	-0.03	0.04
Carnitine Palmitoyltransferase 1A (liver)	CPT1A	0.25	0.01
Carnitine Palmitoyltransferase 1B (muscle)	CPT1B	-0.2	0.01
Acyl-CoA Dehydrogenase, Short/Branched Chain	ACADSB	0.26	0.002
Acyl-CoA Dehydrogenase, C-2 To C-3 Short Chain	ACADS	-0.15	0.05
Acyl-CoA Dehydrogenase, Very Long Chain	ACADVL	-0.37	0.006
Enoyl CoA Hydratase, Short Chain, 1, Mitochondrial	ECHS1	0.15	0.003
Enoyl CoA Hydratase Domain Containing 3	ECHDC3	0.40	0.0004
Hydroxyacyl-CoA Dehydrogenase	HADH	0.31	0.002
Fatty acid synthase	FASN	0.22	0.02
Stearoyl-CoA Desaturase (Delta-9-Desaturase)	SCD	0.68	<0.0001
ELOVL Fatty Acid Elongase 5	ELOVL5	0.36	0.003
ELOVL Fatty Acid Elongase 7	ELOVL7	0.15	0.007
Succinate Dehydrogenase Complex, Subunit C	SDH	0.24	0.005
Succinate Dehydrogenase Complex Assembly Factor 1	SDHAF1	-0.12	0.03
Succinate-CoA Ligase, GDP-Forming, Beta Subunit	SUCLG2	0.16	0.01
Succinate-CoA Ligase, ADP-Forming, Beta Subunit	SUCLA2	0.11	0.02

Table 5.10: Differential expression of significantly up and down regulated genes encoding regulators of lipid metabolism. P value determined by probability distribution of rank product. Colour coding: red, upregulated; blue, downregulated

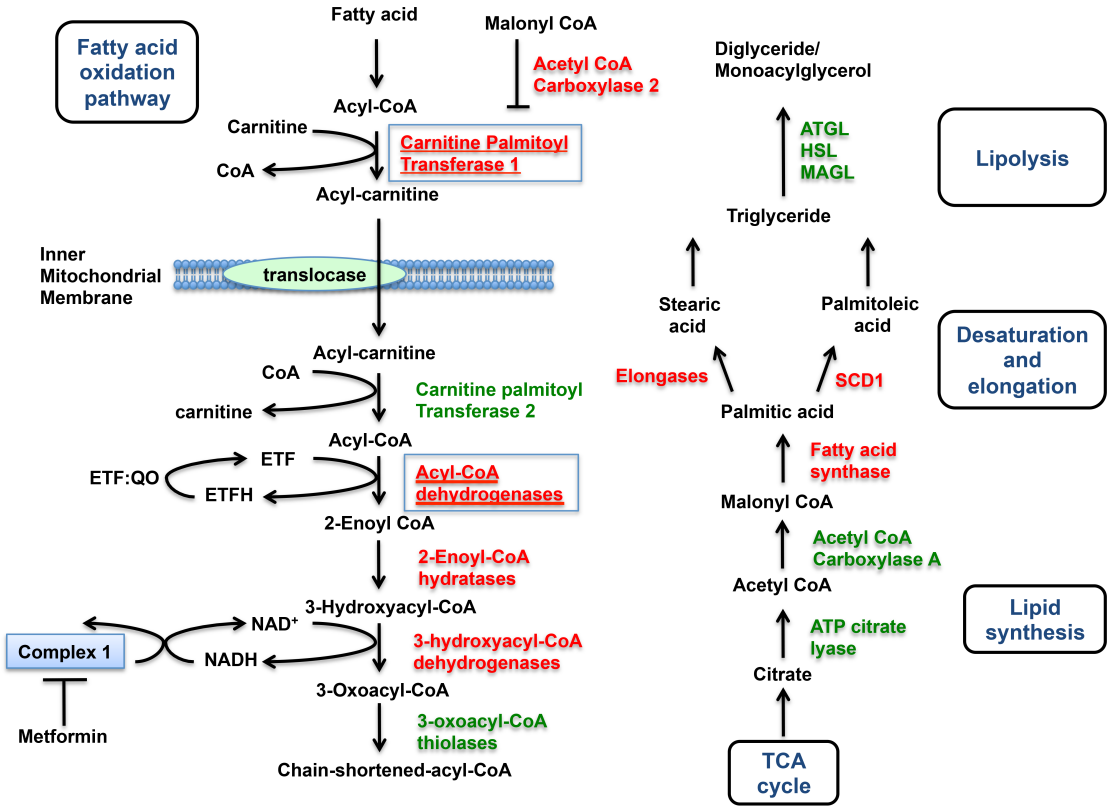


Fig 5.13: Significantly ($p < 0.05$) upregulated (red) and downregulated genes (blue) involved in regulation of lipid synthesis, fatty acid desaturation and elongation, lipolysis and fatty acid oxidation. Genes with different isoforms that are upregulated and downregulated are red surrounded by a blue box and genes that have no significant change in differential expression are in green ($n = 21$).

5.5.7: INSULIN, AMPK, PI3K AND MTOR SIGNALING

There are 7 genes that code for the subunits of AMPK: PRKAA1 and PRKAA2 that code for the alpha subunit; PRKAB1 and PRKAB2 which code for the beta subunit; and PRKAG1, PRKAG2 and PRKAG3 that code for the gamma subunit. Both PRKAA1 and PRKAA2, the 2 subunits of the catalytic alpha domain at which phosphorylation takes place, were upregulated as well as the PRKAB2 and PRKAG1 subunits. LKB1, the upstream threonine kinase was downregulated whilst downstream of AMPK there was some evidence of modulation of the expression of the TSC complex and proteins involved in mTOR signaling. It is however important to be aware that many of the interactions within these pathways are not transcriptional in nature. Lastly several subunits of the PI3K complex were differentially expressed and there was upregulation of insulin receptor gene expression suggesting that there may be altered signaling within the insulin pathway of the cancer cell possibly relevant to a host metabolic effect (**Table 5.11** and **Figure 5.14).**

Protein	Gene	Mean differential expression (log2)	P value
Insulin receptor	INSR	0.14	0.007
Phosphoinositide-3-kinase, regulatory subunit 3	PIK3R3	0.34	0.001
Phosphoinositide-3-kinase, regulatory subunit 5	PIK3R5	-0.35	0.002
Phosphoinositide-3-kinase, regulatory subunit 6	PIK3R6	-0.42	0.0002
Phosphatidylinositol-4,5-bisphosphate 3-kinase, catalytic subunit beta	PIK3CB	0.27	0.01
Phosphatidylinositol-4,5-Bisphosphate 3-Kinase, Catalytic Subunit Gamma	PIK3CG	-0.24	0.02
V-Akt Murine Thymoma Viral Oncogene Homolog 3	AKT3	-0.17	0.02
V-Akt Murine Thymoma Viral Oncogene Homolog 2	AKT2	0.13	0.02
Tuberous sclerosis 1	TSC1	0.02	0.04
Tuberous sclerosis 2	TSC2	0.0003	-0.29
Protein kinase, AMP-activated, alpha 2 catalytic subunit	PRKAA2	0.35	0.0003
Protein kinase, AMP-activated, alpha 1 catalytic subunit	PRKAA1	0.04	0.05
Protein Kinase, AMP-Activated, Beta 2 Non-Catalytic Subunit	PRKAB2	0.24	0.02
Protein Kinase, AMP-Activated, Gamma 1 Non-Catalytic Subunit	PRKAG1	0.12	0.04
serine/threonine kinase 11	STK11	-0.18	0.05
Ras homolog enriched in brain	RHEB	0.13	0.01
regulatory associated protein of MTOR, complex 1	RPTOR	0.02	0.04
Ribosomal Protein S6 Kinase, 70kDa, Polypeptide 2	RPS6KB2	-0.06	0.04
Eukaryotic Translation Initiation Factor 4E Binding Protein 1	EIF4EBP1	-0.10	0.04
Hypoxia Inducible Factor 1, Alpha Subunit	HIF1A	-0.04	0.02
Unc-51 Like Autophagy Activating Kinase 1	ULK1	-0.28	0.006
Unc-51 Like Autophagy Activating Kinase 2	ULK2	0.15	0.009
Unc-51 Like Autophagy Activating Kinase 3	ULK3	-0.17	0.02
Vascular Endothelial Growth Factor C	VEGFC	-0.48	0.0007
Kinase Insert Domain Receptor (A Type III Receptor Tyrosine Kinase)	KDR	0.64	0.001

Table 5.11 – see over: Differential expression of significantly up and down regulated genes encoding regulators of insulin, PI3K, mTOR and AMPK signaling. P value determined by probability distribution of rank product. Colour coding: red, upregulated; blue, downregulated.

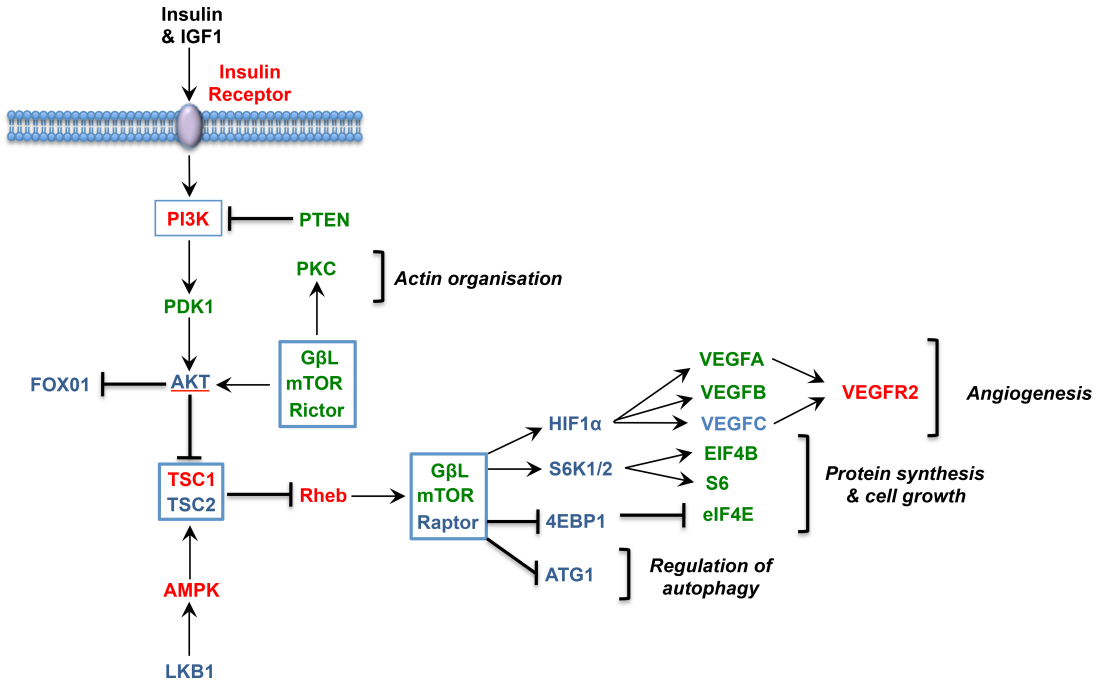


Fig 5.14: Significantly ($p < 0.05$) upregulated (red) and downregulated genes (blue) involved in regulation of the PI3K, AMPK and mTOR pathways. Genes with different isoforms that are upregulated and downregulated are red surrounded by a blue box and genes that have no significant change in differential expression are in green (n = 21).

5.6: IMMUNOHISTOCHEMICAL ANALYSIS

Core biopsies were taken from the primary breast cancer, at the same time as those for RNA sequencing, before and after at least 13 days of metformin treatment under ultrasound guidance by an experienced radiologist. The biopsy samples were then immediately placed in 10% formalin and processed as described in Chapter 2.

5.6.1: Ki67

Ki67 is a well validated marker of cancer cell proliferation [303]. Several prospective studies to date of metformin's effect on Ki67 expression in breast cancer have reported a small decrease in Ki67 of between 3 – 10.5% [105, 215, 216]. The largest study to date suggested that there may only be an effect in patients with features of the metabolic syndrome [105]. In this study, however, there was no evidence of an overall fall in Ki67. There was also much variability in Ki67 expression between paired pre- and post-metformin samples (**Figure 5.15)**.

5.6.1: pAMPK

One study to date has reported an increase in the phosphorylation of AMPK in breast cancer in response to metformin [215]. In this study there was a small increase in the mean pAMPK expression between paired biopsy samples although this did not reach statistical significance on paired t-test (H-score, 2.9 ± 0.5 versus 3.5 ± 0.5, pre- and post-metformin, respectively ($p = 0.16$)) (**Figure 5.16)**. This finding is consistent with metformin being an activator of AMPK in the clinical setting although there is clearly significant variability in response.

5.6.1: pS6

This downstream marker of mTOR activation has not previously been examined in the context of metformin's clinical effect in breast cancer. In this study there was a small decrease in mTOR although again this did not reach statistical significance on paired t-test (H-score, 6.7 ± 0.6 versus 6.0 ± 0.6, pre- and post-metformin, respectively ($p = 0.19$)) (**Figure 5.17)**. Hence, mTOR inhibition may be a mechanism of metformin's anticancer effect.

5.6.1: pE4-BP1

Phosphorylation of 4E-BP1 is another marker of mTOR activation and in this study there was minimal effect on expression of p4E-BP1 and also little variability between biopsy samples (**Figure 5.18).**

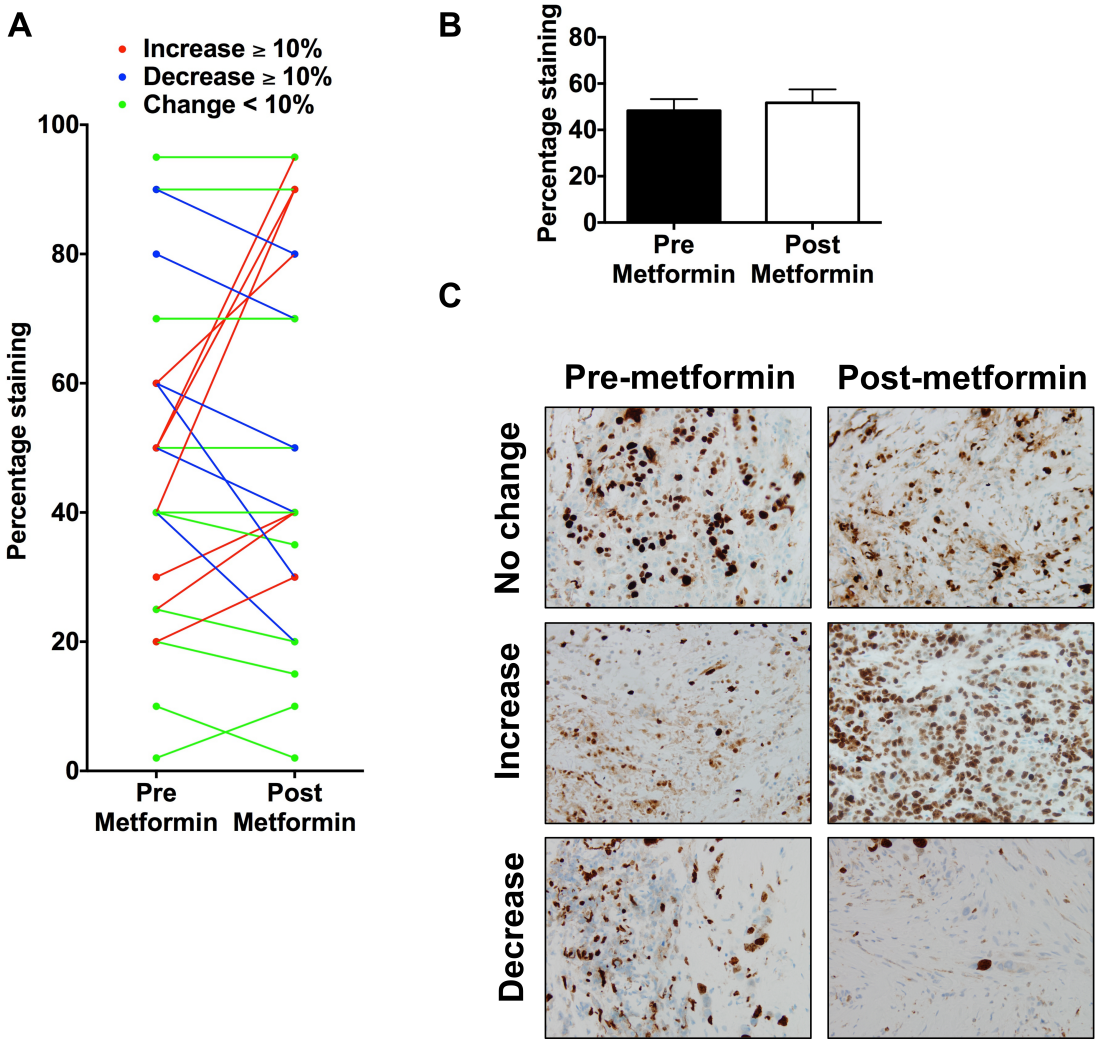


Fig 5.15 A: Baseline and post-metformin immunohistochemical Ki67 expression (percentage of nuclei stained) for each individual primary breast cancer. **B:** Mean baseline and post-metformin immunohistochemical Ki67 expression (percentage of nuclei stained) **C:** Examples of Ki67 immunohistochemical staining for individual patients, **upper panel:** no change after metformin; **central panel:** increase after metformin; **lower panel:** decrease after metformin.

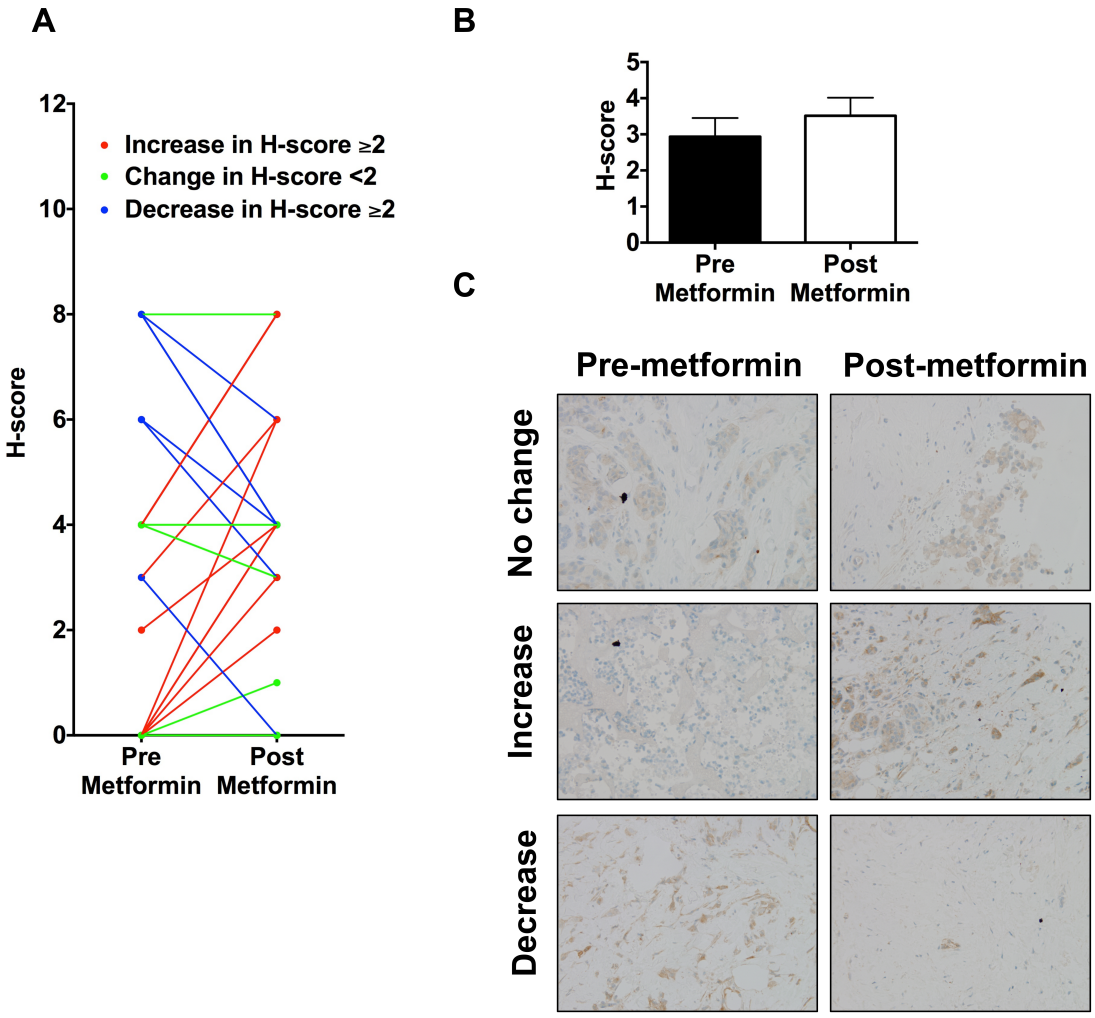


Fig 5.16 A: Baseline and post-metformin immunohistochemical pAMPK expression (H-score) for each individual primary breast cancer. **B:** Mean baseline and post-metformin immunohistochemical pAMPK expression (H-score) **C:** Examples of pAMPK immunohistochemical staining for individual patients, **upper panel:** no change after metformin; **central panel:** increase after metformin; **lower panel:** decrease after metformin.

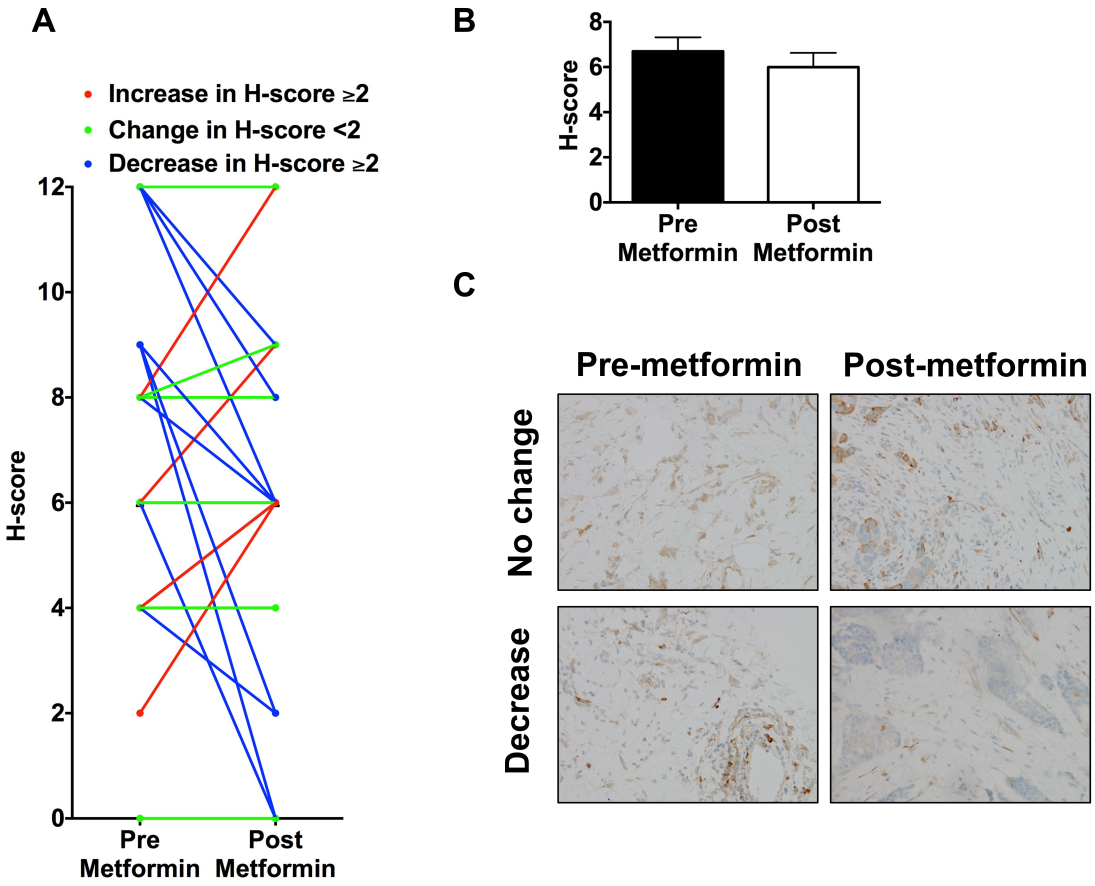


Fig 5.17 A: Baseline and post-metformin immunohistochemical pS6 expression (H-score) for each individual primary breast cancer. **B:** Mean baseline and post-metformin immunohistochemical pS6 expression (H-score) **C:** Examples of pS6 immunohistochemical staining for individual patients, **upper panel:** no change after metformin; **lower panel:** decrease after metformin.

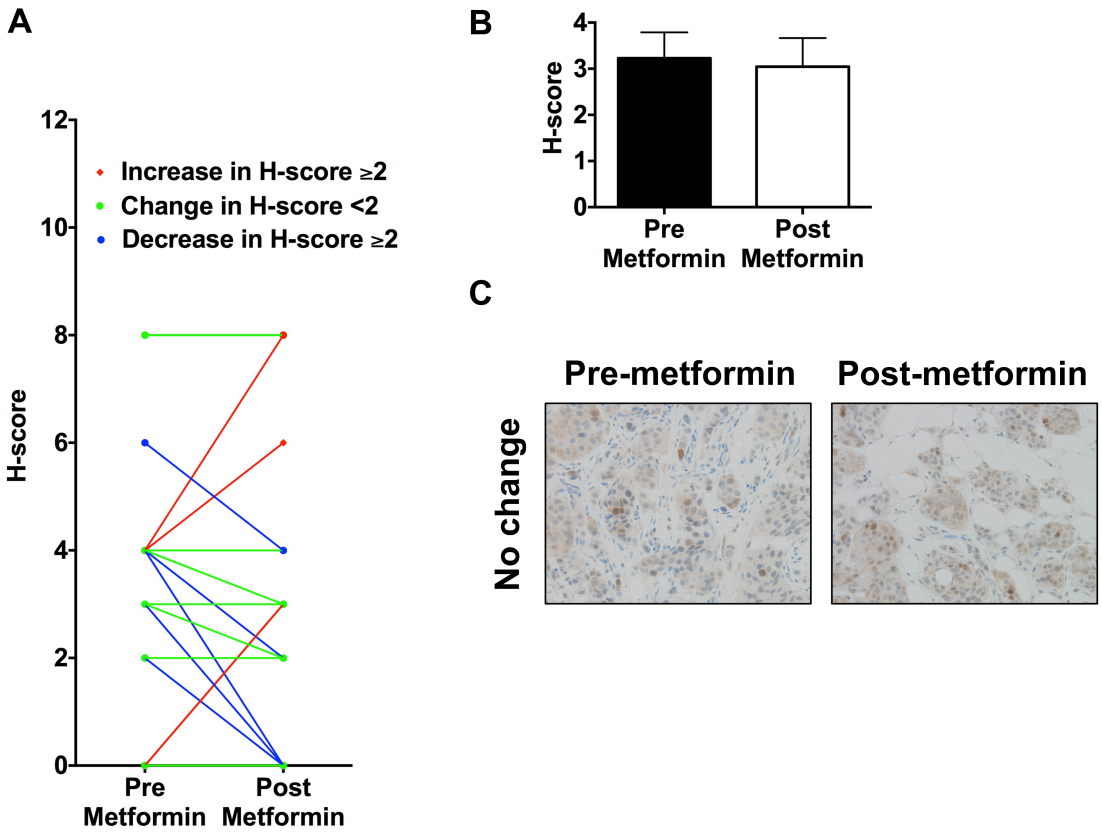


Fig 5.18 A: Baseline and post-metformin immunohistochemical p4E-BP1 expression (H-score) for each individual primary breast cancer. **B:** Mean baseline and post-metformin immunohistochemical p4E-BP1 expression (H-score) **C:** Example of p4E-BP1 immunohistochemical staining for individual patients.

5.7: SERUM METABOLIC MARKERS

Serum metabolic markers were measured before and after 13 days of metformin treatment. Study participants were asked to fast overnight prior to blood sampling and for the second set of blood samples participants were asked to take their metformin on the morning of their study test (approximately 2 hours prior). The data presented here is a preliminary analysis of the paired samples from the first 23 patients.

There was no consistent effect of metformin on serum levels of glucose, lactate, IGF1, IGF2, the ratio of IGF2 to IGF1 or IGF-BP3 (**Figure 5.19A**). Although entry to the study necessitated a fasting blood glucose level on screening tests to be less than 7.0 mmol/L (i.e. not diagnostic of diabetes mellitus), 2 of the 23 patients had a baseline fasting glucose of between 6.1 and 6.9 mmol/L. This is consistent with the WHO criteria for 'impaired fasting glucose' and implies insulin resistance.

There was a trend toward a decrease in serum insulin levels after metformin (67.1 ± 6.4 pmol/L vs 58.1 ± 4.8 pmol/L, pre- and post-metformin, respectively (paired t-test, $p = 0.06$)) and a statistically significant decrease in C-peptide (0.56 ± 0.04 nmol/L vs 0.48 ± 0.02 nmol/L, pre- and post-metformin, respectively (paired t-test, $p = 0.003$)) (**Figure 5.19A)**. Proinsulin C-peptide links the A- and B-chains of insulin during its assembly in the endoplasmic reticulum of the β-cells of the pancreas (**Figure 5.19B**) and equimolar amounts of C-peptide and insulin are then held in the secretory vesicles of the pancreatic β-cells prior to release into the circulation. As the liver extracts a large proportion of insulin form the portal circulation and this varies with the nutritional state of the patient C-peptide is considered a more reliable marker of

insulin secretion when measured in the peripheral circulation than insulin itself [304]. The homeostatic model index (HOMA) is a measure of insulin resistance calculated from the product of glucose (mmol/L) and insulin (mU/L) divided by 22.5. There was a trend toward a reduction in the HOMA index after 2 weeks metformin treatment (2.05 ± 0.17 vs 1.82 ± 0.15 nmol/L, pre- and post-metformin, respectively (paired t-test, p = 0.10)) (**Figure 5.19A)**. Hence this is good evidence that in this essentially normoglycaemic breast cancer population metformin was reducing insulin secretion and possibly insulin resistance. This raises the possibility that this effect is important for metformin's anticancer mechanism, even outside of the diabetes mellitus setting.

There was no clear evidence of an effect on the levels of the serum markers of lipid metabolism, total cholesterol, HDL cholesterol and triglyceride. Leptin is a proteohormone that is understood to play a key role in body weight regulation and has previously been shown to decrease with metformin treatment in patients with type 2 diabetes mellitus [305]. It has also been implicated in tumour stromal interactions that promote cancer invasiveness [306]. However, no effect on serum leptin levels by metformin was seen in this group of patients (**Figure 5.20A)**.

The median serum metformin level was 9.1 (interquartile range, 8.4 – 11.9) nmol/ml (**Figure 5.20B)**. This is consistent with published data [15]. All patients in the study completed compliance forms and there was no suggestion that doses were missed or that there was a marked difference in the timing of sampling.

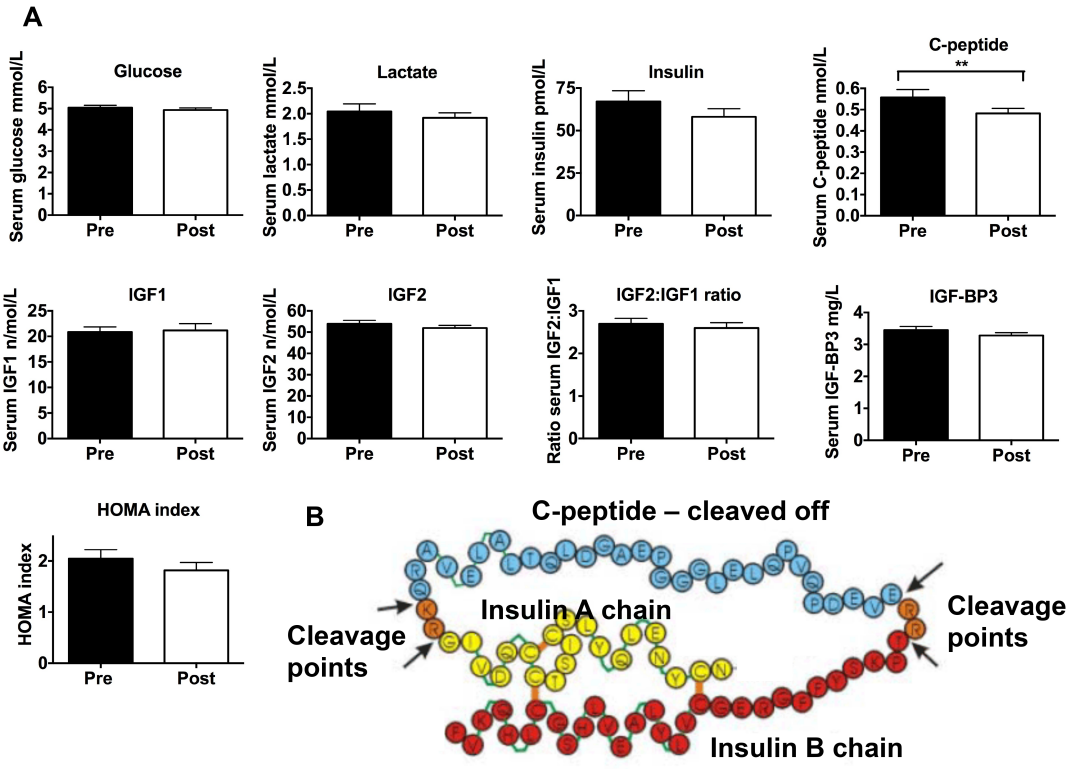


Fig 5.19A: Baseline and post-metformin serum levels of glucose, lactate, insulin, c-peptide, IGF-1, IGF-2, IGF2:IGF1 ratio, IGF-BP3 and HOMA index. **B:** C-peptide is cleaved away from the insulin A and insulin B chain. Data shown are mean ± SEM, **p < 0.01.

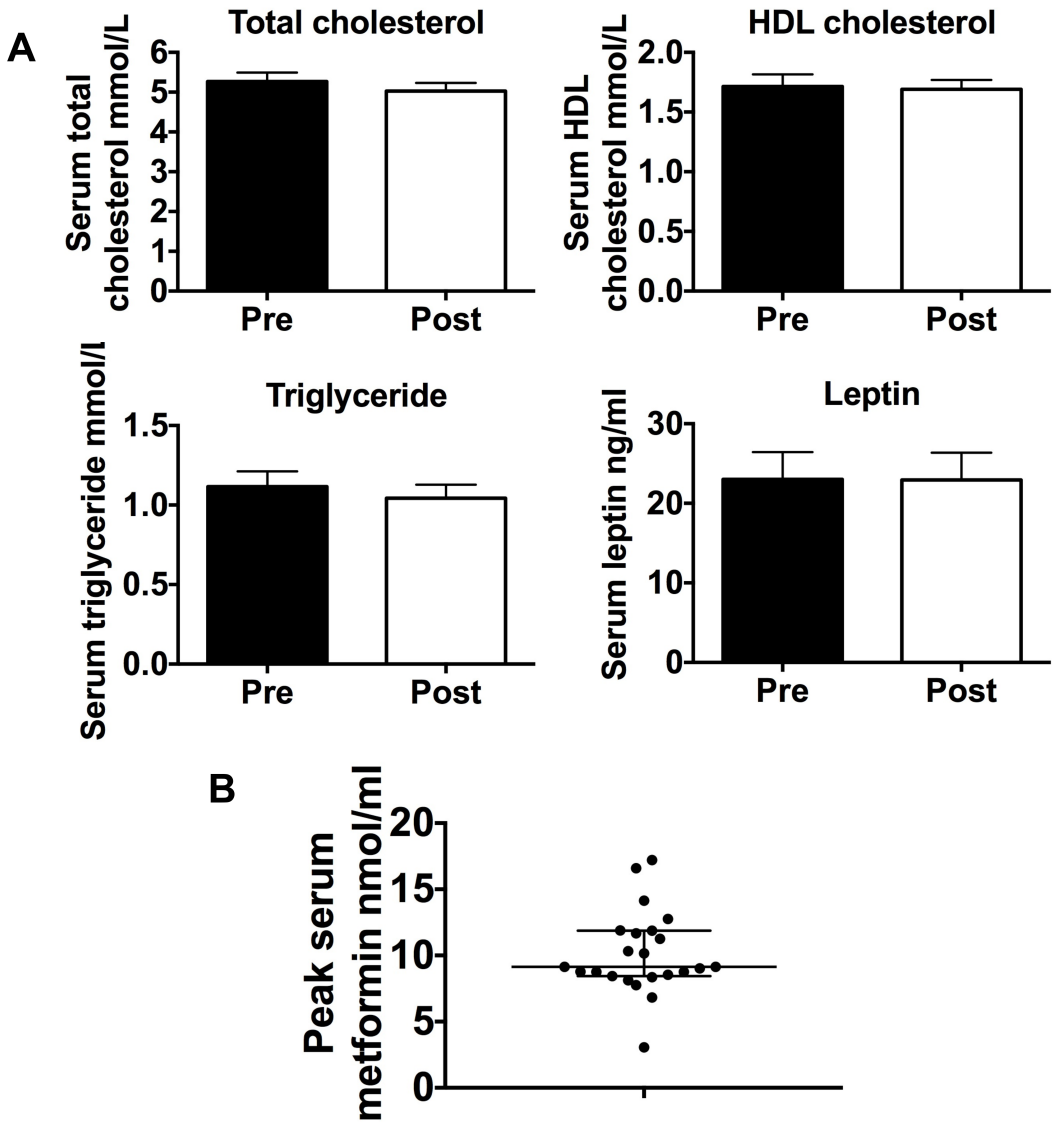


Fig 5.20A: Baseline and post-metformin serum levels of total cholesterol, HDL-cholesterol, triglyceride and leptin. Data shown are mean ± SEM. **B:** Peak serum level of metformin (2 hour post dose). Data shown are median and interquartile range.

5.8: DISCUSSION

5.8.1: mRNA SEQUENCING ANALYSIS IS CONSISTENT WITH A 'DIRECT' METABOLIC EFFECT OF METFORMIN ON CANCER CELLS

The pathway analysis of the mRNA sequencing data was striking in picking out multiple mitochondrial genes and those relevant to the TCA cycle. The degree of differential expression of these genes may well act as a biomarker for metformin's metabolic effect, and ultimately clinical effect, especially if resistance to metformin is predominantly at the mitochondrial level. It was also notable that several glucose and glutamine transporters, the enzymes of fatty acid oxidation, glycolysis and glutaminolysis and also reductive carboxylation were predominantly upregulated suggesting a response to mitochondrial toxicity that is very consistent with our and other's in vitro and xenograft model data (see Chapters 1 and 3 for discussion of this). Hence, the mRNA data is consistent with a direct metabolic effect by metformin on breast cancer cells. The overall increase, although not statistically significant, in AMPK phosphorylation and decrease in S6 phosphorylation also adds weight to this hypothesis.

It is clear that metformin is also having an effect on 'host' metabolism in reducing insulin secretion and correlation of this (and baseline BMI) between individual tumours with changes in mRNA expression of genes relevant to insulin signaling (and other assays in this study) will provide a fuller picture with regards to the intratumoral effect.

5.8.2: CHANGE IN K_2 OF ^{18}[F]-FDG ON DYNAMIC PET-CT IS A POSSIBLE BIOMARKER OF METFORMIN'S METABOLIC EFFECT

The overall decrease in the K_2 variable after metformin on dynamic ^{18}[F]-FDG PET-CT modeling is consistent with a decrease in ^{18}[F]-FDG efflux from the primary breast cancer. It is intriguing that this effect significantly correlated with baseline BMI suggestive of this effect being dependent on the host's metabolic state. Further correlation with other assays in this study, in particular change in c-peptide levels and gene sequencing pathway analysis once the full datasets are available will be important to tease out the importance of this marker in defining metabolic response to metformin. However at this stage it is not clear as to the significance of the change in K_2 as a clinical marker of response as there is very limited published data.

In the light of the upregulation of the glycolysis pathway it is perhaps surprising that there was not an overall increase in the flux, K_1 and K_3 variables from the dynamic ^{18}[F]-FDG PET-CT analysis that would be consistent with an increase in glucose uptake. However, correlation between the change in these variables and the PET-CT data will be intriguing. A full dataset will be required for this to make relevant correlations.

5.8.3: FUTURE WORK

Only the early results from this study are presented here. Analyses of a second cohort of approximately 20 patients for the gene sequencing and serum metabolic marker assays will be available in time and these larger datasets will allow for more comprehensive correlations. Of note, metabolomics and lipidomics analysis is underway of 30 paired tumour samples from this study. This work will not only

enable the comparison of metabolite levels between pre- and post-metformin treated tumours (and correlation with changes in other assays in this study) but also, at baseline, will allow a unique marriage of the datasets for intratumoral metabolites, whole genome mRNA expression, protein expression, functional imaging and the host metabolic state to describe a cohort of 30 untreated primary breast cancers.

CHAPTER 6: FINAL DISCUSSION

6.1: OVERVIEW

Since the genesis of this project the literature and interest in metformin as an anticancer agent has grown exponentially. In the past 4 years the first exploratory studies of metformin's anticancer effect on using clinical cancer specimens have been published. However, although there is now some clinical evidence that metformin may decrease cancer cell proliferation (as measured using Ki67) in an insulin resistant cohort of breast cancer patients [105] many questions remain unanswered. Hence, the overall aims of this DPhil project, as set out in Chapter 1, still remain valid:

a) to further examine the effect of metformin on breast cancer metabolism using in vitro cell line models to gain greater insight into its anticancer mechanism of action;
b) to develop an understanding of pathways that might be targeted to synergise with metformin's anticancer effect;
c) to set up a 'window of opportunity' clinical trial to study metformin's effects on breast cancer metabolism, to develop potential biomarkers of its metabolic effect and further investigate its in vivo mechanism of action.

6.2: INHIBITION OF FATTY ACID OXIDATION CONTRIBUTES TO METFORMIN'S ANTICANCER EFFECT

The data presented in Chapter 4 showed that metformin has pronounced effects on breast cancer cell lipid metabolism. The marked accumulation of lipid droplets in breast cancer cells in vitro and in vivo secondary to the inhibition of fatty acid oxidation by metformin is a novel finding. This occurred as a direct result of complex 1 inhibition and independently of AMPK activation. The combination of metformin with etomoxir, another inhibitor of fatty acid oxidation, further decreased fatty acid oxidation and had an additive antiproliferative effect. The fact that several genes important in regulating fatty acid oxidation were induced in the clinical study (along with many genes encoding for components of complex 1) suggests that this pathway may also be affected at clinically relevant doses.

This discovery is of particular interest in the context of recently published data. The finding that metformin inhibits fatty acid oxidation in breast cancer cell lines is in direct contrast to several published studies of metformin's effects in vitro and in vivo in non-cancer cells. In these studies a decrease in lipid accumulation was observed secondary to increased fatty acid oxidation that is driven by AMPK activation [32, 33, 52, 276, 289]. Metformin has been shown to decrease glucose oxidation and reduce ATP levels in cancer cells [288, 290] and there has been growing interest over the past 2-3 years in the importance of fatty acid oxidation supporting cancer cells under energy stress and its potential as a therapeutic target [307]. Hence the findings presented in this thesis provide good evidence that it is not just the inhibition of

glucose oxidation but a cancer cell's inability to compensate using the fatty acid oxidation pathway that drives the drug's anticancer effect.

This study has important implications for the understanding of how to use metformin in the clinical setting. There has been recent focus on the importance of fatty acid oxidation in cancer stem cell maintenance and our findings may explain metformin's selective targeting of these cells [307]. The anticancer mechanism described here may have implications for future drug development. Lastly, metformin's effect on cancer lipid metabolism may prove a useful biomarker of this drug's anti-cancer effect.

6.3: TARGETING OF GLUTAMINE METABOLISM IN CONJUNCTION WITH METFORMIN TREATMENT SHOULD BE PURSUED AS A TREATMENT STRATEGY

The data presented in Chapter 3 showed that the utilisation of glutamine as a carbon source became increasingly important with metformin treatment in maintaining growth in cancer cells. During the course of this project two other studies were published which confirmed that mitochondrial interference using metformin or otherwise led to dependence on glutamine [143, 151]. The in vitro screen of inhibitors of different steps of the glutaminolysis and reductive carboxylation pathways or glutamine uptake and also the glutamine deprivation experiments showed that this is a compelling strategy to pursue in order to achieve drug synergy with metformin. Given the 'nutrient abundance' necessary in the closed systems of in vitro models it is possible that greater effects and at lower doses may be seen in vivo. In particular, bithionol, a drug that has been shown to inhibit glutamine dehydrogenase and which

is relatively well tolerated in humans had anticancer effects in vitro at dose levels well below peak plasma level both on its own and in synergy with metformin. Given that this drug is already used in the clinic as an anti-parasitic agent it would be a relatively simple step to assess its biological effect and efficacy in a clinical study.

6.4: GENE EXPRESSION DATA FROM CLINICAL SAMPLES CORRELATES WELL WITH IN VITRO WORK

In the analysis of pathways with the most pronounced changes in gene expression, many of the most significant were involved in metabolism. In particular it was striking that so many genes encoding the components of the electron transport chain were differentially expressed as were virtually all the genes key to the TCA cycle, glutaminolysis and glycolysis. This data is the first strong evidence in the clinical setting that metformin is causing an energy stress as a consequence of a direct effect on cancer cells in a similar manner to that observed in vitro. The increase in pAMPK and pS6 expression (although not statistically significant) is also consistent with this effect. However, metformin also reduced insulin secretion as measured by c-peptide levels and there was a correlation between increasing BMI and the degree of decrease in the variable K_2 (a marker of glucose efflux from the tumour). Hence at this stage it is still not clear whether there is also a 'host' indirect effect on the cancer cells related to inhibition of the insulin axis and which is the most clinically relevant. Further correlation of the full serum metabolic marker profile, dynamic PET-CT, immunohistochemistry, RNA sequencing and metabolomics datasets when available should help answer these questions.

6.5: FUTURE DIRECTIONS

In summary, this project has generated a great deal of data on metformin's effects on breast cancer cells both using in vivo and in vitro models and in clinical specimens. Currently only preliminary data is available from the clinical project but in order to maximise the potential of the final dataset and validate its findings it will be important to carry out much more detailed correlations between the different clinical datasets when they are complete. On a similar note, there will be an opportunity to further compare these clinical datasets with the data generated from the in vitro and in vivo models presented in this thesis.

With regard to the work presented in Chapter 3, the most promising avenue of investigation to take forward is to further examine bithionol's anticancer effects both alone and in synergy with metformin. Indeed, glutamine dehydrogenase as a drug target in itself warrants further investigation. Firstly, it would be important to confirm that bithionol is having significant effects on glutamine metabolism the obvious strategy being to use nuclear magnetic resonance techniques to trace metabolism of [U-^{13}C] labeled glutamine in vitro, with and without bithionol. Testing the combination of metformin and bithionol using an in vivo xenograft model will be of particular interest given that the effects of these drugs may be especially acute in a nutrient poor environment. Lastly this combination could be taken into the clinic at an early stage given that their side effect profiles are well understood.

The in vitro finding that metformin inhibited fatty acid oxidation will be examined further in the clinical study. In collaboration with Professor Wakelam at the Babraham Institute, University of Cambridge lipidomic analysis of snap frozen

primary breast cancer biopsy samples obtained in this study should enable an assessment to be made of overall triglyceride accumulation and changes in the profile of metabolic intermediates in the fatty acid oxidation pathway. This could be correlated with the available lipid relevant changes in gene expression. Further work to correlate any changes in the lipid metabolome with other markers in the study, e.g. Ki67 may help to tease out whether this effect is clinically important for metformin's anticancer effect.

With regards to the clinical study a great deal of work still needs to be carried out to maximise the potential of this dataset. A unique opportunity exists to correlate the baseline metabolomic data, functional imaging, next generation gene sequencing, protein expression and host serum metabolite levels in a sizable cohort of breast cancer patients. Indeed, the correlation of metformin's clinical effect on the different assays is a separate but equally important study that should have a major impact on the field. In order to achieve these aims dedicated bioinformatics support will be necessary.

REFERENCES

1. Krall, L.P. and R. Camerini-Davalos, *Early clinical evaluation of a new oral non-sulfonylurea hypoglycemic agent.* Proc Soc Exp Biol Med, 1957. **95**(2): p. 345-7.
2. *Effect of intensive blood-glucose control with metformin on complications in overweight patients with type 2 diabetes (UKPDS 34). UK Prospective Diabetes Study (UKPDS) Group.* Lancet, 1998. **352**(9131): p. 854-65.
3. Lamanna, C., et al., *Effect of metformin on cardiovascular events and mortality: a meta-analysis of randomized clinical trials.* Diabetes Obes Metab, 2011. **13**(3): p. 221-8.
4. Abbasi, F., et al., *Results of a placebo-controlled study of the metabolic effects of the addition of metformin to sulfonylurea-treated patients. Evidence for a central role of adipose tissue.* Diabetes Care, 1997. **20**(12): p. 1863-9.
5. Cusi, K., A. Consoli, and R.A. DeFronzo, *Metabolic effects of metformin on glucose and lactate metabolism in noninsulin-dependent diabetes mellitus.* J Clin Endocrinol Metab, 1996. **81**(11): p. 4059-67.
6. Saenz, A., et al., *Metformin monotherapy for type 2 diabetes mellitus.* Cochrane Database Syst Rev, 2005(3): p. CD002966.
7. Lord, J.M., I.H. Flight, and R.J. Norman, *Metformin in polycystic ovary syndrome: systematic review and meta-analysis.* BMJ, 2003. **327**(7421): p. 951-3.
8. Marchesini, G., et al., *Metformin in non-alcoholic steatohepatitis.* Lancet, 2001. **358**(9285): p. 893-4.
9. Ibanez, L., et al., *Metformin treatment to prevent early puberty in girls with precocious pubarche.* J Clin Endocrinol Metab, 2006. **91**(8): p. 2888-91.
10. http://www.fda.gov.
11. http://www.bnf.org.
12. Pentikainen, P.J., P.J. Neuvonen, and A. Penttila, *Pharmacokinetics of metformin after intravenous and oral administration to man.* Eur J Clin Pharmacol, 1979. **16**(3): p. 195-202.
13. Tucker, G.T., et al., *Metformin kinetics in healthy subjects and in patients with diabetes mellitus.* Br J Clin Pharmacol, 1981. **12**(2): p. 235-46.
14. Scheen, A.J., *Clinical pharmacokinetics of metformin.* Clin Pharmacokinet, 1996. **30**(5): p. 359-71.
15. http://www.bms.com. *Bristol Myers Sqibb prescribing information.*
16. Sirtori, C.R., et al., *Disposition of metformin (N,N-dimethylbiguanide) in man.* Clin Pharmacol Ther, 1978. **24**(6): p. 683-93.
17. Beckmann, R., *[Absorption, distribution in the organism and elimination of metformin].* Diabetologia, 1969. **5**(5): p. 318-24.
18. Hall, H., G. Ramachander, and J.M. Glassman, *Tissue distribution and excretion of phenformin in normal and diabetic animals.* Ann N Y Acad Sci, 1968. **148**(3): p. 601-11.

19. Scheen, A.J., *Drug interactions of clinical importance with antihyperglycaemic agents: an update.* Drug Saf, 2005. **28**(7): p. 601-31.
20. Wilcock, C. and C.J. Bailey, *Accumulation of metformin by tissues of the normal and diabetic mouse.* Xenobiotica, 1994. **24**(1): p. 49-57.
21. Gontier, E., et al., *High and typical 18F-FDG bowel uptake in patients treated with metformin.* Eur J Nucl Med Mol Imaging, 2008. **35**(1): p. 95-9.
22. Gan, S.C., et al., *Biguanide-associated lactic acidosis. Case report and review of the literature.* Arch Intern Med, 1992. **152**(11): p. 2333-6.
23. Kreisberg, R.A. and B.C. Wood, *Drug and chemical-induced metabolic acidosis.* Clin Endocrinol Metab, 1983. **12**(2): p. 391-411.
24. Setter, S.M., et al., *Metformin hydrochloride in the treatment of type 2 diabetes mellitus: a clinical review with a focus on dual therapy.* Clin Ther, 2003. **25**(12): p. 2991-3026.
25. Hundal, R.S., et al., *Mechanism by which metformin reduces glucose production in type 2 diabetes.* Diabetes, 2000. **49**(12): p. 2063-9.
26. Natali, A. and E. Ferrannini, *Effects of metformin and thiazolidinediones on suppression of hepatic glucose production and stimulation of glucose uptake in type 2 diabetes: a systematic review.* Diabetologia, 2006. **49**(3): p. 434-41.
27. Shu, Y., et al., *Effect of genetic variation in the organic cation transporter 1 (OCT1) on metformin action.* J Clin Invest, 2007. **117**(5): p. 1422-31.
28. Shaw, R.J., et al., *The kinase LKB1 mediates glucose homeostasis in liver and therapeutic effects of metformin.* Science, 2005. **310**(5754): p. 1642-6.
29. He, L., et al., *Metformin and insulin suppress hepatic gluconeogenesis through phosphorylation of CREB binding protein.* Cell, 2009. **137**(4): p. 635-46.
30. Kim, Y.D., et al., *Metformin inhibits hepatic gluconeogenesis through AMP-activated protein kinase-dependent regulation of the orphan nuclear receptor SHP.* Diabetes, 2008. **57**(2): p. 306-14.
31. Lee, J.M., et al., *AMPK-dependent repression of hepatic gluconeogenesis via disruption of CREB.CRTC2 complex by orphan nuclear receptor small heterodimer partner.* J Biol Chem, 2010. **285**(42): p. 32182-91.
32. Zang, M., et al., *AMP-activated protein kinase is required for the lipid-lowering effect of metformin in insulin-resistant human HepG2 cells.* J Biol Chem, 2004. **279**(46): p. 47898-905.
33. Zhou, G., et al., *Role of AMP-activated protein kinase in mechanism of metformin action.* J Clin Invest, 2001. **108**(8): p. 1167-74.
34. Kim, E., et al., *Metformin inhibits nuclear receptor TR4-mediated hepatic stearoyl-CoA desaturase 1 gene expression with altered insulin sensitivity.* Diabetes, 2011. **60**(5): p. 1493-503.
35. Evans, J.M., et al., *Metformin and reduced risk of cancer in diabetic patients.* BMJ, 2005. **330**(7503): p. 1304-5.
36. Landman, G.W., et al., *Metformin associated with lower cancer mortality in type 2 diabetes: ZODIAC-16.* Diabetes Care, 2010. **33**(2): p. 322-6.
37. Libby, G., et al., *New users of metformin are at low risk of incident cancer: a cohort study among people with type 2 diabetes.* Diabetes Care, 2009. **32**(9): p. 1620-5.

38. Decensi, A., et al., *Metformin and cancer risk in diabetic patients: a systematic review and meta-analysis.* Cancer Prev Res (Phila), 2010. **3**(11): p. 1451-61.
39. Chlebowski, R.T., et al., *Diabetes, metformin, and breast cancer in postmenopausal women.* J Clin Oncol, 2012. **30**(23): p. 2844-52.
40. Dowling, R.J., et al., *Metformin in cancer: translational challenges.* J Mol Endocrinol, 2012. **48**(3): p. R31-43.
41. Jiralerspong, S., et al., *Metformin and pathologic complete responses to neoadjuvant chemotherapy in diabetic patients with breast cancer.* J Clin Oncol, 2009. **27**(20): p. 3297-302.
42. Bayraktar, S., et al., *Effect of metformin on survival outcomes in diabetic patients with triple receptor-negative breast cancer.* Cancer, 2012. **118**(5): p. 1202-11.
43. Garrett, C.R., et al., *Survival advantage observed with the use of metformin in patients with type II diabetes and colorectal cancer.* Br J Cancer, 2012. **106**(8): p. 1374-8.
44. Mazzone, P.J., et al., *The effect of metformin and thiazolidinedione use on lung cancer in diabetics.* BMC Cancer, 2012. **12**: p. 410.
45. Tan, B.X., et al., *Prognostic influence of metformin as first-line chemotherapy for advanced nonsmall cell lung cancer in patients with type 2 diabetes.* Cancer, 2011. **117**(22): p. 5103-11.
46. Alimova, I.N., et al., *Metformin inhibits breast cancer cell growth, colony formation and induces cell cycle arrest in vitro.* Cell Cycle, 2009. **8**(6): p. 909-15.
47. Zhuang, Y. and W.K. Miskimins, *Cell cycle arrest in Metformin treated breast cancer cells involves activation of AMPK, downregulation of cyclin D1, and requires p27Kip1 or p21Cip1.* J Mol Signal, 2008. **3**: p. 18.
48. Zakikhani, M., et al., *Metformin is an AMP kinase-dependent growth inhibitor for breast cancer cells.* Cancer Res, 2006. **66**(21): p. 10269-73.
49. Liu, B., et al., *Metformin induces unique biological and molecular responses in triple negative breast cancer cells.* Cell Cycle, 2009. **8**(13): p. 2031-40.
50. Blandino, G., et al., *Metformin elicits anticancer effects through the sequential modulation of DICER and c-MYC.* Nat Commun, 2012. **3**: p. 865.
51. Iliopoulos, D., H.A. Hirsch, and K. Struhl, *Metformin decreases the dose of chemotherapy for prolonging tumor remission in mouse xenografts involving multiple cancer cell types.* Cancer Res, 2011. **71**(9): p. 3196-201.
52. Buzzai, M., et al., *Systemic treatment with the antidiabetic drug metformin selectively impairs p53-deficient tumor cell growth.* Cancer Res, 2007. **67**(14): p. 6745-52.
53. Gou, S., et al., *Low concentrations of metformin selectively inhibit CD133(+) cell proliferation in pancreatic cancer and have anticancer action.* PLoS One, 2013. **8**(5): p. e63969.
54. Hirsch, H.A., D. Iliopoulos, and K. Struhl, *Metformin inhibits the inflammatory response associated with cellular transformation and cancer stem cell growth.* Proc Natl Acad Sci U S A, 2013. **110**(3): p. 972-7.
55. Liu, J., et al., *Metformin inhibits renal cell carcinoma in vitro and in vivo xenograft.* Urol Oncol, 2013. **31**(2): p. 264-70.

56. Deng, X.S., et al., *Metformin targets Stat3 to inhibit cell growth and induce apoptosis in triple-negative breast cancers.* Cell Cycle, 2012. **11**(2): p. 367-76.
57. Vazquez-Martin, A., C. Oliveras-Ferraros, and J.A. Menendez, *The antidiabetic drug metformin suppresses HER2 (erbB-2) oncoprotein overexpression via inhibition of the mTOR effector p70S6K1 in human breast carcinoma cells.* Cell Cycle, 2009. **8**(1): p. 88-96.
58. Liu, B., et al., *Potent anti-proliferative effects of metformin on trastuzumab-resistant breast cancer cells via inhibition of erbB2/IGF-1 receptor interactions.* Cell Cycle, 2011. **10**(17): p. 2959-66.
59. Dowling, R.J., et al., *Metformin inhibits mammalian target of rapamycin-dependent translation initiation in breast cancer cells.* Cancer Res, 2007. **67**(22): p. 10804-12.
60. Ben Sahra, I., et al., *The antidiabetic drug metformin exerts an antitumoral effect in vitro and in vivo through a decrease of cyclin D1 level.* Oncogene, 2008. **27**(25): p. 3576-86.
61. Cantrell, L.A., et al., *Metformin is a potent inhibitor of endometrial cancer cell proliferation--implications for a novel treatment strategy.* Gynecol Oncol, 2010. **116**(1): p. 92-8.
62. Gotlieb, W.H., et al., *In vitro metformin anti-neoplastic activity in epithelial ovarian cancer.* Gynecol Oncol, 2008. **110**(2): p. 246-50.
63. Hirsch, H.A., et al., *Metformin selectively targets cancer stem cells, and acts together with chemotherapy to block tumor growth and prolong remission.* Cancer Res, 2009. **69**(19): p. 7507-11.
64. Colquhoun, A.J., et al., *Metformin enhances the antiproliferative and apoptotic effect of bicalutamide in prostate cancer.* Prostate Cancer Prostatic Dis, 2012. **15**(4): p. 346-52.
65. Brown, K.A., et al., *Metformin inhibits aromatase expression in human breast adipose stromal cells via stimulation of AMP-activated protein kinase.* Breast Cancer Res Treat, 2010. **123**(2): p. 591-6.
66. Berstein, L.M., et al., *Isolated and combined action of tamoxifen and metformin in wild-type, tamoxifen-resistant, and estrogen-deprived MCF-7 cells.* Breast Cancer Res Treat, 2011. **128**(1): p. 109-17.
67. Song, C.W., et al., *Metformin kills and radiosensitizes cancer cells and preferentially kills cancer stem cells.* Sci Rep, 2012. **2**: p. 362.
68. Liu, J., et al., *Enhanced cytotoxic effect of low doses of metformin combined with ionizing radiation on hepatoma cells via ATP deprivation and inhibition of DNA repair.* Oncol Rep, 2012. **28**(4): p. 1406-12.
69. Memmott, R.M., et al., *Metformin prevents tobacco carcinogen--induced lung tumorigenesis.* Cancer Prev Res (Phila), 2010. **3**(9): p. 1066-76.
70. Anisimov, V.N., et al., *Effect of metformin on life span and on the development of spontaneous mammary tumors in HER-2/neu transgenic mice.* Exp Gerontol, 2005. **40**(8-9): p. 685-93.
71. Huang, X., et al., *Important role of the LKB1-AMPK pathway in suppressing tumorigenesis in PTEN-deficient mice.* Biochem J, 2008. **412**(2): p. 211-21.
72. Anisimov, V.N., et al., *If started early in life, metformin treatment increases life span and postpones tumors in female SHR mice.* Aging (Albany NY), 2011. **3**(2): p. 148-57.

73. Hosono, K., et al., *Metformin suppresses azoxymethane-induced colorectal aberrant crypt foci by activating AMP-activated protein kinase.* Mol Carcinog, 2010. **49**(7): p. 662-71.
74. Calle, E.E., et al., *Overweight, obesity, and mortality from cancer in a prospectively studied cohort of U.S. adults.* N Engl J Med, 2003. **348**(17): p. 1625-38.
75. Flegal, K.M., et al., *Prevalence and trends in obesity among US adults, 1999-2000.* JAMA, 2002. **288**(14): p. 1723-7.
76. *International Agency for Research on Cancer. Weight Control and Physical Activity*. Vol. 6. 2002: Lyon: International Agency fo Research on Cancer.
77. Phipps, A.I., et al., *Breast density, body mass index, and risk of tumor marker-defined subtypes of breast cancer.* Ann Epidemiol, 2012. **22**(5): p. 340-8.
78. Pierobon, M. and C.L. Frankenfeld, *Obesity as a risk factor for triple-negative breast cancers: a systematic review and meta-analysis.* Breast Cancer Res Treat, 2013. **137**(1): p. 307-14.
79. Mokdad, A.H., et al., *Prevalence of obesity, diabetes, and obesity-related health risk factors, 2001.* JAMA, 2003. **289**(1): p. 76-9.
80. Giovannucci, E., et al., *Diabetes and cancer: a consensus report.* Diabetes Care, 2010. **33**(7): p. 1674-85.
81. Xue, F. and K.B. Michels, *Diabetes, metabolic syndrome, and breast cancer: a review of the current evidence.* Am J Clin Nutr, 2007. **86**(3): p. s823-35.
82. Vigneri, P., et al., *Diabetes and cancer.* Endocr Relat Cancer, 2009. **16**(4): p. 1103-23.
83. Gilbert, C.A. and J.M. Slingerland, *Cytokines, obesity, and cancer: new insights on mechanisms linking obesity to cancer risk and progression.* Annu Rev Med, 2013. **64**: p. 45-57.
84. Roberts, D.L., C. Dive, and A.G. Renehan, *Biological mechanisms linking obesity and cancer risk: new perspectives.* Annu Rev Med, 2010. **61**: p. 301-16.
85. Hankinson, S.E., et al., *Reproductive factors and family history of breast cancer in relation to plasma estrogen and prolactin levels in postmenopausal women in the Nurses' Health Study (United States).* Cancer Causes Control, 1995. **6**(3): p. 217-24.
86. Key, T.J., et al., *Body mass index, serum sex hormones, and breast cancer risk in postmenopausal women.* J Natl Cancer Inst, 2003. **95**(16): p. 1218-26.
87. Missmer, S.A., et al., *Endogenous estrogen, androgen, and progesterone concentrations and breast cancer risk among postmenopausal women.* J Natl Cancer Inst, 2004. **96**(24): p. 1856-65.
88. Nam, S.Y., et al., *Effect of obesity on total and free insulin-like growth factor (IGF)-1, and their relationship to IGF-binding protein (BP)-1, IGFBP-2, IGFBP-3, insulin, and growth hormone.* Int J Obes Relat Metab Disord, 1997. **21**(5): p. 355-9.
89. Pollak, M., *Insulin and insulin-like growth factor signalling in neoplasia.* Nat Rev Cancer, 2008. **8**(12): p. 915-28.
90. Clemmons, D.R., *Modifying IGF1 activity: an approach to treat endocrine disorders, atherosclerosis and cancer.* Nat Rev Drug Discov, 2007. **6**(10): p. 821-33.

91. Milazzo, G., et al., *Insulin receptor expression and function in human breast cancer cell lines.* Cancer Res, 1992. **52**(14): p. 3924-30.
92. Papa, V., et al., *Elevated insulin receptor content in human breast cancer.* J Clin Invest, 1990. **86**(5): p. 1503-10.
93. Goodwin, P.J., et al., *Fasting insulin and outcome in early-stage breast cancer: results of a prospective cohort study.* J Clin Oncol, 2002. **20**(1): p. 42-51.
94. Creighton, C.J., et al., *Insulin-like growth factor-I activates gene transcription programs strongly associated with poor breast cancer prognosis.* J Clin Oncol, 2008. **26**(25): p. 4078-85.
95. Creighton, C.J., et al., *A gene transcription signature of obesity in breast cancer.* Breast Cancer Res Treat, 2012. **132**(3): p. 993-1000.
96. Dunn, S.E., et al., *Dietary restriction reduces insulin-like growth factor I levels, which modulates apoptosis, cell proliferation, and tumor progression in p53-deficient mice.* Cancer Res, 1997. **57**(21): p. 4667-72.
97. Tannenbaum, A. and H. Silverstone, *The influence of the degree of caloric restriction on the formation of skin tumors and hepatomas in mice.* Cancer Res, 1949. **9**(12): p. 724-7.
98. Zhuang, Y. and W.K. Miskimins, *Metformin induces both caspase-dependent and poly(ADP-ribose) polymerase-dependent cell death in breast cancer cells.* Mol Cancer Res, 2011. **9**(5): p. 603-15.
99. Jones, R.G., et al., *AMP-activated protein kinase induces a p53-dependent metabolic checkpoint.* Mol Cell, 2005. **18**(3): p. 283-93.
100. Kalender, A., et al., *Metformin, independent of AMPK, inhibits mTORC1 in a rag GTPase-dependent manner.* Cell Metab, 2010. **11**(5): p. 390-401.
101. Foretz, M., et al., *Metformin inhibits hepatic gluconeogenesis in mice independently of the LKB1/AMPK pathway via a decrease in hepatic energy state.* J Clin Invest, 2010. **120**(7): p. 2355-69.
102. Phoenix, K.N., et al., *Dietary energy availability affects primary and metastatic breast cancer and metformin efficacy.* Breast Cancer Res Treat, 2010. **123**(2): p. 333-44.
103. Algire, C., et al., *Diet and tumor LKB1 expression interact to determine sensitivity to anti-neoplastic effects of metformin in vivo.* Oncogene, 2011. **30**(10): p. 1174-82.
104. Shaw, R.J., et al., *The LKB1 tumor suppressor negatively regulates mTOR signaling.* Cancer Cell, 2004. **6**(1): p. 91-9.
105. Bonanni, B., et al., *Dual effect of metformin on breast cancer proliferation in a randomized presurgical trial.* J Clin Oncol, 2012. **30**(21): p. 2593-600.
106. Xiao, B., et al., *Structure of mammalian AMPK and its regulation by ADP.* Nature, 2011. **472**(7342): p. 230-3.
107. Hardie, D.G., F.A. Ross, and S.A. Hawley, *AMPK: a nutrient and energy sensor that maintains energy homeostasis.* Nat Rev Mol Cell Biol, 2012. **13**(4): p. 251-62.
108. Fogarty, S., et al., *Calmodulin-dependent protein kinase kinase-beta activates AMPK without forming a stable complex: synergistic effects of Ca2+ and AMP.* Biochem J, 2010. **426**(1): p. 109-18.
109. Merrill, G.F., et al., *AICA riboside increases AMP-activated protein kinase, fatty acid oxidation, and glucose uptake in rat muscle.* Am J Physiol, 1997. **273**(6 Pt 1): p. E1107-12.

110. Hardie, D.G., D. Carling, and M. Carlson, *The AMP-activated/SNF1 protein kinase subfamily: metabolic sensors of the eukaryotic cell?* Annu Rev Biochem, 1998. **67**: p. 821-55.
111. Gwinn, D.M., et al., *AMPK phosphorylation of raptor mediates a metabolic checkpoint.* Mol Cell, 2008. **30**(2): p. 214-26.
112. Hoppe, S., et al., *AMP-activated protein kinase adapts rRNA synthesis to cellular energy supply.* Proc Natl Acad Sci U S A, 2009. **106**(42): p. 17781-6.
113. Shackelford, D.B. and R.J. Shaw, *The LKB1-AMPK pathway: metabolism and growth control in tumour suppression.* Nat Rev Cancer, 2009. **9**(8): p. 563-75.
114. Sakamoto, K. and G.D. Holman, *Emerging role for AS160/TBC1D4 and TBC1D1 in the regulation of GLUT4 traffic.* Am J Physiol Endocrinol Metab, 2008. **295**(1): p. E29-37.
115. Barnes, K., et al., *Activation of GLUT1 by metabolic and osmotic stress: potential involvement of AMP-activated protein kinase (AMPK).* J Cell Sci, 2002. **115**(Pt 11): p. 2433-42.
116. Marsin, A.S., et al., *Phosphorylation and activation of heart PFK-2 by AMPK has a role in the stimulation of glycolysis during ischaemia.* Curr Biol, 2000. **10**(20): p. 1247-55.
117. Marsin, A.S., et al., *The stimulation of glycolysis by hypoxia in activated monocytes is mediated by AMP-activated protein kinase and inducible 6-phosphofructo-2-kinase.* J Biol Chem, 2002. **277**(34): p. 30778-83.
118. Koo, S.H., et al., *The CREB coactivator TORC2 is a key regulator of fasting glucose metabolism.* Nature, 2005. **437**(7062): p. 1109-11.
119. Mihaylova, M.M., et al., *Class IIa histone deacetylases are hormone-activated regulators of FOXO and mammalian glucose homeostasis.* Cell, 2011. **145**(4): p. 607-21.
120. Hadad, S.M., et al., *Histological evaluation of AMPK signalling in primary breast cancer.* BMC Cancer, 2009. **9**: p. 307.
121. Baba, Y., et al., *Prognostic significance of AMP-activated protein kinase expression and modifying effect of MAPK3/1 in colorectal cancer.* Br J Cancer, 2010. **103**(7): p. 1025-33.
122. Hawley, S.A., et al., *The antidiabetic drug metformin activates the AMP-activated protein kinase cascade via an adenine nucleotide-independent mechanism.* Diabetes, 2002. **51**(8): p. 2420-5.
123. Owen, M.R., E. Doran, and A.P. Halestrap, *Evidence that metformin exerts its anti-diabetic effects through inhibition of complex 1 of the mitochondrial respiratory chain.* Biochem J, 2000. **348 Pt 3**: p. 607-14.
124. El-Mir, M.Y., et al., *Dimethylbiguanide inhibits cell respiration via an indirect effect targeted on the respiratory chain complex I.* J Biol Chem, 2000. **275**(1): p. 223-8.
125. Perriello, G., et al., *Acute antihyperglycemic mechanisms of metformin in NIDDM. Evidence for suppression of lipid oxidation and hepatic glucose production.* Diabetes, 1994. **43**(7): p. 920-8.
126. Fulgencio, J.P., et al., *Effect of metformin on fatty acid and glucose metabolism in freshly isolated hepatocytes and on specific gene expression in cultured hepatocytes.* Biochem Pharmacol, 2001. **62**(4): p. 439-46.

127. Koopman, W.J., et al., *Mammalian mitochondrial complex I: biogenesis, regulation, and reactive oxygen species generation.* Antioxid Redox Signal, 2010. **12**(12): p. 1431-70.
128. Carvalho, C., et al., *Metformin promotes isolated rat liver mitochondria impairment.* Mol Cell Biochem, 2008. **308**(1-2): p. 75-83.
129. Logie, L., et al., *Cellular responses to the metal-binding properties of metformin.* Diabetes, 2012. **61**(6): p. 1423-33.
130. Anedda, A., E. Rial, and M.M. Gonzalez-Barroso, *Metformin induces oxidative stress in white adipocytes and raises uncoupling protein 2 levels.* J Endocrinol, 2008. **199**(1): p. 33-40.
131. Stambolic, V., et al., *Utility of metformin in breast cancer treatment, is neoangiogenesis a risk factor?* Breast Cancer Res Treat, 2009. **114**(2): p. 387-9.
132. Hirayama, A., et al., *Quantitative metabolome profiling of colon and stomach cancer microenvironment by capillary electrophoresis time-of-flight mass spectrometry.* Cancer Res, 2009. **69**(11): p. 4918-25.
133. Menendez, J.A., et al., *Metformin is synthetically lethal with glucose withdrawal in cancer cells.* Cell Cycle, 2012. **11**(15): p. 2782-92.
134. Hanahan, D. and R.A. Weinberg, *Hallmarks of cancer: the next generation.* Cell, 2011. **144**(5): p. 646-74.
135. Warburg, O., *On the origin of cancer cells.* Science, 1956. **123**(3191): p. 309-14.
136. Vander Heiden, M.G., L.C. Cantley, and C.B. Thompson, *Understanding the Warburg effect: the metabolic requirements of cell proliferation.* Science, 2009. **324**(5930): p. 1029-33.
137. Harris, R.A., et al., *Regulation of the activity of the pyruvate dehydrogenase complex.* Adv Enzyme Regul, 2002. **42**: p. 249-59.
138. Martin, E., R.E. Rosenthal, and G. Fiskum, *Pyruvate dehydrogenase complex: metabolic link to ischemic brain injury and target of oxidative stress.* J Neurosci Res, 2005. **79**(1-2): p. 240-7.
139. Halestrap, A.P. and D. Meredith, *The SLC16 gene family-from monocarboxylate transporters (MCTs) to aromatic amino acid transporters and beyond.* Pflugers Arch, 2004. **447**(5): p. 619-28.
140. Luo, W. and G.L. Semenza, *Emerging roles of PKM2 in cell metabolism and cancer progression.* Trends Endocrinol Metab, 2012. **23**(11): p. 560-6.
141. David, C.J., et al., *HnRNP proteins controlled by c-Myc deregulate pyruvate kinase mRNA splicing in cancer.* Nature, 2010. **463**(7279): p. 364-8.
142. Garcia-Cao, I., et al., *Systemic elevation of PTEN induces a tumor-suppressive metabolic state.* Cell, 2012. **149**(1): p. 49-62.
143. Fendt, S.M., et al., *Metformin Decreases Glucose Oxidation and Increases the Dependency of Prostate Cancer Cells on Reductive Glutamine Metabolism.* Cancer Res, 2013. **73**(14): p. 4429-4438.
144. Phoenix, K.N., F. Vumbaca, and K.P. Claffey, *Therapeutic metformin/AMPK activation promotes the angiogenic phenotype in the ERalpha negative MDA-MB-435 breast cancer model.* Breast Cancer Res Treat, 2009. **113**(1): p. 101-11.
145. Ben Sahra, I., et al., *Targeting cancer cell metabolism: the combination of metformin and 2-deoxyglucose induces p53-dependent apoptosis in prostate cancer cells.* Cancer Res, 2010. **70**(6): p. 2465-75.

146. Cheong, J.H., et al., *Dual inhibition of tumor energy pathway by 2-deoxyglucose and metformin is effective against a broad spectrum of preclinical cancer models.* Mol Cancer Ther, 2011. **10**(12): p. 2350-62.
147. Eagle, H., *Nutrition needs of mammalian cells in tissue culture.* Science, 1955. **122**(3168): p. 501-14.
148. Bergstrom, J., et al., *Intracellular free amino acid concentration in human muscle tissue.* J Appl Physiol, 1974. **36**(6): p. 693-7.
149. Lagranha, C.J., et al., *Glutamine enhances glucose-induced mesangial cell proliferation.* Amino Acids, 2008. **34**(4): p. 683-5.
150. Metallo, C.M., et al., *Reductive glutamine metabolism by IDH1 mediates lipogenesis under hypoxia.* Nature, 2012. **481**(7381): p. 380-4.
151. Mullen, A.R., et al., *Reductive carboxylation supports growth in tumour cells with defective mitochondria.* Nature, 2012. **481**(7381): p. 385-8.
152. Gao, P., et al., *c-Myc suppression of miR-23a/b enhances mitochondrial glutaminase expression and glutamine metabolism.* Nature, 2009. **458**(7239): p. 762-5.
153. Lobo, C., et al., *Inhibition of glutaminase expression by antisense mRNA decreases growth and tumourigenicity of tumour cells.* Biochem J, 2000. **348 Pt 2**: p. 257-61.
154. Seltzer, M.J., et al., *Inhibition of glutaminase preferentially slows growth of glioma cells with mutant IDH1.* Cancer Res, 2010. **70**(22): p. 8981-7.
155. Dang, C.V., et al., *The interplay between MYC and HIF in cancer.* Nat Rev Cancer, 2008. **8**(1): p. 51-6.
156. Yuneva, M., et al., *Deficiency in glutamine but not glucose induces MYC-dependent apoptosis in human cells.* J Cell Biol, 2007. **178**(1): p. 93-105.
157. Medes, G., A. Thomas, and S. Weinhouse, *Metabolism of neoplastic tissue. IV. A study of lipid synthesis in neoplastic tissue slices in vitro.* Cancer Res, 1953. **13**(1): p. 27-9.
158. Menendez, J.A. and R. Lupu, *Fatty acid synthase and the lipogenic phenotype in cancer pathogenesis.* Nat Rev Cancer, 2007. **7**(10): p. 763-77.
159. Ookhtens, M., et al., *Liver and adipose tissue contributions to newly formed fatty acids in an ascites tumor.* Am J Physiol, 1984. **247**(1 Pt 2): p. R146-53.
160. Sabine, J.R., S. Abraham, and I.L. Chaikoff, *Control of lipid metabolism in hepatomas: insensitivity of rate of fatty acid and cholesterol synthesis by mouse hepatoma BW7756 to fasting and to feedback control.* Cancer Res, 1967. **27**(4): p. 793-9.
161. Wymann, M.P. and R. Schneiter, *Lipid signalling in disease.* Nat Rev Mol Cell Biol, 2008. **9**(2): p. 162-76.
162. Alberts, B., et al., *Molecular biology of the cell*. 5 ed. 2008: Garland Science.
163. Salway, J.G., *Metabolism at a glance*. 3 ed. 2004.
164. Baumann, J., C. Sevinsky, and D.S. Conklin, *Lipid biology of breast cancer.* Biochim Biophys Acta, 2013. **1831**(10): p. 1509-17.
165. Milgraum, L.Z., et al., *Enzymes of the fatty acid synthesis pathway are highly expressed in in situ breast carcinoma.* Clin Cancer Res, 1997. **3**(11): p. 2115-20.
166. Swinnen, J.V., K. Brusselmans, and G. Verhoeven, *Increased lipogenesis in cancer cells: new players, novel targets.* Curr Opin Clin Nutr Metab Care, 2006. **9**(4): p. 358-65.

167. Yahagi, N., et al., *Co-ordinate activation of lipogenic enzymes in hepatocellular carcinoma.* Eur J Cancer, 2005. **41**(9): p. 1316-22.
168. Berwick, D.C., et al., *The identification of ATP-citrate lyase as a protein kinase B (Akt) substrate in primary adipocytes.* J Biol Chem, 2002. **277**(37): p. 33895-900.
169. Porstmann, T., et al., *SREBP activity is regulated by mTORC1 and contributes to Akt-dependent cell growth.* Cell Metab, 2008. **8**(3): p. 224-36.
170. Bauer, D.E., et al., *ATP citrate lyase is an important component of cell growth and transformation.* Oncogene, 2005. **24**(41): p. 6314-22.
171. Hatzivassiliou, G., et al., *ATP citrate lyase inhibition can suppress tumor cell growth.* Cancer Cell, 2005. **8**(4): p. 311-21.
172. Migita, T., et al., *ATP citrate lyase: activation and therapeutic implications in non-small cell lung cancer.* Cancer Res, 2008. **68**(20): p. 8547-54.
173. Tong, L., *Acetyl-coenzyme A carboxylase: crucial metabolic enzyme and attractive target for drug discovery.* Cell Mol Life Sci, 2005. **62**(16): p. 1784-803.
174. Swinnen, J.V., et al., *Selective activation of the fatty acid synthesis pathway in human prostate cancer.* Int J Cancer, 2000. **88**(2): p. 176-9.
175. Carretero, J., et al., *Dysfunctional AMPK activity, signalling through mTOR and survival in response to energetic stress in LKB1-deficient lung cancer.* Oncogene, 2007. **26**(11): p. 1616-25.
176. Magnard, C., et al., *BRCA1 interacts with acetyl-CoA carboxylase through its tandem of BRCT domains.* Oncogene, 2002. **21**(44): p. 6729-39.
177. Brusselmans, K., et al., *RNA interference-mediated silencing of the acetyl-CoA-carboxylase-alpha gene induces growth inhibition and apoptosis of prostate cancer cells.* Cancer Res, 2005. **65**(15): p. 6719-25.
178. Chajes, V., et al., *Acetyl-CoA carboxylase alpha is essential to breast cancer cell survival.* Cancer Res, 2006. **66**(10): p. 5287-94.
179. Beckers, A., et al., *Chemical inhibition of acetyl-CoA carboxylase induces growth arrest and cytotoxicity selectively in cancer cells.* Cancer Res, 2007. **67**(17): p. 8180-7.
180. Kuhajda, F.P., *Fatty acid synthase and cancer: new application of an old pathway.* Cancer Res, 2006. **66**(12): p. 5977-80.
181. Alo, P.L., et al., *Expression of fatty acid synthase (FAS) as a predictor of recurrence in stage I breast carcinoma patients.* Cancer, 1996. **77**(3): p. 474-82.
182. Menendez, J.A., et al., *Inhibition of fatty acid synthase (FAS) suppresses HER2/neu (erbB-2) oncogene overexpression in cancer cells.* Proc Natl Acad Sci U S A, 2004. **101**(29): p. 10715-20.
183. De Schrijver, E., et al., *RNA interference-mediated silencing of the fatty acid synthase gene attenuates growth and induces morphological changes and apoptosis of LNCaP prostate cancer cells.* Cancer Res, 2003. **63**(13): p. 3799-804.
184. Pizer, E.S., et al., *Malonyl-coenzyme-A is a potential mediator of cytotoxicity induced by fatty-acid synthase inhibition in human breast cancer cells and xenografts.* Cancer Res, 2000. **60**(2): p. 213-8.
185. Loftus, T.M., et al., *Reduced food intake and body weight in mice treated with fatty acid synthase inhibitors.* Science, 2000. **288**(5475): p. 2379-81.

186. Viollet, B., et al., *Cellular and molecular mechanisms of metformin: an overview.* Clin Sci (Lond), 2012. **122**(6): p. 253-70.
187. Horton, J.D., J.L. Goldstein, and M.S. Brown, *SREBPs: activators of the complete program of cholesterol and fatty acid synthesis in the liver.* J Clin Invest, 2002. **109**(9): p. 1125-31.
188. Ettinger, S.L., et al., *Dysregulation of sterol response element-binding proteins and downstream effectors in prostate cancer during progression to androgen independence.* Cancer Res, 2004. **64**(6): p. 2212-21.
189. Guo, D., et al., *EGFR signaling through an Akt-SREBP-1-dependent, rapamycin-resistant pathway sensitizes glioblastomas to antilipogenic therapy.* Sci Signal, 2009. **2**(101): p. ra82.
190. Williams, K.J., et al., *An essential requirement for the SCAP/SREBP signaling axis to protect cancer cells from lipotoxicity.* Cancer Res, 2013. **73**(9): p. 2850-62.
191. Nieman, K.M., et al., *Adipocytes promote ovarian cancer metastasis and provide energy for rapid tumor growth.* Nat Med, 2011. **17**(11): p. 1498-503.
192. Ros, S., et al., *Functional metabolic screen identifies 6-phosphofructo-2-kinase/fructose-2,6-biphosphatase 4 as an important regulator of prostate cancer cell survival.* Cancer Discov, 2012. **2**(4): p. 328-43.
193. Igal, R.A., *Stearoyl-CoA desaturase-1: a novel key player in the mechanisms of cell proliferation, programmed cell death and transformation to cancer.* Carcinogenesis, 2010. **31**(9): p. 1509-15.
194. Fritz, V., et al., *Abrogation of de novo lipogenesis by stearoyl-CoA desaturase 1 inhibition interferes with oncogenic signaling and blocks prostate cancer progression in mice.* Mol Cancer Ther, 2010. **9**(6): p. 1740-54.
195. Roongta, U.V., et al., *Cancer cell dependence on unsaturated fatty acids implicates stearoyl-CoA desaturase as a target for cancer therapy.* Mol Cancer Res, 2011. **9**(11): p. 1551-61.
196. Pike, L.S., et al., *Inhibition of fatty acid oxidation by etomoxir impairs NADPH production and increases reactive oxygen species resulting in ATP depletion and cell death in human glioblastoma cells.* Biochim Biophys Acta, 2011. **1807**(6): p. 726-34.
197. Samudio, I., et al., *Pharmacologic inhibition of fatty acid oxidation sensitizes human leukemia cells to apoptosis induction.* J Clin Invest, 2010. **120**(1): p. 142-56.
198. Zaugg, K., et al., *Carnitine palmitoyltransferase 1C promotes cell survival and tumor growth under conditions of metabolic stress.* Genes Dev, 2011. **25**(10): p. 1041-51.
199. Jeon, S.M., N.S. Chandel, and N. Hay, *AMPK regulates NADPH homeostasis to promote tumour cell survival during energy stress.* Nature, 2012. **485**(7400): p. 661-5.
200. Peters, J.M., Y.M. Shah, and F.J. Gonzalez, *The role of peroxisome proliferator-activated receptors in carcinogenesis and chemoprevention.* Nat Rev Cancer, 2012. **12**(3): p. 181-95.
201. Bozza, P.T. and J.P. Viola, *Lipid droplets in inflammation and cancer.* Prostaglandins Leukot Essent Fatty Acids, 2010. **82**(4-6): p. 243-50.

202. Takeuchi, K. and K. Reue, *Biochemistry, physiology, and genetics of GPAT, AGPAT, and lipin enzymes in triglyceride synthesis.* Am J Physiol Endocrinol Metab, 2009. **296**(6): p. E1195-209.
203. Diefenbach, C.S., et al., *Lysophosphatidic acid acyltransferase-beta (LPAAT-beta) is highly expressed in advanced ovarian cancer and is associated with aggressive histology and poor survival.* Cancer, 2006. **107**(7): p. 1511-9.
204. Niesporek, S., et al., *Expression of lysophosphatidic acid acyltransferase beta (LPAAT-beta) in ovarian carcinoma: correlation with tumour grading and prognosis.* Br J Cancer, 2005. **92**(9): p. 1729-36.
205. Coon, M., et al., *Inhibition of lysophosphatidic acid acyltransferase beta disrupts proliferative and survival signals in normal cells and induces apoptosis of tumor cells.* Mol Cancer Ther, 2003. **2**(10): p. 1067-78.
206. Douvas, M.G., et al., *Effect of lysophosphatidic acid acyltransferase-beta inhibition in acute leukemia.* Leuk Res, 2006. **30**(8): p. 1027-36.
207. Hideshima, T., et al., *Molecular characterization of PS-341 (bortezomib) resistance: implications for overcoming resistance using lysophosphatidic acid acyltransferase (LPAAT)-beta inhibitors.* Oncogene, 2005. **24**(19): p. 3121-9.
208. Springett, G.M., et al., *Lysophosphatidic acid acyltransferase-beta is a prognostic marker and therapeutic target in gynecologic malignancies.* Cancer Res, 2005. **65**(20): p. 9415-25.
209. Pagel, J.M., et al., *Induction of apoptosis using inhibitors of lysophosphatidic acid acyltransferase-beta and anti-CD20 monoclonal antibodies for treatment of human non-Hodgkin's lymphomas.* Clin Cancer Res, 2005. **11**(13): p. 4857-66.
210. Peterson, T.R., et al., *mTOR complex 1 regulates lipin 1 localization to control the SREBP pathway.* Cell, 2011. **146**(3): p. 408-20.
211. Bagnato, C. and R.A. Igal, *Overexpression of diacylglycerol acyltransferase-1 reduces phospholipid synthesis, proliferation, and invasiveness in simian virus 40-transformed human lung fibroblasts.* J Biol Chem, 2003. **278**(52): p. 52203-11.
212. Das, S.K., et al., *Adipose triglyceride lipase contributes to cancer-associated cachexia.* Science, 2011. **333**(6039): p. 233-8.
213. Nomura, D.K., et al., *Monoacylglycerol lipase regulates a fatty acid network that promotes cancer pathogenesis.* Cell, 2010. **140**(1): p. 49-61.
214. Mehta, S., et al., *Assessing early therapeutic response to bevacizumab in primary breast cancer using magnetic resonance imaging and gene expression profiles.* J Natl Cancer Inst Monogr, 2011. **2011**(43): p. 71-4.
215. Hadad, S., et al., *Evidence for biological effects of metformin in operable breast cancer: a pre-operative, window-of-opportunity, randomized trial.* Breast Cancer Res Treat, 2011. **128**(3): p. 783-94.
216. Niraula, S., et al., *Metformin in early breast cancer: a prospective window of opportunity neoadjuvant study.* Breast Cancer Res Treat, 2012. **135**(3): p. 821-30.
217. Cazzaniga, M., A. Decensi, and G. Pruneri, *Effect of Metformin on apoptosis in a presurgical trial in non-diabetic patients with breast cancer.* Cancer Res, 2012. **72 (24 Suppl.)**: p. 116s.

218. Kalinsky, K., K.D. Crew, and R. S., *Pre-surgical trial of metformin in overweight and obese, multi-ethnic patientswith newly diagnosed breast cancer.* Cancer Res, 2012. **72 (24 Suppl.)**: p. 117s.
219. Ben-Haim, S. and P. Ell, *18F-FDG PET and PET/CT in the evaluation of cancer treatment response.* J Nucl Med, 2009. **50**(1): p. 88-99.
220. Habibollahi, P., et al., *Metformin--an adjunct antineoplastic therapy--divergently modulates tumor metabolism and proliferation, interfering with early response prediction by 18F-FDG PET imaging.* J Nucl Med, 2013. **54**(2): p. 252-8.
221. Ley, T.J., et al., *DNA sequencing of a cytogenetically normal acute myeloid leukaemia genome.* Nature, 2008. **456**(7218): p. 66-72.
222. Wang, Z., M. Gerstein, and M. Snyder, *RNA-Seq: a revolutionary tool for transcriptomics.* Nat Rev Genet, 2009. **10**(1): p. 57-63.
223. Buffa, F.M., et al., *Large meta-analysis of multiple cancers reveals a common, compact and highly prognostic hypoxia metagene.* Br J Cancer, 2010. **102**(2): p. 428-35.
224. Desmedt, C., et al., *Biological processes associated with breast cancer clinical outcome depend on the molecular subtypes.* Clin Cancer Res, 2008. **14**(16): p. 5158-65.
225. Diraison, F., C. Pachiaudi, and M. Beylot, *Measuring lipogenesis and cholesterol synthesis in humans with deuterated water: use of simple gas chromatographic/mass spectrometric techniques.* J Mass Spectrom, 1997. **32**(1): p. 81-6.
226. Diraison, F., P. Moulin, and M. Beylot, *Contribution of hepatic de novo lipogenesis and reesterification of plasma non esterified fatty acids to plasma triglyceride synthesis during non-alcoholic fatty liver disease.* Diabetes Metab, 2003. **29**(5): p. 478-85.
227. Evans, K., et al., *Regulation of dietary fatty acid entrapment in subcutaneous adipose tissue and skeletal muscle.* Diabetes, 2002. **51**(9): p. 2684-90.
228. Giardiello, F.M., et al., *Very high risk of cancer in familial Peutz-Jeghers syndrome.* Gastroenterology, 2000. **119**(6): p. 1447-53.
229. Sanchez-Cespedes, M., et al., *Inactivation of LKB1/STK11 is a common event in adenocarcinomas of the lung.* Cancer Res, 2002. **62**(13): p. 3659-62.
230. Chen, S., et al., *Complementary regulation of TBC1D1 and AS160 by growth factors, insulin and AMPK activators.* Biochem J, 2008. **409**(2): p. 449-59.
231. Chen, S., et al., *Mice with AS160/TBC1D4-Thr649Ala knockin mutation are glucose intolerant with reduced insulin sensitivity and altered GLUT4 trafficking.* Cell Metab, 2011. **13**(1): p. 68-79.
232. Pehmoller, C., et al., *Genetic disruption of AMPK signaling abolishes both contraction- and insulin-stimulated TBC1D1 phosphorylation and 14-3-3 binding in mouse skeletal muscle.* Am J Physiol Endocrinol Metab, 2009. **297**(3): p. E665-75.
233. Wise, D.R., et al., *Myc regulates a transcriptional program that stimulates mitochondrial glutaminolysis and leads to glutamine addiction.* Proc Natl Acad Sci U S A, 2008. **105**(48): p. 18782-7.

234. Javeshghani, S., et al., *Carbon source and myc expression influence the antiproliferative actions of metformin.* Cancer Res, 2012. **72**(23): p. 6257-67.
235. Segal, E.D., et al., *Relevance of the OCT1 transporter to the antineoplastic effect of biguanides.* Biochem Biophys Res Commun, 2011. **414**(4): p. 694-9.
236. Jiang, T., et al., *High levels of Nrf2 determine chemoresistance in type II endometrial cancer.* Cancer Res, 2010. **70**(13): p. 5486-96.
237. Onken, B. and M. Driscoll, *Metformin induces a dietary restriction-like state and the oxidative stress response to extend C. elegans Healthspan via AMPK, LKB1, and SKN-1.* PLoS One, 2010. **5**(1): p. e8758.
238. das Neves, R.P., et al., *Connecting variability in global transcription rate to mitochondrial variability.* PLoS Biol, 2010. **8**(12): p. e1000560.
239. Lee, W.N., et al., *Measurement of fractional lipid synthesis using deuterated water (2H2O) and mass isotopomer analysis.* Am J Physiol, 1994. **266**(3 Pt 1): p. E372-83.
240. Tabernero, J., et al., *Dose- and schedule-dependent inhibition of the mammalian target of rapamycin pathway with everolimus: a phase I tumor pharmacodynamic study in patients with advanced solid tumors.* J Clin Oncol, 2008. **26**(10): p. 1603-10.
241. Chan, T., *Computerized method for automatic evaluation of lean body mass from PET/CT: comparison with predictive equations.* J Nucl Med, 2012. **53**(1): p. 130-7.
242. Carmona-Saez, P., et al., *GENECODIS: a web-based tool for finding significant concurrent annotations in gene lists.* Genome Biol, 2007. **8**(1): p. R3.
243. Nogales-Cadenas, R., et al., *GeneCodis: interpreting gene lists through enrichment analysis and integration of diverse biological information.* Nucleic Acids Res, 2009. **37**(Web Server issue): p. W317-22.
244. Tabas-Madrid, D., R. Nogales-Cadenas, and A. Pascual-Montano, *GeneCodis3: a non-redundant and modular enrichment analysis tool for functional genomics.* Nucleic Acids Res, 2012. **40**(Web Server issue): p. W478-83.
245. Detaille, D., et al., *Obligatory role of membrane events in the regulatory effect of metformin on the respiratory chain function.* Biochem Pharmacol, 2002. **63**(7): p. 1259-72.
246. Zu, X.L. and M. Guppy, *Cancer metabolism: facts, fantasy, and fiction.* Biochem Biophys Res Commun, 2004. **313**(3): p. 459-65.
247. Salas, A., et al., *A critical reassessment of the role of mitochondria in tumorigenesis.* PLoS Med, 2005. **2**(11): p. e296.
248. Wang, J.B., et al., *Targeting mitochondrial glutaminase activity inhibits oncogenic transformation.* Cancer Cell, 2010. **18**(3): p. 207-19.
249. Yang, C., et al., *Glioblastoma cells require glutamate dehydrogenase to survive impairments of glucose metabolism or Akt signaling.* Cancer Res, 2009. **69**(20): p. 7986-93.
250. Karbowski, M. and R.J. Youle, *Dynamics of mitochondrial morphology in healthy cells and during apoptosis.* Cell Death Differ, 2003. **10**(8): p. 870-80.

251. Meeusen, S., J.M. McCaffery, and J. Nunnari, *Mitochondrial fusion intermediates revealed in vitro.* Science, 2004. **305**(5691): p. 1747-52.
252. Turturro, F., G. Von Burton, and E. Friday, *Hyperglycemia-induced thioredoxin-interacting protein expression differs in breast cancer-derived cells and regulates paclitaxel IC50.* Clin Cancer Res, 2007. **13**(12): p. 3724-30.
253. Hirschhaeuser, F., et al., *Multicellular tumor spheroids: an underestimated tool is catching up again.* J Biotechnol, 2010. **148**(1): p. 3-15.
254. Sonveaux, P., et al., *Targeting lactate-fueled respiration selectively kills hypoxic tumor cells in mice.* J Clin Invest, 2008. **118**(12): p. 3930-42.
255. Esslinger, C.S., K.A. Cybulski, and J.F. Rhoderick, *Ngamma-aryl glutamine analogues as probes of the ASCT2 neutral amino acid transporter binding site.* Bioorg Med Chem, 2005. **13**(4): p. 1111-8.
256. Bode, B.P., et al., *Glutamine transport in isolated human hepatocytes and transformed liver cells.* Hepatology, 1995. **21**(2): p. 511-20.
257. Bode, B.P. and W.W. Souba, *Modulation of cellular proliferation alters glutamine transport and metabolism in human hepatoma cells.* Ann Surg, 1994. **220**(4): p. 411-22; discussion 422-4.
258. Collins, C.L., et al., *Determinants of glutamine dependence and utilization by normal and tumor-derived breast cell lines.* J Cell Physiol, 1998. **176**(1): p. 166-78.
259. Hassanein, M., et al., *SLC1A5 mediates glutamine transport required for lung cancer cell growth and survival.* Clin Cancer Res, 2013. **19**(3): p. 560-70.
260. Meng, M., et al., *Nitrogen anabolism underlies the importance of glutaminolysis in proliferating cells.* Cell Cycle, 2010. **9**(19): p. 3921-32.
261. Ronzio, R.A. and A. Meister, *Phosphorylation of methionine sulfoximine by glutamine synthetase.* Proc Natl Acad Sci U S A, 1968. **59**(1): p. 164-70.
262. Catane, R., et al., *Azaserine, DON, and azotomycin: three diazo analogs of L-glutamine with clinical antitumor activity.* Cancer Treat Rep, 1979. **63**(6): p. 1033-8.
263. Li, M., et al., *Novel inhibitors complexed with glutamate dehydrogenase: allosteric regulation by control of protein dynamics.* J Biol Chem, 2009. **284**(34): p. 22988-3000.
264. Saunders, L.P., et al., *Identification of small-molecule inhibitors of autotaxin that inhibit melanoma cell migration and invasion.* Mol Cancer Ther, 2008. **7**(10): p. 3352-62.
265. Edwards, L.A., et al., *Combined inhibition of the phosphatidylinositol 3-kinase/Akt and Ras/mitogen-activated protein kinase pathways results in synergistic effects in glioblastoma cells.* Mol Cancer Ther, 2006. **5**(3): p. 645-54.
266. Mizuno, Y., T. Saitoh, and N. Sone, *Inhibition of mitochondrial alpha-ketoglutarate dehydrogenase by 1-methyl-4-phenylpyridinium ion.* Biochem Biophys Res Commun, 1987. **143**(3): p. 971-6.
267. Goncharov, N.V., R.O. Jenkins, and A.S. Radilov, *Toxicology of fluoroacetate: a review, with possible directions for therapy research.* J Appl Toxicol, 2006. **26**(2): p. 148-61.

268. Timmerman, L.A., et al., *Glutamine sensitivity analysis identifies the xCT antiporter as a common triple-negative breast tumor therapeutic target.* Cancer Cell, 2013. **24**(4): p. 450-65.
269. Singh, T.S., H. Sugiyama, and A. Rangsiruji, *Paragonimus & paragonimiasis in India.* Indian J Med Res, 2012. **136**(2): p. 192-204.
270. Robinson, A.C., et al., *The effects of metformin on glycemic control and serum lipids in insulin-treated NIDDM patients with suboptimal metabolic control.* Diabetes Care, 1998. **21**(5): p. 701-5.
271. Jeppesen, J., et al., *Effect of metformin on postprandial lipemia in patients with fairly to poorly controlled NIDDM.* Diabetes Care, 1994. **17**(10): p. 1093-9.
272. Zavaroni, I., et al., *Inhibition of carbohydrate-induced hypertriglyceridemia by metformin.* Horm Metab Res, 1984. **16**(2): p. 85-7.
273. Marchetti, P., et al., *Effect of plasma metformin concentrations on serum lipid levels in type II diabetic patients.* Acta Diabetol Lat, 1988. **25**(1): p. 55-62.
274. Riccio, A., et al., *Glucose and lipid metabolism in non-insulin-dependent diabetes. Effect of metformin.* Diabete Metab, 1991. **17**(1 Pt 2): p. 180-4.
275. http://www.clinicaltrials.gov.
276. Cool, B., et al., *Identification and characterization of a small molecule AMPK activator that treats key components of type 2 diabetes and the metabolic syndrome.* Cell Metab, 2006. **3**(6): p. 403-16.
277. Saeedi, R., et al., *Metabolic actions of metformin in the heart can occur by AMPK-independent mechanisms.* Am J Physiol Heart Circ Physiol, 2008. **294**(6): p. H2497-506.
278. Merrill, G.M., et al., *AICAR decreases malonyl-CoA and increases fatty acid oxidation in skeletal muscle of the rat.* Am. J. Physiol, 1997. **273**: p. E1107–E1112.
279. Habets, D.D., et al., *Crucial role for LKB1 to AMPKalpha2 axis in the regulation of CD36-mediated long-chain fatty acid uptake into cardiomyocytes.* Biochim Biophys Acta, 2009. **1791**(3): p. 212-9.
280. Henin, N., et al., *Inhibition of fatty acid and cholesterol synthesis by stimulation of AMP-activated protein kinase.* FASEB J, 1995. **9**(7): p. 541-6.
281. Muoio, D.M., et al., *AMP-activated kinase reciprocally regulates triacylglycerol synthesis and fatty acid oxidation in liver and muscle: evidence that sn-glycerol-3-phosphate acyltransferase is a novel target.* Biochem J, 1999. **338 (Pt 3)**: p. 783-91.
282. Foretz, M., et al., *AMP-activated protein kinase inhibits the glucose-activated expression of fatty acid synthase gene in rat hepatocytes.* J Biol Chem, 1998. **273**(24): p. 14767-71.
283. Kuhajda, F.P., et al., *Synthesis and antitumor activity of an inhibitor of fatty acid synthase.* Proc Natl Acad Sci U S A, 2000. **97**(7): p. 3450-4.
284. Swinnen, J.V., et al., *Androgens, lipogenesis and prostate cancer.* J Steroid Biochem Mol Biol, 2004. **92**(4): p. 273-9.
285. Demierre, M.F., et al., *Statins and cancer prevention.* Nat Rev Cancer, 2005. **5**(12): p. 930-42.
286. Bhalla, K., et al., *Metformin prevents liver tumorigenesis by inhibiting pathways driving hepatic lipogenesis.* Cancer Prev Res (Phila), 2012. **5**(4): p. 544-52.

287. Bartlett, K. and S. Eaton, *Mitochondrial beta-oxidation.* Eur J Biochem, 2004. **271**(3): p. 462-9.
288. Lee, W.J., et al., *AMPK activation increases fatty acid oxidation in skeletal muscle by activating PPARalpha and PGC-1.* Biochem Biophys Res Commun, 2006. **340**(1): p. 291-5.
289. Ahmadian, M., et al., *Desnutrin/ATGL is regulated by AMPK and is required for a brown adipose phenotype.* Cell Metab, 2011. **13**(6): p. 739-48.
290. Corton, J.M., et al., *5-aminoimidazole-4-carboxamide ribonucleoside. A specific method for activating AMP-activated protein kinase in intact cells?* Eur J Biochem, 1995. **229**(2): p. 558-65.
291. Carracedo, A., et al., *A metabolic prosurvival role for PML in breast cancer.* J Clin Invest, 2012. **122**(9): p. 3088-100.
292. Schafer, Z.T., et al., *Antioxidant and oncogene rescue of metabolic defects caused by loss of matrix attachment.* Nature, 2009. **461**(7260): p. 109-13.
293. Ito, K., et al., *A PML-PPAR-delta pathway for fatty acid oxidation regulates hematopoietic stem cell maintenance.* Nat Med, 2012. **18**(9): p. 1350-8.
294. Wang, Y.C., et al., *Health and economic burden of the projected obesity trends in the USA and the UK.* Lancet, 2011. **378**(9793): p. 815-25.
295. Cuber, J.C., et al., *Metabolic and drug distribution studies do not support direct inhibitory effects of metformin on intestinal glucose absorption.* Diabete Metab, 1994. **20**(6): p. 532-9.
296. Turkheimer, F.E., R. Hinz, and V.J. Cunningham, *On the undecidability among kinetic models: from model selection to model averaging.* J Cereb Blood Flow Metab, 2003. **23**(4): p. 490-8.
297. Dimitrakopoulou-Strauss, A., L. Pan, and L.G. Strauss, *Parametric imaging: a promising approach for the evaluation of dynamic PET-18F-FDG studies - the DKFZ experience.* Hell J Nucl Med, 2010. **13**(1): p. 18-22.
298. Iozzo, P., et al., *Insulin stimulates liver glucose uptake in humans: an 18F-FDG PET Study.* J Nucl Med, 2003. **44**(5): p. 682-9.
299. Cheng, T., et al., *Pyruvate carboxylase is required for glutamine-independent growth of tumor cells.* Proc Natl Acad Sci U S A, 2011. **108**(21): p. 8674-9.
300. Brown, R.S., et al., *Glucose transporters and FDG uptake in untreated primary human non-small cell lung cancer.* J Nucl Med, 1999. **40**(4): p. 556-65.
301. Higashi, K., et al., *Correlation of Glut-1 glucose transporter expression with.* Eur J Nucl Med, 2000. **27**(12): p. 1778-85.
302. Higashi, T., et al., *FDG uptake, GLUT-1 glucose transporter and cellularity in human pancreatic tumors.* J Nucl Med, 1998. **39**(10): p. 1727-35.
303. Dowsett, M., et al., *Assessment of Ki67 in breast cancer: recommendations from the International Ki67 in Breast Cancer working group.* J Natl Cancer Inst, 2011. **103**(22): p. 1656-64.
304. Bonser, A.M. and P. Garcia-Webb, *C-peptide measurement: methods and clinical utility.* Crit Rev Clin Lab Sci, 1984. **19**(4): p. 297-352.
305. Nar, A. and O. Gedik, *The effect of metformin on leptin in obese patients with type 2 diabetes mellitus and nonalcoholic fatty liver disease.* Acta Diabetol, 2009. **46**(2): p. 113-8.

306. Barone, I., et al., *Leptin mediates tumor-stromal interactions that promote the invasive growth of breast cancer cells.* Cancer Res, 2012. **72**(6): p. 1416-27.
307. Vance, J.E. and D.E. Vance, *Phospholipid biosynthesis in mammalian cells.* Biochem Cell Biol, 2004. **82**(1): p. 113-28.